Disorder in holographic field theories

inhomogeneous geometries, momentum relaxation and SYK models

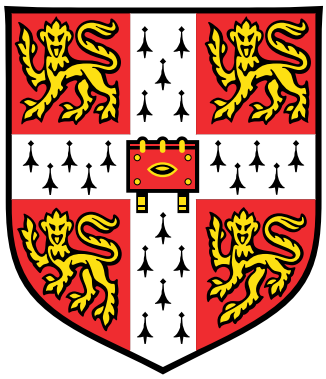

Bruno Loureiro

Gonville and Caius College
University of Cambridge

Supervisors: Prof Antonio Miguel García-García
Prof Emilio Artacho

This dissertation is submitted for the degree of Doctor of Philosophy

April, 2018

Morte e vida das hipóteses. Da equação eu parte do Cosmos ao axioma Cosmos parte do eu. Subsistência. Conhecimento. Antropofagia.

Manifesto Antropofágico, Oswald de Andrade.

Declaration

I hereby declare that except where specific reference is made to the work of others, the contents of this dissertation are original and have not been submitted in whole or in part for consideration for any other degree or qualification in this, or any other university. This dissertation is my own work and contains nothing which is the outcome of work done in collaboration with others, except as specified in the text and Acknowledgements. This dissertation contains fewer than 60,000 words including appendices, bibliography, footnotes, tables and equations and has fewer than 150 figures.

The core part of the thesis is based on research published in:

- AM Garcia-Garcia, B Loureiro, "*Marginal and irrelevant disorder in Einstein-Maxwell backgrounds*", Phys. Rev. D 93 065025 (2016)
- A.M. Garcia-Garcia, B. Loureiro and A. Romero-Bermudez, "*Transport in a gravity dual with a varying gravitational coupling constant*", Phys. Rev. D 94 086007 (2016)
- A.M. Garcia-Garcia, B. Loureiro, A. Romero-Bermudez and T. Masaki, "*Chaotic-Integrable Transition in the Sachdev-Ye-Kitaev Model*", Phys. Rev. Lett. 120, 241603 (2018)
- A.M. Garcia-Garcia, B. Loureiro, Tomás Andrade, "*Coherence effects in disordered geometries with a field-theory dual* ", J. High Energ. Phys. (2018) 2018: 187.

Bruno Loureiro
April, 2018

Acknowledgments

First and foremost, I would like to thank Antonio - supervisor, advisor, collaborator and mentor. His meticulous dosage of rigour, support and inspiration have been invaluable in my academic and personal development during this arduous process called PhD.

If I ever made it here, it was because of the unconditional support and love of my mother, Marcia. During our first visit to Cambridge, she asked me: 'fancy studying here when you grow up?'. I was 9 years old. Look what happened.

I would also like to thank the rest of my family, major witnesses in this conspiracy. In particular, my grandmother Maria, tia Katita, dinda Lucia, my father Hugo and my belle-mère Manou.

I am grateful to Eduardo and Valeria, for the support, advice and numerous interesting conversations in London.

Marisa, Giorgio, Pippo and nonna Leonora, vi ringrazio per l'affetto con cui mi avete sempre accolto. Sarete per sempre la mia famiglia italiana.

Amigos da terra. De terreiros. Ctônicos. Ian, devir amigo. Breno, não fazemos drama. Clarissa, fais gaffe aux mouettes. Clarissa, há verdade. Claudio++. Serenojoviais, sempre.

A huge thanks to all the friends with whom I have shared the untold story of this thesis. Salvatore, lo zio. Aurelio, colleague, collaborator and friend. Beñazinho. Alan, the chef. Hippolyte. Cambyse and Karina. Marianne. Simon San. Miguelito. The Brazilian gang: Luiza, Josie, Renata, Elton, Matheusão, Isa, Livia, Flávia, Maria, Denise, Jana, Carol, Philipe, Alê, Manou, Ildo, Vanessa, Rodrigo, Camila, Cris, Leo, Rayner, Giorgia. The TCM colleagues and friends: Victor, Daniel Rowlands, Daniel Malz, Adam, Ezequiel, Joas. And also a big thanks to all the TCM staff who have always been friendly and supportive.

Aline and Erick, friends of the house, friends of the routine. Small family in this unfamiliar place.

Giuseppe, fratello, carioca del tuorlo e amiguinho 100%. Loucura é pensar que precisei cruzar um atlântico para encontrar um irmão.

Lavinia, amore mio. Pensei em tudo que é possível falar, que sirva apenas para nós dois... But you taught me that it only takes a small thought to fill a whole life.

Summary

Holographic dualities are now an established tool in the study of universal properties of strongly coupled field theories. Yet, theories without translational symmetry are still poorly understood in this context. In this dissertation, we investigate three new approaches to this challenging problem.

The first part of the dissertation concerns a class of phenomenological holographic models in which momentum relaxation can be achieved without breaking translational symmetry in the dual geometry. In particular, we focus on an example in which the dual geometry is similar to anti-de Sitter (AdS) Brans-Dicke theory. We study the thermodynamic and transport properties of the model and show that for strong momentum relaxation and low temperatures the model has insulator-like behaviour.

In the second part, we go beyond the effective description and consider holographic theories which explicitly break translational symmetry. From the perspective of gravity, these theories translate to geometries that vary explicitly in the boundary space-like coordinates. We refer to these geometries as '*inhomogeneous*' and investigate two approaches to study them. The first is motivated by the question: "*what happens to a homogeneous geometry when coupled with a field varying randomly in space?*". Starting from an AdS geometry at zero or finite temperature, we show that a spatially varying random Maxwell potential drives the dual field theory to a non-trivial infra-red fixed point characterised by an emerging scale invariance. Thermodynamic and transport properties of this disordered ground state are also discussed. The second is motivated by the complementary question: "*how does a random geometry affect a probe field*?". In the weak disorder limit, we show that disorder induces an additional power-law decay in the dual correlation functions. For certain choices of geometry profile, this contribution becomes dominant in the infra-red, indicating the breaking of perturbation theory and the possible existence of a phase transition induced by disorder.

The third and last part of this dissertation switches from the gravity to the field theoretical side of the duality. We discuss the Sachdev-Ye-Kitaev (SYK) model, a disordered many-body model with distinctive black hole-like properties. We provide analytical and numerical evidence that these *holographic* properties are robust against a natural one-body deformation for a finite range of parameters. Outside this interval, this system undergoes a chaotic-integrable transition.

Contents

List of Illustrations

Tables

Figures

Nomenclature

Abbreviations

AdS_d	d-dimensional anti-de Sitter
BD	Brans-Dicke
CFT	Conformal field theory
EMd	Einstein-Maxwell-dilaton
Eq(s).	equation(s)
i.i.d.	Independent and identically distributed
IR	Infra-red
KSS	Kovtun-Son-Starinets
OTO	Out-of-time-order
QCD	Quantum chromodynamics
QFT	Quantum field theory
RN	Reissner-Nordström
SYK	Sachdev-Ye-Kitaev
SYM	Super Yang-Mills
UV	Ultra-violet

Symbols

Δ_g	Laplace-Beltrami operator
Λ	Cosmological constant
$\mathbb{E}[\dots]$	Expected value

$\mathbb{M}^d$	d-dimensional Minkowski spacetime
$\mathbb{R}^d$	d-dimensional Euclidean space
$\sigma(\omega)$	ac-conductivity
σ_{dc}	dc-conductivity
σ_{Q}	Regular part of the translational invariant dc-conductivity
l_{AdS}	anti-de Sitter radius
T	Temperature
e	Maxwell coupling

Conventions

In this dissertation we adopt the following conventions.

Natural units

We set $\hbar = c = G = k_{\mathrm{B}} = 1$. Space, time, mass and temperature are all given in terms of energy dimensions.

With a few stated exceptions, we also set the electron charge e and the AdS radius l_{AdS} to unit.

Metric signature

The spacetime metric signature is mostly plus, $(-, +, \ldots, +)$.

Bulk vs. boundary

Unless otherwise stated, d will always denote the number of dimensions in the **boundary** field theory.

The latin letters $a, b, c, d = 1, \cdots, d+1$ are reserved as bulk indices, while the greek letters $\mu, \nu = 1, \ldots, d$ for boundary indices. The spacelike boundary coordinates are usually indexed by the latin letters $i, j, k, l = 1, \cdots, d-1$.

1 | Introduction and overview

The *holographic duality* relating strongly-coupled quantum field theories in d dimensions and classical theories of gravity in $d+1$-dimensional anti-de Sitter (AdS) spacetime has become an important tool in the modern repertoire of techniques employed to study strongly-interacting systems. Despite undoubtful progress, the field remains limited by the artificial set of symmetries commonly imposed when solving Einstein's equations analytically. This dissertation is part of a collective research effort in relaxing these symmetry constraints, and focus in particular on the problem of translational symmetry breaking and disorder in holographic field theories.

We start with a brief storyline of the developments that are at the heart of our research questions.

The birth of applied holography

Fruit of years of collaborative work [1], the holographic duality, also known as AdS/CFT correspondence, first formally appeared in the work of Maldacena in 1997 [2]. In his seminal paper, Maldacena proposed that the strong coupling regime of $\mathcal{N}=4$ super Yang-Mills (SYM) theory admitted a dual description in terms of the $\mathrm{AdS}_5 \times S^5$ solution of general relativity [2][1]. With a few exceptions - such as integrable theories at low dimensions - the strong coupling regime of generic field theories is inaccessible by conventional perturbative techniques. On the other hand, general relativity is concerned with finding solutions for Einstein's equations, a hard but well-understood problem. It is precisely in this imbalance that lies the appeal of the duality.

Maldacena's proposal unfolded in several generalizations. Works by Witten [3], Gubser, Klebanov and Polyakov [4] have drawn a practical dictionary to translate observables from the field theory side to geometric quantities in general relativity. New dualities were established, and a fast-paced research field started gaining shape [5]. Indeed, it took less than four years from Maldacena's work to the first application of the holographic duality to a practical problem in nuclear physics, the *quark-gluon plasma* [6].

Heavy-ion collisions in the LHC produce a strongly-interacting deconfined phase of quantum chromodynamics (QCD) known as the quark-gluon plasma. Experiments suggest

[1] Note that S^n denote the n-dimensional unit sphere

that this soup of quarks and gluons interacts strongly and behave as an almost ideal fluid [7]. Research for an effective model describing the experiments requires an estimate of the thermodynamic and transport coefficients governing the hydrodynamical expansion of QCD. Conventional techniques, such as diagrammatic expansions and lattice simulations are conceptually limited to the weak coupling regime of QCD, providing poor extrapolated results at strong-coupling. Starinets, Policastro and Son were the first to realise the potential of applying the holographic duality to this problem. Regarding the strongly-coupled phase of $\mathcal{N} = 4$ super Yang-Mills as a toy-model for the quark-gluon plasma, they employed the duality to estimate that the shear viscosity to entropy ratio is given by the constant $\eta/s = (4\pi)^{-1}$ [6, 8]. Surprisingly, this value is in good agreement with the heavy-ion collision experiments in the LHC [9]. Based on the previous weak coupling result for η/s, that suggested it is an increasing function of the coupling parameter, and on the notion of *universality* of the hydrodynamical description, Kovtun, Starinets and Son later conjectured that the value $(4\pi)^{-1}$ should be a lower bound for the shear viscosity to entropy ratio of fluids [10, 11]. Although this celebrated result was shown later to be violated in generalised holographic field theories, it is astoundingly satisfied by most real-life fluids [9].

The KSS bound, as it is now known, has laid the groundwork of applied holography, and became a landmark for how the duality can be employed to provide insight about some universal properties of strongly-coupled field theories [12].

Holography and criticality

Behind the unreasonable effectiveness of the holographic approach to the quark-gluon plasma, is the key notion of *universality*. Holographic field theories should be thought as *phenomenological*, rather than *microscopic* descriptions for a system. For instance, it would be misleading to picture $\mathcal{N} = 4$ SYM as a faithful description of deconfined quarks. Instead, we can motivate this similarity by thinking in terms of the *renormalization group flow*. Despite being radically different in the ultra-violet, at strong coupling, these theories flow to a common infra-red fixed point described by a universal hydrodynamic expansion, which can be effectively studied using the holographic duality.

The idea of studying holographic field theories to intuit the universal behaviour of strongly-interacting fixed points found a fertile ground in the field of condensed matter, where universality has been a paradigm since the work of Kadanoff and Wilson [13–15]. At the core of condensed matter theory is the classification of phases of matter and the transitions between them. In the vicinity of a phase transition, critical theories develop long-range correlations characterised by an emerging scale invariance of the physical observables. Correlation functions in the system become independent of the underlying microscopic theory at large scales and can be described by an effective quantum field theory. From the renormalization group perspective, classifying the universality classes of phase transitions is translated to classi-

fying the long-range behaviour of scale-invariant quantum field theories [16, 17]. In $d = 1, 2$ dimensions, scale invariance is strong enough to provide a comprehensive classification of the critical points. However, at higher dimensions, the conventional techniques are limited to weak coupling. Holography is a promising tool to address the strong coupling limit. As we will discuss in Chapter 2, the holographic duality can be thought as a geometrization of the renormalization group flow, naturally embodying scale invariance on the asymptotically AdS boundary conditions.

The pioneering work of Hartnoll, Sachdev, Müller and Kovtun [18] have laid the groundwork for a fast-paced research program inspired by criticality, drawing ever-growing attention from high energy and condensed matter physicists alike [19–23]. However, it was soon realised that the simplest holographic field theories fail to capture some of the important features of critical condensed matter systems. For instance, the early holographic field theories were all relativistic, a limitation which was rapidly addressed [20, 21, 24–26]. Since the first works from 2008, many similar questions have been addressed, and the list of effective holographic theories motivated by condensed matter systems is ever-growing. As a side effect, general relativity has also benefited from the outburst engendered by applied holography. To cite an example, superconductivity was the driving motivation behind the discovery of the first hairy black hole in AdS [27–30].

Despite these unquestionable successes, the field of applied holography is far from mature, and many ubiquitous concepts in condensed matter physics still lack a holographic counterpart. A key example is provided by disordered field theories. Disorder is widely employed in condensed matter to model phenomena that vary from sample to sample, such as defects and impurities in metals, frustration in glasses, turbulence in fluids and more broadly noise in experiments [31]. It is of paramount importance whenever translational symmetry is broken at the microscopic scale, and essential for predicting realistic experimental results, as for example the finite dc-conductivity of standard metals [32]. From the perspective of gravity, a disordered field theory is dual to a random metric solving stochastic Einstein's equations [22, 33]. Due to the non-linearity of the field equations, a brute force approach to this problem is doomed. Finding novel clever approaches to this problem thus constitutes a *essential* part of the applied holography program, and is at the core of this dissertation.

Disorder can be regarded, to first order, as a mechanism for breaking translational symmetry. As it was previously mentioned, translational invariant theories can lead to unphysical results, particularly when it comes to transport. The linear response coefficient of any operator coupling to the conserved momentum operator is infinite, translating the fact that all frames are equivalent. A concrete example is the infinite dc-conductivity of the homogeneous free electron gas. In this case, a small disordered potential can be introduced as a mechanism to relax momentum, leading to the expected finite result given by Drude's formula [34]. Disorder induces a crossover in the kinetic behaviour of the electrons from

ballistic to diffusive, the last being closely related to the dc-conductivity through Einstein's relations. But the phenomenology associated with disorder can be richer than only relaxing momentum. As it was first remarked by Phil Anderson in 1958, the interplay between *quantum coherence* and disorder yield the total suppression of quantum diffusion in $d = 1, 2$ dimensions [35], translating to an insulating behaviour of the disordered electron gas. In higher dimensions $d > 2$, a metal-insulator transition occurs as a function of disorder strength [35–39]. Anderson localization has been experimentally observed in optical [40–43] and acoustic systems [44] and in a Bose-Einstein condensates [45], but it was long believed that electron-electron interactions spoil localization [46–48], impeding an experimental observation in the solid state. It was only in 2006 that Basko, Aleiner and Altshuler have shown using diagrammatic techniques that the strongly-disordered Anderson localised phase is stable against weak interactions [49,50]. This novel state of quantum matter usually referred to as many-body localised, became an area of intense investigation, with many standing open questions regarding its properties (see [51, 52] for two recent reviews). Many-body localisation is yet another example of the rich phenomenology associated with disordered systems.

In a close analogy with the free electron gas, the dc-conductivity of the simples charged holographic theory - the Reissner-Nordström (RN) black hole - is divergent, a direct consequence of the translation invariance of the geometry. Motivated by the limitations of the RN solution as a realistic model for a charged strongly-coupled plasma, research in incorporating translational symmetry breaking and momentum relaxation in the Einstein-Maxwell theory has flourished [33, 53–65]. We can roughly separate the to-date literature on this front in two rough categories.

Effective field theories of momentum relaxation

The first category is composed of theories which judiciously capture the phenomenology of momentum relaxation but avoid dealing with Einstein's equations in the presence of spatially inhomogeneous sources. For this reason, we refer to these theories as *effective field theories of momentum relaxation*. In holographic field theories, the momentum operator is encoded in the tx-component of the boundary energy-momentum, dual to the geometry metric tensor. Since the metric couples to all fields in the theory through the volume form, translational symmetry can be broken by introducing a field, in the simplest case a scalar ϕ, that explicitly depends on the boundary spacelike coordinates. As we will discuss in detail in Section 2.3, the scalar field introduce a *source* s that couples to a scalar operator $\mathcal{O}$ of the dual field theory, through a term $\sim \int \mathrm{d}^d x \; s(t, \mathbf{x})\mathcal{O}(t, \mathbf{x})$ in the field theory action. The relationship between the source s, operator $\mathcal{O}$ and momentum p_x is given by a Ward identity, $\partial_t \langle p_x \rangle = \nabla_x s \; \langle \mathcal{O} \rangle$. Relaxation of momentum would be represented by a term $\partial_t \langle p_x \rangle = -\tau^{-1} \langle p_x \rangle + \dots$ in the equation above, with τ parametrising the typical relaxation

time. This term can be introduced by choosing a spatially-dependent source $s(x)$ (say in the x-direction) that couples to the momentum operator. However, note that a generic inhomogeneous source inevitably leads to solving non-linear partial differential equations for the geometry. The first works to consider relaxation introduced such term by hand [18, 22], avoiding to solve for the geometry. The major breakthrough was achieved only five years later, when it was realised that, since Einstein's equations couples to a massless source only through second derivative terms, engineering a source term $s(x) = \tau^{-1}x$ introduced a relaxation term in the boundary Ward identity without introducing explicit x dependent in the field equations [53, 54]. It turns out that implementing this idea on the gravity side of the duality is closely related to the *Stueckelberg mechanism* in massive gravity [53]. The major success of this model is that, since Einstein's equations are symmetric, the dual geometry can be found explicitly and the dc-conductivity can be computed analytically. Interestingly, the simplest flavour of this geometry provides a model for the crossover between a standard (or coherent) and a bad (or incoherent) metal. This celebrated result will be discussed in detail in Section 2.5.2.

Similar mechanisms for relaxing momentum while keeping the geometry spatially homogeneous have also been studied in holography. Two notable examples are the helical lattices [58, 66–69] and the Q-lattices [70–72]. These models rely on the symmetries of a class of known string theory solutions supported by complex one-forms that are also linear in the spacelike boundary coordinates. The addition of other fields allows for engineering other phases in the infra-red (IR). As a trade-off between complexity and flexibility, these models can reproduce not only the coherent/incoherent crossover of the simple Stueckelberg-based models but can also be tuned to have an insulating behaviour IR [67].

In Chapter 3 we discuss a new model that introduces a non-minimal coupling between the Stueckelberg fields and the Ricci scalar, similar to the Brans-Dicke theory in cosmology. The non-trivial coupling enriches the phenomenology of the previous Stueckelberg-based models, introducing an insulator-like behaviour when the relaxation parameter is large.

It is important to stress that, despite the working simplicity of the aforementioned holographic models, they fail to capture the rich phenomenology of strongly-disordered systems previously discussed. For instance, there is no sign of coherence effects at any value of the relaxation parameter. The investigation of models in which the geometry explicitly depends on the spacelike boundary coordinates is essential to go beyond relaxation.

Inhomogeneous holographic theories

In contrast with the effective models discussed above, the second category consists of theories dual to geometries that are an explicit function of the spacelike boundary coordinates. This can be achieved, for instance, by coupling the geometry to non-linear inhomogeneous source $s(x)$, and we here refer to the dual of these geometries as *inhomogeneous holographic*

theories.

Motivated by the ubiquitous role that lattices play in Condensed Matter systems - and in particular in the context of band theory - the first steps in this direction have studied the dual field theory in the presence of periodic sources $s(x) \propto \cos(kx)$, the so-called *holographic lattices* [73–77]. Early numerical results indicated that, as expected, the ac-conductivity in the presence of a holographic lattice followed Drude's formula for low frequencies. Furthermore, a cross-over to power-law scaling $\sigma(\omega) \sim \omega^\gamma$ with $\gamma = 2/3$ at intermediate frequencies was observed [75, 76]. This scaling behaviour is consistent with cuprates, a family of high-T_c superconducting materials largely believed to be described by a strongly-interacting field theory [78–81]. It was later shown that the holographic lattices introduced an effective mass in the gravity side, establishing a bridge with the aforementioned Stueckelberg-based models [64]. An important progress in this field was the introduction by Donos and Gauntlett of a simpler approach to computing the dc-conductivity which allowed to establish a generic formula in terms of the behaviour of the geometry at the horizon [82, 82–85]. The same authors later showed that the holographic conductivities are closely related to the diffusion of charge and heat in the black hole horizon [86].

The second major line in the investigation of inhomogeneous holographic theories is motivated by disorder. Early works on disorder in the context of holography have avoided directly dealing with disordered sources, and instead studied effective mechanisms such as the memory function method [63] and replica theories [22]. Disordered sources were first studied in the *probe limit*, neglecting the effect of disorder in the geometry, which is fixed [87–89]. Clearly, the probe limit avoids the kernel of the problem. However, these works bair merit for introducing a model of disorder which is particularly adapted to the context of gravity. The idea is to decompose the disordered source as a finite sum of oscillating terms with i.i.d. uniform random phases $s(x) = \sum_{n=1}^{N} A_n \cos(k_n x + \gamma_i)$, $\gamma_i \in [0, 2\pi)$. In the large N limit, this sum provides a discrete and smooth representation of a random Gaussian process. For this reason, it is particularly suited for holography and was adopted by most of the later works. A detailed discussion of general *spectral representations* for disorder is given in Chapter 2.3.3.

The dc-conductivity of a charged holographic field theory is closely related to the near-horizon region of the geometry. As will be discussed in 2.3.3, this region encodes the IR behaviour of the dual field theory. The probe limit where the geometry is fixed by hand is only justified when the disordered source is an *irrelevant* deformation of the boundary field theory. According to the renormalization group (RG), when disorder is a *relevant* deformation of the ultra-violet (UV) Lagrangian, it is expected to grow in the IR, driving the theory to a *disordered fixed point* [90]. In terms of the gravity dual, this is the regime where the back reaction cannot be neglected and corresponds to a genuine inhomogeneous solution of Einstein's equations. The first analytical attempt to study disorder in this regime was by Adam and Yaida, who investigated the marginal case in perturbation theory [91]. It was found that

disorder, in this case, is *marginally relevant*, yielding logarithm divergences in the free energy of the dual field theory. Drawing on this result and on the previously introduced spectral representation of disorder, Santos and Hartnoll proposed a resummation scheme for the logarithm divergence [33, 92]. Surprisingly, the resummed geometry acquires an emergent scale invariance in the IR, known in the holography literature as *Lifshitz scaling* [93]. The scalar source considered by Hartnoll and Santos can be chosen to be a marginal deformation by appropriately tuning the mass. The lack of a mass parameter was a hindrance to generalise this result to charged systems, where the chemical potential is always relevant. A first attempt was made by Peet and O'Keeffe who found higher order divergences that precluded a simple resummation [94]. In Chapter 4, we discuss a solution for this problem involving a judicious choice for the distribution of disorder. We carry the resummation for the disordered Einstein-Maxwell system and find that the geometry interpolates between AdS in the ultra-violet and a Lifshitz fixed point in the infra-red. We establish a close relationship between the disorder correlation and the emergent scale invariance, suggesting that the IR Lifshitz scaling is closely related to the marginally relevant disorder. At $T = 0$, the dc-conductivity of the disordered plasma increases, reflecting the presence of the weakly-disordered chemical potential. In contrast, at $T > 0$ the dc-conductivity is not affected to lowest order in disorder.

Other works on disordered sources in holographic field theories include brane models [95] and effective hydrodynamical theories [96]. It is worth mentioning a recent front of research focusing in bounds for the transport coefficients of disordered holographic theories [97–99]. The general expressions for the holographic conductivities obtained by Donos and Gauntlett allow to establish bounds for a class of disordered theories exempt from the full geometry.

It is important to emphasise that research in disordered holographic theories is a fairly recent topic. Introducing disorder in boundary source fields has been the driving set-up for studying this problem. Ideally, one would hope to observe signs of coherence effects in the strong-disorder limit. But going beyond perturbation theory is challenging both analytically and numerically, severely limiting the study of relevant strongly-disordered geometries. Although it is early to be assertive, the perturbative results so far contain no footprint of coherence effects, and the bounds in transport seem to preclude a metal-insulator transition for a wide class of systems. In Chapter 5 we propose a new setting to study disordered systems in holography in which coherence effects between a disordered geometry and a probe source can be implemented, opening a new direction of research in this field.

A disordered many-body toy-model for holography

Most of the research effort highlighted in this introduction focus on pushing the boundaries of the holographic toolbox. In the last chapter we switch gears and discuss a solvable quantum many-body model introduced by Kitaev in 2015 [100] for an explicit realisation of the holographic duality in one dimension. Curiously, disorder makes yet another appearance as

a key ingredient in this model named after Sachdev, Ye and Kitaev (SYK).

Interest in the SYK model is manifold. It is by far the simplest example of holographic theory, being dual to Jackiw-Teitelboim gravity [101]. It thus offers unique insight into the mechanisms of the duality. From the perspective of gravity, the SYK model can be studied as a toy-model for the microscopic degrees hidden behind black hole horizons, and there is hope it can shed light into quantum properties of black holes [101–104]. Finally, the SYK model has drawn the attention of condensed matter physicists as a rare example of an interacting quantum many-body theory which is solvable at strong coupling. An ever-growing number of works have employed generalised SYK models to investigate strongly-correlated metals [105], chaotic/non-chaotic transitions [106–108], Mott insulators [109] and many-body localised phases [110,111]. Even experimental realisations of the SYK model have been proposed in cold atoms systems [112] and in condensed matter [113,114].

Due to the lack of locality, the SYK model is better understood as an effective model for the infra-red behaviour of some higher dimensional quantum field theory. From the renormalization group perspective, a central question is understanding to which extent the appealing holographic properties survive the presence of relevant deformations of the theory. Chapter 6 addresses this question in detail. We carry an analytical and numerical investigation of the natural one-body relevant deformation of the theory. Our results suggest that while the thermodynamical properties of the deformed theory are dominated by the relevant one-body term, there is a finite region of parameters where the model retains some of its holographic features, such as the exponential growth of the OTO four-point function. Our perturbative results suggest that outside this region there is a chaotic-integrable transition, in line with the cross-over of spectral correlations from Wigner-Dyson to Poisson statistics observed in [115].

Overview

The first chapter of this dissertation is dedicated to setting the concepts and conventions that will be used in what follows and contains no original work by the author. We start by introducing the toolbox of applied holography. The holographic dictionary and how it can be used to compute thermodynamic and transport properties are explained. Next, we work two celebrated examples that illustrate the philosophy and *modus operandi* of applied holography. The first example is the ac-conductivity of a strongly-coupled charged plasma in $d = 3$ dimensions, dual to the Reissner-Nordström black hole. As expected for a translational invariant geometry, the zero frequency limit of the conductivity is divergent. This naturally leads us to introduce the Stueckelberg fields as a mechanism for relaxing momentum. It is shown that the resulting dc-conductivity is finite and consistent with Drude's formula.

Chapters 3 to 6 are the bulk of the dissertation, and contain my original contribution to

the field. Chapter 3 investigates a model where gravity is coupled to a scalar field, similarly to Brans-Dicke gravity in anti-de Sitter. The motivation for studying this model is that, when the field is chosen to depend linearly on the spatial coordinates, this model presents insulator-like features. More precisely, for strong relaxation and low temperatures, the electric conductivity is a decreasing function of temperature. We also study the thermodynamics and the shear viscosity to entropy ratio, which is always lower than the celebrated Kovtun-Son-Starinets (KSS) bound.

In Chapter 4 we study Einstein's equations in the presence of a charged disordered field. The probability distribution of disorder is chosen to be a centred normal, with the standard deviation parametrising the amplitude of the field. The equations can be solved explicitly in the perturbative regime of weak disorder when the charged field represent a random deformation of the fixed homogeneous geometry. The holographic dual is a strongly-interacting plasma in the presence of a random chemical potential. We explore the consequences of this deformation both at zero and finite temperature and study the dc-conductivity of the random geometry.

Chapter 5 pursues the investigation of explicitly random geometries from a complementary perspective. Instead of sourcing disorder as a random deformation of a translational invariant geometry, we study a family of three-dimensional inhomogeneous geometries which solve Einstein's equations. This family is indexed by an arbitrary function which we take to be either oscillating or random. By studying the dynamics of a probe scalar field in this disordered geometry, we are able to observe, for the first time, signs of coherence effects. This result opens new directions in the investigation of disorder in the AdS/CFT correspondence.

In chapter 6 we change sides in the duality and discuss the celebrated Sachdev-Ye-Kitaev (SYK), model. The SYK model is a rare example of a disordered interacting many-body model that is analytically tractable in the strongly-coupled regime. It has been the object of intense research recently since Kitaev showed that it shares many properties with the near-horizon geometry of extremal AdS black holes [102]. These *holographic properties* suggest the SYK model is an explicit realisation of the AdS/CFT correspondence. In this chapter, we investigate the robustness of the holographic properties against the most natural one-body deformation of the model.

2 | A brief guide to holography

The *holographic* or *AdS/CFT duality* is a correspondence between strongly-coupled quantum field theories in d dimensions and asymptotically AdS_{d+1} solutions of classical general relativity. Its history is rooted in years of research in string theory, and most notably in the period known as *second superstring revolution* [1], when non-perturbative properties of string theory started being uncovered. Although string theory is necessary for a deep understanding of the mechanism underlying the duality, it can be motivated and formulated without reference to strings. This philosophy, commonly referred as *bottom-up approach*, is the perspective adopted throughout this dissertation. Therefore, for the interest of conciseness, we will avoid references to string theory outside the preamble, focusing on the *modus operandi* of the holographic duality instead. The curious reader can find more information on the stringy history of the duality in the seminal papers on the subject [3, 5, 116], or in the excellent recent reviews [117–121].

2.1 Preamble

It was long known that gauge theories and general relativity coexisted in different sectors of string theory. Gauge theories emerge naturally as low-energy excitations in the spectra of open strings. The celebrated work of t' Hooft matching the large N expansion of interaction diagrams in $SU(N)$ Yang-Mills theory with the topological expansion of string diagrams is probably the first concrete example of the gauge theory/string connection [122]. On the other hand, general relativity corresponds to the low-energy limit of type IIB, a theory of closed strings. The prolific research on the landscape of gravitational solutions in string theory was motivated by the attempt to describe the degrees of freedom responsible for the thermodynamic properties of black holes, the so-called *information paradox* [118, 123, 124]. Although the low-energy sectors of closed and open strings are limits of the same theory, in principle there is no reason for them to overlap. The bridge was only established in 1995, with a celebrated work by Polchinski, who showed that D-branes - extended objects that naturally appear in the open string low-energy sector - are actually non-perturbative solutions of string theory, valid at all energies. In particular, they are also present in type IIB, and surprisingly play an important role supporting the black hole solutions on this side

of the theory.

This result motivated Juan Maldacena, about twenty years ago, to match the symmetries of two well-known solutions on each side of the two low-energy sectors. The equivalence between the symmetries of $\mathcal{N} = 4$ super Yang-Mills (SYM) with the isometries of $\mathrm{AdS}_5 \times S^5$ allied to Polchinski's result led Maldacena to conjecture that they were two faces of the same Dp-brane configuration, and should, therefore, be equivalent [116]. This construction became known as *AdS/CFT correspondence* or *holographic duality*[2].

Maldacena's conjecture holds in a conjunction of two limits:

a) First, the large-N limit. In the field theory side, N is the number of colours in the gauge group, and for large-N the path integral can be expanded around the classical saddle-point solution of the theory. Therefore it corresponds to a *semi-classical* or *mean field expansion*. From the perspective of closed strings, this is the limit in which type IIB reduces to classical supergravity (SUGRA).

b) Second, the strong-coupling limit. From the perspective of the field theory, this limit corresponds to taking the interaction term in the Lagrangian to be dominant. Together with large-N, it is known as the t' Hooft limit, since it corresponds to the original limit used by t' Hooft in [122]. From the perspective of closed strings, this limit corresponds to an asymptotic AdS region of the Dp-brane solution of SUGRA.

$\mathcal{N} = 4$ super Yang-Mills is one of the many $U(N)$ gauge theories that can be engineered from Dp-brane configurations in string theory. Maldacena's conjecture led to a research effort in the directions of extending the duality to other gauge theories. In the years that followed, other dualities between large-N strongly coupled gauge theories and asymptotically AdS solutions of SUGRA have been established [119].

Later, it was shown that the role played by supersymmetry could be attenuated [126], and it was conjectured that the AdS/CFT correspondence should hold beyond the low-energy string sectors [4,119]. In 1998, Gubser, Klebanov, Polyakov [4] and Witten [3] gave a generic prescription to compute the generating function of the dual gauge theory in terms of the on-shell action of the SUGRA solution. The *GKPW prescription*, also broadly referred as the *holographic dictionary* was an important step towards an operational formulation of the duality independently from string theory. The systematic mapping between the QFT generating functional and the dual SUGRA action became a shortcut to the lengthy and technical process of identifying the appropriate QFT dual to a given SUGRA brane configuration. Furthermore, by following the GKPW prescription for any geometry satisfying asymptotic AdS boundary conditions, one can compute properties of a potential dual field theory -

[2]The holographic principle was proposed in 1995 by 't Hooft and Susskind, and postulate that a state corresponding to a region in a quantum gravity theory can be characterised entirely by the information in the boundary of the region [125]. The AdS/CFT correspondence, being a duality between a theory in four dimensions ($\mathcal{N} = 4$ SYM) and a gravity theory in five dimensions (AdS_5), realises the holographic principle.

which is, however, not guaranteed to exist. This *bottom-up approach*[3] became the motor of an intense research program consisting of studying the field theory properties of known asymptotically AdS backgrounds. However, it is important to mention that most of the celebrated bottom-up theories have a rigorous embedding in string theory, even if sometimes the embedding was found after these geometries had been proven useful for the purpose of holography, as in the case of the holographic superconductor [29, 127]. Throughout this dissertation, we will often use the term *holographic field theory* as a short for a QFT defined via the holographic dictionary.

In the next section, we introduce the AdS geometry and discuss the coordinate charts used throughout this dissertation. The holographic dictionary is discussed next, and we illustrate the *modus operandi* of the bottom-up approach to holography with two examples that are closely related to the discussion in the following chapters.

2.2 The geometry of anti-de Sitter spacetime

Anti-de Sitter spacetime is a vacuum solution of the Einstein's field equations with negative cosmological constant $\Lambda < 0$:

$$R_{ab} - \frac{1}{2}(R + 2\Lambda)g_{ab} = 0 \tag{2.1}$$

In $d+1$ dimensions, we will usually parametrise $\Lambda = -\frac{d(d-1)}{l_{\text{AdS}}^2}$. AdS_{d+1} can be seen as a hyperboloid embedded in $\mathbb{R}^{2,d}$ given by the equation:

$$X_0^2 + X_{d+1}^2 - \sum_{i=1}^{d} X_i^2 = l_{\text{AdS}}^2, \tag{2.2}$$

where $l_{\text{AdS}} > 0$ is a positive length scale called *AdS radius*. From now on we set $l_{\text{AdS}}^2 = 1$ unless stated otherwise. The induced metric has signature $(2, d)$:

$$\mathrm{d}s^2 = -\mathrm{d}X_0^2 - \mathrm{d}X_{d+1}^2 + \sum_{i=1}^{d} \mathrm{d}X_i^2$$

Figure 2.1 shows a plot of AdS_2 as embedded in $\mathbb{R}^{1,2}$. Note that by construction the

[3] As opposed to the *top-down approach* which consists of carefully establishing dualities from sensible low-energy limits of string configurations.

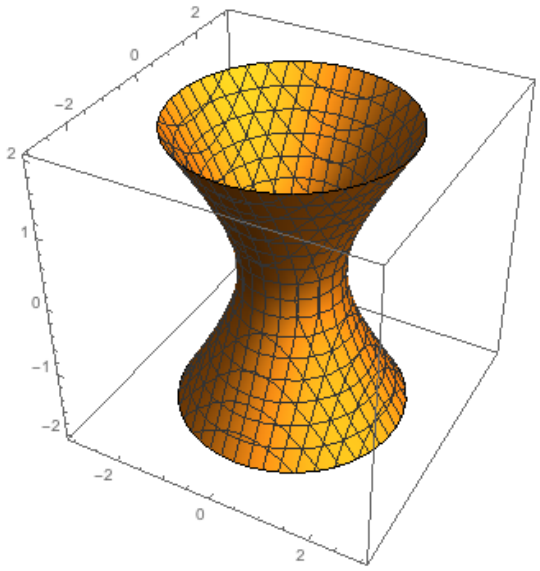

Figure 2.1: Hyperboloid $x^2 + y^2 - z^2 = 1$

isometry group of this spacetime is $SO(2, d)$. We can solve 2.1 by choosing *global Coordinates*:

$$\begin{aligned} X_0 &= \cosh(\rho)\cos\tau \\ X_{d+1} &= \cosh(\rho)\sin\tau \\ X_i &= r_i \sinh(\rho)\sin\tau \end{aligned}$$

where the constraint is now $\sum_{i=1}^{d}(r_i)^2 = 1$ and we have $\tau \in [0, 2\pi)$, $r \in (0, \infty)$ and $\rho \in \mathbb{R}$. The induced metric in these coordinates become:

$$\mathrm{d}s^2 = -\cosh^2(\rho)\ \mathrm{d}\tau^2 + \mathrm{d}\rho^2 + \sinh^2(\rho)\ \mathrm{d}\Omega_{d-1}^2,$$

where $\mathrm{d}\Omega^2$ is the metric element of the S^{d-1} sphere. Often one works with the universal covering of AdS_{d+1} by allowing $\tau \in \mathbb{R}$ to avoid unphysical periodic timelike directions.

2.2.1 A note on coordinate charts

Different coordinate charts are useful in holography applications, and it is fairly common to see different coordinates systems being used throughout the literature. As a reflection of that, we will employ three different coordinate charts throughout this dissertation. These charts only differ in the definition of the AdS radial component, thus not changing the physics of the boundary dual field theory. To avoid confusion, when employing each of these coordinate systems, we will consistently use the same notation as defined in this section.

Poincaré chart I

The first useful coordinate chart we will define is the *Poincaré chart* $x^a = (u, t, \mathbf{x})$. It is defined by making the following change of coordinates with respect to embedding coordinates Eq.(2.1),

$$\begin{aligned} X_0 &= \tfrac{1}{2u}\left[1 + u^2\left(1 + \sum_{i=1}^{d-1}(x_i)^2 - t^2\right)\right], & X_{d+1} &= ut, \\ X_d &= \tfrac{1}{2u}\left[1 - u^2\left(1 + \sum_{i=1}^{d-1}(x_i)^2 - t^2\right)\right], & X_i &= ux_i, \quad \text{for } i \in \{1, \ldots, d-1\}, \end{aligned}$$

with $\mathbf{x} \in \mathbb{R}^{d-1}$, $t \in \mathbb{R}$ and $u \in [0, \infty)$. These coordinates make explicit the invariance under scaling transformations $(u, t, \mathbf{x}) \to (\lambda^{-1}u, \lambda t, \lambda \mathbf{x})$. Note that, in contrast with the global coordinates, these coordinates only cover part of AdS_{d+1}. The induced metric in Poincaré Coordinates is given by

$$\mathrm{d}s^2 = u^{-2}\mathrm{d}u^2 + u^2\left(-\mathrm{d}t^2 + \mathrm{d}\mathbf{x}^2\right). \tag{2.3}$$

From where is clear that each constant u slice is conformally equivalent to $\mathbb{M}^d$. Note that t is a nontrivial function of (τ, ρ, r_i) and so global time τ is different from Poincaré time t. In holography applications, the Poincaré time is always used, since it is the physical timelike coordinate in the boundary spacetime. These coordinates will be used in Chapter 3.

Poincaré chart II

A closely related flavour of Poincaré chart is given by taking $r = u^{-1}$. The metric is given in the chart $x^a = (r, t, \mathbf{x})$ by

$$\mathrm{d}s^2 = r^{-2}\left(\mathrm{d}r^2 - \mathrm{d}t^2 + \mathrm{d}\mathbf{x}^2\right). \tag{2.4}$$

This chart has the convenience that all coordinates have the same dimensions, and under a conformal transformation they scale uniformly $(r, t, \mathbf{x}) \to \lambda(r, t, \mathbf{x})$. These coordinates will be used in Chapter 4.

Fefferham-Graham coordinates

The Fefferham-Graham coordinate chart $x^a = (\rho, t, \mathbf{x})$ is defined by taking $\rho = r^2$ in the Poincaré chart II. The metric reads,

$$\mathrm{d}s^2 = \frac{\mathrm{d}\rho^2}{4\rho^2} + \frac{1}{\rho}\left(-\mathrm{d}t^2 + \mathrm{d}\mathbf{x}^2\right). \tag{2.5}$$

These coordinates are going to be used in Chapter 5. The name is an allusion to the geometers Fefferham and Graham, who used this coordinates in their work to prove an important general theorem about asymptotically AdS geometries [128],

Theorem 1 *Any solution of the $d+1$ dimensional Einstein Equations 2.1 with negative cosmological constant can be written locally in the chart $x^a = (\rho, x^\mu)$ as*

$$ds^2 = \frac{d\rho^2}{4\rho^2} + \frac{1}{\rho} g_{\mu\nu}(\rho, x^\mu) dx^\mu dx^\nu \tag{2.6}$$

for $\mu, \nu \in \{0, 1, \ldots, d\}$. Moreover, the following near-boundary expansion holds,

$$g_{\mu\nu}(\rho, x) \underset{\rho=0}{\sim} g^{(0)}_{\mu\nu}(x^\mu) + \rho\, g^{(2)}_{\mu\nu}(x^\mu) + \cdots + \rho^{d/2}\, g^{(d)}_{\mu\nu}(x^\mu) + \rho^{d/2} h^{(d)}(x^\mu) \log\rho + \ldots \tag{2.7}$$

where only even coefficients $g^{(d)}, h^{(d)}$ are present in the expansion.

2.3 The dictionary

2.3.1 Matching symmetries and dimensions

As was previously discussed in the Preamble, the first instance of the holographic duality was the equivalence between the strongly-coupled phase of $\mathcal{N} = 4$ Super Yang-Mills (SYM) in four-dimensional Minkowski Spacetime $\mathbb{M}^4$ and classical supergravity in $\text{AdS}_5 \times S^5$. The motivation for this relationship was the observation that these theories have the same symmetries. On one side, fields of $\mathcal{N} = 4$ SYM transform under the representations of $PSU(2,2|4)$. For example, bosons transform under $SO(4,2) \times SO(6)$, which is exactly the isometry group of $\text{AdS}_5 \times S^5$. A similar argument applies to the fermionic sector [4]. This example carries over for any dimension and conformal theory since it is a general fact that the isometries of AdS_{d+1} are exactly given by the d-dimensional conformal group.

Matching symmetries provides the right track to find the map between observables on both sides of the correspondence since any sensible map must preserve the symmetries of gauge invariant objects. Take for example a composite scalar operator $\mathcal{O}_\Delta$ of conformal dimension Δ (given, for example, by the trace [5] over some fields in $\mathcal{N} = 4$). This operator transforms under a representation of $SO(6)$ with Dynkin label $[\Delta, 0, 0]$. The possible dual fields in the gravity side should be those transforming under the same representation of $SO(6)$.

Since the discovery of the equivalence between $\mathcal{N} = 4$ and the $\text{AdS}_5 \times S^5$ geometry, other dualities have been established by looking at other embeddings of supersymmetric

[4] See for example references in [116].
[5] The trace ensures gauge invariance.

gauge theories in string theory. On general grounds, the dualities give the equivalence between conformal field theories in $\mathbb{M}^d$ and $\text{AdS}_{d+1} \times X$ geometries, where X is a compact Einstein manifold of dimension $10 - d + 1$ which we will omit from now on. The matching of symmetries was the object of intense study in the early days of AdS/CFT (see for example [129]), and led to a dictionary between operators in d dimensional CFTs and gravitational fields in the $d + 1$ dimensional AdS space, which we summarise in table 2.1.

Type of gravity field	Relation between mass and conformal dimension
massive scalars and spin 2 fields	$m^2 l^2_{\text{AdS}} = \Delta(\Delta - d)$
massless spin 2 field (graviton)	$m^2 l^2_{\text{AdS}} = 0$, $\Delta = d$
p-forms	$m^2 l^2_{\text{AdS}} = (\Delta - p)(\Delta - d + p)$
spin 1/2 or 3/2	$\lvert m \rvert L = \Delta - \frac{d}{2}$

Table 2.1: Holographic dictionary.

2.3.2 The GKPW prescription

The above formulation of the AdS/CFT correspondence is of little practical use. It establishes a relationship between gravitational fields and gauge invariant operators, but gives no information on how to compute observables such as correlation functions. A practical prescription was given independently in 1998 by Gubser, Klebanov, Polyakov, and Witten [3, 4]. Accounting for the mismatch of dimensions, Witten has proposed that the d-dimensional conformal field theory lives on the boundary of the dual AdS_{d+1} geometry, which is exactly given by $\partial \text{AdS}_{d+1} = \mathbb{M}^d$. Witten's proposal is enough to establish a mathematical relationship between the observables in both sides of the duality. As we discuss now, this relationship is given by matching the generating functional in both sides of the duality.

Let S_{CFT} be the action for a d-dimensional conformal field theory living in $\mathbb{M}^d$, and consider a global chart $x^\mu = (t, \mathbf{x})$ with $\mathbf{x} \in \mathbb{R}^{d-1}$, $\mu = 0, \ldots, d$[6]. Usually the observables of interest in a CFT are the correlation functions, which give information about the statistics of excitations in the theory. Consider a generic conformal operator $\mathcal{O}^I_\Delta(x)$ with mass dimension Δ in the CFT and with some generic index I, which can be either a spin, colour or spacetime index. Suppose we are interested in calculating the n-point correlation function of this operator. Following a general prescription in quantum field theory [130], we introduce an auxiliary source field $s_I(x)$ and add the following term to the CFT action,

$$S_{\text{CFT}} \to S_{\text{CFT}} - i \int \mathrm{d}^d x \; s_I(x) \mathcal{O}^I_\Delta(x). \tag{2.8}$$

The correlation functions can then be computed by taking functional derivatives with respect

[6] To lighten notation, we often omit the spacetime hypersrcipt μ. In this case, spacelike coordinates $\mathbf{x}$ are always in bold, to contrast with the spacetime coordinates x.

to the generating functional and setting the source field to zero,

$$\langle \mathcal{O}_\Delta^{I_1}(x_1)\dots\mathcal{O}_\Delta^{I_n}(x_n)\rangle = (-i)^n \left.\frac{\delta^n W[s(x)]}{\delta s_{I_1}(x_1)\dots\delta s_{I_n}(x_n)}\right|_{s=0}. \tag{2.9}$$

where W is the generating functional CFT. Based on the symmetry arguments discussed in Section 2.3, adding the source $s_I(x)$ on CFT side is equivalent to adding a field in the gravity side. The exact nature of this field will depend on the nature of the index I, with the most common pairs given in Table 2.1. For example, if $\mathcal{O}_\Delta$ is a scalar operator with mass dimension Δ, $s(x)$ should also be taken to be a scalar, with mass dimension $d-\Delta$, and the field to be added in the gravity side is a scalar field with mass $m^2 = \Delta(\Delta - d)$. Another common example is when $\mathcal{O}_\Delta^I = E_i$ is an electric field in the i-th direction. In this case, $s^I = J^i$ is an electric current also in the i-th direction, and the dual gravity field should be a massless vector potential.

For the sake of illustration, let's focus on the simplest case of a scalar operator $\mathcal{O}_\Delta$. According to Witten's proposal, the CFT should live in the boundary of AdS_{d+1}. Fixing Fefferham-Graham coordinates $x^a = (\rho, x^\mu)$,

$$\mathrm{d}s^2 = \frac{\mathrm{d}\rho^2}{4\rho^2} + \frac{1}{\rho}(-\mathrm{d}t^2 + \mathrm{d}\mathbf{x}^2). \tag{2.10}$$

Note that indeed the boundary $\rho = 0$ is conformally equivalent to $\mathbb{M}^d$ with the previously fixed chart $x^\mu = (t, \mathbf{x})$. As we previously argued, the addition of the term $\sim \int s(x)\mathcal{O}(x)$ in the CFT action should correspond to the addition of a minimally coupled scalar field with mass $m^2 = \Delta(\Delta - d)$ in the AdS_{d+1} geometry,

$$S_{\text{SUGRA}} \to S_{\text{SUGRA}} - \frac{i}{2}\int \mathrm{d}\rho\mathrm{d}^d x \left(\mathrm{d}\psi \wedge \star\mathrm{d}\psi + m^2\psi^2\right). \tag{2.11}$$

Note that we denoted S_{SUGRA} the supergravity action supporting the $\text{AdS}_{d+1}\times X$ solution dual to our CFT. Technically, this action is composed by a consistent reduction of type IIB string theory and depends on the specific duality in question. For the purpose of the bottom-up approach we follow throughout this dissertation, the exact form of S_{SUGRA} will not be relevant, and we refer the curious reader to [118, 119]. Note that we can relate the addition of this scalar field term to the addition of a term in the boundary of AdS_{d+1} by integrating by parts and using Stoke's theorem,

$$\int \mathrm{d}\rho\mathrm{d}^d x \left(\mathrm{d}\psi \wedge \star\mathrm{d}\psi + m^2\psi^2\right) = -\int \mathrm{d}\rho\mathrm{d}^d x\, \psi\left(\mathrm{d}\star\mathrm{d}\psi - m^2\psi\right) + \int_{\rho=0}\mathrm{d}^d x\, \psi\star\mathrm{d}\psi. \tag{2.12}$$

When varied, the first term gives the scalar field equations of motion,

$$\left(\Delta_g - m^2\right)\psi = 0, \tag{2.13}$$

where $\Delta_g = \mathrm{d}\star\mathrm{d}$ is the Laplace-Beltrami operator, written in a chart x^a as $\Delta_g = \frac{1}{\sqrt{-g}}\partial_a\left(\sqrt{-g}g^{ab}\partial_b\right)$. According to Witten's proposal, the boundary term corresponds to the addition of a term in the CFT action. Precisely this term should be compared to Eq.(2.8). In order to evaluate it, we need to solve Eq.2.13.

It is possible to find a full solution of Eq.(2.13) for the metric (2.10) by exploiting homogeneity and working in Fourier space. This technical computation is given in Appendix A.1, and is also discussed in the specific case of $d = 2$ in Chapter 5. However, for evaluating the boundary term we only need the *near-boundary* expansion of ψ. We take this opportunity to present a more general result valid for a scalar field in *any* asymptotically AdS_{d+1} geometry. It states that solutions of Eq.(2.13) written in Fefferham-Graham coordinates Eq.(2.6) admit the following near-boundary expansion,

$$\psi(\rho, x) \underset{\rho=0}{\sim} \rho^{\frac{d-\Delta}{2}}\left(\psi_{(0)}(x) + \rho\psi_{(2)} + \cdots + \rho^{\frac{2\Delta+d}{2}}\left(\psi_{(2\Delta+d)} + \phi_{(2\Delta+d)}\log\rho\right)\right). \tag{2.14}$$

where *all* coefficients $\psi_2, \psi_{(4)}, \ldots, \phi_{(2\Delta+d)}$ can be fixed as functions of $\psi_{(0)}$ by evaluating Eq.(2.13) close to the boundary, with the exception of $\psi_{(2\Delta+d)}$, which requires solving the equation outside the near-boundary region [131].

In the coordinates of Eq.(2.10), the on-shell action reads,

$$S_{\text{on-shell}} = -\frac{i}{2}\int_{\rho=0}\mathrm{d}^d x\,\sqrt{-\gamma}\,\psi n^a\partial_a\psi \tag{2.15}$$

where $n = -2\rho\partial_\rho|_{\rho=0}$ is the normal unit vector pointing in the outward normal direction along the boundary, and γ is the induced metric at the boundary $\rho = 0$. Note that naively inserting the expansion Eq.(2.14) in Eq.(2.15) lead to a diverging on-shell action at the boundary for any $m^2 > -d^2/4$. We therefore introduce a cutoff at $\rho = \lambda \ll 1$ and evaluate Eq.(2.15) at this hypersurface instead,

$$\begin{aligned} S_{\text{on-shell}} &= -\frac{i}{2}\int_{\rho=\lambda}\mathrm{d}^d x\,\sqrt{-\gamma}\,\psi n^a\partial_a\psi \\ &= i\int\mathrm{d}^d x\left(\lambda^{\frac{d-2\Delta}{2}}(d-\Delta)\psi_{(0)}(x)^2 + \cdots + d\,\psi_{(0)}(x)\psi_{(2\Delta+d)}(x)\right). \end{aligned} \tag{2.16}$$

Note that we have singled out only the most diverging term $\propto \psi_{(0)}^2$, and omitted the others in the ellipsis. Comparing with Eq.(2.8), this expansion suggests that, up to these diverging terms, we should identify the source with the normalisable mode $s \propto \psi_{(0)}$ and the

expectation value of the dual scalar operator with the non-normalisable mode $\langle \mathcal{O} \rangle \propto \psi_{(2\Delta+d)}$[7]. Recalling that all other coefficients $\psi_2, \psi_{(4)}, \ldots, \phi_{(2\Delta+d)}$ can be expressed as functions of $\psi_{(0)}$, with this identification, the diverging terms are all proportional to the square of the source. These correspond to *contact terms* in the field theory correlation function, and should be systematically removed by adding counter-terms. In holography, the counter-terms correspond to boundary terms in the action Eq.(2.11), and the systematic procedure of removing the divergences is known as *holographic renormalization* [131, 132]. We discuss an explicit example of this procedure in Appendix A.2.

Our discussion can be summarised in the following identification between the generating functional in the CFT and the on-shell, renormalised SUGRA action,

$$W[s(x)] = \left\langle \exp\left(\int \mathrm{d}^d x \; s(x) \mathcal{O}(x) \right) \right\rangle_{\text{CFT}} = S_{\text{SUGRA}}[\psi]|_{\lim\limits_{\rho \to 0} \rho^{\frac{\Delta - d}{2}} \psi(\rho, x) = s(x)} \,. \tag{2.17}$$

This relation, also known as *GKPW prescription*, can be easily generalised for other fields. For example, a current $J^\mu(x)$ of conformal dimension Δ will be sourced by a vector potential A_μ through a coupling $\sim i \int d^d x \; A_\mu^{(0)}(x) J^\mu(x)$. In this case we solve for the Einstein-Maxwell system in AdS_{d+1} with boundary condition $A_\mu^{(0)} = \lim\limits_{r \to 0} A_\mu$. Since A_μ is a massless 1-form, table 2.1 indicates it must have conformal dimension 1.

2.3.3 An interpretation of the extra dimension

Consider a generic quantum field theory in $\mathbb{M}^d$ with action $S(g)$, where g is one of the theory's coupling constants. Under the flow of the renormalization group (RG) the coupling runs according to

$$u \frac{\partial g(u)}{\partial u} = \beta(g(u)),$$

where u parametrises the local RG energy scale, and $\beta(u)$ is the theory's beta function. At the critical point, $\beta(g(u)) = 0$ and the theory become scale invariant, i.e. invariant under scaling transformations of the coordinates $x^\mu \to \lambda x^\mu$. In principle, the RG energy scale u is unrelated to the field theory spacetime coordinates $x^\mu = (t, \mathbf{x})$. However, one can attempt to "geometrise" u by promoting it to a coordinate in a $d+1$-dimensional field theory that effectively accounts for the flow of the RG as part of the spacetime dynamics. The set of new coordinates $(u, t, \mathbf{x})$ transforms now under $(t, \mathbf{x}, u) \to (\lambda^{-1} u, \lambda t, \lambda \mathbf{x})$ since u has energy dimensions. The right metric that encodes this invariance is naturally given by the AdS_{d+1}

[7] Note that in the mass window where both $\psi_{(0)}$ and $\psi_{(2\Delta+d)}$ are normalisable, the role of source and operator can be interchanged, leading to equivalent quantisation schemes (see Appendix A.1). The exact prefactors depend on the boundary counter-terms required to remove the contact terms and on the quantisation.

metric in Poincaré I coordinates,

$$\mathrm{d}s^2 = \frac{l_{\mathrm{AdS}}^2}{u^2}\mathrm{d}u^2 + \frac{u^2}{l_{\mathrm{AdS}}^2}\eta_{\mu\nu}\mathrm{d}x^\mu \mathrm{d}x^\nu.$$

This observation is just a re-statement of the previous claim about the isometries of AdS_{d+1} being exactly the conformal group in d-dimensions[8]. This construction suggests a RG interpretation of the holographic coordinate $r = \frac{l_{\mathrm{AdS}}^2}{u}$. The hypersurfaces $r =$ constant, which are isomorphic to $\mathbb{M}^d$, correspond to field theories at different energy scales. Dynamics in this direction is given by the flow of the RG group, and the boundary theory corresponds to the critical point of the flow, where the geometry is conformal.

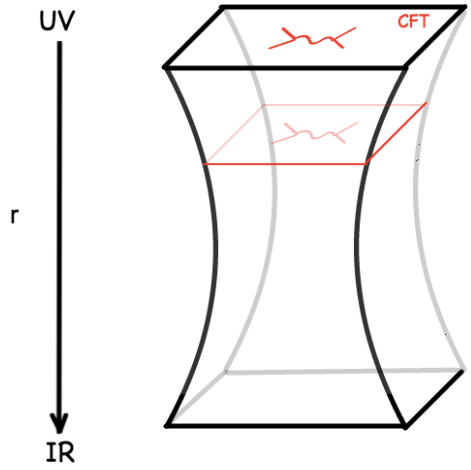

Figure 2.2: Holography as geometrization of the RG flow. Field theories of different lengthscales live in different r slices.

2.3.4 Generalization to thermal States

So far we only considered the duality for CFTs at zero temperature. Temperature can be introduced in CFTs by the standard procedure of compactifying the Euclidean time direction in the Matsubara formalism for equilibrium field theory. This procedure is similar to the Gibbons-Hawking prescription in the context of black holes [133], which consists in avoiding conic singularities of the spacetime metric by imposing periodicity on the Euclidean time coordinate. Due to their thermodynamic properties, black holes are thus the natural candidates for the gravity duals of finite temperature CFTs. Further evidence is given by the observation that the radius of the compactified time circle increases with the radial direction

[8] The constant l is a length scale required for the metric to have the right dimension, and is known as the *AdS radius*.

and asymptotes to $\frac{\hbar}{k_B T_H}$, where T_H is the Hawking temperature associated with a black hole. But, in these coordinates (Poincaré I) , radial infinity is exactly where our CFT lives, and therefore the radius of the compactified Euclidean quantum field theory must coincide with the asymptotic radius of the Euclidean black hole.

The conclusion is that thermal states in holographic field theories are encoded by a black hole in the bulk of spacetime. This is also consistent with our RG picture for holography: since the correspondence takes place in the boundary of the $d+1$ spacetime (which corresponds to the ultra-violet (UV) of the field theory) any asymptotically AdS spacetime that solves the appropriate equations of motion complies with the conjecture. This encodes how different infra-red (IR) geometries that are not necessarily pure AdS but rather *asymptotically AdS* can influence the ultra-violet (UV) physics living in the boundary.

2.4 Holographic toolbox

In the previous sections we have introduced the AdS/CFT correspondence between strongly-coupled CFTs in Minkowski spacetime and the AdS_{d+1} geometry. We have discussed how the idea that the CFT lives in the boundary AdS_{d+1} can be combined with symmetry arguments to provide a well-defined relationship between the generating functional of the CFT and the renormalised on-shell action of the gravitational field. We have crucially remarked that the GKPW prescription only relates the CFT to the near-boundary behaviour of AdS_{d+1}, suggesting that the duality should hold for generic *asymptotically AdS* geometries. This important observation is in line with a renormalization group picture of the duality, where the near-boundary region correspond to the UV energy scales. As an example, we briefly motivated how to heat the CFT up by introducing an asymptotically AdS black hole in the bulk of the spacetime. An explicit calculation involving thermal field theories will be discussed in Section 2.5.1. But before, we discuss in detail the subtleties using the relation in Eq.(2.17) to compute two particular observables of interest: the two-point functions and transport coefficients.

2.4.1 Two-point function

The GKPW prescription gives a well-defined recipe to compute the partition function of holographic field theories. At finite temperature, the thermodynamical properties can be obtained by calculating the corresponding thermodynamical potentials and their derivatives. An observable of interest that characterises the statistics of the theory is the two-point function. For weakly-interacting field theories, the two-point function gives information about the single-particle spectrum of the theory. Even though a quasi-particle picture is not well-adapted to strongly-coupled theories - and holography in particular - the two-point

function still provides rich information. As we will see in Section 2.4.2, it is related to the transport coefficients through Kubo's formula.

Formally, Eqs.(2.17) and (2.9) provide all ingredients one needs to compute the two-point correlation function. It suggests that for computing the two-point functions all we need is to solve for the gravity dynamics, insert the near-boundary behaviour of the solution in the renormalised on-shell action and take two functional derivatives with respect to the source. But, in principle, how can one differentiate an Euclidean two-point function from a real-time retarded or advanced two-point function? This was an important question in the early days of the duality, and was addressed in the works of Son, Starinets [134] and Herzog [135]. When the covariant momentum $k^2 = -\omega^2 + \mathbf{k}^2$ in the Fourier decomposition of the field ψ is negative $k^2 < 0$, there are two solutions corresponding to an incoming and an outgoing wave at the Poincaré horizon. It is precisely this ambiguity that account for the different correlators. It can be shown, by explicit comparison in both sides of this simple case, that the advanced/retarded two-point functions correspond to the choice outgoing/incoming wave boundary condition at the horizon [135]. Note that in Euclidean signature we always have $k^2 > 0$, and therefore there is only one choice of propagator: the Euclidean propagator. We now illustrate this construction in the Euclidean scalar field case.

Following the calculation in Section 2.3.2, the renormalised on-shell action reads

$$S^{\text{ren}}_{\text{on-shell}} \propto \int \mathrm{d}^d x \; \psi_{(0)}(x)\psi_{(2\Delta+d)}(x) \propto \int \frac{\mathrm{d}^d k}{(2\pi)^d} \; \psi_{(0)}(-k)\frac{\psi_{(2\Delta+d)}(k)}{\psi_{(0)}(k)}\psi_{(0)}(k). \tag{2.18}$$

where in the last equality we have simply written in Fourier space and multiplied and divided by $\psi_{(0)}$. As previously discussed, the exact prefactor depend on renormalisation, see Appendix A.2 for an example or [131] for the general case. From the general solution discussed in Appendix A.1, we can show that the ratio is independent of $\psi_{(0)}$. Therefore the two-point function in Fourier space is simply given by

$$\langle \mathcal{O}(k)\mathcal{O}(-k)\rangle = \frac{\delta^2 S^{\text{ren}}_{\text{on-shell}}}{\delta\psi_{(0)}(k)\delta\psi_{(0)}(-k)} = \frac{\psi_{(2\Delta+d)}(k)}{\psi_{(0)}(k)} \propto k^{2\nu} \tag{2.19}$$

where $\nu = \sqrt{\frac{d^2}{4} + m^2}$. In real Euclidean coordinates this corresponds to $\langle \mathcal{O}(x)\mathcal{O}(0)\rangle \propto |x|^{-2\Delta}$ which is precisely the expected result for an Euclidean two-point function of a conformal operator with mass dimension Δ. The advanced/retarded two-point functions can be obtained following exactly the same procedure, with the only difference that the ratio in Eq.(2.19) will be given by the coefficients corresponding to the outgoing/incoming wave boundary condition at the Poincaré horizon.

The procedure outlined above is general for other types of operators in Table 2.1 and for other asymptotically AdS geometries. In particular, the finite temperature two-point

functions are obtained from black hole geometries. Below we give a step-by-step summary of the discussion for a general field ϕ (not necessarily a scalar) and asymptotically AdS geometry.

1. Following Table 2.1, determine the gravity field ϕ which is dual to the operator of interest.

2. Introduce the corresponding field in the gravity action. Solve the equations of motion for the gravity field imposing the following boundary condition

$$s(x) = \lim_{\rho\to 0} \rho^{\frac{d-\Delta}{2}} \phi(\rho, x) \tag{2.20}$$

   together with regularity (if in Euclidean signature) or outgoing/incoming wave boundary condition (if in real time) at the horizon (or Poincaré horizon, if at zero temperature). The function $s(x)$ represents a source in the boundary field theory, which should be kept arbitrary. Note that we have written this relation in Fefferham-Graham coordinates, and it can be easily adapted to the other coordinates in Section 2.2.1.

3. Insert the solution in the on-shell action and renormalise if needed. Schematically, the final action in Fourier space will take the form $S^{\text{ren}}_{\text{on-shell}} = K \int \frac{\mathrm{d}^d k}{(2\pi)^d} s(-k)\mathcal{F}(\rho, k)s(k)\Big|^{\rho_h}_{\rho=0}$, where $\rho_h = \infty$ in the case of pure AdS (zero temperature) or the horizon position for a black hole geometry (finite temperature).

4. The two-point correlation function of interest is given by $G(k) = -2\,\mathcal{F}(\rho, k)|_{\rho=0}$.

Note that, in contrast with the usual quantum field theory procedure of computing the two-point function, the recipe above makes no allusion to the basis the operators are written, and therefore can be calculated independently of a quasiparticle description. An alternative procedure is to relate the two-point function in the boundary to the gravity two-point function in the bulk. This alternative is illustrated in Appendix A.3 for the massive scalar field case, and will be used throughout Chapter 5.

2.4.2 Transport coefficients

Consider a generic QFT with action S_0, and let $s_I(x)$ be a source coupling to an operator of the theory $\mathcal{O}_I(x)$ (again, I is a generic index that can denote spin, colour, spacetime coordinates, etc.),

$$S = S_0 + i \int \mathrm{d}^d x\; s_I(x)\mathcal{O}^I(x). \tag{2.21}$$

What is the effect of this new term in the expectation value $\langle\mathcal{O}\rangle_0$ to first order in s? The answer is given by *Kubo's formula*, which states that the change $\delta\langle\mathcal{O}^I\rangle = \langle\mathcal{O}^I\rangle - \langle\mathcal{O}^I\rangle_0$ is

given by

$$\delta\langle\mathcal{O}^I(x)\rangle = \int \mathrm{d}^d y\, \chi^{IJ}(x,y)s_J(y) + O\left(s^2\right), \tag{2.22}$$

where the function χ is generically refereed as a *transport coefficient*, and is given by

$$\chi^{IJ}(x,y) = i\theta(t-t')\langle[\mathcal{O}^I(x),\mathcal{O}^J(y)]\rangle = G_R^{IJ}(x,y), \tag{2.23}$$

Note that, quite surprisingly, the response of the system is completely determined by the retarded Green's function G_R of the operators coupling to the perturbation. This result is non-trivial since G_R is a measure of the statistics of the theory, and is completely independent of the source profile $s(x)$. The transport coefficients are usually referred by specific names depending on the operators $\mathcal{O}$. For instance, when the operator is an electric current J^i in the spacelike direction $x^i \in \mathbb{R}^{d-1}$, the corresponding transport coefficient is the electric conductivity σ_{ij}. Some of the most common pairs are given in Table 2.2. In the chapters that

Transport Coefficient	Source	Associated operator
Susceptibility χ	scalar fluctuation $\delta\psi$	Scalar operator $\mathcal{O}$
Conductivity σ	vector fluctuation δA_μ	Current J^μ
Shear Viscosity η	metric fluctuation δh_{ij}	T^{ij}

Table 2.2: Transport coefficients and the respective sources

follow we will be mostly interested in the conductivity σ_{ij}. As mentioned before, the indices i,j are spacelike indices. When $i=j$, we refer to $\sigma_i = \sigma_{ii}$ as the *longitudinal conductivity* in direction i, and when σ_{ij} for $i \neq j$ as the *transversal conductivity*. In particular, we will be interested in the longitudinal *ac-conductivity* (in the direction x, for example), which is the response of the system to an electric field constant in space but oscillating in time. Since the field is homogeneous, it is convenient to work in a Fourier basis, where Eq.(2.22) simplifies to

$$\delta\langle J^x(\omega)\rangle = \sigma_x(\omega)E_x(\omega) \tag{2.24}$$

and therefore the ac-conductivity can be obtained by simply dividing the observed fluctuation in the current by the sourced field. From the ac-conductivity, we can compute the *dc-conductivity*, defined as the zero-frequency limit $\sigma_{\mathrm{dc}} = \lim_{\omega\to 0}\sigma_x(\omega)$. In the next section we study how Kubo's formula can be used to measure the longitudinal ac-conductivity of the simplest charged holographic field theory.

2.5 Case studies

In the previous sections, we have introduced the holographic dictionary and explained how transport coefficients of holographic field theories can be computed by following a systematic prescription. In this section, we illustrate this methodology in two important examples that are cornerstones of discussion that will follow in the next chapters. The first is the computation of the ac-conductivity of the Reissner-Nordström black hole - a background dual to a charged strongly-interacting plasma. The upshot of the calculation is that the zero-frequency limit or dc-conductivity is divergent due to the translational symmetry of the geometry. The second example introduces the Stueckelberg mechanism discussed in the introduction to break translational symmetry and induce momentum relaxation. The resulting dc-conductivity is shown to be finite and consistent with Drude's formula.

2.5.1 Conductivity of the Reissner-Nordström black hole

We now compute the electric conductivity of the simplest strongly-coupled holographic QFT with a charge density ρ and a constant chemical potential μ at finite temperature T. Following the bottom-up philosophy, the first step consists in finding a geometry that supports these properties. Charge is introduced by minimally coupling the metric to a Maxwell term

$$S = \int \mathrm{d}^{d+1}x\sqrt{-g}\left(R - 2\Lambda - \frac{1}{4e^2}F^2\right), \tag{2.25}$$

where e is the Maxwell coupling constant. The equations derived from the action in Eq.(2.25) are known as the *Einstein-Maxwell system*. For simplicity, we focus on $d = 3$. Since we want a theory at finite temperature, according to the discussion in Section 2.3.4 we should look for black hole solutions. The simplest black hole solution for the Einstein-Maxwell system is the Reissner-Nordstrom (RN) geometry, given in $d + 1 = 4$ dimensions by

$$\begin{aligned} \mathrm{d}s^2 &= r^{-2}\left[-f(r)\mathrm{d}t^2 + \frac{\mathrm{d}r^2}{f(r)} + \mathrm{d}x^2 + \mathrm{d}y^2\right], \\ f(r) &= 1 - \left(1+Q^2\right)\left(\frac{r}{r_0}\right)^3 + Q^2\left(\frac{r}{r_0}\right)^4, \\ A &= \mu\left(1 - \frac{r}{r_0}\right)\mathrm{d}t, \end{aligned} \tag{2.26}$$

where r_0 is the location of the black hole horizon and $Q = \frac{\mu^2 r_0^2}{4}$ is defined for notational convenience. Note that we have set the AdS radius $l^2_{\text{AdS}} = 1$ and the Maxwell coupling $e = 1$ for simplicity. The free parameters of the model are (r_0, μ).

Thermodynamically, the RN black hole is similar to a charged plasma at finite temperature.

Its temperature is obtained by following the Hawking-Gibbons prescription, giving $T = \frac{f'(r)}{4\pi} = \frac{1}{4\pi r_0}(3 - Q^2)$. The entropy density of the black hole is proportional to the horizon area $s = \int_{r=r_0} \mathrm{d}^2x\sqrt{-\gamma} = 4\pi r_0^2$. Finally, the charge density is given by the timelike component of the current, $\rho = \langle J^t \rangle = F^{tr} = \mu r_0^{-1}$, and the energy density by the tt-component of the energy momentum tensor $\epsilon = \langle T^{tt} \rangle = 2(1+Q^2)$. The free energy is given by computing the on-shell action, i.e. inserting Eq.(2.26) back into the action Eq.(2.25). One can show that the free energy density computed in this way satisfy the usual thermodynamic relation for a charged system $f = \epsilon - Ts - \mu\rho$. Varying the free energy with respect to (ρ, T), it can be shown that the first law of thermodynamics holds

$$\mathrm{d}f = -s\,\mathrm{d}T - \rho\mathrm{d}\mu \tag{2.27}$$

In Section 2.3.3 we heuristically argued that the r-slices can be thought as an energy scale for the dual field theory. While the boundary $r = 0$ corresponds to the UV, the horizon parametrise the IR scale of the dual theory. By construction, the boundary condition at $r = 0$ fix the UV geometry to be AdS_4. However note that the near-horizon geometry is not fixed. To find it for the RN solution, we change coordinates to $\rho = r - r_0$ and do a Taylor series expansion of Eq.(2.26). Inserting $f(\rho) = 4\pi T\rho + O(\rho^2)$ in the expression for $\mathrm{d}s^2$, it is easy to see that the near-horizon geometry is conformally equivalent to AdS_4, with a renormalised AdS radius proportional to the temperature T. Note that this argument is not specific to the RN, but apply identically to any simple black hole solution with metric $\mathrm{d}s^2 \propto \left(-f\mathrm{d}t + f^{-1}\mathrm{d}r + \mathrm{d}\mathbf{x}^2\right)$ and $T > 0$. However note that for $Q = \sqrt{3}$, we have $T = 0$ even though $r_0 < \infty$. This is not possible for the Schwarzschild solution corresponding to $\mu = 0$, since in this case $T = T(r_0)$ and the only way to tune $T = 0$ is to have no horizon, $r_0 \to \infty$. Black holes which have $T \propto f'(r_0) = 0$ with finite horizon radius are known as *extremal*. At extremality, we let $r = r_0 + \lambda\rho + O(\lambda^2)$ for $\lambda \ll 1$ and expand $f(\rho) = f''(0)\lambda^2\rho^2 + O(\lambda^3)$, and the near horizon geometry is given by

$$\mathrm{d}s^2 \sim -\left(\frac{\rho}{r_0}\right)^2 \mathrm{d}\tau^2 + \left(\frac{\rho}{r_0}\right)^{-2} \mathrm{d}\rho^2 + r_0^{-2}\left(\mathrm{d}x^2 + \mathrm{d}y^2\right), \tag{2.28}$$

where we have rescaled $\tau = \lambda t$. This metric corresponds to a $AdS_2 \times S^2$ geometry. The field theory dual to the extremal RN geometry has a non-trivial RG flow given by $AdS_4 \to AdS_2 \times S^2$. According to the holographic dictionary, this result indicates that the quantum critical IR fixed point of the strongly-coupled charged plasma is governed by an effective conformal field theory in $d = 1$. The infra-red physics correspond to the long-time, large-scale behaviour of the system. Indeed, as it was shown in [82, 136], the dc-conductivities (zero-frequency, long-times) is completely determined from the knowledge of the near-horizon region. A distinctive property of this fixed point is that the entropy density s is

positive at $T = 0$. This unusual property is typical of frustrated systems, although there is no sign of frustration in the gravity side. As it is evident from the calculation, a large class of extremal black holes share this same $AdS_2 \times S^2$ fixed point. There is a consensus in the literature that the ubiquitous $AdS_2 \times S^2$ geometry carries deep meaning in terms of the universal IR behaviour of strongly-coupled theories [137, 138]. However, a clear understanding of this statement remains an open question. Early research in the nature of the AdS_2 fixed point was motivated by the black hole information paradox [139–146]. The debate was revived recently with the proposal by Kitaev of a one-dimensional many-body model that share the key distinctive properties with the AdS_2 fixed point. These holographic properties suggest that the model, known as the Sachdev-Ye-Kitaev model, is an effective microscopic description of extremal black hole horizons. In Section 6 we introduce the SYK model and discuss the stability of the holographic properties.

According to the discussion in Section 2.4.2, to compute the longitudinal ac-conductivity of the dual theory we need to introduce a time-dependent electric field. In the gauge invariant formulation, this is achieved by sourcing a time-dependent fluctuation in the vector potential $A \to A + \delta A_x(t)\mathrm{d}x$. In principle, Einstein's equations can couple this fluctuation to all metric components, which would oblige us to consider further fluctuations $\delta g_{\mu\nu}$ for consistency. However, it can be shown that δA_x only couples to δg_{tx}, and we can consistently set all other metric fluctuations to zero [147]. The equations of motion for these perturbations are given by the linearised Einstein's equations and the Maxwell equations. We can combine both non-trivial equations to eliminate δg_{tx}, giving one-second order ODE for δA_x:

$$(f(r)\delta A_x')' + \frac{\omega^2}{f(r)}\delta A_x - 4Q^2\frac{r^2}{r_0^2}\delta A_x = 0 \tag{2.29}$$

According to the holographic dictionary (Table 2.1), near the boundary $r = 0$ we have $\delta A_x = \delta A_{x(0)} + rA_{x(1)} + \ldots$, where $\langle j^x \rangle = A_{x(1)}$, and the electric field at the boundary is given by $E_i = \lim_{r\to 0} i\omega\delta A_x = i\omega\delta A_{x(0)}$. Combining the prescription from section 2.4.1 and Eq.(2.24),

$$\sigma_x(\omega) = \frac{1}{i\omega}\frac{\delta A_{x(1)}}{\delta A_{x(0)}}. \tag{2.30}$$

We are left with a completely technical task: solve Eq.(2.29), apply incoming boundary conditions at $r = r_0$ and insert the near-horizon expansion of the solution in Eq.(2.30). Unfortunately, this equation cannot be solved analytically, and we recur to numerical integration. Figure 2.3 show the behaviour of the real and imaginary part of the conductivity σ_x as a function of the frequency for different choices of chemical potential μ. Note however that at the neighbourhood of $\omega = 0$ these numerical results should be taken with a pinch of salt. Indeed, it can be shown that the imaginary part of the ac-conductivity diverges as $\mathrm{Im}\sigma_x \underset{\omega\to 0}{\sim} \omega^{-1}$. According to the *Kramers-Kronig relations*, this implies that $\mathrm{Re}(\sigma_x) =$

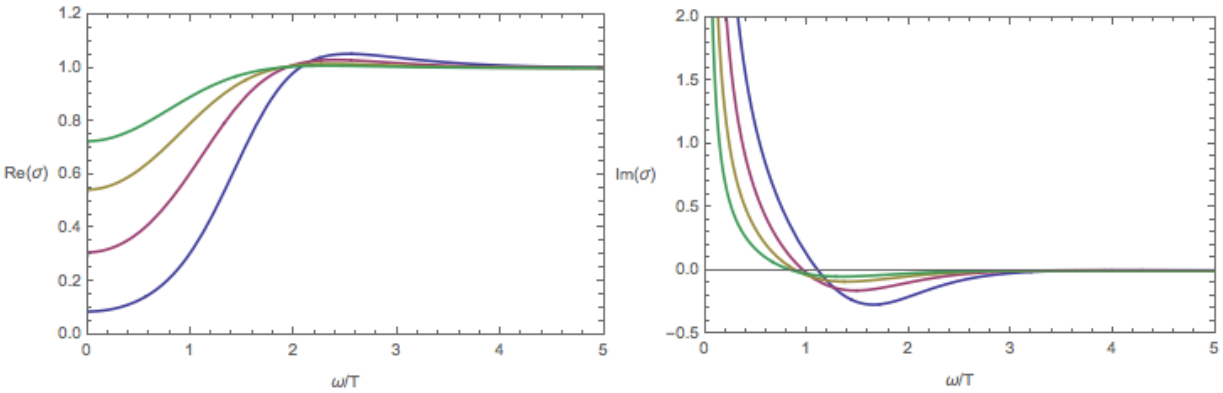

Figure 2.3: Electrical conductivity for the Reissner-Nörsdtrom geometry for different chemical potentials μ.

$\mathrm{P}\int_{\mathbb{R}} \frac{d\omega'}{\pi} \frac{\mathrm{Im}(\sigma_x)}{\omega-\omega'} \underset{\omega\to 0}{\sim} K\delta(\omega)$. The delta function is, of course, not captured by the numerics. It can be shown that the precise behaviour of the dc-conductivity in the neighbourhood of $\omega = 0$ is given by

$$\sigma(\omega) \underset{\omega\to 0}{=} \sigma_Q + K\left(\delta(\omega) - \frac{1}{i\omega}\right) + O\left(\omega^2\right), \tag{2.31}$$

where the *regular part* of the dc-conductivity σ_Q and the *Drude weight* K are completely determined by the near-horizon data [148]. Note that the Drude weight K can be computed by taking the limit $\lim_{\omega\to 0} \frac{1}{\omega}\mathrm{Im}(\sigma(\omega))$. In Chapter 3 we will discuss the analytic calculation of the regular part σ_Q for a more general charged model. One way to think about the delta function divergence of σ at low-frequencies is as a Drude peak with infinite scattering time. As it was discussed in the introduction, this behaviour is typical of translational invariant systems. It is easy to see that the metric Eq.(2.26) is invariant under translations along the spacelike boundary coordinates $(x, y) \to (x + x_0, y + y_0)$. Note that momentum is also conserved at every r-slice, since $\partial_0 T^{0i} = 0$. The RN black hole thus behaves as a typical translational invariant charged QFT.

2.5.2 A simple model for momentum relaxation

We now introduce the Stueckelberg mechanism for the specific example of the Einstein-Maxwell system in $d + 1 = 4$ dimensions. The key idea is to introduce a family of $d - 1$ massless scalar fields which depend only linearly on the spacelike boundary coordinates. To be precise, we fix a coordinate chart $x^a = (r, t, x, y)$, and define the *Stueckelberg fields* $\phi_a = \alpha\delta_{aj}x^j = \alpha(0, 0, x, y)$, $i \in \{x, y\}$. The action is given by minimally coupling the scalars

to gravity,

$$S = \int \mathrm{d}^4x\sqrt{-g}\left(R + 6 - \frac{1}{4}F^2 - \frac{1}{2}(\partial_x\phi_x)^2 - \frac{1}{2}(\partial_y\phi_y)^2\right). \tag{2.32}$$

Since the wave equation for the scalars is second order in the derivatives, the linear profile trivially satisfy the equations of motion. However, the energy momentum tensor associated with the scalars has constant non-zero components given by $T^{\phi}_{ii} = -\frac{1}{2}(\alpha_i)^2$ for $i \in \{x, y\}$. Since the equations of motion do not depend explicitly on (x, y), the Einstein-Maxwell system can be solved, as before, by imposing radial symmetry, and is given by

$$\begin{aligned}
\mathrm{d}s^2 &= r^{-2}\left[-f(r)\mathrm{d}t^2 + \frac{\mathrm{d}r^2}{f(r)} + \mathrm{d}x^2 + \mathrm{d}y^2\right], \\
f(r) &= 1 - \frac{\alpha^2 r^2}{2} - \left(1 + Q^2 - \frac{\alpha^2 r_0^2}{2}\right)\left(\frac{r}{r_0}\right)^3 + Q^2\left(\frac{r}{r_0}\right)^4 \\
A &= \mu\left(1 - \frac{r}{r_0}\right)\mathrm{d}t, \qquad \phi_x = \alpha x, \quad \phi_y = \alpha y.
\end{aligned} \tag{2.33}$$

As with the RN geometry, r_0 is the black hole horizon and we defined $Q^2 = \frac{\mu^2 r_0^2}{4}$ for convenience. The free parameters of the model are (r_0, μ, α). To have an intuition for this new parameter, it is useful to look at the thermodynamics of the model. For instance, the temperature and the energy density now depend on α, $T = \frac{1}{4\pi r_0}\left(3 - Q^2 - \frac{1}{2}\alpha^2\right)$, $\epsilon = \langle T^{tt}\rangle = 2\left(1 + Q^2 - \frac{1}{2}\alpha^2\right)$, while the entropy and charge density remain the same $s = 4\pi r_0^{-2}$ and $\rho = \mu r_0^{-1}$. Again, the free energy of the system satisfy $f = \epsilon - sT - \rho\mu$. However it can be shown that the first law of thermodynamics picks a contribution from the new parameter α [54]:

$$\mathrm{d}f = -s\ \mathrm{d}T - \rho\mathrm{d}\mu - r_0^{-1}\mathrm{d}(\alpha^2). \tag{2.34}$$

This shows that the Stueckelberg fields affect the dual field theory similarly to applying a constant magnetic field of strength α. Note that, as with the RN geometry, it is possible to tune (μ, α) to get $T = 0$ with $r_0 < \infty$, and the IR fixed point at extremality is also given by $\mathrm{AdS}_2 \times S^2$.

The longitudinal ac-conductivity in the x-direction can be computed analogously to the RN background. Since the Stueckelberg field ϕ_x couples to the vector potential A through the geometry, for consistency we also have to consider a fluctuation in this direction. We are thus led to consider the following set of time-dependent fluctuations,

$$A \to A + a_x(r,t)\mathrm{d}x, \qquad \mathrm{d}s^2 \to \mathrm{d}s^2 + 2g_{tx}(r,t)\mathrm{d}x\mathrm{d}t, \qquad \phi_x \to \phi_x + \chi(r,t). \tag{2.35}$$

One could proceed by writing the equations of motion for the fluctuations in Fourier space

and solving them numerically, as exemplified in Section 2.5.1. However, we now illustrate an alternative approach introduced by Gauntlett and Donos to analytically compute the dc-conductivity directly [82]. It consists of making the following ansatz for the fluctuations

$$a_x(r,t) = a_x(r) - Et, \qquad g_{tx}(r,t) = g_{tx}(r), \qquad \chi(r,t) = \chi(r). \tag{2.36}$$

Note that by construction the ansatz for the vector potential fluctuation corresponds to a constant electric field E at the boundary. Denoting $' = \partial_r$, Maxwell's equations imply that the electric current in the x direction is radially conserved,

$$J^x = f(r)a_x' - \rho\, g_{tx} = \text{constant} \tag{2.37}$$

By definition, the dc-conductivity in this context is given by $J^x = \sigma_{\text{dc}} E$, and thus all we need is to show that Eq.(2.37) is proportional to the electric field E at the boundary. Since this quantity is radially conserved, the strategy is to evaluate it in the horizon where the the boundary conditions can be applied to fix the terms. For instance, the term $f(r)a_x'$ can be fixed straightaway. Following the holographic dictionary, close to the horizon $r = r_0$, we must impose ingoing boundary conditions for a_x. In Eddington-Finkelstein coordinates $(u, v) = (t + r_*, t - r_*)$, $\mathrm{d}r_* = f^{-1}\mathrm{d}r$, this means that $a_x(r,t) \propto v$, which imply that close to the boundary we must impose $a_x' \underset{r=r_0}{\sim} f^{-1}E$. For the second term, we evaluate the (xt) components of Einstein's equation close to the horizon, giving $g_{tx} \underset{r=r_0}{\sim} -\frac{r_0\mu}{\alpha^2}E$. The dc-conductivity is thus given by

$$\sigma_{\text{dc}} = 1 + \frac{\mu^2}{\alpha^2} = 1 + \frac{4\pi\rho^2}{s\,\alpha^2}. \tag{2.38}$$

Different from the RN geometry example, the dc-conductivity now reflects the break of translation invariance and is finite. As expected, it is proportional to the charge density and inversely proportional to the parameter α, which measures the amplitude of the Stueckelberg field. In the limit $\alpha \to 0$, the dc-conductivity diverges as expected for a translational invariant system. The parameter α can be thought as an inverse "relaxation time". Consider for instance the Ward identities of the dual boundary theory in the x-direction

$$\partial_t \delta\langle p_x\rangle = -\alpha\delta\langle\mathcal{O}\rangle + \rho\partial_t a_x^{(0)}, \tag{2.39}$$

where $a_x^{(0)}$ is the vector potential fluctuation evaluated at the boundary, and $\delta\langle p_x\rangle$, $\delta\langle\mathcal{O}\rangle$ are the boundary operators dual to the fluctuations (g_{tx}, χ). The second term has a clear interpretation: it is the flux of momentum generate by the applied external field. By solving the equations of motion for χ, it can be shown that for small $\alpha/\mu \ll 1$, $\langle\mathcal{O}\rangle \propto p_x$, suggesting that α^{-1} can be interpreted as a relaxation rate. However for $\alpha/\mu \gg 1$, $\langle\mathcal{O}\rangle$ has higher order

contributions which are not simply proportional to the flux of momentum [56, 149, 150]. This is known in the literature as the *incoherent regime*, in which the underlying strongly-coupled degrees of freedom do not respond well to the external field. The dc-conductivity in the incoherent phase asymptotically approaches a constant for any fixed charge density and driving electric field. For this reason, this geometry is thought to model the crossover between a standard strongly-coupled metal and a *bad metal* [151].

Note however that the well-defined limit of strong relaxation $\alpha/\mu \to \infty$ is still metallic, which is both odd and unphysical. In Chapter 3, we discuss a solution to the lack of insulating behaviour at strong relaxation by introducing a simple model in which the Stueckelberg fields are coupled to the Ricci scalar in the action.

3 | Momentum relaxation in Brans-Dicke holography[†]

In this chapter we study holographic models where a scalar is coupled to the Ricci scalar R. Similar models have been studied in the cosmology literature, where they are known as AdS Brans-Dicke (BD) models. In terms of the holographic duality, they can be interpreted as effective models of metals with a varying coupling constant. We show that, for translational invariant backgrounds, the regular part of the dc-conductivity σ_Q deviates from the universal result of Einstein-Maxwell-Dilaton (EMD) models. However, the shear viscosity to entropy ratio saturates the Kovtun-Son-Starinets (KSS) bound. Similar results apply to more general $f(R)$ gravity models. In four bulk dimensions we study momentum relaxation induced by Stueckelberg fields coupled to the gravity and electromagnetic sectors. For sufficiently strong momentum dissipation induced by the former, a recently proposed bound on the dc-conductivity σ is violated for any finite electromagnetic axion coupling. Interestingly, in more than four bulk dimensions, the dc-conductivity for strong momentum relaxation decreases with temperature in the low-temperature limit. In line with other gravity backgrounds with momentum relaxation, the shear viscosity to entropy ratio is always lower than the KSS bound. The numerical computation of the ac-conductivity reveals a linear growth with the frequency in the limit of low temperature, low frequency and large momentum relaxation. We also show that the module and argument of the ac-conductivity for intermediate frequencies are not consistent with cuprates experimental results, even assuming several channels of momentum relaxation.

3.1 Introduction

Einstein general relativity assumes that gravity is mediated by a tensor two particle. Despite its immense conceptual and phenomenological success, generalizations [153] of general relativity, where gravity is also mediated by a scalar or a vector, have been intensively

[2]This Chapter is based on Ref. [152], and was done in collaboration with Antonio M. García-García and Aurelio Romero Bermúdez. The author would like to acknowledge A.R. Bermúdez for the numerical work in Section 3.2.

studied mostly for its potential interest in cosmology but also simply as toy models of new ideas in gravity. One of the most influential, though not the earliest [153], is the so called Brans-Dicke gravity [154] that aimed to reconcile Mach's principle with general relativity. Gravity is also mediated by a scalar coupled linearly to the Ricci tensor. The action also has a kinetic term for the scalar so BD has two coupling constants. Physically this scalar can be understood as a gravitation constant G that varies in time and space. General relativity is usually preferred as it predicts the same physics with less free parameters. Interestingly, after a conformal transformation, BD gravity maps into Einstein gravity with a dilaton field. As a result of this mapping, explicit analytical solutions of the BD gravity equations of motion are known not only for Einstein gravity but also for asymptotically dS and AdS spaces even if the theory also contains massless photons modelled by the Maxwell tensor. For a certain region of parameters it is also possible [155] to map onto BD more general $f(R)$ models where the action is not linear in the Ricci tensor R.

In light of this rich phenomenology, we study BD backgrounds with AdS asymptotic as effective duals of strongly coupled metals. Previous holographic studies [156, 157] involving BD backgrounds were restricted to thermodynamic properties only. By contrast here we focus on transport observables such as the optical, dc-conductivity and shear viscosity in asymptotically AdS Brans-Dicke backgrounds. Our motivation is to explore the impact of the BD scalar running in the radial dimension, that acts as an effective gravitational constant, on the transport properties of holographic metals [158, 159].

More specifically we address whether the universality of the shear viscosity [6] and the dc-conductivity [57, 160–162], reported in translational invariant Einstein-Maxwell-Dilaton (EMD) [158, 159] backgrounds with massless photons and no dilaton coupling to the Maxwell tensor also holds in BD background. We have found that, while the universal shear viscosity ratio also holds in BD background, the dc-conductivity deviates from the universal result of EMD theories.

We also investigate momentum relaxation by gravitational Stueckelberg fields, namely, Stueckelberg fields coupled to the Ricci tensor, a simplified form of BD backgrounds where the scalar has no dynamics. Stueckelberg fields [54] together with massive gravitons, or simply a random chemical potential [33, 61, 88–90, 94, 95], break translational invariance which modifies substantially the conductivity and other transport properties. For weak momentum relaxation the conductivity is to a good extent described by Drude physics. For low temperatures or frequencies the conductivity is large, the so called Drude peak, and decreases monotonously. It was observed, in all models studied, that no matter the strength of the momentum relaxation the conductivity of Einstein-Maxwell holographic metals was always above a certain bound which precludes a metal-insulator transition. In part based on this numerical evidence, it was conjectured [97] the existence of a lower bound in the conductivity of more complicated holographic models. However, in two

recent papers [163, 164] violations of this bound have been reported in models where the Stueckelberg field is coupled to the Maxwell tensor, effectively screening charge. Here we show that gravitational Stueckelberg fields, that do not screen charge, also lead to violations of the bound in the limit of strong, although still parametrically small with respect to the rank of the gauge group, Stueckelberg field gravity coupling. For three space dimensions the dc-conductivity decreases with T for low temperatures even without any other source of momentum relaxation.

We also study the ac-conductivity in BD backgrounds. The ac-conductivity in EMD models with translational invariance in the limit of small frequencies and temperatures is controlled by the infrared (IR) geometry that for Reissner-Nordstrom background is AdS_2 leading to $\sigma \underset{\omega\to 0}{\sim} \omega^2$. The effect of momentum relaxation in the ac-conductivity of EMD theories was investigated in [159] but it is not yet fully understood whether, for low-frequencies and strong momentum relaxation, the conductivity scales as a power-law faster than linear as in Mott insulators and many-body localised states [165].

By contrast, in a model in which momentum relaxation occurs by an oscillatory chemical potential, it was claimed [166] the modulus of the ac-conductivity for intermediate frequencies decays as a power-law with an exponent equal to that observed in most cuprates. Here we find that, even assuming several channels of momentum dissipation, we cannot reproduce the modules and argument observed in cuprates. However, we have found that, for strong momentum dissipation and close to zero temperature, the ac-conductivity increases linearly, not quadratically with the frequency, for both gravitational and electromagnetic Stueckelberg fields. Finally, we have computed the ratio of the shear viscosity and the entropy density in BD holography with momentum relaxation. We have observed that, unlike the translational invariant case, the ratio is temperature dependent. It decreases as the strength of momentum relaxation increases and it is always below the KSS bound. It can be made arbitrarily small for a finite amount of momentum relaxation.

The organization of the chapter is as follows: in section two we compute analytically the dc-conductivity and show that the shear viscosity to entropy ratio in translational invariant BD backgrounds and other generalised theories of gravity is given by the KSS bound. In section three we study the dc-conductivity in BD like backgrounds with momentum relaxation induced by coupling the Stueckelberg field and the Ricci tensor in two boundary space dimensions. In section four we address momentum relaxation by gravitational Stueckelberg fields in higher space dimensions. In section five we study the ac-conductivity in BD backgrounds. We also compute the module and argument of the complex conductivity in order to compare with results in cuprates. In section six we compute the shear viscosity to entropy density ratio including different sources of momentum relaxation. We end up with a list of interesting problems for further research and a short summary of the main results.

Next we introduce the BD action, the equations of motion and its analytical solution.

3.2 Dc-conductivity in translationally invariant BD holography

We start our analysis by introducing the BD action and the equations of motion. We then compute the conductivity for a general background ansatz and show it is expressed in terms of thermodynamic quantities and the value of the scalar at the horizon. This is different from EMD models with no coupling between the dilaton and the Maxwell field where it only depends on thermodynamic quantities.

We then find that a calculation in the Einstein frame, resulting from a conformal transformation, leads to the same result. Finally, we discuss other modified gravity models that fall within the BD universality class.

3.2.1 Brans-Dicke Action and equations of motion

The Brans-Dicke-Maxwell action in a $d+1$-dimensional manifold is given by

$$S = \int_{\mathcal{M}} \mathrm{d}^{d+1}x\sqrt{-g}\left[\phi R - \frac{\xi}{\phi}(\nabla\phi)^2 - V(\phi) - \frac{Y}{4}F^2\right]. \tag{3.1}$$

Note that we are working in units where $2\kappa^2 = 16\pi G_N = 1$ and we include a non-trivial coupling $Y(\phi)$ between the Brans-Dicke scalar ϕ and the Maxwell term, as well as a (for now arbitrary) scalar potential $V(\phi)$. In this model gravity is not only mediated by the massless symmetric rank two tensor g but also by the real scalar field which has its own dynamics and a kinetic term parameterise by $\xi \geq 0$[9]. Intuitively the non-minimal coupling ϕR can be interpreted as the running of Newton's constant "$G(x) \equiv G_N/\phi(x)$" [155].

Variation of this action gives the following equations of motion:

$$\begin{aligned}
\phi\left(R_{ab} - \frac{1}{2}Rg_{ab}\right) =& \frac{\xi}{\phi}\left(\nabla_a\phi\nabla_b\phi - \frac{1}{2}(\nabla\phi)^2\, g_{ab}\right) - \frac{1}{2}V(\phi) + (\nabla_a\nabla_b\phi - \Box\phi\, g_{ab}) \\
&- \frac{Y}{2}\left(F_{ac}F^c_{\ b} + \frac{1}{4}F^2\, g_{ab}\right), \\
\partial_a\left(\sqrt{-g}Y(\phi)F^{ab}\right) &= 0, \\
\Box\phi &= \frac{1}{2(d-1)\xi + 2d}\Big((d-1)\phi V'(\phi) - (d+1)V(\phi) - \frac{(d-3)}{4}F^2 - \frac{Y'(\phi)}{4}\phi F^2\Big).
\end{aligned}$$

First, note that there is an extra term $(\nabla_a\nabla_b\phi - \Box\phi\, g_{ab})$ for the scalar in the Einstein's equations. This term comes from the Palatini identity $\delta_g R = R_{ab}\delta g^{ab} - \nabla_c\left(\delta\Gamma^c_{ab} - g^{ac}\delta\Gamma^b_{cb}\right)$ which in Einstein gravity can be integrated to give a boundary term. Evaluating this term in

[9] The standard notation in the literature for the Brans-Dicke coupling is ω. We refrain from this notation to avoid confusion with the frequency ω in the ac-conductivity $\sigma(\omega)$.

normal coordinates and using Stoke's theorem yields the extra term previously mentioned. Second, terms on the left hand side of the scalar equation come from the Ricci scalar factor that is solved by taking the trace of Einstein's equations.

An important observation is that for $Y = 1$ and $d = 3$ the Maxwell term in the scalar equation vanishes. This is a consequence of the fact that in $d = 3$ the electromagnetic energy-momentum tensor is conformal and therefore traceless, and do not source the Ricci scalar. This invariance will play later a crucial role in our analysis.

3.2.2 Regular part of the dc-conductivity for a general ansatz

We now present the computation of the conductivity at zero-frequency in a generic static and spherically symmetric AdS_{d+1} black brane. As usual in translationally invariant theories, for vanishing frequency $\sigma(\omega) \underset{\omega\to 0}{\sim} \sigma_Q + K\delta(\omega)$, where we use the standard notation introduced in Section 2.5.1: K for the Drude weight and σ_Q for the regular part of the dc-conductivity. In this section we are only interested in the latter. We derive a general expression for σ_Q that highlights the universality of our results. An explicit solution for the background is worked out in Appendix C.1.

Background and conserved charges

Consider the following static and spherically symmetric ansatz for the field equations,

$$\mathrm{d}s^2 = -A(u)\mathrm{d}t^2 + B(u)\mathrm{d}u^2 + C(u)\delta_{ij}\mathrm{d}x^i\mathrm{d}x^j, \tag{3.2a}$$

$$A = a_t(u)\mathrm{d}t, \tag{3.2b}$$

$$\phi = \phi(u). \tag{3.2c}$$

We assume this chart is globally defined and describes an asymptotically AdS_{d+1} black hole. More precisely, we require that $A(u) = B(u)^{-1} = C(u) = u^2$ as $u \to \infty$ (assymptotic boundary) and that $A(u) \sim B(u)^{-1} \sim 4\pi T(u - u_0)$ for $u_0 > 0$. In what concerns the fields, we need to require that $Y(\infty) = 1$, $\phi(\infty) \neq 0$ and $V(\phi) \sim 2\Lambda\phi$ close to the boundary and that they are regular at the horizon $u = u_0$. Moreover we impose $a_t(u_0) = 0$.

For this ansatz we use the existence of two radially conserved charges in order to simplify the computation of the conductivity. The simplest one is the charge density, that can be obtained by looking at the (t) component of Maxwell's equations,

$$\partial_a\left(\sqrt{-g}Y(\phi)F^{at}\right) = \partial_u\left(\sqrt{-g}Y(\phi)g^{uu}g^{tt}a_t'\right) = 0\,.$$

Therefore the charge density

$$\rho = \frac{Y C^{\frac{d-1}{2}}}{\sqrt{AB}} a_t' \tag{3.3}$$

is radially conserved. The second conserved quantity is related to the geometry. Consider the (tt) and the (xx) components of the Brans-Dicke equations with one raised index

$$\phi\left(R^t{}_t - \frac{1}{2}R\, g^t{}_t\right) = -\frac{Y}{2}F_{tu}F^{tu} + \left(-\frac{Y}{8}F^2 + \frac{\xi}{2\phi}(\nabla\phi)^2 + \frac{1}{2}V - \Box\phi\right) g^t{}_t + \nabla^t\nabla_t\phi\,,$$
$$\phi\left(R^x{}_x - \frac{1}{2}R\, g^x{}_x\right) = \left(-\frac{Y}{8}F^2 + \frac{\xi}{2\phi}(\nabla\phi)^2 + \frac{1}{2}V - \Box\phi\right) g^x{}_x + \nabla^x\nabla_x\phi.$$

Note that the assumption $\partial_t\phi = \partial_x\phi = 0$ is crucial in this analysis. For our ansatz, $g^t{}_t = g^x{}_x = 1$ and therefore we subtract the above expression to give

$$\phi\left(R^t{}_t - R^x{}_x\right) = -\frac{Y}{2}F_{ut}F^{ut} + \nabla^t\nabla_t\phi - \nabla^x\nabla_x\phi\,. \tag{3.4}$$

In order to write this as a total derivative, we will make use of the following identities

$$\sqrt{-g}R^t{}_t = -\frac{1}{2}\partial_u\left(\frac{1}{\sqrt{AB}}C^{\frac{d-1}{2}}A'\right),$$
$$\sqrt{-g}R^x{}_x = -\frac{1}{2}\partial_u\left(\sqrt{\frac{A}{B}}C^{\frac{d-3}{2}}C'\right).$$

Which is subtracted to give

$$\sqrt{-g}(R^t{}_t - R^x{}_x) = -\frac{1}{2}\partial_u\left(\frac{1}{\sqrt{AB}}C^{\frac{d+1}{2}}\left(\frac{A}{C}\right)'\right).$$

Regarding the right hand side, we have

$$\nabla^t\nabla_t\phi - \nabla^x\nabla_x\phi = g^{tt}\nabla_t\nabla_t\phi - g^{xx}\nabla_x\nabla_x\phi = -\left(g^{tt}\Gamma^r_{tt} - g^{xx}\Gamma^r_{xx}\right)\phi' = \frac{1}{2B}\left(\frac{A'}{A} - \frac{C'}{C}\right)\phi',$$

and therefore

$$\sqrt{-g}\left(\nabla^t\nabla_t\phi - \nabla^x\nabla_x\phi\right) = \frac{C^{\frac{d+1}{2}}}{2\sqrt{AB}}\left(\frac{A}{C}\right)'\phi'.$$

Taking into account that $\sqrt{-g}YF^{ut} = \rho$, we finally rewrite Eq. (3.4) as

$$\phi\,\partial_u\left(\frac{1}{\sqrt{AB}}C^{\frac{d+1}{2}}\left(\frac{A}{C}\right)'\right) = \rho a_t' - \frac{C^{\frac{d+1}{2}}}{\sqrt{AB}}\left(\frac{A}{C}\right)'\phi'.$$

which is expressed as a total derivative,

$$\partial_u \left(\frac{\phi}{\sqrt{AB}} C^{\frac{d+1}{2}} \left(\frac{A}{C} \right)' - \rho a_t \right) = 0 \, . \tag{3.5}$$

In previous works, this conserved charge was related to thermodynamical quantities [148, 160, 161]. Indeed, by integrating it, evaluating it at the horizon and using the boundary condition $a_t(u_0) = 0$ we get

$$\frac{\phi}{\sqrt{AB}} C^{\frac{d+1}{2}} \left(\frac{A}{C} \right)' \Big|_{u=u_0} = \frac{\phi(u_0)}{\sqrt{AB}} C(u_0)^{\frac{d-1}{2}} A'(u_0) = sT$$

which is exactly the same results obtained previously. Note that we use the fact that the entropy in BD theory satisfies

$$S = \frac{1}{4} \int_{u=u_0} \mathrm{d}^d x \, \phi \sqrt{-g}$$

instead of the standard area law. This is another simple manifestation that the strength of gravity in BD backgrounds is not constant, as in Einstein gravity, but governed by the scalar "G/ϕ"[10] [155]. Surprisingly, the scalar field fits nicely to produce the same thermodynamic result.

For a general r, we then have

$$sT = \frac{\phi}{\sqrt{AB}} C^{\frac{d+1}{2}} \left(\frac{A}{C} \right)' - \rho a_t . \tag{3.6}$$

Note that in particular $a_t(\infty) = \mu$. Therefore using the Smarr relation $sT + \mu\rho = \epsilon + P$ and the above expression evaluated at the boundary $u \to \infty$ we get

$$\epsilon + P = \frac{\phi}{\sqrt{AB}} C^{\frac{d+1}{2}} \left(\frac{A}{C} \right)' \Big|_{u=\infty} .$$

Fluctuations

In order to compute conductivities, we need to study fluctuations around the background solutions. It is sufficient to consider the following set of consistent fluctuations

$$\mathrm{d}s^2 \to \mathrm{d}s^2 + 2h_{tx}(u,t)\mathrm{d}t\mathrm{d}x \, , \qquad\qquad A \to A + a_x(u,t)\mathrm{d}x \, .$$

[10] Note that in standard units the area law is $S = \frac{1}{4G} \int_{u=u_0} \mathrm{d}^d x \sqrt{-g}$

The equation of motion for a_x is obtained by linearizing the (x) component of Maxwell's equations,

$$\begin{aligned}\partial_a\left(\sqrt{-g}Yg^{ac}g^{xd}F_{cd}\right) &= \partial_u\left(\sqrt{-g}Yg^{uu}g^{xx}\partial_u a_x\right) - \partial_u\left(\sqrt{-g}Yg^{uu}g^{xt}a_t'\right) + \partial_t\left(\sqrt{-g}Yg^{tt}g^{xx}\partial_t a_x\right) \\ &= \partial_u\left(\sqrt{\frac{A}{B}}C^{\frac{d-3}{2}}Y\partial_u a_x\right) - \sqrt{\frac{B}{A}}C^{\frac{d-3}{2}}Y\partial_t^2 a_x + \rho\partial_u\left(g^{xx}h_{tx}\right) = 0\ .\end{aligned}$$

To eliminate the h_{tx} term in the above expression we look at the constraint equation given by the linearised (rx) Brans-Dicke equation,

$$\partial_u\left(g^{xx}h_{tx}\right) = -\frac{g^{xx}}{\phi}Ya_t'a_x\ .$$

Inserting this in the above expression and solving for a_t' in function of the charge density we get

$$\frac{\phi\, C^{\frac{d+1}{2}}}{\sqrt{AB}}\partial_u\left(\sqrt{\frac{A}{B}}C^{\frac{d-3}{2}}Y\partial_u a_x\right) - \sqrt{\frac{B}{A}}C^{\frac{d-3}{2}}Y\partial_t^2 a_x - \rho^2 a_x = 0\ .$$

We now use the conserved charge (3.5) to rewrite the above equation as,

$$\partial_u\left(\frac{C^{d-1}Y\phi}{B}\left(\frac{A}{C}\right)'\partial_u a_x - \frac{A}{C}\rho^2 a_x\right) - \sqrt{\frac{B}{A}}C^{\frac{d-3}{2}}Y\partial_t^2 a_x = 0\ .$$

As long as we are ony interested in the regular part of the dc-conductivity, we can set $\partial_t^2 a_x = 0$. The resulting equation is easily integrated to give,

$$\frac{C^{d-1}Y\phi}{B}\left(\frac{A}{C}\right)'\partial_u a_x - \frac{A}{C}\rho^2 a_x = \text{constant}\ .$$

Black brane boundary conditions set $A(u_0) \sim 1/B(u_0) = 0$. Regularity of the fields at the horizon fixes the constant above to zero. Moreover,without loss of generality we set $\lim_{u\to\infty}\phi(u) \equiv 1$ at the boundary. With this information the equation for the fluctuation is easily integrated:

$$a_x^{(0)}(u) = \exp\left\{-\int_u^\infty \frac{AB\rho^2}{Y\phi(A/C)'C^{d-2}}\mathrm{d}u\right\} = \exp\left\{-\int_u^\infty \frac{Y(a_t')^2}{\phi C(A/C)'}\mathrm{d}u\right\}\ ,$$

where $a_x^{(0)}(u)$ is the independent solution of the equation that tends to one at the boundary and determines the regular part of the conductivity [11]. We can use the charges (3.3) and

[11] The second solution can be obtained using the Wronskian. For further details see [148].

(3.6) to perform the integral explicitly:

$$\int_u^\infty \frac{Y(a_t')^2}{\phi C(A/C)'}\mathrm{d}u = \int_u^\infty \frac{a_t'}{a_t + sT/\rho}\mathrm{d}u = \log(a_t(u)\rho + sT)|_u^\infty = \log\frac{\epsilon + P}{a_t(u)\rho + sT} \,,$$

where we have used the Smarr relation. This implies that

$$a_x^{(0)}(u) = \frac{a_t(u)\rho + sT}{\epsilon + P} \,,$$

and in particular

$$a_x^{(0)}(u_0) = \frac{sT}{\epsilon + P} \,,$$

where we use the boundary condition $a_t(u_0) = 0$. Finally, the regular part of the dc-conductivity is given by

$$\sigma_Q = Y(u_0)C(u_0)^{\frac{d-3}{2}}(a_x^{(0)}(u_0))^2 = Y(u_0)C(u_0)^{\frac{d-3}{2}}\left(\frac{sT}{\epsilon + P}\right)^2 .$$

This result is the same as the one obtained in EMD models [148, 160, 161]. It is interesting to observe that in these works $T_t^t = T_x^x$ is given as a necessary condition for the universality of σ_Q. Here this condition is clearly violated, but we can still write the equation for the fluctuation as a total derivative. However, we need to take into account the modified area law for the entropy density, yielding

$$\sigma_Q = \frac{Y(u_0)}{\phi(u_0)^{\frac{d-3}{d-1}}}\left(\frac{s}{4\pi}\right)^{\frac{d-3}{d-1}}\left(\frac{sT}{\epsilon + P}\right)^2 . \tag{3.7}$$

Note the explicit dependence of σ_Q on the BD field ϕ. For $d > 3$, we thus expect the scalar field to renormalise the universal contribution to the conductivity. To understand better the possible effects of ϕ, we need to evaluate its behavior at the horizon, in particular, the low and high temperature scaling of $\phi(u_0)$.

In contrast with the previous discussion, those questions do not have a universal answer. It depends on the particular solution for the background. In next section, we will see that the BD model can be formally mapped onto an EMD model by a conformal transformation. Explicit solutions for the latter have been widely studied in both the context of gravity [167, 168] and of holography [158, 169] (and references therein). As an illustration of this method we study in Appendix C.1 a particular solution, and show explicitly how it is mapped to BD.

A simple numeric fit for the solution (C.1) suggests two scaling regimes. For low temperature, $\phi(T) \sim a$ tends, for a fixed charged density, to a temperature independent constant $0 < a < 1$. This indicates that close to extremality the temperature scaling of σ_Q

coincides with EMD result, although up to a numerical prefactor a. For high temperatures, we find that $\phi(T) \sim T^{-\delta}$ for $\delta \geq 0$, suggesting that $\phi \to 0$ asymptotically at the horizon for sufficiently high temperatures. Here δ is a function of both the Brans-Dicke parameter ξ and the dimensionality d, and monotonically decreases with $\xi \geq 0$ for fixed d. For example, for $d = 4$ and $\xi = 0$, we have $\delta \approx 0.4$, while $\delta \approx 0.22$ for $\xi = 1$. In particular we have $\delta \to 0$ as $\xi \to \infty$ for any dimension $d > 2$.

One can interpret this behavior in a heuristic way. First note that Newton's constant G is related to the string coupling constant $g_s \sim G$. If we naively interpret the BD coupling "G/ϕ" as a dynamical Newton's constant, the flow of ϕ can be interpret as a flow from weaker ($\phi \gg 1$) to stronger ($\phi \ll 1$) coupling. More specifically, for the background solution of Appendix C.1 $\phi \in [0, \phi(u_0)]$ with $0 < \phi(u_0) \leq 1$. Therefore the running of ϕ from the boundary to the horizon corresponds in the dual field theory to a flow from weaker to stronger coupling. For the purpose of the conductivity, this running has the effect of increasing σ_Q by a factor $\phi(u_0)^{-\frac{d-3}{d-1}}$. Although tempting, one needs to be cautious with this heuristic interpretation. In the saddle point approximation, exact only in $N \to \infty$ limit, we always have $g_s \ll 1$ and $\lambda = g_s N \gg 1$. Thus this interpretation should not be taken seriously in the limit of fixed large N and $\phi(u_0) \to 0$, where the saddle point is clearly not valid.[12]

Conformal transformations and universality

The explicit result for the regular part of the dc conductivity (3.7) is also expected from a well known trick broadly used in the Brans-Dicke literature that we now discuss (see for example [170] and references within).

Consider the following conformal mapping of the metric g,

$$\bar{g} = \phi^{\frac{2}{d-1}} g \, .$$

Taking into account the transformation in the volume element and in the Ricci scalar, the action reads

$$\bar{S} = \int_{\mathcal{M}} \mathrm{d}^{d+1}x\sqrt{-g}\left[\bar{R} - \frac{4}{d-1}(\bar{\nabla}\bar{\phi})^2 - \bar{V}(\bar{\phi}) - \frac{\bar{Y}(\bar{\phi})}{4}\bar{F}^2\right],$$

where we have defined

$$\alpha = \frac{d-3}{2\sqrt{(d-1)\xi + d}} \qquad \bar{\phi} = \frac{d-3}{4\alpha}\log\phi \tag{3.8}$$

$$\bar{V}(\bar{\phi}) = \phi^{-\frac{d+1}{d-1}} V(\phi) \qquad \bar{Y}(\bar{\phi}) = Y(\bar{\phi}) e^{-\frac{4\alpha\bar{\phi}}{d-1}}, \tag{3.9}$$

and all bar $\bar{.}$ quantities are computed with respect to the metric $\bar{g}$. Note that for $d = 3$

[12] For this reason we employ the term "weaker" instead of "weak".

the Maxwell coupling is not affected by the conformal mapping. This is a consequence of the fact that electromagnetism is conformal in $d = 3$. It is also useful to note that $\bar{\phi}$ is well defined for $d = 3$ since α has a factor $d - 3$ as well.

This is nothing but the well known Einstein-Maxwell-Dilaton action. This action has been widely studied in the context of string theory and effective holographic models [157–159, 171]. This map provides a useful way of constructing solutions to BD gravity, since solutions of EMD theory are well known. A particular explicit solution that illustrates this point is given in Appendix C.1. More interestingly, it is known that the regular part of the dc-conductivity in such models take the (almost-)universal form

$$\bar{\sigma}_Q = \bar{Y}(u_0) \left(\frac{\bar{s}}{4\pi}\right)^{\frac{d-3}{d-1}} \left(\frac{\bar{s}\bar{T}}{\bar{\epsilon} + \bar{P}}\right)^2 .$$

It is not hard to check that the thermodynamic quantities $(\bar{s}, \bar{T}, \bar{\epsilon}, \bar{P})$ are invariant under the conformal mapping [13]. The only part of $\bar{\sigma}_Q$ that is not invariant is the non-universal charge coupling $\bar{Y}$, which transforms as $\bar{Y}(\bar{\phi}) = \phi^{-\frac{d-3}{d-1}} Y(\phi)$ and give the explicit result computed in the previous section.

This raises the interesting question of whether there are other theories of modified gravity that can be cast as an EMD theory in the Einstein frame, and if so, which those theories are. Indeed, this question has been much discussed in the gravity literature [172–174]. There has been a controversial debate on whether theories that are related by field redefinition or conformal transformation describe *gravitationally* [14] the same theory or not [175]. A full discussion of those intricate questions is beyond the scope of this work. Here we limit our discussion to the fact that conformal transformations are a convenient tool to study dynamically equivalent theories.

A well known class of theories that can be mapped into BD are $f(R)$ theories of gravity, defined through the action

$$S = \int_{\mathcal{M}} \mathrm{d}^{d+1}x \sqrt{-g} f(R) + S_{\text{matter}} ,$$

where $f(R)$ is a generic function of the Ricci scalar R and S_{matter} include any other fields coupled to the metric, but not to R. One can introduce an auxiliary field χ to rewrite the above equation as

$$S = \int_{\mathcal{M}} \mathrm{d}^{d+1}x \sqrt{-g} \left[f(\chi) + f'(\chi)(R - \chi)\right] + S_{\text{matter}} .$$

[13] This is essentially a consequence of the regularity of ϕ at the horizon.

[14] By gravitationally we mean the geodesics, conservation of the energy-momentum tensor, energy conditions, etc.

Variation with respect to χ give $f''(\chi)\,(R-\chi)=0$, so as long as $f''(\chi)\neq 0$ this constraint imposes $\chi = R$ and we recover the initial action. Note that this is also a sufficient condition for $f(R)$ to be invertible. Now defining $\phi = f'(\chi)$ and $V(\phi) = \chi(\phi)\phi - f(\chi(\phi))$ we can write

$$S = \int_{\mathcal{M}} \mathrm{d}^{d+1}x\sqrt{-g}\,(\phi R - V(\phi)) + S_{\text{matter}}\ ,$$

which is precisely a BD action with $\xi = 0$ and potential $V(\phi)$. This procedure is nothing but the Legendre transform of the action with respect to the conjugate field ϕ. Taking $S_{\text{matter}} = -\frac{1}{4}\int Y(u)F^2$, we proceed with the computation of the regular part of the conductivity as before to get

$$\sigma_Q = \frac{Y(u_0)}{f'(R(u_0))^{\frac{d-3}{d-1}}}\left(\frac{s}{4\pi}\right)^{\frac{d-3}{d-1}}\left(\frac{sT}{\epsilon+P}\right)^2 .$$

This illustrates how a combination of a conformal transformation and a Legendre transform can be used to considerably simplify calculations. Indeed, this procedure is much more general, and can be applied to other theories such as Palatini gravity or $f(\phi)$ couplings to the Ricci [175]. An interesting example of the latter is a conformal coupling $f(\phi) = 1 + \frac{1}{6}\phi^2$ that appears naturally in one-loop diagrams of string theory [176].

It is tempting to apply this construction to other theories of gravity such as Gauss-Bonnet, which in holography effectively correspond to leading $1/N$ corrections in the dual field theory. However, Gauss-Bonnet contain terms such as $R_{ab}R^{ab}$ which introduce further non-linearity and thus makes difficult the Legendre transformation [174]. Therefore Gauss-Bonnet gravity do not fall under BD universality.

A natural question to ask is what happens with other transport coefficients. For example, both the shear viscosity and the entropy contain the same power of G, and therefore η/s does not depend on G. As a consequence, we expect $\eta/s = 1/4\pi$ in BD holography to saturate the KSS bound. This is just a particular example of a general result that any theory related to standard gravity via a conformal transformation indeed saturates the KSS bound [177, 178]. However, quantities such as the entanglement entropy should be sensitive to ϕ in the expected way ($G \to G\phi^{-1}$). Indeed this was explicitly calculated in the context of $f(R)$ theories, and agrees with our discussion since $\phi = f'(R)$ [179–181].

This discussion applies only to theories with no momentum relaxation. In the rest of the section we focus on the description of transport in BD holography with momentum dissipation.

3.3 Momentum relaxation and dc-conductivity in BD holography

We now study the effect of momentum relaxation in the transport properties of the field theory dual of BD gravity. We consider the linear coupling to the Ricci scalar to be a function of the gradient of the Stueckelberg fields, that explicitly break diffeomorphism invariance in the boundary spacelike coordinates:

$$S = \int \mathrm{d}^{d+1}x\sqrt{-g}\left[Z(TrX)R - 2\Lambda - V(TrX) - \frac{Y(TrX)}{4}F^2\right] , \tag{3.10}$$

where $TrX = \frac{1}{d-1}\sum_I \nabla_\mu X^I \nabla^\mu X^I$ and $X^I = \alpha x^I$. We use the metric ansatz of Eq. (3.2) with $A = g$, $B = 1/g$ and $C = u^2 c$:

$$\mathrm{d}s^2 = -g(u)\mathrm{d}t^2 + \frac{\mathrm{d}u^2}{g(u)} + u^2 c(u)\delta_{ij}dx^i dx^j , \quad i = 1, \ldots, d-1 , \quad r \in [u_0, \infty) . \tag{3.11}$$

Assuming that $g \to u^2$ and $c \to 1$ for large u, and that g has a (double) single zero at (zero) finite temperature defining the horizon, we follow the procedure devised by Donos and Gauntlett [182] to compute the dc-conductivity from the solution of the equations of motion at the horizon.

We add a perturbation in A_x linear in time, while the Stueckelberg field and metric perturbations are independent of time,

$$\begin{aligned} A &\to A + (a_x(u) - Et)\,\mathrm{d}x, \\ X^x &\to X^x + \chi(u), \\ \mathrm{d}s^2 &\to \mathrm{d}s^2 + 2u^2 h_{tx}(u)\,\mathrm{d}t\mathrm{d}x + 2u^2 h_{ux}(u)\,\mathrm{d}u\mathrm{d}x. \end{aligned}$$

Maxwell's equation for a_x is:

$$\partial_u\left[Y\sqrt{-g}g^{uu}(g^{tx}F_{ut} + g^{xx}F_{ux})\right] = 0 , \tag{3.12}$$

which leads to the radially conserved quantity:

$$J = -Yr^{d-3}c^{\frac{d-3}{2}}ga_x' - h_{tx}\frac{\rho}{c} . \tag{3.13}$$

This conserved quantity is evaluated at the horizon where h_{tx} and a_x are obtained as we discuss below.

The perturbation on the gauge field close to the horizon is obtained from Eq. (3.13) by

choosing J such that a_x is ingoing in the horizon:

$$a_x' \sim -\frac{E}{g} \implies a_x \sim -Ev \,, \tag{3.14}$$

where v is the ingoing Eddington-Finkelstein coordinate $v = t + u_*$, given in terms of the tortoise coordinate $\mathrm{d}u_* = \frac{\mathrm{d}u}{g}$.

Eq. (3.14) gives the first term inside the parenthesis of Eq. (3.13). To obtain the second term, we combine the (xt) and (xx) Einstein's equations. Since we will evaluate them at the horizon, we will only write down explicitly the non-zero terms after taking the limit $u \to u_0$.

For clarity we write down Einstein's equations only for $d = 3$:

$$ZG_{ab} = \frac{1}{2}T_{ab} + \frac{1}{2}\mathcal{Z}_{ab} \,, \tag{3.15}$$

$$T_{ab} = Y\left(F_a^c F_{bc} - \frac{1}{4}g_{ab}F^2\right) - (2\Lambda + V)g_{ab} + \sum_I \nabla_a X^I \nabla_b X^I \left(-\dot{V} - \frac{\dot{Y}}{4}F^2 + \dot{Z}R\right) \,, \tag{3.16}$$

$$\mathcal{Z}_{ab} = 2(\nabla_a\nabla_b - g_{ab}\nabla_c\nabla^c)Z, \tag{3.17}$$

where the dot derivative stands for derivative with respect to $TrX = \frac{1}{2}g^{ab}\sum_I \partial_a X^I \partial_b X^I$ and R is the Ricci scalar.[15]

The (tx) Einstein's equation is,

$$\mathcal{O}(h_{tx}', h_{tx}'') + \frac{u^2}{2}Zh_{tx}u^2\left[g'' + g'\left(\frac{2}{c} + \frac{c'}{c}\right) + \dots\right] = \tag{3.18}$$

$$\frac{u^2}{4}h_{tx}\left(-4\Lambda - 2V + Ya_t'^2\right) + \frac{1}{2}gYa_t a_x' + \frac{1}{2}u^2 g\dot{Z}TrX'h_{tx}' - \frac{rh_{tx}}{2c}\left[2rcg'\dot{Z}TrX' + \dots\right], \tag{3.19}$$

where the dots and the terms $\mathcal{O}(h_{tx}', h_{tx}'')$ are zero at the horizon, the prime derivative is with respect to r and $TrX' = \partial_u TrX$. The first two terms on the right-hand side come from T_{ab} and the last term from $\mathcal{Z}_{ab}$. In order to simplify Eq. (3.18) we eliminate $c''(u)$ from the (tt) Einstein's equation and substitute it into the (xx) Einstein's equation. The result is given in

[15]The full dynamical stability of the model Eq. (13) is beyond the scope of this work. We thank Oriol Pujolàs and Matteo Baggioli for pointing out the occurrence of third order time derivatives. These occur beyond the linear analysis and have the potential to further restrict the parameters for which the model is stable.

Eq. (3.20) by specifying G_{xx}, T_{xx} and $\mathcal{Z}_{xx}$ separately,

$$ZG_{xx} = \frac{u^2 c}{2} Z g'' + \frac{u^2 Z}{4}\left(\frac{c'}{c} + \frac{2}{r}\right) g' + \frac{r^4 Z}{8}\frac{4\Lambda + 2V + Y a_t'^2}{k^2 \dot{Z} - u^2 c Z} + \dots \,, \tag{3.20}$$

$$\mathcal{Z}_{xx} = \frac{\alpha^2 \dot{Z} g'}{2}\left(\frac{c'}{c} + \frac{2}{r}\right) + \frac{\alpha^2 u^2 c \dot{Z}}{4}\frac{4\Lambda + 2V + Y a_t'^2}{\alpha^2 \dot{Z} - u^2 c Z} + \dots \,, \tag{3.21}$$

$$\frac{1}{2} T_{xx} = \frac{\alpha^2 \dot{Z}}{2} g'' + \frac{\alpha^2 \dot{Z}}{2}\left(\frac{c'}{c} + \frac{2}{r}\right) g' + \frac{u^2 Z}{4}\frac{u^2 c(4\Lambda + 2V - Y a_t'^2) + \alpha^2(-2\dot{V} + \dot{Y} a_t'^2)}{\alpha^2 \dot{Z} - u^2 c Z} \tag{3.22}$$

$$+ \frac{\dot{Z}}{4}\frac{2\alpha^2 \dot{V} + (2\alpha^2 u^2 c Y - \alpha^4 \dot{Y}) a_t'^2}{\alpha^2 \dot{Z} - u^2 c Z} + \dots, \tag{3.23}$$

where the dots vanish at the horizon. Combining eqs. (3.20) and (3.18) allows to eliminate h_{tx}. Its value at the horizon $u = u_0$, is used to calculate the dc-conductivity from $\mathrm{Re}(\sigma_{\mathrm{dc}}) = J/E$. Before we do so, we define the expansions of the metric functions g and c close to the horizon as:

$$g \sim g_1\left(1 - \frac{u_0}{r}\right) + \dots,$$
$$c \sim c_0 + c_1\left(1 - \frac{u_0}{r}\right) + \dots$$

Restoring arbitrary bulk dimensionality $d+1$, the temperature is

$$T = \frac{1}{4\pi}\,\frac{c_0 u_0}{2c_0 + c_1}\,\frac{4\Lambda + 2V(u_0) + Y(u_0) a_t'(u_0)^2}{\frac{2\alpha^2 \dot{Z}(u_0)}{u_0^2 c_0} - (d-1) Z(u_0)}\,, \tag{3.24}$$

where we have used $TrX = \frac{\alpha^2}{u^2 c}$ to simplify the denominator. The dc-conductivity, obtained from eqs. (3.13), (3.14) and the value of h_{tx} at the horizon, calculated as indicated previously, are given by the following compact expression,

$$\mathrm{Re}(\sigma_{\mathrm{dc}}) = Y_0 u_0^{d-3} c_0^{\frac{d-3}{2}} + \frac{\rho^2}{m_{\text{eff}}^2}\,, m_{\text{eff}}^2 = 2 c_0^{\frac{d-1}{2}} u_0^{d-1}\left(T\mathcal{A} + Z_0^2 \mathcal{B} + \dot{Z}_0 \mathcal{C}\right), \tag{3.25}$$

where T is the temperature Eq. (3.24) and $\mathcal{A}$, $\mathcal{B}$ and $\mathcal{C}$ are given in Eq. (3.26). The term $a_t' = \frac{\rho}{Y(u) r^{d-1} c(u)^{\frac{d-1}{2}}}$ is also evaluated at the horizon. The subscripts $'0'$ in eqs. (3.25) and (3.26) indicate the variable is evaluated at the horizon. Equation (3.25) suggests that even at zero temperature the conductivity receives a correction given by the $\dot{Z}_0^2 \mathcal{C}$ term. We note that although this is a fully analytical expression for the conductivity the metric at the horizon

may only be computed numerically.

$$\mathcal{A} = \frac{4\pi(2c_0+c_1)}{u_0^3 c_0^3}\frac{\frac{(d-1)(d-2)}{4}u_0^4c_0^2Z_0^2-(d-2)\alpha^2u_0^2c_0Z_0\dot{Z}_0+2\alpha^4\dot{Z}_0^2}{(d-1)Z_0-\frac{2\alpha^2\dot{Z}_0}{u_0^2c_0}}, \tag{3.26}$$

$$\mathcal{B} = \frac{(d-1)c_0}{4\left[(d-1)Z_0-\frac{2\alpha^2\dot{Z}_0}{u_0^2c_0}\right]^2}\left[(d-2)u_0^2c_0\big(4\Lambda+2V_0+Y_0a_t'^2\big)+2\alpha^2\big(2\dot{V}_0-\dot{Y}_0a_t'^2\big)\right], \tag{3.27}$$

$$\mathcal{C} = \frac{\alpha^2}{u_0^2c_0^2\left[(d-1)Z_0-\frac{2\alpha^2\dot{Z}_0}{u_0^2c_0}\right]^2}\Big\{\alpha^2\dot{Z}_0\big(4\Lambda+2V_0-Y_0a_t'^2\big)- \tag{3.28}$$

$$Z_0\Big[\frac{d-1}{2}u_0^2c_0\big(12\Lambda+6V_0+Y_0a_t'^2\big)+\alpha^2\big(2\dot{V}_0-\dot{Y}_0a_t'^2\big)\Big]\Big\}. \tag{3.29}$$

3.3.1 Conductivity reduction induced by charge screening

Our result for the dc-conductivity generalises those obtained previously from the AdS RN+Stueckelberg background ($Z=1, Y=1\ V=TrX$) [54], and from the backgrounds studied in [163, 164] with $Z=1, Y=e^{-\kappa TrX}\ V=TrX$, $\kappa>0$. In these models the Ricci scalar is not coupled directly to the Stueckelberg field. However, the Stueckelberg-dependent coupling Y has a crucial role in the dc-conductivity.

For sufficiently large κ and α, and for low temperature, the dc-conductivity increases with temperature, a behaviour previously referred to as *insulating* [163, 164]. We note that the physical reason for this behavior is not a smaller scattering time but the simple fact that Y screens the charge at low temperature and consequently reduces the conductivity which is proportional to the charge. While the overall temperature dependence is similar to that expected in a system approaching an insulating state, it should be noted the conductivity is *always* finite so the system is metallic in all cases. Moreover, the scattering time, controlled by the parameter α, in this model has the same temperature dependence than in RN+Stueckelberg background for which no insulating behavior was observed. Very likely, a truly insulating behavior would lead to a qualitative change in the background something that is not observed in [163, 164].

In the following sections we identify a region of parameters in BD holography where we have found similar features which are not induced by charge screening. However, we do not claim that our system is an insulator because the conductivity is always finite even at zero temperature.

3.3.2 The dc-conductivity in BD-Stueckelberg backgrounds

In this section we explore the effect of the BD-type coupling Z on the background and on the dc-conductivity in $d = 3$ boundary dimensions. More specifically, we break translational invariance by using an Stueckelberg-dependent BD coupling $Z(TrX)$. First we consider the simpler case $V = TrX = \frac{1}{d-1}\sum_I \nabla_\mu X^I \nabla^\mu X^I = 0$ in Eq. (3.10) and later study a more general BD-like model where $V = TrX \neq 0$ is also present. Initially we restrict our analysis to two space dimension. The dependence on dimensionality of our results is discussed in the last part of the section.

We note physically $Z(TrX)$ is an Stueckelberg-dependent gravitational coupling constant that runs from the boundary to the horizon. For that reason we will refer to these Stueckelberg fields coupled to the Ricci tensor as gravitational Stueckelberg fields. The qualitative effect of this running in the holographic dimension, from weak to strong coupling, is less obvious than for $Y \neq 1$ or in the translational invariant case.

Momentum relaxation with $Z \neq 1$, $Y = 1$ and $V = 0$

We start our analysis with the simpler case of no Stueckelberg field potential and trivial coupling to the Maxwell tensor,

$$Z = e^{\lambda TrX}\,, \quad \dot{Z} = \lambda Z\,, \quad TrX = \frac{\alpha^2}{u^2 c}\,, \tag{3.30}$$

$$V = 0\,, \qquad \dot{V} = 0\,, \tag{3.31}$$

$$Y = 1\,, \qquad \dot{Y} = 0, \tag{3.32}$$

Although, *a priori*, λ and α are independent parameters, it is easy to see from Eq. (3.30) that these parameters appear only in Z as a single parameter $\lambda_{\text{eff}} = \lambda\alpha^2$. Translational symmetry is broken for both $\lambda_{\text{eff}} > 0$ and $\lambda_{\text{eff}} < 0$. In the first case $c(u_0) < 1$ while in the second $c(u_0) > 1$. However, for $\lambda < 0$ the squared 'effective mass' m^2_{eff} in Eq. (3.25) is negative. Therefore, λ_{eff} should be constrained to positive values.[16]

At high temperature, the background tends to AdS RN+Stueckelberg [54] ($Z = 1, Y = 1$, $V = TrX$): it has a similar blackening factor and $c \to 1$ for all r. The effect of the coupling Z in the background is more evident at low temperatures where $c(u)$ has a stronger dependence on the radial dimension.

Regarding the dc-conductivity, this model has qualitatively similar properties to that of the RN+Stueckelberg. For example, for the allowed range of parameters, the dc conductivity increases as the temperature decreases and $\text{Re}(\sigma_{\text{dc}}) > Y_0 = 1$. Moreover, it is known [54] that for RN+Stueckelberg in four bulk dimensions, this condition is $\text{Re}(\sigma_{\text{dc}}) > u_0^{d-3}$. In the

[16] As we will demonstrate later in a similar background we have observed that $\lambda < 0$ also leads to the violation of the null energy condition. Therefore, we restrict to positive λ_{eff}.

model Eq.(3.30) the condition is $\mathrm{Re}(\sigma_{\mathrm{dc}}) > (u_0^2 c_0)^{\frac{d-3}{2}}$, where $c(u_0) = c_0$.

It would be interesting to compare the dc-conductivity for a fixed scattering time in the model of Eq.(3.30) with the well-studied AdS RN+Stueckelberg model. However, it is clear that both models display similar features since the respective actions are related by a conformal transformation. As was explained in detail in sec. 3.2.2.3 for the translational invariant case, under a conformal transformation, the action of Eq. (3.10) can be transformed into an action with $Z = 1$. The change of the Ricci scalar under this transformation involves additional terms which depend on TrX and contain the usual kinetic term proportional to $\sum_I \nabla_\mu X^I \nabla^\mu X^I$, $X^I = \alpha x^I$.
Moreover, as mentioned in sec. (3.2.2.3), in $d = 3$ dimensions electromagnetism is conformal, therefore, the conformal transformation does not change the coupling of the F^2 term in the action, see Eq. (3.8). This is consistent with the fact that for the choice of couplings given in Eq. (3.30), the zero temperature dc-conductivity is larger than one, as in the RN+Stueckelberg model [54]. In higher dimensions, however, it is expected the model specified by Eq. (3.30) will yield $\mathrm{Re}(\sigma_{\mathrm{dc}}) < 1$ in some range of parameters. Indeed we will see that this is the case in sec. 3.4.

In the next section we study a more general model with a finite potential (V) and non-trivial BD (Z) and Maxwell (Y) couplings in four bulk dimensions.

Momentum relaxation with $Z \neq 1$, $Y \neq 1$ and $V \neq 0$

Before showing the results for the dc-conductivity, it is illuminating to comment the general features of the gravitational background given in Eq. (3.11) for the following choice of couplings,

$$Z = e^{\lambda TrX} , \qquad \dot{Z} = \lambda Z , \tag{3.33}$$

$$V = TrX = \frac{\alpha^2}{u^2 c(u)} , \ \dot{V} = 1 , \tag{3.34}$$

$$Y = e^{-\kappa TrX} , \qquad \dot{Y} = -\kappa Y, \tag{3.35}$$

where $\alpha, \kappa > 0$ and λ is real.

The extremal charge density is:

$$\rho_e = u_0^2 c_0 \sqrt{Y(-2\Lambda - V)} . \tag{3.36}$$

It is clear that ρ_e decreases as Y decreases, which for the choice of Eq. (3.33) corresponds to increasing α and κ. Similarly, for smaller $c(u_0) = c_0$ the extremal charge density is smaller.

We now comment on the allowed range of the BD coupling parameter λ according

to the properties of the background. Similarly to sec. 3.3.2.1, $\lambda > 0$ ($Z > 1$) is allowed, in which case the g/u^2 and $c(u)$ increase monotonically towards the boundary. Contrary to the model of sec. 3.3.2.1, $\lambda = 0$ is also allowed due to the presence V, which breaks translational invariance. In this case the BD coupling is trivial $Z = 1$ and has been studied previously [163, 164].

Moreover, we also find backgrounds satisfying all boundary conditions for $\lambda < 0$ ($Z < 1$). However, in this case g/u^2 does not increase monotonically towards the boundary; there exists a point inside the bulk where the derivative of g/u^2 vanishes. This suggests the odd feature that the background displays a repulsive behavior between this point and the boundary, which may violate energy null condition.[17] In [183] the energy conditions in theories of gravity different from Einstein's gravity have been re-derived from Raychaudhury's equation and imposing gravity to be attractive. For the action given in Eq.(3.10) the null energy condition reduces to

$$\frac{1}{Z}(T_{ab} + \mathcal{Z}_{ab})n^a n^b \geq 0 \,, \tag{3.37}$$

for all null vectors n^a and where T_{ab} and $\mathcal{Z}_{ab}$ are defined in Eq. (3.15). We have found that for $\lambda < 0$ the background violates the null energy condition Eq. (3.37). This is easily seen by expressing the background Eq. (3.11) in the variable $u = u_0/r$ and plugging the following null vector: $N^t = 1/\sqrt{g}$, $N^u = \sqrt{g}$, $N^i = 0$ in Eq. (3.37), which reduces to

$$(T_{ab} + \mathcal{Z}_{ab})N^a N^b \propto \ddot{Z}TrX'^2 + \dot{Z}TrX'' \propto c'(u)^2 - 2c(u)c''(u) \geq 0 \,. \tag{3.38}$$

For $\lambda \geq 0$, $c''(u) \leq 0$ and the null energy condition for this null vector is satisfied, however we have observed that for any $\lambda < 0$ this condition is violated.

Regarding the metric function $c(u)$, as the temperature increases, it becomes almost independent of the holographic coordinate $c(u) \approx c(u_0) = c_0 \to 1$. The blackening function is also modified in such a way that the geometry approaches that of AdS RN+Stueckelberg. In the allowed region: $\lambda \geq 0$, the horizon value of c satisfies $c_0 \leq 1$ and c_0 decreases for larger λ. We have already observed this behavior in the model of Sec. 3.3.2.1 ($Y = 1$ and $V = 0$). On the other hand, in the forbidden region $\lambda < 0$, $c(u_0) = c_0 > 1$ and c_0 increases for smaller λ. We note that, at low temperatures the spatial metric functions $g_{ii} = u^2 c(u)$ could, in principle, be better understood in terms of Lifshitz and hyperscaling violation anomalous exponents, similarly to EMD theories [159]. While we do not rule out the behavior of g_{ii} close to the horizon may actually be cast using various anomalous exponents, we have not been able to re-express the metric at low temperatures using a single anomalous exponent.

Finally, in this model, contrary to that of sec. 3.3.2.1, λ and α are independent parameters. In the presence of $V = TrX = \frac{\alpha^2}{u_0^2 c_0}$, the parameter α appears independently of the parameter λ in the action and the equations of motion. Therefore, it is expected that these two cannot

[17] We thank Roberto Emparan for discussion and suggestions on this matter.

be relabelled into a single parameter. For more explicit results regarding the background for different choices of the parameters, see the Appendix C.2.

The dc-conductivity

We depict in Figs. 3.1 and 3.2 the dc-conductivity Eq.(3.25), in two space dimensions as a function of temperature for a wide range of the BD parameter λ and the charge screening parameter κ. The effect of λ and κ is very similar: both control the strength of momentum dissipation.

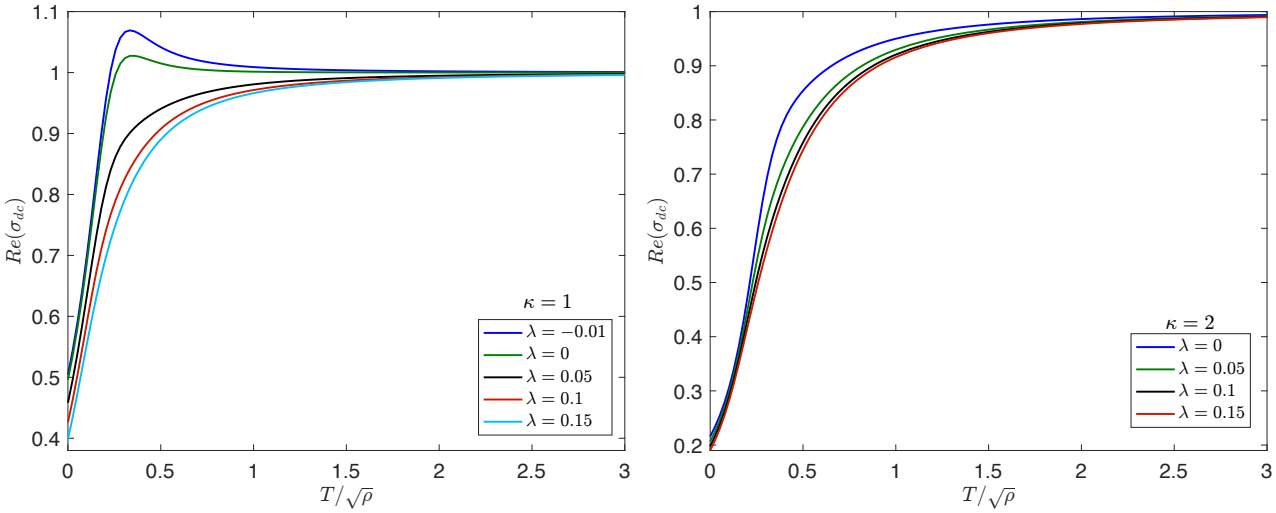

Figure 3.1: Temperature dependence of the dc-conductivity Eq. (3.25) for fixed axion parameter $\alpha = 1$ and charge density $\rho = 1$. The charge screening parameter κ and the BD-coupling parameter λ are indicated in the plots. The effect of increasing λ for fixed κ is similar to increase κ for fixed λ. The case $\lambda < 0$ suggests that the effect of a weaker gravitational coupling $Z < 1$ on the dc-conductivity is to weaken momentum dissipation. However, we stress this limit violates the null energy condition Eq. (3.38) and should be excluded.

In Fig. 3.1 we observe that the increase of either the charge screening or the effective gravitational coupling ($Z > 1$) yields a lower dc-conductivity especially for low temperatures and sufficiently large values of $\lambda > 0, \kappa$. We note that that in this range of parameters the conductivity is below the bound only because of charge screening.

However, in Fig. 3.2 we observe that, even though the BD parameter does not appear explicitly in the Maxwell coupling Y, its effect is to *renormalise* the charge screening parameter κ through the change in the geometry. More explicitly, through the value of the metric function $c(u)$ at the horizon: c_0. This is possible even for small κ. As mentioned before, increasing λ leads to a smaller c_0 and BD coupling which manifests as stronger momentum dissipation. This is a quite interesting and unexpected feature of the model. For instance, the bound in the conductivity of [97] is violated, even for very weak charge screening $\kappa = 0.1$ provided that momentum dissipation by gravitational Stueckelberg fields is strong

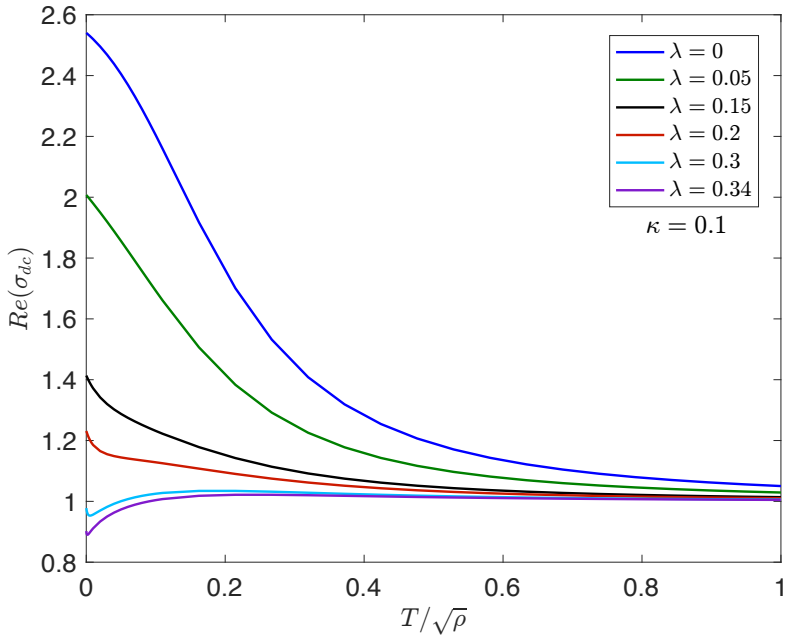

Figure 3.2: Temperature dependence of the dc-conductivity Eq. (3.25) for fixed axion parameter $\alpha = 1$ and charge density $\rho = 1$. The charge screening parameter κ and the BD-coupling parameter λ are indicated in the plot. The effect of the BD parameter is similar to the charge screening parameter. Increasing λ yields a smaller $u_0^2 c_0$; as a consequence the first term in Eq. (3.25): $Y_0 = \exp\left[-\kappa\alpha^2/(u_0^2 c_0)\right]$ decreases. The bound of [97] is violated for large λ even for weak charge screening.

enough $\lambda \geq 0.3$. The change in the temperature dependence of the dc-conductivity at low temperature for different values of the parameters is not caused by charge screening but by the effective running of the gravitational coupling. As anticipated in sec. 3.3.1, a decrease in the conductivity for low temperatures sometimes occur in systems that approach an insulating transition. However, in our case the conductivity, though substantially suppressed, it never vanishes. Therefore the model we study is never an insulator.

Notice that in the left plot of Fig. 3.1 we have included a case in the forbidden range of the BD parameter: $\lambda < 0$, which corresponds to a BD coupling satisfying $Z < 1$ and $\dot{Z} = \partial_{TrX} Z < 0$. We have included this value only to tentatively suggest that the effect of a weaker gravitational interaction could be to effectively reduce the strength of momentum dissipation. Moreover, we have observed that the effective mass in Eq. (3.25) becomes negative for some $\lambda_m < 0$, which depends on the rest of the parameters. A negative effective mass has been linked to instabilities of the theory [163]. However, we emphasise that, even for our choice of the BD coupling Z there is a region $\lambda_m < \lambda < 0$ in which the effective mass is positive but the null energy condition Eq.(3.38) is violated.

3.4 BD holography in higher dimensions

So far we have restricted our analysis to $d+1=4$ bulk dimensions. Here we briefly discuss the most salient features of higher dimensional backgrounds. The motivation to study $d>3$ is to observe the explicit effect of the running of the gravitational constant associated to the extra factor $g_{xx}^{\frac{d-3}{2}} = u_0^{d-3} c_0^{\frac{d-3}{2}}$ in the first term of the conductivity Eq. (3.25),

$$\mathrm{Re}(\sigma_{\mathrm{dc}}) = Y_0 u_0^{d-3} c_0^{\frac{d-3}{2}} + \dots \,. \tag{3.39}$$

The presence of this term is not exclusive to the BD model. Indeed, in EMD models where translational invariance is broken by axion fields, the same factor is present, [55]. We note however that, at least in EMD theories where the Stueckelberg fields and the dilaton are coupled *minimally* through a dilaton-dependent coupling constant, [55, 159, 162], the metric function c is trivial, $c=1$, [18]. Therefore, in EMD-axion theories , $c_0=1$.

We now discuss the two models of Secs. 3.3.2.1 and 3.3.2.2 for $d=4,5$ boundary spacetime dimensions. In Fig. 3.3 we plot the metric function $c(u)$ used in the ansatz Eq. (3.11), in the model of Eq. (3.33). In the absence of $V(TrX)$, Eq. (3.30), the background has similar features.

The results, depicted in Fig. 3.3, indicate that increasing dimensionality decreases the curvature of the metric function c. This is more easily seen at low temperature (top row), where $c_0 = c(u=u_0)$ increases for $\lambda>0$ and decreases for $\lambda<0$. Though not shown in the figure, a similar effect is also observed in the blackening function. This is a manifestation of the large-dimensionality limit, [184, 185] where the shape of g and c is such that the gravitational effects are stronger closer to the horizon but weaker far from it.

Dimensionality effects on the dc-conductivity Eq. (3.39) are directly related to the dependence of c_0 and u_0 on the dimension. The quantities with tilde are in $\tilde{d}$ dimensions and those without tilde in d dimensions. If $\tilde{d}>d$, we observe that:

- For $\lambda>0$ and low (high) temperature: $\tilde{c}_0 > (<) c_0$ and $\tilde{u}_0 < (>) u_0$.
- For $\lambda<0$ (forbidden by the null energy condition) and low (high) temperature: $\tilde{c}_0 < (>) c_0$ and $\tilde{u}_0 > (<) u_0$.

For the temperature range studied, $\tilde{u}_0^2 \tilde{c}_0 < u_0^2 c_0$. Moreover, for low temperature $u_0^2 c_0 < 1$ but for large temperature $u_0^2 c_0 > 1$. Therefore, for low temperature one expects the suppression of the dc-conductivity to be smaller for larger dimensionality.

We show in Fig. 3.4 that the term $g_{xx}^{\frac{d-3}{2}}$ in Eq. (3.39) leads to a suppression of σ_{dc} at low temperature in three space (boundary) dimensions ($d=4$). In order to isolate the effect

[18] An additional difference in the background is that in the metric ansatz given in Eq. (3.11), $g_{tt} = -1/g_{rr}$, which is not the case in a EMD plus axion theory, [159, 162].

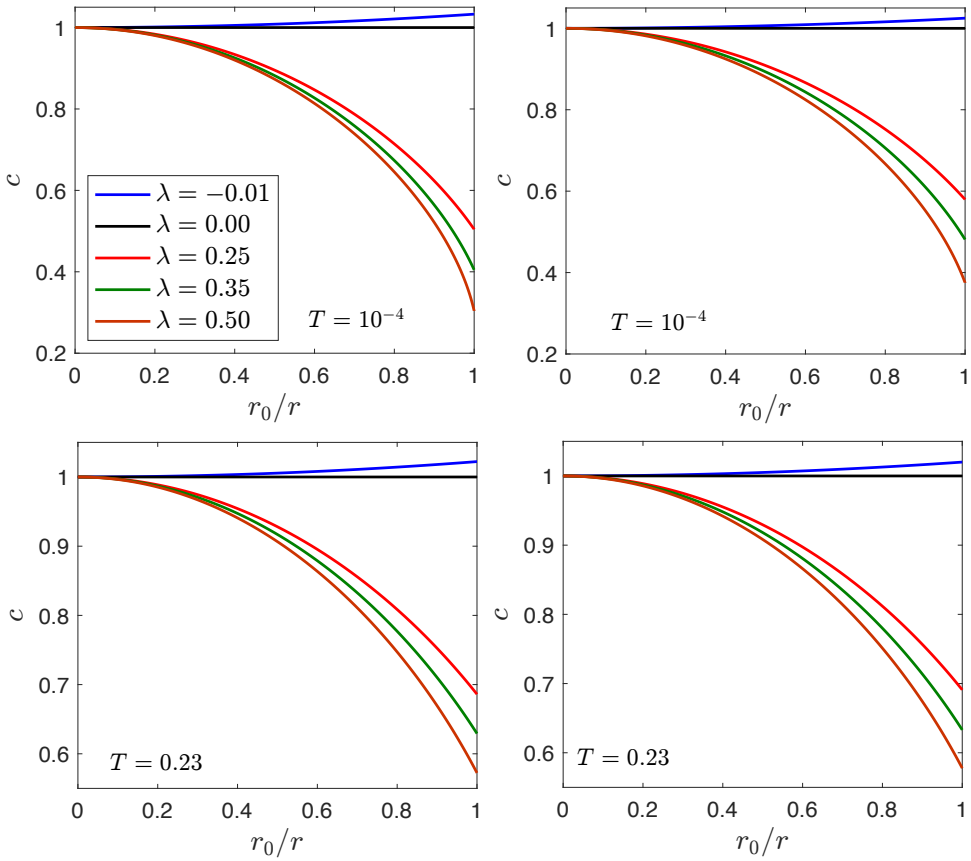

Figure 3.3: Metric function c , Eq. (3.11), in $d+1=5$ (left column) and $d+1=6$ (right column) bulk dimensions for the model given in Eq.(3.33). The temperature is indicated in the plots and the charge density is $\rho = 1$. The charge screening parameter $\kappa = 1$ and the axion parameter $\alpha = 1$. The BD-coupling parameter λ is indicated in the legend, which refers to all figures. While the boundary conditions for $\lambda < 0$ are satisfied, this case leads to violation of the null energy condition.

of the background we couple the Maxwell field minimally by setting $Y = 1$, namely, the couplings used are those given in Eq. (3.40).

$$Z = e^{\lambda TrX} \,, \qquad \dot{Z} = \lambda Z \,, \tag{3.40}$$

$$V = TrX = \frac{\alpha^2}{u^2 c(u)} \,, \; \dot{V} = 1 \,, \tag{3.41}$$

$$Y = 1 \,, \qquad \dot{Y} = 0. \tag{3.42}$$

A similar effect, depicted in Fig. (3.5), is observed even in the absence of $V(TrX)$ in the action (3.10), namely, we choose the couplings of Eq. (3.30). As was explained in Sec. 3.3.2.1, in the absence of V, there is a single parameter that controls momentum dissipation $\lambda_{\text{eff}} = \lambda\alpha^2 > 0$. In summary, our results suggest that for higher dimensions gravitational effects, including those of the gravitational Stueckelberg fields are suppressed

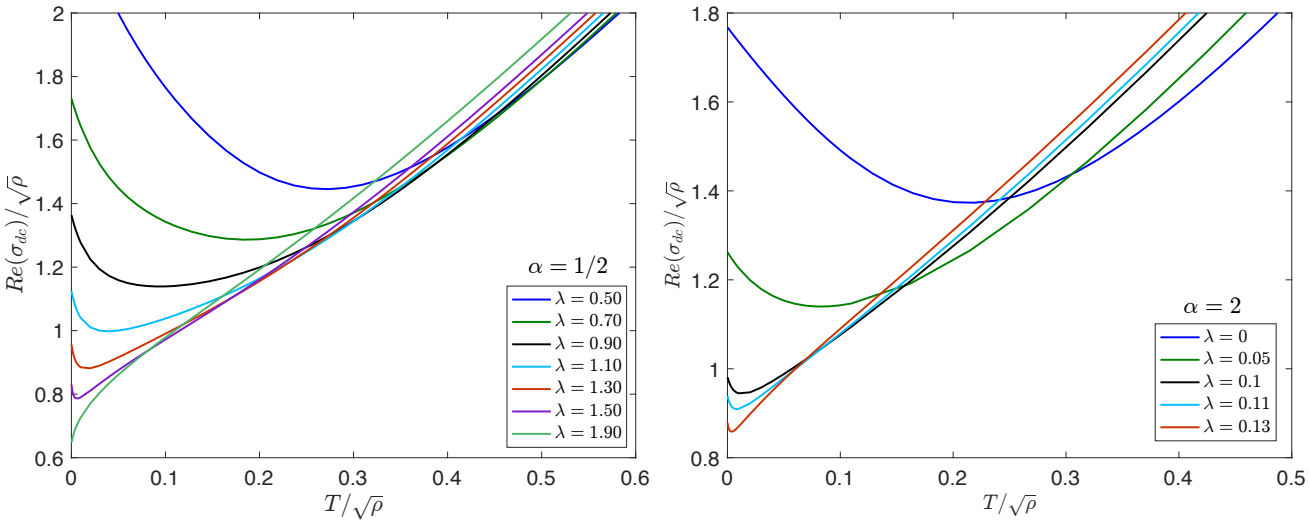

Figure 3.4: zero-frequency conductivity Eq. (3.25) in $d+1=5$ bulk dimensions in a model with a minimally coupled Maxwell field, Eq.(3.40). When the BD coupling λ is larger than some positive value the dc-conductivity at zero temperature is below 1. This effect is due to the background rather than to an axion-dependent Maxwell coupling as in Fig. 3.1. The charge density is fixed $\rho = 1$.

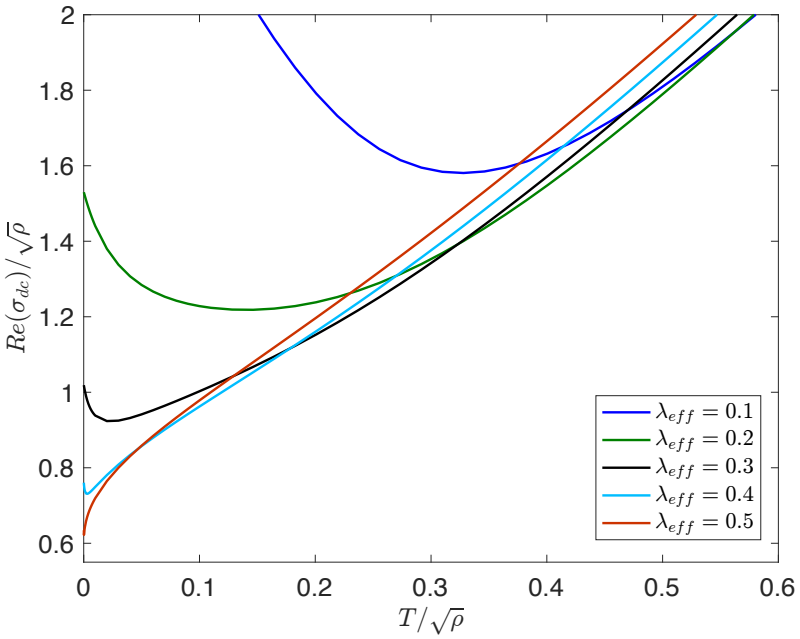

Figure 3.5: zero-frequency conductivity Eq. (3.25) in $d+1=5$ bulk dimensions in a model with a minimally coupled Maxwell field and $V(TrX) = 0$, Eq.(3.30). Similar behavior as in Fig.3.4 is observed despite the absence of the usual kinetic term in the action ($V = 0$). Again, the effective change in the gravitational interaction, through the BD coupling ZR, parametrised by $\lambda_{\text{eff}} = \alpha^2\lambda$, allows to decrease the dc-conductivity despite the absence of charge screening $Y = 1$. The charge density is fixed $\rho = 1$.

except close to the horizon. As a consequence, the conductivity is closer to the RN limit for high temperature. However close to zero temperature, where gravitational effects are

still important, the dc-conductivity is heavily suppressed for strong momentum relaxation induced by the gravitational axion only.[19] Therefore, also in this case, the background induces a important suppression of the conductivity without the need of any external source of charge screening. Obviously the system studied in this chapter is always a metal, however it would be interesting to explore whether there are other backgrounds within BD holography that reproduce genuine insulating features in the dual field theory.

3.5 Ac-conductivity in BD holography with momentum relaxation

We continue our analysis of transport properties of BD holography by investigating the ac-conductivity. We focus first in the low frequency scaling of the real part of the conductivity. We found that the conductivity grows linearly with the frequency for low temperatures but strong momentum relaxation. In the second part of the section we show that BD holography, even if combined with other sources of momentum relaxation, does not reproduce the intermediate-frequency scaling of the absolute value and argument of the ac-conductivity observed in cuprates.

3.5.1 Low-frequency behavior of the conductivity

In the context of massive gravity the equation for the perturbation leading to the ac-conductivity at extremality has been solved analytically for low frequencies by using the method of matched asymptotic expansions [186]. In [54] it was shown that, in the previous model, the dc conductivity is equivalent to that obtained in the RN+Stueckelberg model, upon a convenient identification of the parameters. Using the method of matched asymptotic expansions we have observed (not shown) that, as in massive gravity, the low-frequency behavior of the ac-conductivity of the extremal RN+Stueckelberg model is also linear in frequency with an always negative slope, which is consistent with Drude physics.

Although we have not been able to obtain analytical results of the low-frequency scaling for arbitrary couplings Z and Y, we observe numerically, see Fig. 3.6, the same linear scaling of the conductivity for small frequencies. Interestingly, provided that momentum relaxation is strong enough, the slope of this linear growth is positive, namely, the conductivity increases with the frequency. This is not exclusive of BD holography, it is also observed for $\lambda = 0$ in the limit of strong momentum relaxation induced by the axion coupled to the Maxwell field. This is an interesting feature which we are not aware to have been reported in holographic systems which do not include charge screening.

[19] Although, as the case with charge screening of sec. 3.3.2.2, the conductivity never vanishes.

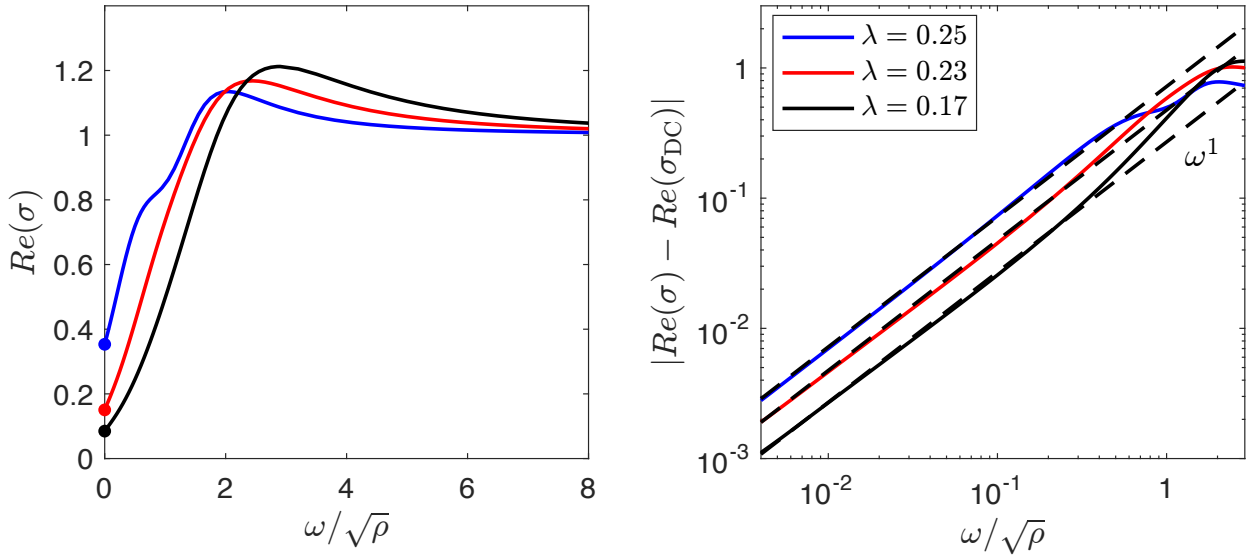

Figure 3.6: Zero temperature [extremal background of Eqs.(3.10), (3.33)] ac-conductivity for strong breaking of translational symmetry. The charge screening parameter is $\kappa = 1$ and the axion parameter is $\alpha = 1$ (blue lines), $\alpha = 1.5$ (red lines) and $\alpha = 2$ (black continuous lines). The BD-coupling parameter λ, given in the legend, is fixed close to the maximum value allowed by the background boundary conditions. The extremal charge density is $\rho = 1$. The dashed black lines correspond to the linear scaling $\beta\omega$, where β is fixed from the lowest frequency point of the numerical data.

At nonzero temperature, the numerical results of Fig.3.7 show that the subleading term depends quadratically on the frequency. We conclude therefore that for the general class of models with action Eq.(3.10), and for low frequency, the ac-conductivity is

$$\mathrm{Re}(\sigma) - \mathrm{Re}(\sigma_{\mathrm{dc}}) = a\omega + b\omega^2 + \dots \tag{3.43}$$

where $b \to 0$ for $T \to 0$ and, for $T \gg 0$, both constants tend to zero, but a does it faster than b. In other words, at large temperature we have observed a subleading contribution dominated by ω^2 while in the limit of zero temperature is proportional to ω^1. As was mentioned above, for $Z = 1$ and a minimally a coupled Maxwell field ($Y = 1$), the constants a and b are always negative, describing the broadening of the Drude peak. For $Y \neq 1$ and both $Z \neq 1$ and $Z = 1$, a is negative when $\mathrm{Re}(\sigma_{\mathrm{dc}}) > 1$ and positive when $\mathrm{Re}(\sigma_{\mathrm{dc}}) < 1$.

For $Y \neq 1$ and both at zero (not shown) and nonzero temperature (bottom left plot in Fig. 3.7), we have observed a range of parameters for which the ac-conductivity has a local maximum for relatively small frequencies. In Fig. 3.7 we observe that in the high temperature limit the local peak is smeared. A similar feature in the dc-conductivity has been recently reported in [163]. Similarly to the phenomenology observed in the temperature dependence of the dc-conductivity, we believe that, in the range of parameters of Fig. 3.7, this intermediate peak is a consequence of charge screening induced by a non-trivial

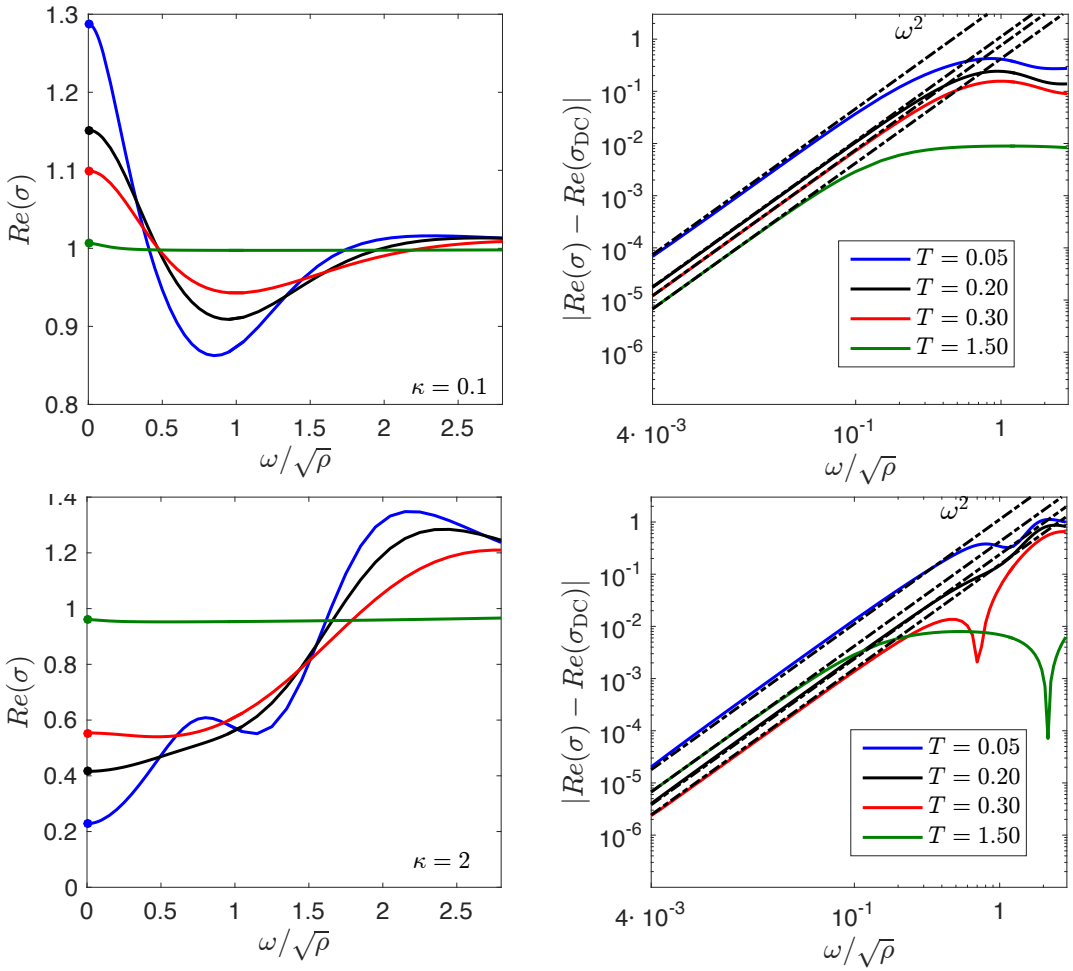

Figure 3.7: Ac-conductivity at finite temperature in the background given in Eqs. (3.10) and (3.33). Each line corresponds to a fixed temperature, indicated in the legend of the right-hand side plots. The dashed-dotted black lines correspond to the quadratic scaling and are fixed in the same way as in Fig. 3.6. As temperature decreases (blue lines) a slight disagreement is observed. We expect for near extremal solutions the frequency scaling is given by Eq.(3.43). The charge density $\rho = 1$, $\alpha = 1$, $\lambda = 0.15$ and κ is indicated in the left-hand side plots.

axion-dependent Maxwell coupling and therefore it is not a precursor of insulating behavior. Indeed the conductivity is always finite.

We have observed that a stronger gravitational interaction (larger BD coupling Z) has a similar impact on the intermediate peak as increasing momentum dissipation. As was mentioned in Sec. 3.3.2.2, in $d = 3$ boundary dimensions this is a nontrivial effect: a conformal transformation of the action Eq. 3.10 with $d > 3$ renormalises the Maxwell coupling in an analogous way to the conformal transformation of the BD model, see Eq. (3.8). However, for $d = 3$ the Maxwell coupling is invariant under such transformation and one could expect therefore the Maxwell coupling to be unchanged by a change in the BD coupling. Nonetheless, from a holographic point of view, it is known that the

observables in the boundary theory are roughly determined by the gravitational background (plus boundary values of bulk fields). Therefore, at intermediate energy scales, and despite the fact the Maxwell coupling is invariant under a conformal transformation for $d = 3$, one should expect the features of the BD background at intermediate length-scales to determine the ac-conductivity.

3.5.2 Argument and modulus of the ac-conductivity in BD gravity with momentum relaxation

A well known property of the ac-conductivity in most cuprates is that for intermediate frequencies the module of the conductivity scales as $\omega^{-2/3}$. It has been recently claimed [166] that a holographic setup where momentum relaxation is introduced by a modulating chemical potential share similar properties. However, we note that this holographic setup does not reproduce another property of the ac-conductivity in cuprates: the argument of the conductivity is constant in the same range of frequencies. In this section we study whether field theory duals of gravity models with different channels of momentum dissipation can reproduce these features of the ac-conductivity in cuprates.

Results for different values of the parameters are depicted in Fig. 3.8. Either the constant argument or the desired $2/3$ power-law decay can be observed for some values of the parameters. However, it is clear from our results that even by fine tuning all the available parameters we could not reproduce both features for a single set of parameters.

3.6 Ratio of shear viscosity and entropy density in BD with momentum relaxation

In this section we study the ratio η/s between the shear viscosity η and the density of entropy s for BD holography with momentum relaxation. In a quantum field theory the viscosity is defined through the Kubo formula:

$$\eta = -\lim_{\omega\to 0}\frac{1}{\omega}\mathrm{Im}G^R_{T^{xy}T^{xy}}(\omega, q=0)\ , \tag{3.44}$$

where T^{xy} is the xy component of the stress-energy tensor. In order to compute the viscosity in the model of Eq.(3.10) we use the membrane paradigm in a similar way as it has been used in sec. 3.2.2 for the calculation of the regular part of the dc-conductivity. While we restrict ourselves to numerical results we expect that, as shown in [187], it should be possible to derive quasi-analytical approximations at low and large temperatures.[20]

[20] An analytical calculation in terms of the background expansion close to the boundary is possible, however, the background needs to be computed numerically.

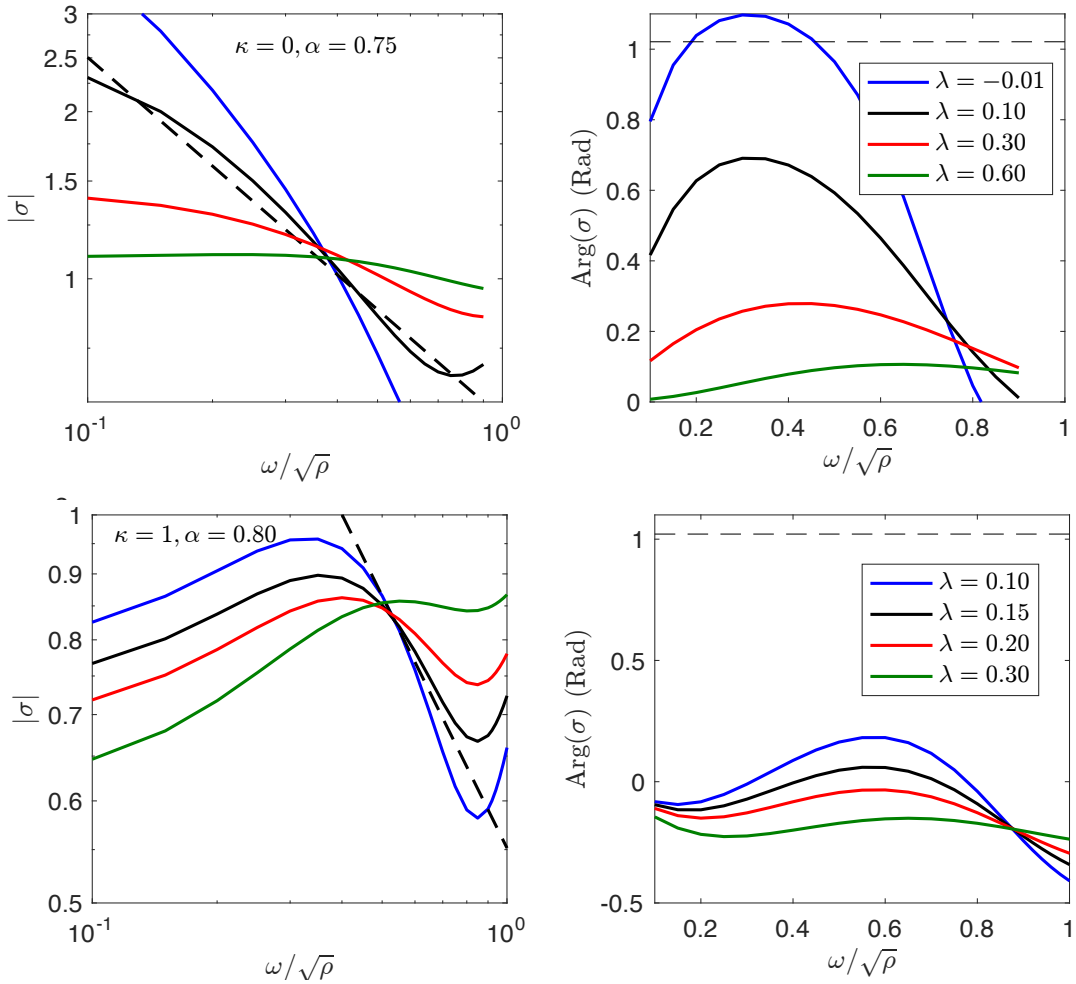

Figure 3.8: Absolute value and argument of the ac-conductivity for different values of the parameters. The temperature and charge density are $T = 0.05$ and $\rho = 1$. The BD model with the couplings of Eq. (3.33) does not describe the experimental behavior for intermediate frequencies observed for cuprates. The dashed lines are the exponent ξ, $|\sigma| = \omega^a$, $a = 1.35 - 2 = -0.65$, and $\arg(\sigma) = \frac{\pi}{2}(2 - 1.35) = 1.01$ Rad, according to experiments.

Previously it has been reported that in the presence of momentum relaxation [72,187–190] or anisotropy [191–193][21] the ratio is temperature dependent and in most cases below the KSS bound. We find similar results in the case of BD holography. For our analysis we use the couplings of Eq. (3.33) with $V = TrX$ (Fig. 3.9) and $V = 0$ (Fig. 3.10) which include, as a particular case, some of the previously studied cases of AdS RN+Stueckelberg [72, 187]. In the full range of parameters we have explored, the ratio decreases with temperature and is always below the KSS bound. It also decreases as the strength of momentum relaxation increases, by any of the channels explored. It seems that it can be made arbitrarily close to zero even for a finite momentum relaxation. We do not have a clear understanding of

[21] We note that in these models the effective mass of the graviton is nonzero. As shown in [194] this is a necessary condition to observe violation of the KSS bound. However, in theories without translational invariance and massless graviton [194] the KSS bound remains valid. Our model falls in the first class of theories.

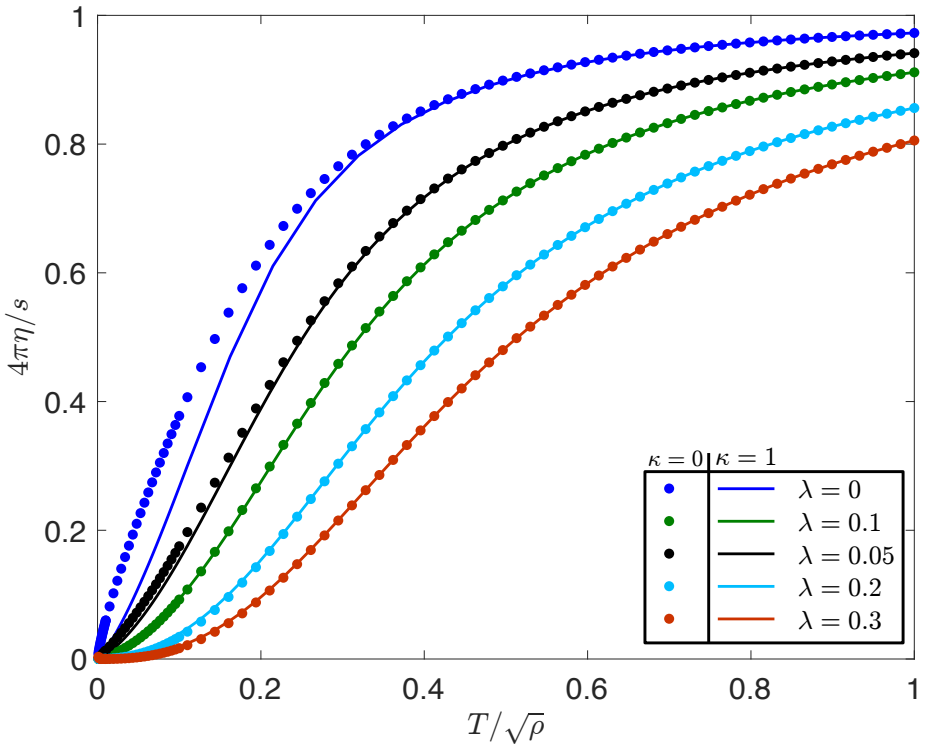

Figure 3.9: Shear viscosity to entropy density ratio (η/s) for the couplings of Eq. (3.33) in the model defined in eqs.(3.10) and Eq.(3.33). The axion parameter $\alpha = 1$ and the charge density $\rho = 1$.

the physical reasons behind this behavior however we note that similar results have been observed [195] in the context of the quark-gluon plasma with quenched impurities in the limit in which the phenomenon of Anderson localization becomes important.

3.7 Outlook and Conclusions

The potential interest of BD backgrounds in holography is well beyond the problems discussed in this work. For instance, the entanglement entropy depends explicitly on the gravity coupling constant and it is also very sensitive to the strength of bulk interactions. Therefore we expect that the holographic entanglement entropy in inhomogeneous BD backgrounds may reveal interesting features not found in previous holographic duals. These features would not only be present to leading order (area of minimal surface) but also in the quantum correction originated by the entanglement between the bulk and the minimal surface [196]. Another topic of potential interest is that of holographic superconductivity. It is well known that the ratio between the order parameter at zero temperature and the critical temperature, or the width of the coherence peak are useful indicators of the strength of the interactions binding the condensate. For the former, values much larger than the Bardeen-Cooper-Schrieffer prediction, suggesting strong interactions, are expected. It would

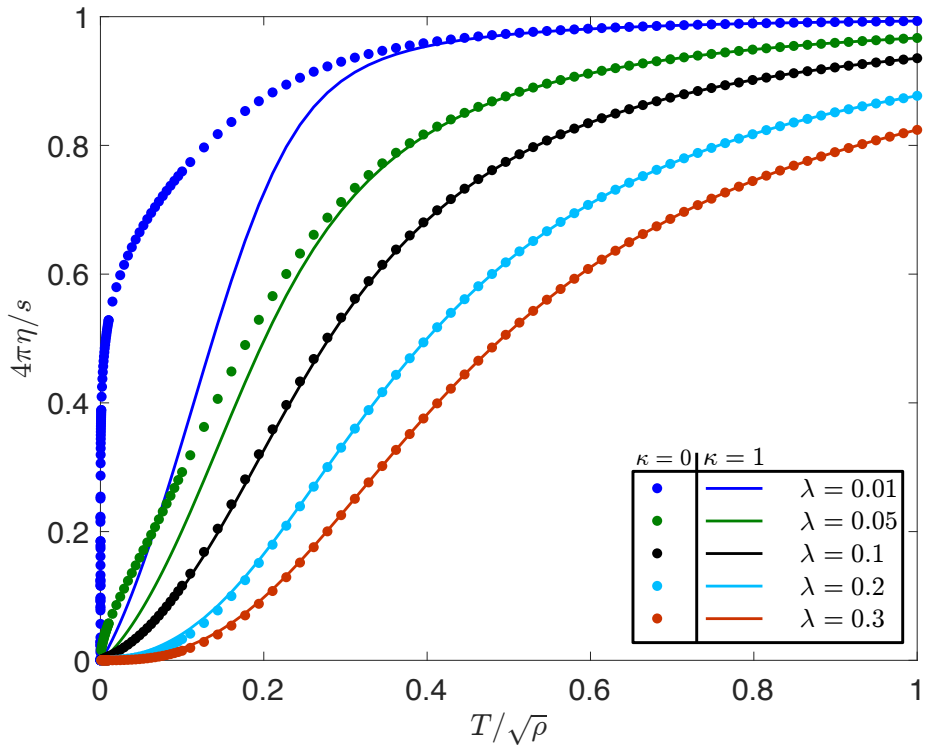

Figure 3.10: Shear viscosity to entropy density ratio (η/s) for the couplings of Eq.(3.33) in the model defined in eqs. (3.10) and Eq.(3.33) but taking $V = 0$ and $\dot{V} = 0$. The axion parameter $\alpha = 1$ and the charge density $\rho = 1$. As discussed in Sec. 3.3.2.1, for $\kappa = 0 \implies Y = 1$(dots) the theory has a single parameter that controls momentum dissipation, namely $\lambda_{\text{eff}} = \lambda\alpha^2$.

be interesting to investigate whether it is possible to tune this ratio in BD backgrounds. That would be a smoking gun that the scalar in BD backgrounds effectively controls the interactions in the bulk. Finally, we note that the introduction of randomness in the scalar is qualitatively different from other forms of disorder used in holography. It amounts to a random strength of the gravitational interaction. Mobile charge introduced through the gauge field will feel these random interactions not very differently from the way in which electrons felt quench impurities. This is in stark contrast with the effect of a random chemical potential, quite popular in holography, where the mobile carriers are by construction randomly but homogeneously distributed through the sample. Coherence phenomena like Mott-Anderson localization could not be observed in this setting.

In summary, we have investigated the transport properties of strongly coupled field theories whose gravity-dual is a Brans-Dicke action where gravity is mediated by both a tensor, the graviton, and a scalar that depends on the radial dimension. In the translational invariant limit we have computed analytically several transport properties. The finite part of the dc-conductivity σ_Q, expressed in terms of thermodynamic quantities, is different from the universal prediction for EMD backgrounds [161] however the shear viscosity ratio is still given by the KSS bound. Similar results apply to other generalised $f(R)$ gravity

backgrounds that can be mapped onto BD. The difference with EMD models is that the entropy does not hold an area law as it also depends on the value of the scalar at the horizon.

Momentum relaxation is induced by a gravitational axion, namely, the linear coupling of the Ricci tensor and the axion. Following the procedure pioneered by Donos and Gauntlett [182] we compute analytically the dc-conductivity as a function of the metric at the horizon which is evaluated numerically. In $d+1=4$ bulk dimensions momentum relaxation by a BD Stueckelberg field is qualitatively similar to the results obtained by other mechanism of momentum relaxation [54,163,164] in the limit of strong charge screening. Interestingly for strongly coupled gravitational Stueckelberg fields, that induce strong momentum relaxation, the conductivity bound [97] is violated for any finite charge screening induced by the electromagnetic axion [163,164].

In higher spatial dimensions the dc-conductivity for sufficiently strong momentum relaxation decreases in the low temperature limit. This suggests that the analogous conductivity bound is violated even if there is no coupling between the axion and the Maxwell field. We have also computed numerically the ac-conductivity in BD backgrounds with momentum relaxation. For sufficiently strong breaking of translational invariance, the conductivity grows linearly with the frequency in the limit of small frequencies and very low temperatures though it remains finite for any temperature and frequency. We have also evaluated numerically the modulus and the argument of the ac-conductivity for different momentum relaxation channels in order to find out whether the phenomenology of this model is similar to that of the cuprates for intermediate frequencies. Our results are not very encouraging. For any value of the parameters we could not reproduce the experimental results for both quantities simultaneously. Finally, we have shown that the shear viscosity to entropy ratio decreases with temperature and the KSS bound is violated by any strength of the momentum relaxation.

4 | Marginal and Irrelevant Disorder in Einstein-Maxwell backgrounds†

In this chapter we study analytically the effect of a weak random chemical potential of zero average in an Einstein-Maxwell background. For uncorrelated disorder this perturbation is relevant however we show that it can become marginal or even irrelevant by tuning disorder correlations. At zero temperature we find that, to leading order in the disorder strength, the correction to the conductivity for irrelevant perturbations vanishes. In the marginal case, in order to renormalise a logarithmic divergence, we carry out a resummation of the perturbative expansion of the metric that leads to a Lifshitz-like geometry in the infrared. Disorder in this case also induces a positive correction to the conductivity. At finite temperature the black hole acquires an effective charge and the thermal conductivity has the expected Drude peak that signals the breaking of translational invariance. However the electric conductivity is not affected by the random chemical potential to leading order in the disorder strength.

4.1 Introduction

Disorder plays an important role on the transport properties of interacting electrons in solids. A small amount of disorder in systems with translational symmetry makes the dc-conductivity finite. Similarly, disorder slows down the classically diffusive dynamics of electrons in solids at finite temperature. In real materials disorder is typically introduced by chemical doping which in some cases obscures its effect: the conductivity may increase because the slow down of the motion caused by disorder is counterbalanced by the addition of new carriers.

By contrast, in the limit of vanishing temperature and interactions quantum coherence phenomena enhance dramatically the effect of disorder. According to the one parameter scaling theory of localisation [38], classical diffusion in two and lower dimensions is completely arrested for any disorder and sufficiently long times. This quantum coherence phenomenon, usually referred to as Anderson localisation [35], also occurs in higher dimensions [197] for sufficiently strong disorder. Qualitative calculations [49, 50] in the physics literature and

[2]This Chapter is based on Ref. [61], and was done in collaboration with Antonio M. García-García.

more rigorous, but restricted to mean-field interactions, mathematical results [198] agree that Anderson localisation for sufficiently strong disorder still persists in the presence of weak interactions. This novel state of quantum matter is usually referred to as many-body localised. However the stability of the many-body localised phase in strongly-interacting regimes remain an open question. The detailed understanding of the interplay between disorder and interactions is seriously hampered by computational limitations and the lack of analytical tools to tackle strong interactions. This rich repertoire of disorder-induced phenomenology summed to the challenging open problems regarding the interplay between disorder and strong-interactions in electronic systems offer sufficient motivation for studying disorder in the context of charged holographic theories.

Indeed there are already several studies of the role of disorder in a strongly-coupled field theory with a gravity-dual. Originally disorder was introduced [22,63,74] as a deformation of the boundary field theory that coupled the random potential to an operator of the conformal field theory. The addition of this perturbation breaks translational invariance so effectively the role of disorder was to induce momentum relaxation which alters substantially the transport properties of the dual field theory.

In the context of holographic superconductors the effect of a random chemical potential has been studied numerically but only in the probe limit where disorder does not backreact in the metric [87, 88]. Disorder has also been considered in hyperscaling violating backgrounds, also in the probe limit [199–201]. Backreaction effects of a weak but marginally disordered scalar at zero temperature leads to logarithmic divergences in the infrared that suggest an instability of the perturbation theory [90, 91]. However it was later proposed [33] that that these divergences were an artefact of the perturbation theory in non-linear problems that could be cured by the Poincaré-Lindstedt method. The resulting metric in the infrared, after an effective resummation of logarithmic corrections, becomes Lifshitz-like with a dynamical critical exponent that depends on the strength of disorder. In the infinite temperature case [92, 202] it seems that the presence of a horizon prevents any Lifshitz scaling in the infrared. Numerical simulations for stronger disorder [33, 202], still for a disordered scalar at zero and finite temperature, have not shown any qualitative change to these results.

In the context of Einstein-Maxwell theories it has been recently proposed [59, 83] a general expression for the averaged conductivity in gravity-duals, modified by disorder or any other source of inhomogeneity, in terms of the solution of the Einstein equations for the metric. The study of these solutions has just started: the effect of weak disorder in the Einstein-Maxwell theory induced by a random chemical potential including backreaction effects, recently studied by O'Keefe and Peet [94], reveals surprising features like a conductivity that increases with disorder. We note that the disorder investigated in Ref. [94] is a relevant perturbation that leads to linear, instead of logarithmic, divergences in the metric. Although the Poincaré-Lindstedt method is technically applicable in this case it is less clear that these

divergences are really an artefact of the perturbation theory.

Here we revisit this problem by studying an Einstein-Maxwell background with a random, but in general correlated, chemical potential of zero average at zero and finite temperature. By modifying the correlations of the disordered chemical potential we tune the conformal dimension of the gauge field so that we can also investigate irrelevant and marginal perturbations. In the limit of zero temperature we have found that, to leading order, irrelevant perturbations do not modify the conductivity in the limit of zero temperature. By contrast, for marginal disorder the corrections to the conductivity are positive. In this case the metric develops perturbative logarithmic singularities in the infrared that can be resummed by using the Poincaré-Lindstedt method [33]. The resulting geometry is Lifshitz-like in the infrared with a dynamical critical exponent that depends on the disorder strength. In the finite temperature case the effect of perturbative disorder is weaker. The electrical conductivity does not get corrections in the disorder strength to leading order though the black-hole becomes charged even in this limit.

We start by introducing the Einstein-Maxwell theory with a random but correlated chemical potential.

4.2 Correlated Disorder in the Einstein-Maxwell background

We investigate the interplay of disorder and interactions in field theories with a gravity dual. For that purpose we study an asymptotic AdS Einstein-Maxwell theory in $d+1=4$ space-time dimensions with a random chemical potential given by the action

$$S=\int \mathrm{d}^4x\sqrt{-g}\left(R+6-\frac{1}{4}F^2\right), \tag{4.1}$$

where F is the Maxwell tensor, R the scalar curvature. For convenience we have set $l_{\mathrm{AdS}_4}=2\kappa_4^2=e^2=1$. We choose to work in Fefferman-Graham coordinates $\mathrm{d}s^2=r^{-2}\left(\mathrm{d}r^2+g_{\mu\nu}(r,x^\mu)\mathrm{d}x^\mu\mathrm{d}x^\nu\right)$ which we suppose are globally defined. Here $r=0$ is the AdS boundary, with coordinates $x^\mu=(t,x,y)$. The equations of motion are given by

$$R_{ab}+3g_{ab}=\frac{1}{4}F^c{}_aF_{bc}-\frac{1}{8}g_{ab}F^2, \tag{4.2a}$$

$$\partial_a\left(\sqrt{-g}F^{ab}\right)=0. \tag{4.2b}$$

We are only interested in spatially inhomogeneous solutions of the equations above, for which neither the metric components nor the gauge field depend on time. Therefore the $U(1)$ gauge field $A=a_t(r,\mathbf{x})\mathrm{d}t$, which we assume is the only non-zero component, and the

metric $g_{\mu\nu}(r,\mathbf{x})$ depends explicitly on the bulk (r) and the boundary spacelike coordinates ($\mathbf{x}$). This system of equations support both zero and finite temperature solutions, which are specified by the IR and UV boundary conditions. For the zero temperature case, we require all metric components and the gauge field to be regular at the Poincaré horizon $r \to \infty$. For the finite temperature case, we require the existence of a horizon, *i.e.* a point $r_0 \in (0,\infty)$ such that $g_{tt}(r,\mathbf{x}) \sim \gamma_{tt}(\mathbf{x})(r-r_0) + O\left((r-r_0)^2\right)$ and $g_{rr}(r,\mathbf{x}) \sim \frac{\gamma_{rr}(\mathbf{x})}{r-r_0} + O\left(1\right)$ for $|r-r_0| \ll 1$, with all other components g_{ij} regular. Similarly, close to the boundary we impose,

$$\lim_{r\to 0} g_{ab}\mathrm{d}x^a\mathrm{d}x^b = r^{-2}\left(\mathrm{d}r^2 - \mathrm{d}t^2 + \mathrm{d}x^2 + \mathrm{d}y^2\right), \tag{4.3a}$$

$$\lim_{r\to 0} a_t(r,\mathbf{x}) = \mu(\mathbf{x}). \tag{4.3b}$$

According to the holographic dictionary the bulk action Eq.(4.1), with the above boundary conditions, is dual to a $d=3$ conformal field theory at finite chemical potential $\mu(\mathbf{x}) = \lim_{r\to 0} a_t(r,x)$. Disorder is introduced, in one or both boundary directions, through a random chemical potential in the boundary $\mu(\mathbf{x})$. Next we give a detailed account of the properties of this random chemical potential so that we can use it to model irrelevant and marginal perturbations in the dual field theory.

4.2.1 Correlated disorder and relevance of perturbations

We introduce disorder in the holographic setting by imposing that the chemical potential $\mu(\mathbf{x})$ is a stochastic field depending on the spacelike boundary coordinates. This random boundary condition promotes the vector potential $A = a_t(r,\mathbf{x})\mathrm{d}t$ and the metric components to stochastic processes indexed by $\mathbf{x}$. Similarly the equations of motion Eqs.(4.2a) and (4.2b) becomes stochastic equations.

We specify the distribution of $\mu(\mathbf{x})$ by a spectral decomposition

$$\mu(\mathbf{x}) = \bar{V}\int_{\mathbb{R}^n} \frac{\mathrm{d}^n k}{(2\pi)^n}\, e^{i\mathbf{k}\cdot\mathbf{x}}\mu_{\mathbf{k}}, \tag{4.4}$$

where $n=1$ if disorder is only in one direction or $n=2$ if disorder is in both directions and the parameter $\bar{V}$ measures the amplitude of the source ($\mu \sim O\left(\bar{V}\right)$). Further, we assume $\mu_{\mathbf{k}}$ is a spectral stochastic process taking values in a normal distribution with zero average $\mathbb{E}[\mu_{\mathbf{k}}] = 0$ and variance $\sigma^2_{\mathbf{k}}$, with $\mathbb{E}[\dots]$ denoting the average with respect to the normal distribution. From now on we will restrict ourselves to isotropic disorder $\mu_{\mathbf{k}} = \mu_k$ so that Eq.(4.4) can be written effectively as a one-dimensional integral $\int_{\mathbb{R}^n}\mathrm{d}^n k = \mathrm{Vol}(\mathbb{S}^n)\int_{0^+}^{\infty}\mathrm{d}k\; k^{n-1}$. We stress that even though μ_k is normally distributed, this does not imply $\mu(\mathbf{x})$ is also normal. This will be the case only if σ_k^2 is independent of k. It was shown recently [94] that when $\sigma_k^2 = 1$, the weak disordered chemical potential $\bar{V} \ll 1$ is relevant perturbation in the RG sense,

casting some doubts on the reliability of their perturbative approach.

Interestingly the relevance, or not, of the deformation depends on the disorder correlations as the mass dimension of $\bar{V}$ is controlled by the mass dimension of σ_k^2. Specifically, we have $[\mu] = [\bar{V}] + n + [\mu_k] = [\bar{V}] + \frac{1}{2}(n + [\sigma_k^2])$. Therefore introducing powers of k in σ_k makes disorder more and more irrelevant. For instance assuming $\sigma_k^2 \propto k^s$

$$[\bar{V}] = 1 - \frac{n+s}{2}. \tag{4.5}$$

Therefore disorder is relevant ($\bar{V} > 0$) when $n + s < 2$, marginal ($\bar{V} = 0$) when $n + s = 2$ and irrelevant ($\bar{V} < 0$) when $n + s > 2$. In the following we will restrict to marginal and irrelevant perturbations by employing correlated potentials such that $n + s \geq 2$. Surprisingly, we shall see that this *a priori* naive power counting actually determines the perturbative flow of the RG in the Einstein-Maxwell system. Finally we note that for a fixed s, increasing the number of dimensions in which we introduce disorder makes disorder less relevant. The fact that translation invariance is left unbroken in a bulk direction constrains the dynamics of the fields to the orthogonal directions. It is therefore no surprise that disorder is more relevant in this case. Indeed it is a well known result in condensed matter systems that disorder is more relevant in lower dimensional systems [38].

4.2.2 Explicit implementation of disorder

We have now all the ingredients to define the correlated disordered potential to be employed in the rest of the paper. For most of the analytical calculations we shall employ Eq.(4.4) assuming isotropic disorder [22] and a normal μ_k with zero average $\mathbb{E}[\mu_k] = 0$ and variance given by

$$\sigma_k^2 = 2^{s+1} k^s e^{-2ka}. \tag{4.6}$$

Note that the exponential factor assures convergence of the boundary deformation by smoothly suppressing high-momenta modes. This introduces a UV length scale $a = 1/k_0$, necessary to cure divergences for irrelevant perturbations, which can be interpreted as a lattice constant that effectively suppresses modes with wavelength smaller than the lattice spacing. We stress that since we are interested on averaged quantities that are computed analytically an explicit expression for $\mu(\mathbf{x})$ is not necessary.

However in the finite temperature case we shall find more convenient at times to employ the following discrete representation of the random chemical potential commonly used in

[22] When working in higher dimensions, we denote $k = |\mathbf{k}|$. In one dimension we explicitly include the modulus to avoid ambiguities.

the holography literature [33, 87–89, 92, 94, 202, 203],

$$\mu(\mathbf{x}) = \bar{V} \sum_{\{m_i\}=1}^{N-1} A_{\{m_i\}} \prod_{i=1}^{n} \cos(k_{m_i} x^i + \gamma_m). \tag{4.7}$$

where $A_{\{m_i\}} = \bar{V}(\sqrt{\Delta k \sigma_{\{m_i\}}})^n$ with $\Delta k = k_0/N$ and $k_{m_i} = m_i \Delta k$. Here $\gamma_m \in [0, 2\pi)$ are i.i.d. uniform random phases. Further, we define $\Delta k = k_0/N$ and $k_{m_i} = m_i \Delta k$. Averages $\mathbb{E}[\cdots]$ in this representation are taken with respect to uniformly distributed random phases γ_m, the variance is given by Eq. (4.6). Note that, different from the continuous representation in Eq.(4.7), here the UV cutoff $k_0 = 1/a$ is sharp and applied directly to the sum. Note that in this representation there is also a natural IR scale $k_* = 1/L = 1/Na$ which is only taken to zero in the averaging procedure.

Both the discrete and the continuous representations are equivalent in the limit $a \to 0$ and $L \to \infty$. For finite values of the cutoffs we still expect qualitatively similar results.

4.3 Random chemical potential at zero temperature

In this section we study the $d + 1 = 4$ Einstein-Maxwell action at zero temperature in the presence of a weak and correlated random chemical potential. We investigate the cases of disorder acting in one and two boundary space dimensions. Although both cases are quantitatively different, they have a similar IR behaviour as long as correlations are chosen so that disorder is marginal. For marginal disorder we find logarithmic IR divergences in the metric that can be resummed by the Poincaré-Lindstedt method leading to a Lifshitz-like metric. We proceed with the calculation of the DC conductivity for both irrelevant and marginal disorder. We find the perturbative correction vanishes for irrelevant disorder and is positive for marginal disorder. The divergence of the marginal flow signals an instability of the system towards, possibly to a charged ground state at finite temperature.

4.3.1 Metric corrections for disorder in one dimension

Consider the action (4.1) with boundary conditions (4.3) at zero temperature. We fix coordinates $x^\mu = (t, x, y)$ in the boundary and restrict disorder to act only in the x direction. Following the discussion in section 4.2.1, we introduce disorder by requiring $\mu(x)$ to be a homogeneous random field with spectral decomposition

$$\mu(x) = \bar{V} \int_{\mathbb{R}} \frac{\mathrm{d}k}{2\pi}\, e^{ikx} \mu_k,$$

where μ_k is a gaussian spectral process with zero mean. Finding exact solutions of the system (4.2) is a hard task so we restrict ourselves to a perturbative analysis in disorder

strength $\bar{V}$. According to Eq.(4.5), for $\sigma_k = 1$ we have $[\bar{V}] = 1/2 > 0$ and therefore disorder is relevant in this case. A perturbative analysis is therefore inadequate, as disorder can drive the theory to a new fixed point far from AdS_4. This lead us to consider correlated disorder with $\sigma_k = 2^{s+1}|k|^s e^{-2|k|a}$. It is easy to see that by choosing $s = 1$ disorder will be marginal. Therefore we might be able to find new disordered fixed points close to AdS_4 by adapting the analysis of Hartnoll and Santos [33] for a scalar coupled to gravity to the case of Einstein-Maxwell theory.

To set up the perturbation theory, we write the most general static line element in Fefferman-Graham coordinates compatible with our boundary conditions

$$\mathrm{d}s^2 = r^{-2}\left[-A(r,x)\mathrm{d}t^2 + \mathrm{d}r^2 + B(r,x)\mathrm{d}x^2 + D(r,x)\mathrm{d}y^2\right],$$

and proceed with a perturbative expansion in $\bar{V} \ll 1$

$$\begin{aligned} A(r,x) &= 1 + \bar{V}^2\alpha(r,x) + O(\bar{V}^2), & B(r,x) &= 1 + \bar{V}^2\beta(r,x) + O(\bar{V}^2), \\ D(r,x) &= 1 + \bar{V}^2\delta(r,x) + O(\bar{V}^2), & a_t(r,x) &= \bar{V}\varphi(r,x) + O(\bar{V}^3), \end{aligned}$$

where all $\alpha, \beta, \delta, \varphi$ have been lifted to stationary stochastic processes via the boundary conditions and Einstein's Equations. Note that to order $\bar{V}^0$ the background is pure AdS_4. To order $\bar{V}^1$, Maxwell's Equation (4.2b) is a Laplace equation

$$\partial_r^2\varphi + \partial_x^2\varphi = 0,$$

which can be solved by decomposing $\varphi(x) = \int \frac{\mathrm{d}k}{2\pi}\, e^{ikx}\varphi_k(r)$ and imposing the boundary conditions (4.4) together with regularity at $r \to \infty$:

$$\varphi(r,x) = \int \frac{\mathrm{d}k}{2\pi}\, e^{-|k|r+ikx}\mu_k. \tag{4.8}$$

We now need to insert this into the $O(\bar{V}^2)$ Einstein's Equations, that can be reorganised to give:

$$\partial_r\left[r^{-2}\partial_r(\alpha+\delta)\right] = \frac{1}{2}\left[(\partial_r\varphi)^2 - (\partial_x\varphi)^2\right], \tag{4.9a}$$

$$r^2\partial_r\left(r^{-1}\partial_r\beta\right) = -\partial_r(\alpha+\delta), \tag{4.9b}$$

$$\partial_r\partial_x(\alpha+\delta) = r^2\partial_r\varphi\partial_x\varphi, \tag{4.9c}$$

$$2r^3\partial_r\left[r^{-2}\partial_r(\alpha-\delta)\right] + 2r\partial_x^2(\alpha-\delta) = 2r^3\left[(\partial_r\varphi)^2 + (\partial_x\varphi)^2\right]. \tag{4.9d}$$

In practice this can be solved explicitly by inserting Eq. (4.8) in the right hand side of the above equation, developing α, β, γ in harmonics and integrating the resulting einstein-max:eq:eom's. However, since we are not interested in the specific realizations of the random

geometry but rather in the possible IR averaged fixed points, we take the average of the above equations:

$$\mathbb{E}[(\partial_r\varphi)^2 - (\partial_x\varphi)^2] = 0, \tag{4.10a}$$

$$\mathbb{E}[(\partial_r\varphi)^2 + (\partial_x\varphi)^2] = \int_{0^+}^{\infty} \frac{\mathrm{d}k}{2\pi}\, 2^{s+2}k^{s+2}e^{-2k(r+a)} = \frac{\Gamma(s+3)}{4\pi(r+a)^{s+3}}. \tag{4.10b}$$

where we assumed $s > -3$ [23]. From the above it is clear that the solutions of equations (4.9a) and (4.9b) are regular for all $r \geq 0$ while solutions of (4.9d) can develop divergences depending of the value of s. Explicitly we have:

$$\mathbb{E}[\alpha + \delta] = \eta, \tag{4.11a}$$

$$\mathbb{E}[\beta] = \eta, \tag{4.11b}$$

$$\mathbb{E}[\alpha - \delta] = -\frac{\Gamma(s+3)}{4\pi(s+2)} \int \frac{\mathrm{d}r}{(r+a)^s} \propto \begin{cases} \log(r+a) & \text{for } s = 1, \\ (r+a)^{1-s} & \text{for } s \neq 1. \end{cases} \tag{4.11c}$$

where we have imposed regularity at $r \to \infty$ and the boundary conditions $\mathbb{E}[(\alpha-\delta)(x,0)] =$ const. Note that this result reproduces exactly what we naively expect from the power counting analysis: for $s < 1$, disorder is relevant and therefore the perturbation scheme breaks down with the appearance of power law divergences in the deep IR $r \to \infty$. For $s > 1$, disorder is irrelevant, and indeed the background flows to pure AdS_4 in the IR. For $s = 1$ disorder is marginally relevant, as signalled by a log divergence as we flow towards the IR. This log behaviour was first observed in [91] and later reproduced in [33, 92] in the case of a disordered scalar. Our analysis for the charged case suggests that the log divergences for marginal deformations are a quite general feature of holographic disorder.

Resummation of the metric for marginal disorder

In a perturbative RG analysis, one is interested in how the deformation of a given action can change the IR behaviour of the theory. Divergences signal an instability of the flow towards new fixed points. In particular, logarithmic divergences are usually associated with marginal deformations which can sometimes be resummed, to all orders, to give the explicit IR effective action [16]. A similar procedure to resum log divergences in Holography was first proposed by Hartnoll and Santos [33]. As was mentioned in the introduction, the upshot is that log divergences in holography are associated with IR geometries that can be characterised by their scaling properties. In the case of scalar deformations, they found an emergent Lifshitz scaling with dynamical critical exponent $\bar{z}(\bar{V})$ which is an increasing function of disorder.

[23] We are not interested in the range $s < 0$ since we already know disorder is relevant in this case a perturbative approach is not adequate.

The general idea is to modify the metric ansatz by including a function that regularise the divergences order by order in perturbation theory, similar to the Poincaré-Lindsteadt method used in the study of non-linear oscillators. Our ansatz is

$$\mathrm{d}s^2 = \frac{1}{r^2}\left[-\frac{A(r,x)}{F_1(r)^{p(\bar{V})}}\mathrm{d}t^2 + \mathrm{d}r^2 + B(r,x)\mathrm{d}x^2 + \frac{D(r,x)}{F_2(r)^{q(\bar{V})}}\mathrm{d}y^2\right],$$

and consists of corrections only to the IR diverging components of the metric. Since divergences appear in the second order of perturbation theory, we can expand $p(\bar{V}) = p_2\bar{V}^2 + O(\bar{V}^4)$ and $q(\bar{V}) = q_2\bar{V}^2 + O(\bar{V}^4)$ and require $\lim_{r\to 0} F_{1,2} = 1$ in order to preserve the UV physics. The equations of motion (4.9) now read:

$$\begin{aligned}
\partial_r\left[r^{-2}\partial_r\left(\alpha+\delta-\log F_1^{p_2}F_2^{q_2}\right)\right] &= \frac{1}{2}\left[(\partial_r\varphi)^2-(\partial_x\varphi)^2\right],\\
r^2\partial_r\left(r^{-1}\partial_r\beta\right) &= -\partial_r\left(\alpha+\delta-\log F_1^{p_2}F_2^{q_2}\right),\\
\partial_r\partial_x(\alpha+\delta) &= r^2\partial_r\varphi\partial_x\varphi,\\
r^2\partial_r\left[r^{-2}\partial_r\left(\alpha-\delta-\log\frac{F_1^{p_2}}{F_2^{q_2}}\right)\right] + \partial_x^2\left(\alpha-\delta\right) &= r^2\left[(\partial_r\varphi)^2+(\partial_x\varphi)^2\right].
\end{aligned}$$

From the above it is clear that choosing $F_1 = F_2 = F$ and tuning $p = 1/4 = -q$ leaves $\alpha+\delta$ and β unchanged while shifts $\alpha-\delta \to \alpha-\delta-\log F(r)^{1/2}$ by the log of an arbitrary function $F(r)$. Any choice of $F(r)$ satisfying the constraint $F(0) = 1$ and such that $F(r) \sim r^2$ as $r\to\infty$ will regularise the IR log divergence previously found (*e.g.* $F(r) = 1 + (r/a)^2$). Up to a rescaling of the coordinates by a constant, the averaged IR metric can then be written as:

$$\mathbb{E}[\mathrm{d}s^2_{IR}] \sim -\frac{\mathrm{d}t^2}{r^{2b_1}} + \frac{\mathrm{d}r^2+\mathrm{d}x^2}{r^2} + \frac{\mathrm{d}y^2}{r^{2b_2}},$$

for $b_1 = 1 + \bar{V}^2/4 + O(\bar{V})^4$ and $b_2 = 1 - \bar{V}^2/4 + O(\bar{V})^4$. The emergent IR metric has an anisotropic scaling symmetry in the bulk directions. This should not be a surprise since isotropy is broken by disorder. Next we show isotropy is recovered by considering disorder in both boundary space directions.

4.3.2 Metric corrections for disorder in two dimensions

In the previous section, we found that working with the averaged geometry is enough to determine the instability of the RG flow. The way the metric diverges is intimately connected to the emergent scaling behaviour of the IR disordered fixed points. In this section we show that a similar log divergence emerges when disorder is considered in all space boundary directions. The advantage is that isotropy is recovered, making easier to generalise to higher dimensions and finite temperature. As expected, the resulting metric

has an emergent Lifshitz scaling in the IR.

The framework used above can be generalised to include disorder in both bulk directions (x, y) with the changes:

$$k \to \mathbf{k} = (k_x, k_y), \qquad x \to \mathbf{x} = (x, y), \qquad \int \mathrm{d}k \to \int \mathrm{d}^2 k.$$

The power counting (4.5) now give us $[\bar{V}] = -s/2$, and disorder is marginal for $s = 0$. This is not surprising, since by performing the above changes in Eq. (4.10b), it is clear that the double integral contributes with an additional power of k.

The only difference in the averaged equation of motion is the appearance of non-trivial y dependence in the gauge field A components. They can be conveniently rearranged as [24]:

$$4\partial_r \left[r^{-2}\partial_r \alpha\right] = \mathbb{E}\left[3(\partial_r\varphi)^2 + (\nabla\varphi)^2\right] = \frac{3}{2\pi}(r+a)^{-4}, \tag{4.12a}$$

$$2\partial_r \left[r^{-2}\partial_r \left(\beta+\delta\right)\right] = -\mathbb{E}\left[(\partial_r\varphi)^2 + (\nabla\varphi)^2\right] = -\frac{3}{4\pi}(r+a)^{-4}, \tag{4.12b}$$

$$\partial_r \left[r^{-2}\partial_r \left(\beta-\delta\right)\right] = \mathbb{E}\left[(\partial_x\varphi)^2 - (\partial_y\varphi)^2\right] = 0, \tag{4.12c}$$

$$2\partial_r \left[r^{-2}\partial_r \left(\alpha+\beta+\delta\right)\right] = r\,\mathbb{E}\left[(\partial_r\varphi)^2 - (\nabla\varphi)^2\right] = 0, \tag{4.12d}$$

where we introduced the bulk gradient $\nabla = (\partial_x, \partial_y)$. As advertised, now disorder does not break isotropy in the bulk, and this is reflected in the equations of motion (4.12b). In the one dimensional case $\mathbb{E}[\partial_y\varphi] = 0$ and the average in the right hand side do not vanish. The equations above can be easily solved to give:

$$\alpha = -(\beta+\delta) = -\frac{1}{8\pi}\log(r+a),$$

which is in agreement with marginally relevant deformations. In analogy with the one dimensional case, it is again possible to resum these logarithmic corrections. Up to a coordinate redefinition, the IR geometry will take the form:

$$\mathbb{E}[\mathrm{d}s^2_{IR}] \sim -\frac{\mathrm{d}t^2}{r^{2\bar{z}}} + \frac{\mathrm{d}r^2}{r^2} + \frac{\mathrm{d}x^2+\mathrm{d}y^2}{r^2}.$$

with $\bar{z} = 1 + \bar{V}^2/2 + O(\bar{V}^4)$. This IR fixed point corresponds to a quantum field theory with *Lifshitz* scaling, since it is invariant under $(t, x, y) \to (\lambda^{\bar{z}}t, \lambda x, \lambda y)$. The emergence of Lifshitz scaling in the context of disordered holography was first observed in [33]. It is an interesting fact that Lifshitz-like scaling emerges in different dimensions and for different random sources. This suggests that Lifshitz geometries in the IR are a robust feature of marginal disorder in holography.

[24] To avoid charging the notation, we conveniently denote $\mathbb{E}[\alpha(r,x)] = \alpha(r)$, etc.

4.3.3 Conductivity of the dual field theory

We now turn our attention to how disorder affects the transport of the dual theory. In condensed matter, the effect of weak disorder in a metal is to decrease the conductivity [204]. This is the first sign that for strong enough disorder the system undergoes a metal-insulator transition. According to the *scaling theory of localisation* [38, 205] (or [204] for a review) the knowledge of the scaling of the conductance with the system size allows to derive a real space RG equation and eventually to establish the existence of the metal-insulator transition.

In holography, it was established that a range of theories in both zero and finite temperature have a finite and constant incoherent contribution to the conductivity in addition to the usual coherent contribution coming from a finite charge density [57]. In particular this contribution is also present at zero temperature and charge density [8, 136]. Our aim is to understand how disorder affects this contribution. For simplicity, we work with disorder in one dimension and compute the dc-conductivity in this direction. We will show that an irrelevant disordered chemical potential does not contribute to the conductivity, while a marginal deformation has the effect of increasing it. In both cases disorder does not suppress the incoherent contribution to the conductivity. It is an open question why those degrees of freedom seem to be protected from relaxation. In principle this is different from the behaviour expected in condensed matter systems where disorder always suppresses the conductivity. We note that a direct comparison is difficult as our perturbation may also induce a net increase of carriers that enhance the conductivity.

Computing transport coefficients in inhomogeneous backgrounds is an involved task. Since we are only interested in the DC conductivity, we are going to take a shortcut first proposed by Donos and Gauntlett in Ref. [59] which consist in applying a constant electric field $E^x \equiv E$ in the disordered direction at the dual boundary theory. In the bulk, this is implemented by a fluctuation in the vector potential that solves the time dependence of the Maxwell's Equations,

$$\delta A = (a_x(r,x) - Et)\mathrm{d}x.$$

This fluctuation generates a non-trivial boundary current obtained via the usual holographic dictionary $j^x = \lim_{r\to 0} \partial_r a_x$. The conductivity is then defined as

$$\sigma = \left.\frac{\mathbb{E}[j^x]}{E}\right|_{r=0}. \tag{4.13}$$

The fluctuation above also couples to the metric via the Einstein's Equations, and consistency require turning on metric fluctuations. In a radial gauge $h_{ra} = 0$ for $a \in \{r, t, x, y\}$, the Einstein's Equations decouple in two sectors, and is sufficient to consider only the metric fluctuation h_{tx}.

As in the previous section, we proceed with a perturbative analysis. Inspection of the equations of motion to first order in E and second order in $\bar{V}$ requires

$$a_x(r,x) = a_x^{(0)}(r,x) + \bar{V}^2 a_x^{(2)}(r,x) + O(\bar{V}^4), \qquad h_{tx}(r,x) = \bar{V} h_{tx}^{(1)} + O(\bar{V}^3).$$

Note in particular that we need to expand the fluctuation a_x to $O(\bar{V}^2)$ in order to respect the holographic dictionary and match the boundary current $j^x = \lim_{r\to 0} \partial_r a_x$ to the bulk current $\sqrt{-g}F^{xr}$. To compute the conductivity from Eq.(4.13) we need to solve the Einstein-Maxwell system order by order for $\{a_x^{(0)}, a_x^{(2)}, h_{tx}^{(1)}\}$ and take the relevant average over disorder. As boundary conditions for the fluctuations, we require δA_x to be ingoing and the dual field theory Minkowski metric to be fixed, or in other words $\lim_{r\to 0} r^2 h_{tx} = 0$[25].

To order $\bar{V}^0$, the (r) and (x) Maxwell's Equations give

$$\begin{aligned} \partial_r \partial_x a_x^{(0)}(r,x) &= 0, \\ \partial_r^2 a_x^{(0)}(r,x) &= 0, \end{aligned}$$

which implies $\partial_r a_x^{(0)} =$ constant. To fix this constant, we need to apply ingoing boundary conditions. Note that $\bar{r} = t - r$ and $v = t + r$ are the two null coordinates in AdS_4. Therefore for the fluctuation to be ingoing, we require $\delta A_x(r,t,x) = \delta A_x(x,v)$ which fixes $\partial_r a_x^{(0)} = -E$. This gives the order $O(\bar{V}^0)$ contribution to the DC conductivity $\sigma = 1 + O(\bar{V}^2)$, which agrees with the pure AdS_4 value.

The order $O(\bar{V}^2)$, the (r) and (x) Maxwell's Equations read

$$\partial_r \left[E(\alpha - \beta + \delta) - 2r^2 h_{tx}^{(1)} \partial_r \varphi - 2\partial_r a_x^{(2)} \right] = 0, \tag{4.14}$$

$$\partial_x \left[E(\alpha - \beta + \delta) - 2r^2 h_{tx}^{(1)} \partial_r \varphi - 2\partial_r a_x^{(2)} \right] = 0, \tag{4.15}$$

Note that these are exactly the equations for the conservation of the bulk current to $O(\bar{V}^2)$. They fix

$$\partial_r a_x^{(2)} = c - 2r^2 h_{tx}^{(1)} \partial_r \varphi + \frac{E}{2}(\alpha - \beta + \delta), \tag{4.16}$$

for an arbitrary constant c. Note that the average of the above is exactly the numerator in (4.13). Since $\mathbb{E}[\alpha - \beta + \delta] = 0$ everywhere in the bulk from Eqs. (4.11a), (4.11b) and $\lim_{r\to 0} \mathbb{E}[r^2 h_{tx}^{(1)} \partial_r \varphi] = 0$ to avoid deformations of the dual field theory Minkowski metric, c is exactly the correction the the conductivity we are after. To fix c, we need to impose ingoing boundary conditions in the Poincaré horizon $r = \infty$, or in other words $\delta A_x(r,t,x) =$

[25] We are grateful to Andrew Lucas for pointing this out.

$\delta A_x(v,x)$ for $v = t + r$. This fixes $\lim_{r\to\infty} \partial_r a_x^{(2)}(r,x) = 0$, and we can formally write

$$c = \lim_{r\to\infty} 2\mathbb{E}[r^2 h_{tx}^{(1)} \partial_r \varphi]. \tag{4.17}$$

As we mentioned before, the Einstein's equations for $h_{tx}^{(1)}$ decouple from the background

$$\partial_r \partial_x \left(r^2 h_{tx}^{(1)}\right) = r^2 E \partial_x \varphi,$$
$$\partial_r \left(r^{-2} \partial_r (r^2 h_{tx}^{(1)})\right) = E \partial_r \varphi,$$

and can be readily solved by inserting the source (4.8) and integrating,

$$r^2 h_{tx}^{(1)}(r,x) = E \int \frac{\mathrm{d}k}{2\pi} \mu_k 2^{s+1} k^{-3} e^{-kr+ikx} \left(2 + 2kr + k^2 r^2\right) + C(x),$$

where $C(x)$ is a (random) integration constant. We suppose $C(x)$ admits a spectral representation with gaussian measure and write $C(x) = \int \frac{\mathrm{d}k}{2\pi} e^{ikx} \mu_k c_k$ for a deterministic constant c_k. The boundary condition $\lim_{r\to 0} r^2 h_{tx} = 0$ then fixes $c_k = -2k^{-3}$. Note that with this choice we have in particular $\lim_{r\to 0} \mathbb{E}[r^2 h_{tx}^{(1)} \partial_r \varphi] = 0$ as claimed before. We can now explicitely fix c by computing the average in Eq. (4.17)

$$c = \begin{cases} 0 & \text{for } s > 1, \\ \frac{8\log 2 - 5}{\pi} & \text{for } s = 1. \end{cases}$$

Therefore for irrelevant disorder there are no corrections to the background conductivity to second order, $\sigma = 1 + O(\bar{V}^4)$, while for marginal disorder we have

$$\sigma = 1 + \bar{V}^2 \gamma + O(\bar{V}^4),$$

for $\gamma = \pi^{-1}(8\log 2 - 5) > 0$. This result is consistent with the previously discussed fact that for irrelevant deformations the background AdS_4 remains the IR fixed point of the system, while for marginal deformations the background geometry receives logarithmic corrections. Note that for $s < 1$ the deformation is relevant. In this case c diverges polynomially and perturbation theory breaks down.

One might ask if the resummation carried out in the last sections alters the computation of the conductivity. This is not the case since as we argued before the metric fluctuations decouple from the background equations of motion. Resumming the background IR divergence for marginal deformations therefore does not change the conductivity, which is finite in the IR.

4.4 Random chemical potential at finite temperature

A natural generalization of the previous discussion is to include the effects of temperature. In practice, this is equivalent to imposing an AdS black hole boundary condition to the vacuum, around which we carry out a perturbative calculation. From the field theory perspective, we will be studying the perturbative effect of a random chemical potential in a quantum field theory at finite temperature. In practice, the presence of a horizon spoils the symmetry between the boundary coordinates (t, x, y), which makes the calculations more involved. Following some previous ideas [92], we will see that the problem can be analysed in two opposite limits: high and low momenta modes. The high momenta modes will be exactly those that will contribute to the leading divergences of the metric components, therefore determining the emerging IR scaling. On the other hand, low momenta modes are constant along the bulk and will have the effect of renormalizing the temperature and charge of the black hole. We shall see that the initially uncharged black hole geometry develops an effective net charge proportional to the strength of the perturbation. Moreover to leading order in the disorder strength the thermal conductivity, but not the electrical conductivity, develops a Drude peak consistent with the breaking of translational symmetry by the random chemical potential.

4.4.1 Equations of Motion

Consider again the action (4.1). If $A = 0$, this action supports a finite temperature vacuum given by a $d+1 = 4$ AdS Schwarzschild black hole. Introducing a random chemical potential (4.4) in the boundary can be seen as perturbation around this vacuum as long as $T \gg \bar{V}$. However, in order for disorder to be still relevant we need $k_0 = 1/a \gg T$. Therefore we are working with the hierarchy $k_0 \gg T \gg \bar{V}$. In analogy with the zero temperature case, we can set up a perturbative calculation around this background by looking at solutions of the system (4.2) with the ansatz:

$$\mathrm{d}s^2 = r^{-2}\left[-f(r)A(r)\mathrm{d}t^2 + \frac{\mathrm{d}r^2}{f(r)} + B(r)(\mathrm{d}x^2 + \mathrm{d}y^2)\right], \tag{4.18a}$$

$$A = a_t(r, \mathbf{x})\mathrm{d}t. \tag{4.18b}$$

Following our previous discussion we are working directly with the averaged metric $A(r) = \mathbb{E}[A(r, \mathbf{x})]$, $B(r) = \mathbb{E}[B(r, \mathbf{x})]$ and with disorder in both boundary directions (x, y), for which we can imposed isotropy. We also suppose that f is a function of the holographic coordinate r with a first order pole at a point r_0. It will be convenient to consider the rescaling $\bar{r} = r/r_0$, such that $f(\bar{r} = 1) = 0$. As before, we set up our perturbation theory by

letting

$$A(\bar{r}) = 1 + \bar{V}^2\alpha(\bar{r}) + O(\bar{V}^2), \qquad B(\bar{r}) = 1 + \bar{V}^2\beta(\bar{r}) + O(\bar{V}^2),$$
$$a_t(\bar{r}, x) = \bar{V}\varphi(\bar{r}, x) + O(\bar{V}^3).$$

The task is to solve the system (4.9) together with the boundary conditions $\alpha(0) = \beta(0)$ and $\lim_{u\to 0} \varphi(\bar{r}, \mathbf{x}) = \int \frac{\mathrm{d}^2k}{2\pi}\, e^{i\mathbf{k}\cdot\mathbf{x}}\mu_{\mathbf{k}}$. Further, we impose regularity and ingoing boundary conditions at the horizon $\bar{r} = 1$.

To order $\bar{V}^0$, the equations of motion are those for the AdS Schwarzschild background,

$$-6 + 6f - 4\bar{r}f' + \bar{r}^2 f'' = 0,$$
$$3 - 3f + \bar{r}f' = 0,$$

which are trivially satisfied by $f = 1 - \bar{r}^3$. To order $\bar{V}$, we have Maxwell's Equations for the vector potential, while no further metric equations are sourced:

$$f\partial_{\bar{r}}^2\varphi + r_0^2\partial_x^2\varphi = 0.$$

Again, we decompose $\varphi = \int \frac{\mathrm{d}^2k}{(2\pi)^2}\, e^{i\mathbf{k}\cdot\mathbf{x}}\varphi_{\mathbf{k}}(\bar{r})$ to get:

$$f\varphi_\kappa'' - \kappa^2\varphi_k = 0, \tag{4.19}$$

where we have defined the dimensionless momentum $\kappa = r_0|\mathbf{k}|$. Unfortunately we cannot solve the above equation explicitly. However we will be interested in two limits, the low (or zero) $\kappa \ll 1$ and high $\kappa \gg 1$ momentum modes. In the first limit, we have $\varphi_0' = \eta$ which is constant, while in the second limit $\kappa \gg 1$ we can rely on the WKB approximation

$$\varphi_k(\bar{r}) = \mu_k f^{-1/4} e^{-\kappa\int f^{-1/2}}.$$

To order $\bar{V}^2$, Einstein's Equations give:

$$f\alpha'' + \frac{(\bar{r}f' - 2f)}{2\bar{r}}(3\alpha' + \beta') = -\frac{\bar{r}^2 r_0^2}{2f}\mathbb{E}\left[f(\partial_{\bar{r}}\varphi)^2 + r_0 r_0^2(\nabla\varphi)^2\right],$$
$$f\alpha'' + 2f\beta'' + \frac{3\bar{r}f' - 2f}{2\bar{r}}\alpha' + \frac{\bar{r}f' - 2f}{2\bar{r}}\beta' = \frac{\bar{r}^2 r_0^2}{2f}\mathbb{E}\left[-f(\partial_{\bar{r}}\varphi)^2 + r_0^2(\nabla\varphi)^2\right],$$
$$f\beta'' - \frac{f}{\bar{r}}\alpha' - \frac{\bar{r}f' - 4f}{\bar{r}} = \frac{\bar{r}^2 r_0^2}{2f}\mathbb{E}\left[f(\partial_{\bar{r}}\varphi)^2 - r_0^2(\partial_x\varphi)^2 + r_0^2(\partial_y\varphi)^2\right],$$
$$f\beta'' - \frac{f}{\bar{r}}\alpha' - \frac{\bar{r}f' - 4f}{\bar{r}} = \frac{\bar{r}^2 r_0^2}{2f}\mathbb{E}\left[f(\partial_{\bar{r}}\varphi)^2 + r_0^2(\partial_x\varphi)^2 - r_0^2(\partial_y\varphi)^2\right].$$

where we made use of the zeroth order equations. These can be explicitly decoupled in two

second order equations

$$(3+f)^2 f^{-1/2}\partial_{\bar{r}}\left(\frac{f^{3/2}}{\bar{r}^2(3+f)}\partial_{\bar{r}}\alpha\right) = r_0^2\,\mathbb{E}[3(\partial_{\bar{r}}\varphi)^2 + r_0^2(\nabla\varphi)^2], \tag{4.20a}$$

$$4f^{3/2}\partial_{\bar{r}}\left(\frac{f^{1/2}}{\bar{r}^2}\partial_{\bar{r}}\beta\right) = -r_0^2\,\mathbb{E}[f(\partial_{\bar{r}}\varphi)^2 + r_0^2(\nabla\varphi)^2]. \tag{4.20b}$$

4.4.2 High momenta modes

The effect of modes with $\kappa \gg 1$ was first discussed in Ref. [92] in the context of a random scalar deformation. Since the calculations for the high momenta modes for the charged deformation is similar, we only review the results and direct the reader to Ref. [92] for the technical details.

An explicit calculation shows that for $\kappa \gg 1$ the main contribution to integrating equations (4.20a) and (4.20b) comes from the near boundary region $\bar{r} = 0$. Note that in this region these equations reduce to (4.12b) and (4.12a), giving logarithmic corrections to the metric coefficient $\alpha \sim \log r_0/a$. The important remark is that the second order correction to the surface gravity of the background is proportional to α. In particular, this implies that the temperature of the black hole receives second order logarithmic corrections from the high momenta modes. If we further assume that these corrections can be resummed as in the zero temperature setting, the temperature will develop a Lifshitz scaling $T \sim r_0^{-\bar{z}}$ with the horizon. The upshot is that all other thermodynamic quantities are affected by the way they scale with temperature. It is important to note that this is a direct consequence of the logarithmic corrections for the metric coefficient α. Since we find a similar correction, the results of Ref. [92] should apply here.

What about lower momenta modes? From Eq. (4.19), it is clear that for $\kappa \ll 1$ the source is approximately constant in the bulk, and therefore does not contribute to the singular behaviour of the metric. From the RG point of view, these modes are irrelevant and can only possibly renormalise the background geometry. As we will discuss below, this is indeed the case.

4.4.3 Low momenta modes

We will show that low momenta modes play the role of renormalizing the background by introducing a charge $Q \sim \bar{V}$ in the originally neutral black hole.

Consider the renormalised blackening factor $f = \bar{f} + \bar{V}^2\delta f$ where $\bar{f}(\bar{r}) = 1 - \bar{r}^3$ with ansatz (4.18). This shift has no effect in the zeroth and first order equations. However, it

introduces an extra factor in Eq. (4.20b):

$$\left(\bar{r}^{-3}\delta f\right)' - \bar{f}^{1/2}\partial_{\bar{r}}\left(\frac{\bar{f}^{1/2}}{\bar{r}^2}\partial_{\bar{r}}\beta\right) = \frac{r_0^2}{4\bar{f}}\,\mathbb{E}[\bar{f}(\varphi'_\kappa)^2 + \kappa^2\varphi_\kappa^2].$$

In particular, for $\kappa \ll 1$ the left hand side is constant, since by Maxwell's Equations (4.19) $(\varphi'_{\kappa\ll 1})^2 = \mu_0^2$. This is precisely the statement that low momenta modes are constant along the bulk. Close to the horizon $\bar{r} = 1$ the first term on the right hand side drops, giving:

$$(\bar{r}^{-3}\delta f)' = \frac{r_0^2}{4}\mu_0^2,$$

which can be easily solved by $\delta f(\bar{r}) = \frac{r_0^2}{4}\mu_0^2\,(\bar{r}^4 - \bar{r}^3)$ and requiring $\delta f(0) = \delta f(1) = 0$. This correction gives precisely the blackening factor $f(\bar{r}) = 1 - (1+Q^2)\bar{r}^3 + Q^2\bar{r}^4$ expected for an AdS Reissner-Nordstrom black hole with charge,

$$Q^2 = \frac{r_0^2}{4}\mu_0^2\bar{V}^2.$$

Therefore the constant low momenta modes have the effect of renormalizing the near horizon geometry of the initially uncharged black hole, adding a charge proportional to the sourced disorder. However note that this only contributes to the previous discussion at order $O(\bar{V}^4)$.This explains why to leading order it is justified to look only at high momenta modes when analysing the divergences of the metric under the flow of the renormalization group. We expect the full non-linear solution to be a charged black hole with a temperature reflecting both contributions discussed above.

4.4.4 Conductivity and momentum dissipation

Recent works by Donos, Gauntlett [59, 82, 84, 85], built upon previous membrane paradigm ideas [136], have simplified enormously the task of computing averaged DC conductivities in inhomogeneous backgrounds at finite temperature. Specifically, in [59] they provide an explicit formula for the DC conductivity of the Einstein-Maxwell system sourced by a periodic potential in terms of near horizon data. The generalization of their results to our model read

$$\sigma = 1 + \bar{V}^2 X^{-1}\mathbb{E}\left[\frac{\varphi_{(0)}}{A_{(0)}}\right]^2, \tag{4.21}$$

where $X = \mathbb{E}\left[\left(\frac{\varphi^{(0)}}{A_{(0)}}\right)^2\right] - \mathbb{E}[B_{(0)}^{-3}\partial_x B_{(0)}] - \mathbb{E}\left[\frac{\varphi_{(0)}}{A_{(0)}}\right]^2$ and the metric and gauge field are evaluated at the horizon $\bar{r} = 1$. In order to compute the corrections to the conductivity is necessary to take averages of fractions, which is usually a hard task. However we can still get

a qualitative picture without having to compute the averages explicitly. First, it is clear that generically $X \neq 0$ since the first term is an average over a second moment. The same is *a priori* not clear for the numerator, which is an average over a first moment.

In perturbation theory, $A = 1 + \bar{V}^2\alpha$, and we can expand the denominator for small $\bar{V}$: $\mathbb{E}\left[\varphi_{(0)}/A_{(0)}\right] \sim \mathbb{E}\left[\varphi_{(0)}\right] - \bar{V}^2\mathbb{E}[\alpha_{(0)}\varphi_{(0)}\big] + O(\bar{V}^4)$. By construction we have $\mathbb{E}[\varphi_{(0)}] = 0$, and the problem simplifies to computing $\mathbb{E}[\alpha_{(0)}\phi_{(0)}]$. In principle to compute this average explicitly one needs the exact background to second order. However by looking at the most general spectral decomposition of α that solves the equations of motion one can compute the average (4.21) in function of the coefficients $\alpha_{\mathbf{k}}$. Without loss of generality we can write $\alpha = \alpha_{\text{hom}}(\bar{r}) + \alpha_{\text{inh}}(\bar{r}, \mathbf{x})$. It is clear that only α_{inh} contributes to the perturbative corrections of the conductivity, since any homogeneous part (which is a constant at the horizon) vanishes when averaged with the source $\phi_{(0)}$. From the equations of motion we can write (c.f. Appendix D.1 for further details)

$$\alpha_{\text{inh}}(\bar{r}, \mathbf{x}) = \sum_{\mathbf{k}} \alpha^0_{\mathbf{k}}(\bar{r}) \prod_i \cos 2\theta_{i,\mathbf{k}} + \sum_{\mathbf{k}\neq\mathbf{l}} \alpha^+_{\mathbf{k},\mathbf{l}}(\bar{r}) \prod_i \cos\theta^+_{i,\mathbf{k},\mathbf{l}} + \sum_{\mathbf{k}\neq\mathbf{l}} \alpha^-_{\mathbf{k},\mathbf{l}}(\bar{r}) \prod_i \cos\theta^-_{i,\mathbf{k},\mathbf{l}},$$

where we used a discrete representation for simplicity (c.f. Eq. (4.7)), and defined $\theta^{\pm}_{i,k_i,l_i} = \theta_{i,k_i} \pm \theta_{i,l_i}$. Letting $\varphi = \sum_{\mathbf{k}} \varphi_{\mathbf{k}}(\bar{r}) \prod_i \cos\theta_{i,\mathbf{k}}$ and evaluating at $\bar{r} = 1$, one check that $\mathbb{E}[\alpha_{inh(0)}\phi_{(0)}] = 0$ and therefore

$$\sigma = 1 + O(\bar{V}^4).$$

One could be tempted to extend this argument to fourth or higher orders in $\bar{V}$. However this is a really hard task as it would also require the computation at least of the third order contribution to the vector potential as well as the fourth order contribution to the metric.

It is intriguing that the random chemical potential does not contribute, to leading order at least, to the background electric conductivity. The likely physical reason for that behaviour is a peculiar feature of this realisation of disorder: charge carriers, whose average charge vanishes, and that naturally contributes to the electrical conductivity, are at the same time the source of disorder in the system. This dual role is rather unusual in condensed matter systems where scatterers are typically uncharged and quenched and therefore do not contribute to the electrical conductivity.

We confirm that this unexpected result is a peculiarity of the electrical conductivity in this model of disorder by computing the thermal conductivity κ [26], which describes transport

[26] Not to be mistaken with the dimensionless momentum we defined before.

of energy instead of charge. Following again the results of [59], κ is given by,

$$\kappa = \frac{(4\pi)^2 T}{X + \mathbb{E}\left[\frac{\varphi_{(0)}}{A_{(0)}}\right]^2}.$$

It is straightforward to check that now the thermal conductivity depends on disorder, even to leading order, since we have an average over a second moment of the source φ inside X, which gives a non-zero contribution to second order. We can estimate this in the high temperature limit $T \gg k_0$ where the main contribution to the geometry is $\varphi_{\kappa \ll 1} = (1 - \bar{r})\mu(x, y)$. Therefore $\kappa = \frac{(4\pi)^4 T^3}{9} \frac{1}{\mathbb{E}[\mu^2]}$ which leads to,

$$\kappa = \frac{(4\pi)^3}{9} \frac{T^3}{k_0 \bar{V}^2}. \tag{4.22}$$

As was expected, in the absence of disorder $\bar{V} \to 0$, κ diverges as $1/\bar{V}^2$ since for no disorder translational invariance is recovered. The expression (4.22) also suggests that the relaxation scale of momentum is given by $\tau^{-1} \sim k_0 \bar{V}^2$. This is in full agreement with recent results in a set up similar to ours where disorder is introduced by a random scalar field in the boundary [202].

Finally, it is important to stress that all these results are restricted to averaged conductivities. It would be interesting to know higher moments and the full probability distribution of the relevant observables. That for instance could provide additional information on the effect of a random chemical potential on the electrical conductivity for which we have clearly observed that a simple average misses important features.

4.5 Conclusions

We have studied analytically the role of weak disorder in Einstein-Maxwell theory and its relation, by holography, with the transport properties of the dual field theory. Disorder is introduced through a random correlated chemical potential whose conformal dimension can be tuned by modifying the strength of the correlations. In that way we can investigate, within the Einstein-Maxwell theory, irrelevant, marginal or relevant perturbations. We have focused in the first two cases where we have found that, to leading order, irrelevant perturbations do not alter the conductivity while marginal perturbations induce a positive correction. Both results are in agreement with the recently proposed bound [96–98] for the dc-conductivity at finite temperature. Curiously disorder does not seem to suppress incoherent transport even at zero temperature. It would be interesting to understand why these field theory degrees of freedom are protected from disorder. In the marginal case at zero temperature we also found infrared logarithmic singularities in the metric that, after

resummation as in Ref. [33], lead to a Lifshitz-like geometry. At finite temperature we have shown that despite the fact that the chemical potential has zero average the black hole develops some net charge. The thermal conductivity is consistent with a disordered potential that induces relaxation of momentum. However the average electrical conductivity, as in the zero temperature case, is still not affected by disorder to leading order in perturbation theory.

5 | Coherence effects in disordered geometries with a field-theory dual[†]

In this chapter we investigate the holographic dual of a probe scalar in an asymptotically anti-de Sitter disordered background which is an exact solution of Einstein's equations in three bulk dimensions. Unlike other approaches to model disorder in holography, we are able to explore quantum wave-like interference effects between an oscillating or random source and the geometry. In the weak-disorder limit, we compute analytically and numerically the one-point correlation function of the dual field theory for different choices of sources and backgrounds. The most interesting feature is the suppression of the one-point function in the presence of an oscillating source and weak random background. We have also computed analytically and numerically the two-point function in the weak disorder limit. We have found that, in general, the perturbative contribution induces an additional power-law decay whose exponent depends on the distribution of disorder. For certain choices of the gravity background, this contribution becomes dominant for large separations which indicates breaking of perturbation theory and the possible existence of a phase transition induced by disorder.

5.1 Introduction

Holographic dualities, that relate classical theories of gravity to strongly-coupled quantum field theories, are now a forefront research area not only in high energy physics but also in quantum information and condensed matter physics. In the latter, it is emerging as a powerful tool to describe universal properties of strongly-correlated quantum systems. One of the main challenges for the application of holographic techniques in this context is the description of disorder, which is ubiquitous in realistic systems and directly responsible for a broad variety of phenomena ranging from momentum relaxation to quantum interference leading to different forms of localization [35, 37, 50, 207, 208]. The introduction of disorder in gravity backgrounds with a negative cosmological constant relevant for holography requires

[2]This Chapter is based on Ref. [206], and was done in collaboration with Antonio M. García-García and Tomás Andrade. The author would like to acknowledge T. Andrade for the numerical work in Section 5.4.

the solution of spatially inhomogeneous Einstein's equations, in general a difficult task.

Different approximation schemes have been proposed to make the problem technically tractable while keeping some of the expected phenomenology related to the introduction of disorder. For instance, momentum relaxation, a rather general consequence of any form of disorder, can be achieved by adding a massless scalar [54, 209–211] that depends linearly on the boundary coordinates. Since the scalar field only couples to gravity through its derivatives, translation invariance is broken by the background but the equations of motion are still independent of the spatial coordinates which facilitates substantially the calculation, in many cases analytical, of transport properties.

As was expected, the electrical conductivity is always finite and depends directly on the strength of the translational symmetry breaking characterised by the slope, with respect to the spatial coordinates, of the scalar field in the boundary. For weak momentum relaxation, the electrical conductivity reproduces the expected phenomenology of Drude's model, which includes a peak at low frequencies, remnant of the broken translational symmetry, followed by a decay for higher frequencies. For stronger relaxation the Drude peak is suppressed, leading to an incoherent 'bad-metal' behaviour [57, 149, 212, 213]. However even in the limit of infinite relaxation no insulating behaviour is observed. Recently, models that consider the coupling of the scalar field to the gravity and the Maxwell term managed to reproduce a vanishing conductivity in the limit of infinite relaxation [152, 163, 164]. Yet, in this limit the effective charge in these models vanish, so strictly speaking they cannot be considered insulators. Other effective models of momentum relaxation in holography include the memory matrix formalism [22, 200, 201, 214], helical and Q-lattices [60, 67, 182] and massive gravity [53, 65, 186, 215]. Similar results [59, 73, 75, 76, 216–218] have been obtained even for Maxwell fields with a spatially oscillating chemical potentials in the boundary leading to inhomogeneous Einstein's equations. We note that effects such as localization are precluded by design since a random but homogeneously distributed, and therefore delocalised, chemical potential is an input in this approach.

Disorder has also been introduced at the level of the action by a random source coupled to the dual conformal field theory operator [63, 219]. By using the replica trick, it is possible to integrate out the random coupling resulting in a double trace deformation of the non-disordered theory. For marginal perturbations, renormalization group techniques suggest the existence of logarithmic corrections in the two-point correlation function that spoils conformal symmetry. Interestingly, this is in agreement with the expected behaviour of certain two dimensional conformal field theories perturbed by disorder (see [220] and references therein).

Another popular approach is to consider a random field in the boundary, in most cases a random chemical potential (source) for gauge (scalar) fields, but neglecting the backreaction in the gravity background (probe limit) [62, 87–89, 95, 200, 203, 221, 222]. Analytical

attempts to go beyond this probe limit have found logarithmic infra-red (IR) divergences in the gravity background, signaling the breakdown of perturbation theory [90, 91]. A resummation scheme for the divergent expansion was proposed in [92, 151, 187, 202] resulting in an averaged gravity background with an emerging Lifshitz scaling symmetry, which was shown to be a generic feature of marginal disordered deformations [94, 152]. For geometries with a horizon, the most general result in this context is that of Gauntlett, Donos and collaborators [59, 70, 82–84, 86] who found closed expressions for the dc conductivity and other averaged transport coefficients in generic inhomogeneous backgrounds. As a direct consequence, bounds on the electric and thermal conductivity were proposed [96–99].

The conclusion of this more direct approach is similar to the one from the phenomenological models of momentum relaxation discussed previously, namely, it is not possible to reach an insulating state which is believed to be a distinctive feature of strong disorder in condensed matter systems. Even simpler coherence effects such as weak-localization [223], which are precursors of a metal-insulator transition, have not yet been clearly identified.

In this manuscript we propose a new approach to model disorder in holography which has the potential to reproduce some of these coherent effects. We switch perspectives and consider the effect of a disordered geometry with no horizon on a probe scalar field. This is accomplished by considering a family of three dimensional random geometries that solve Einstein's equations exactly[27] and neglecting the backreaction of the scalar in the geometry. This family is indexed by a parameter which we take to be a random function of the boundary coordinates. The scalar field feels the geometry as an effective inhomogeneous coefficient in the equations of motion. This is reminiscent, though we cannot establish a precise mapping, of a one-dimensional wave equation with a random refractive index [207, 208] plus additional terms that control the evolution in the radial direction which are related to interactions in the boundary.

According to the holographic dictionary, the geometry is dual to a strongly-coupled disordered plasma living at the boundary, and the scalar field sources a boundary dual operator. We investigate numerically and analytically the properties of this disordered plasma by looking at one and two-point functions of this scalar operator. For the one-point function our main result is the observation of coherence effects, due to interference between an oscillating source and the random geometry, that, in some cases, leads to the strong suppression of oscillations even for weak disorder. The contribution to the two-point function for a weak random Gaussian geometry is still a power-law decay for large distances with an exponent that depends on both the scalar mass and disorder correlations modelled by a non-trivial power spectrum. In some cases, this correction becomes dominant for large distances which suggests the breaking of perturbation theory and the possible transit of the

[27] We can find an exact solution of Einstein's equations involving a free function due to the fact that all vacuum solutions are pure diffeomorphisms in three dimensions. The generalization to higher dimensions would involve solving the equations numerically.

system to a new disorder-driven fixed point.

The chapter is organised as follows. In the next section we introduce the geometry we will be studying and discuss the equation of motion for the probe scalar. In section 5.3 we solve these equations analytically in the limit of a weak-disordered background. The one and two-point functions of the dual operator are computed for different choices of both sources and inhomogeneous geometries. In section 5.4, we solve the equation of motion by numerical techniques and compute in certain cases the one and two-point correlation function of dual scalar. Section 5.5 is devoted to a comparison of our results with previous approaches to disorder in holography. We conclude in section 5.6 with a summary of results and ideas for future work. The appendices offer a wider discussion of technical points which are used throughout the main body of the paper.

5.2 Setup

In this section we introduce our objects of study. First, we introduce a family of geometries in $d+1=3$ spacetime dimensions. This family is characterised by an arbitrary function which we can take to be random. We next introduce a minimally coupled scalar field and discuss its equation of motion and associated boundary conditions. The aim is to use this field to probe the properties of the inhomogeneous geometry, which holographically can be interpreted as a strongly-coupled disordered field theory.

5.2.1 Geometry

Solutions of the vacuum $d+1$-dimensional Einstein's Equations with a negative cosmological constant have been classified in the pioneering work of Fefferham and Graham [128, 224]. For $d>2$, we can integrate Einstein's Equations in a neighbourhood of the boundary by requiring that the Weyl tensor vanish. This condition constrains the boundary metric to be conformally flat. However, in $d=2$ the Weyl tensor vanishes exactly, leaving the conformal class of the boundary metric arbitrary [225].

In this manuscript we will be mainly interested in the following family of metrics defined by a global coordinate patch $x^a=(\rho,t,x)$ as

$$\mathrm{d}s^2=\frac{\mathrm{d}\rho^2}{4\rho^2}+\frac{1}{\rho}\left(-\mathrm{d}t^2+\mathrm{d}x^2+2g_{tx}(x)\mathrm{d}t\mathrm{d}x\right), \tag{5.1}$$

where $g_{tx}(x)$ is an arbitrary function of the boundary coordinate x. In line with our discussion above, it is easy to check that this family satisfies Einstein's Equations in $d=2$ dimension with a negative cosmological constant for any g_{tx}. In these coordinates, the conformal boundary is located at $\rho=0$ and the induced conformal metric $g^{(0)}$ is given by $\rho\,\mathrm{d}s^2|_{\rho=0}=$

$-\mathrm{d}t^2 + \mathrm{d}x^2 + 2g_{tx}(x)\mathrm{d}t\mathrm{d}x$. The Poincare horizon is parametrised by $\rho = \infty$.

From a holographic perspective, this space-time encodes the degrees of freedom of a strongly-coupled field theory living on the boundary metric described above. However, the dual stress tensor vanishes since this change in the boundary metric does not induce sub-leading terms in the bulk metric. This resembles the situation we encounter in the axion model of [54], where the marginal, spatially dependent, scalar sources do not excite a vacuum expectation value. In the next sections we will be interested in studying the family of geometries in Eq.(5.1) for different choices of g_{tx}. In particular, we will be interested in the case where $g_{tx}(x)$ is a random Gaussian process, as introduced in Appendix B. We will study the dynamics of a minimally coupled scalar field as a way of probing the effects of the disordered geometry. The aim is to get an insight into the nature of the strongly-coupled disordered dual field theory.

5.2.2 Scalar Field and Equations of Motion

We consider a probe scalar field ψ of mass m minimally coupled to the geometry in Eq.(5.1). The equation of motion is given by $(\Delta_g - m^2)\psi = 0$, where the curved Laplacian can be written in a chart x^a as $\Delta_g = \frac{1}{\sqrt{-g}}\partial_a\left(\sqrt{-g}\, g^{ab}\partial_b\right)$. Since ∂_t is a killing vector for Eq.(5.1), we can restrict our attention to static configurations $\psi = \psi(\rho, x)$. In these coordinates, the equation of motion thus reads

$$4\rho^2\partial_\rho^2\psi - \rho\frac{g_{tx}\partial_x g_{tx}}{(1+g_{tx}^2)^2}\partial_x\psi + \rho\frac{1}{1+g_{tx}^2}\partial_x^2\psi - m^2\psi = 0. \tag{5.2}$$

We are interested in solutions satisfying the following boundary conditions,

$$\lim_{\rho\to\infty}\psi(\rho, x) < \infty, \tag{5.3a}$$

$$\lim_{\rho\to 0}\rho^{\frac{\nu-1}{2}}\psi(\rho, x) = s(x), \tag{5.3b}$$

where we have defined $\nu = \sqrt{1+m^2}$. The first boundary condition assures regularity of the solution at the Poincaré horizon $\rho = \infty$. As discussed in Appendix A.2, the second boundary condition defines a field $s(x)$ living in the boundary $\rho = 0$ with conformal dimension $\Delta_- = 1 - \nu$. This field sources a dual boundary operator $\mathcal{O}(x) \sim \rho^{-\frac{\nu+1}{2}}\psi$ of conformal dimension $\Delta_+ = 1 + \nu$.

Even for simple choices of g_{tx}, Eq.(5.2) remains largely intractable analytically. However when g_{tx} is small we can compute perturbative corrections to the plain AdS_3 result analytically, helping us to build an intuition of the effects of the weakly disordered geometry. We will recur to numerical methods to test the analytical prediction and also to explore the region of stronger disorder not accessible to an analytical treatment.

5.3 Perturbative analysis of the one-point and two-point correlation functions

In this section we study Eq.(5.2) perturbatively for different choices of g_{tx}. For convenience, we will set $m^2 = -\frac{3}{4}$ throughout this section, which is equivalent to choosing $\nu = \frac{1}{2}$. Note this choice respects the Breitenlohner-Freedman bound, $m^2 \geq -1$ in $d = 2$, [226, 227]. We will divide our discussion by order in perturbation theory, and focus in two observables: the expectation value of the dual boundary operator (one-point function) and the two-point function. We can obtain both these quantities by solving the perturbative equations with the appropriate boundary conditions.

5.3.1 Zeroth Order

To set up the perturbative analysis, let $g_{tx}(x) = \epsilon\, g(x)$ for a parameter $\epsilon \ll 1$ measuring the amplitude of g_{tx} fluctuations. For $\epsilon = 0$, Eq.(5.2) reduces to the equation of a massive scalar field in AdS_3 given by

$$4\rho^2\partial_\rho^2\psi_{(0)} + \rho\partial_x^2\psi_{(0)} + \frac{3}{4}\psi_{(0)} = 0.$$

Letting $\psi_{(0)}(\rho, x) = \int_{\mathbb{R}} \frac{\mathrm{d}k}{2\pi} e^{ikx} f_k(\rho)$, the equation above reduces to

$$4\rho^2 f_k'' - \left(\rho k^2 - \frac{3}{4}\right) f_k = 0, \tag{5.4}$$

which has general solution

$$f_k(\rho, x) = a_k \rho^{1/4} e^{-k\sqrt{\rho}} + b_k \rho^{1/4} e^{k\sqrt{\rho}}. \tag{5.5}$$

Regularity at the Poincaré horizon Eq.(5.3a) requires that $a_k = 0$ for $k < 0$ and $b_k = 0$ for $k > 0$, which can be written compactly as $f_k(\rho) = a_k \rho^{1/4} e^{-|k|\sqrt{\rho}}$ for a different constant a_k. Now letting $s(x) = \int_{\mathbb{R}} \frac{\mathrm{d}k}{2\pi} e^{ikx} s_k$, boundary condition Eq.(5.3b) can be imposed coefficient wise to yield $a_k = s_k$. The full solution therefore reads

$$\psi_{(0)}(\rho, x) = \rho^{1/4} \int_{\mathbb{R}} \frac{\mathrm{d}k}{2\pi} e^{ikx} e^{-|k|\sqrt{\rho}} s_k. \tag{5.6}$$

Note that this depends directly on the Fourier components of the source. We are interested in a few particular cases that we outline below.

Constant source If $s(x) = s = \int_{\mathbb{R}} \frac{\mathrm{d}k}{2\pi} e^{ikx} 2\pi\delta(k) s$ is constant, we have $\psi_{(0)}(\rho, x) = \rho^{1/4} s$. This sources a dual boundary operator with expectation value $\langle \mathcal{O}(x) \rangle = 2\nu \lim_{\rho \to 0} \rho^{-\frac{\nu+1}{2}} \psi_{(0)} =$

0.

Oscillating source If $s(x) = s\cos qx = s\int_{\mathbb{R}} \frac{\mathrm{d}k}{2\pi} e^{ikx}\pi\left[\delta(k-q)+\delta(k+q)\right]$ for $q \in \mathbb{R}$, we have $\psi_{(0)}(\rho, x) = s\rho^{1/4}e^{-|q|\sqrt{\rho}}\cos qx$. This sources a dual boundary operator with expectation value given by $\langle\mathcal{O}(x)\rangle = -s|q|\cos qx$.

Superposition of oscillations Consider now a source given by a superposition of N oscillating modes $s(x) = \sum_{n=1}^{N} s_n \cos(q_n x + \gamma_n)$, where s_n, q_n and γ_n can be freely chosen. Noting that the finite sum can be exchanged with the integral and following the same steps as above mode-wise we find $\psi_{(0)}(\rho, x) = \rho^{1/4}\sum_{n=1}^{N} s_n e^{-|q_n|\sqrt{\rho}}\cos(q_n x + \gamma_n)$. The one-point function thus reads $\langle\mathcal{O}(x)\rangle = -\sum_{n=1}^{N} s_n|q_n|\cos(q_n x + \gamma_n)$.

Delta source and two-point function As discussed in Appendix A.3, the boundary-to-bulk propagator is given by solving the equations of motion with a delta source, $s(x) = \delta(x) = \int_{\mathbb{R}} \frac{\mathrm{d}k}{2\pi} e^{ikx}$. We thus have,

$$K_{(0)}(\rho, x-y) = \rho^{1/4}\int_{\mathbb{R}} \frac{\mathrm{d}k}{2\pi} e^{ik(x-y)}e^{-|k|\sqrt{\rho}} = \frac{1}{\pi}\frac{\rho^{3/4}}{(x-y)^2+\rho}.$$

which follows the shape of a Lorentzian (or Cauchy) distribution. Following the discussion in Appendix A.2, the boundary two-point function can be obtained by

$$\langle\mathcal{O}(x)\mathcal{O}(y)\rangle = 2\nu\lim_{\rho\to 0}\rho^{-\frac{1+\nu}{2}}K_{(0)}(\rho; x-y) = \frac{1}{\pi}\frac{1}{(x-y)^2}. \tag{5.7}$$

Note this is not the expected result for an operator of conformal dimension $2\Delta_+ = 3$ but rather for an operator of conformal dimension $2\Delta_+ = 2$. This is because, by considering a static field, we effectively reduce the conformal dimension of the problem. Since we will be interested in static inhomogeneous configurations in what follows, this is the object we will be computing corrections for.

5.3.2 Second Order

Note that since g_{tx} appears only quadratically in Eq.(5.2), there are no non-trivial order one corrections to $\psi_{(0)}$. It is thus sufficient to consider $\psi = \psi_{(0)} + \epsilon^2\psi_{(2)} + O(\epsilon^4)$. Inserting into Eq.(5.2) and expanding up to second order leads to

$$4\rho^2\partial_\rho^2\psi_{(2)} + \rho\,\partial_x^2\psi_{(2)} + \frac{3}{4}\psi_{(2)} = \rho\, g(x)^2\partial_x^2\psi_{(0)} + \rho\, g(x)\partial_x g(x)\partial_x\psi_{(0)}. \tag{5.8}$$

Note that the zeroth order solution act as a source for the perturbative correction. Since the full solution has to satisfy the boundary conditions, we have to apply them order by

order. For instance every term in the ϵ-expansion has to be regular at the Poincaré horizon. However since we have enforced boundary condition Eq.(5.3b) at zeroth order, we have to set $\lim_{\rho\to 0}\rho^{\frac{\nu-1}{2}}\psi_{(2)}=0$ for the inhomogeneous geometry not to correct the fixed boundary source $s(x)$. Summarizing, we have to solve Eq.(5.8) subjected to

$$\lim_{\rho\to\infty}\psi_{(2)}(\rho,x)<\infty, \tag{5.9a}$$

$$\lim_{\rho\to 0}\rho^{\frac{\nu-1}{2}}\psi_{(2)}(\rho,x)=0. \tag{5.9b}$$

If g_{tx} is of Schwarz class, we can attempt to solve Eq.(5.8) in Fourier space as we did for the zeroth-order result. Letting $\psi_{(2)}(\rho,x)=\int_{\mathbb{R}}\frac{\mathrm{d}k}{2\pi}e^{ikx}f_k(\rho)$ and $g(x)=\int_{\mathbb{R}}\frac{\mathrm{d}k}{2\pi}e^{ikx}g_k$, we can rewrite Eq.(5.8) in Fourier space as

$$4\rho^2 f_k''-\left(\rho k^2-\frac{3}{4}\right)f_k=-\frac{\rho^{5/4}}{2}\int_{\mathbb{R}}\mathrm{d}l\int_{\mathbb{R}}\mathrm{d}q\;(k-l)(2k-l)e^{-|k-l|\sqrt{\rho}}g_{l-q}g_q s_{k-l} \tag{5.10}$$

where the right-hand side has been evaluated applying the convolution theorem with the zeroth order solution Eq.(5.6)[28]. This integral-differential equation cannot be solved in a closed form. In the following subsections we discuss solutions for specific inhomogeneous configurations. For each choice of g, we can consider different choices of source and study the interplay between the source, the geometry and the resulting expectation value and two-point function of the dual boundary operator.

Constant geometry

The simplest example is given by taking $g(x)=2\pi\;g$ to be a constant. In this case $g_k=g\delta(k)$ and for generic source

$$4\rho^2 f_k''-\left(\rho k^2-\frac{3}{4}\right)f_k=-\rho^{5/4}k^2e^{-|k|\sqrt{\rho}}s_k g^2.$$

Note that the linear differential operator on the left-hand side is exactly the same as for the zeroth-order equation. This is generic and hold at all orders in perturbation theory. The only difference is the source term on the right-hand side. By linearity, the general solution will be a linear combination of the solution for the homogeneous equation plus a particular solution. As before, the homogeneous solution has one exponentially diverging piece which should be set to zero by regularity at the Poincaré horizon. This leads to

$$f_k(\rho)=a_k\rho^{1/4}e^{-|k|\sqrt{\rho}}+\frac{g^2}{4}\rho^{1/4}e^{-|k|\sqrt{\rho}}\left(1+2|k|\sqrt{\rho}\right)s_k,$$

[28] Note that the convolution representation is not unique, but all representations are equivalent up to a translation in the momentum integration.

where a_k is an integration constant. Close to the boundary $\rho = 0$, the solution behaves as

$$f_k(\rho) \underset{\rho=0}{\sim} \left(a_k + \frac{g^2}{4} s_k\right) \rho^{1/4} + O\left(\rho^{3/4}\right),$$

and therefore boundary condition Eq.(5.9b) imposes $a_k = -\frac{g^2}{4} s_k$. Finally, we can write

$$\psi_{(2)}(\rho, x) = \frac{1}{2} \rho^{3/4} g^2 \int_{\mathbb{R}} \frac{\mathrm{d}k}{2\pi} e^{ikx} |k| e^{-|k|\sqrt{\rho}} s_k.$$

As in the zeroth-order solution, we discuss below a few cases of interest.

Constant source Let $s(x) = s$ be a constant. Inserting in the above leads trivially to $\psi_{(2)}(\rho, x) = 0$. Therefore the off-diagonal constant metric does not affect the zeroth order boundary one-point function.

Oscillating source Let $s(x) = s \cos qx$. Inserting in the above leads to

$$\psi_{(2)}(\rho, x) = \frac{\rho^{3/4} g^2}{2} |q| e^{-|q|\sqrt{\rho}} s \cos qx.$$

At the boundary $\rho = 0$ this induces a correction to the zeroth-order one-point function which is proportional to g,

$$\langle \mathcal{O}(x) \rangle = -|q| \left(1 - \frac{\epsilon^2}{2} g^2 + O(\epsilon^4)\right) s \cos qx.$$

Superposition of oscillations Let $s(x) = \sum_{n=1}^{N} s_k \cos\left(q_n x + \gamma_n\right)$. This case is similar to the above, since we can integrate term by term in the sum to give,

$$\psi_{(2)}(\rho, x) = \rho^{3/4} \frac{g^2}{2} \sum_{n=1}^{N} |q_n| e^{-|q_n|\sqrt{\rho}} s_n \cos(q_n x + \gamma_n).$$

The correction to the boundary one-point reads

$$\langle \mathcal{O}(x) \rangle = -\sum_{n=1}^{N} |q_n| \left(1 - \frac{\epsilon^2}{2} g^2 + O(\epsilon^4)\right) s_n \cos(q_n x + \gamma_n).$$

Again, it represents just a renormalization of the amplitude of the zeroth one-point function.

Delta source and two-point function Recall that, as discussed in the previous section and in the Appendix A.3 that the boundary-to-bulk propagator $K(\rho; x, y)$ can be

computed by solving the equations of motion with $s(x) = \delta(x)$. We thus have $K_{(2)}(\rho; x) = \frac{g^2}{2\pi}\rho^{3/4}\frac{x^2-\rho}{(\rho+x^2)^2}$. Evaluating at the boundary leads to a correction to the first zeroth-order two-point function,

$$\langle \mathcal{O}(x)\mathcal{O}(y)\rangle = \left(1 - \frac{\epsilon^2}{2}g^2 + O(\epsilon^4)\right)\frac{1}{\pi}\frac{1}{|x-y|^2}. \tag{5.11}$$

Note that for all the cases above the constant off-diagonal metric element perturbatively decreases the amplitude of the boundary one-point function and two-point function. Since in perturbation theory the equations are linear this case can be interpreted as the mean result for a inhomogeneous geometry. The amplitude damping raises the question on whether in a non-perturbative setup the geometry can effectively suppress the boundary correlation functions.

Oscillating geometries

We now consider a generic superposition of N oscillating modes, $g(x) = \sum_{n=1}^{N} A_n e^{i\omega_n x}$ for $\omega_n \in \mathbb{R}$. For example, an interesting particular case is $\omega_1 = -\omega_2 = \omega$, $A_1 = A_2 = \frac{g}{2}$ and $A_n = 0$ for $n > 2$ which correspond to $g(x) = g\cos\omega x$. The Fourier modes are given by a Dirac comb $g_k = \sum_{n=1}^{N} A_n\delta(k-\omega_n)$ and for a generic source the equations of motion in Fourier space read,

$$4\rho^2 f_k'' - \left(\rho k^2 - \frac{3}{4}\right) f_k = -\rho^{5/4}\sum_{n=1}^{N}\sum_{m=1}^{N} A_n A_m (k-\omega_n-\omega_m)(2k-\omega_n-\omega_m)\times \\ \times\, e^{-|k-\omega_n-\omega_m|\sqrt{\rho}} s_{k-\omega_n-\omega_n}.$$

By linearity, we can solve the equation above term by term. The regular solution at the Poincaré horizon is given by the homogeneous solution Eq.(5.5) plus the sum of each individual particular solution

$$f_k(\rho) = \frac{\rho^{1/4}}{2}\sum_{n=1}^{N}\sum_{m=1}^{N} A_n A_m \frac{k-\omega_n-\omega_m}{\omega_n+\omega_m}\left[e^{-|k-\omega_n-\omega_m|\sqrt{\rho}} - e^{-|k|\sqrt{\rho}}\right] s_{k-\omega_n-\omega_m}.$$

Taking the Fourier transform, we arrive at an implicit solution for the generic source

$$\psi_{(2)}(\rho, x) = \frac{\rho^{1/4}}{2}\sum_{n=1}^{N}\sum_{m=1}^{N}\frac{A_n A_m}{\omega_n+\omega_m}\int_{\mathbb{R}}\frac{\mathrm{d}k}{2\pi}e^{ikx}(k-\omega_n-\omega_m)\left[e^{-|k-\omega_n-\omega_m|\sqrt{\rho}} - e^{-|k|\sqrt{\rho}}\right]\times \\ \times s_{k-\omega_n-\omega_m}. \tag{5.12}$$

As before, we now analyse some interesting particular cases where the above integral can be done explicitly.

Constant source Let $s(x) = s$ be a constant, i.e. $s_k = \delta(k)$. As before, the above integral trivially gives $\psi_{(2)} = 0$. There are no corrections to the boundary dual operator.

Plane wave source Let $s(x) = se^{iqx}$, i.e. $s_k = s\delta(k-q)$. The Fourier transform is given by

$$\psi_{(2)}(\rho, x) = \rho^{1/4} s e^{iqx} \frac{q}{2} \sum_{n=1}^{N} \sum_{m=1}^{N} \frac{A_n A_m}{\omega_n + \omega_m} e^{i(\omega_n+\omega_m)x} \left[e^{-|q|\sqrt{\rho}} - e^{-|\omega_n+\omega_m+q|\sqrt{\rho}} \right].$$

Close to the boundary, this gives a correction to the dual one-point function

$$\delta\langle \mathcal{O}(x) \rangle = s e^{iqx} \frac{q}{2} \sum_{n=1}^{N} \sum_{m=1}^{N} \frac{A_n A_m}{\omega_n + \omega_m} e^{i(\omega_n+\omega_m)x} \left(|\omega_n + \omega_m + q| - |q| \right).$$

There are a couple of particular cases of special interest,

- $g(x) = ge^{-i\omega x}$ ($A_1 = g$, $\omega_1 = -\omega$, all other zero):

$$\begin{aligned} \langle \mathcal{O}(x) \rangle &= -q \left(1 - \frac{\epsilon^2}{4\omega} \left(|q - 2\omega| - |q| \right) g^2 e^{-2i\omega x} \right) s e^{iqx}, \\ &= -q \left(1 - \frac{\epsilon^2}{4\omega} \left(|q - 2\omega| - |q| \right) g(x)^2 \right) s(x). \end{aligned}$$

  Consider $q, \omega \geq 0$ and define the relative correction $\Delta(x) = \frac{\delta\langle \mathcal{O} \rangle}{\langle \mathcal{O} \rangle_{(0)}}$, where $\langle \mathcal{O} \rangle_{(0)}$ is the zeroth order one-point result. We can identify three distinct regimes. For $q > 2\omega$, the relative correction to the one-point function is positive and simply proportional to the geometry $\Delta(x)_{q \geq 2\omega} = -\frac{\epsilon^2}{2} g(x)^2 = -\frac{1}{2} g_{tx}(x)^2$, while for $q < 2\omega$ the result depends explicitly on the relative strength of the modes, $\Delta(x)_{q<2\omega} = -\frac{\epsilon^2}{2} \left(\frac{q}{\omega} - 1 \right) g(x)^2 = -\frac{1}{2} (\frac{q}{\omega} - 1) g_{tx}^2$. For $q < \omega$ the relative correction will be positive, while in the window $\omega < q < 2\omega$ it becomes negative. Therefore the inhomogeneous geometry can either suppress ($q > \omega$) or enhance ($q < \omega$) the expectation value of the dual operator, depending on the coherence between the modes. The discussion is summarised in Fig.5.1.

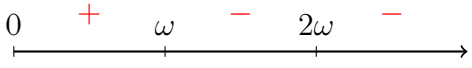

Figure 5.1: Sign of the relative correction $\Delta(x)$ for different $q \geq 0$ and fixed ω.

- $g(x) = g \cos \omega x$ ($A_1 = A_2 = \frac{1}{2} g$, $\omega_1 = -\omega_2 = \omega$, all other zero):

By linearity, this case can be obtained by summing the above with the reversed $q \to -q$. The relative correction $\Delta(x) = \frac{\delta\langle\mathcal{O}\rangle}{\langle\mathcal{O}\rangle_{(0)}}$ is given by

$$\Delta(x) = -\epsilon^2 \frac{g^2}{8}\left[\frac{|q+2\omega|-|q|}{2\omega}e^{2i\omega x} - \frac{|q-2\omega|-|q|}{2\omega}e^{-2i\omega x} + 2\right].$$

Note that, different from the above in general it is not possible to rewrite the relative correction as an explicit function of the geometry. First, lets consider the case $q, \omega \geq 0$. Then $q + 2\omega \geq 0$ and we have two subcases: $q \geq 2\omega$ and $q < 2\omega$. These are given by

$$\Delta(x)_{q\geq 2\omega} = -\frac{\epsilon^2}{4}g^2\left(\cos 2\omega x + 1\right) = -\frac{\epsilon^2}{4}g^2\cos^2\omega x = -\frac{1}{2}g_{tx}^2$$
$$\Delta(x)_{q<2\omega} = -\frac{\epsilon^2}{8}g^2\left[e^{2i\omega x} + \left(\frac{q}{\omega} - 1\right)e^{-2i\omega x} + 2\right]$$

The two modes $e^{2i\omega}$ and $e^{-2i\omega}$ can interfere constructively or destructively depending on the relative sign of q and ω. Note that the correction is symmetric under $\omega \to -\omega$ as expected. The $q, \omega < 0$ case is similar up to a change of sign.

Oscillating Source We now build on the previous results to analyse more intricate cases. Let $s(x) = s\cos qx$. Linearity of Eq.(5.12) together with the example above can be used to get the following correction,

$$\delta\langle\mathcal{O}(x)\rangle = \epsilon^2 s\frac{q}{4}\sum_{n=1}^{N}\sum_{m=1}^{N}\frac{A_n A_m}{\omega_n+\omega_m}\Big[\, e^{i(\omega_n+\omega_m+q)x}\left(|\omega_n+\omega_m+q|-|q|\right) + \\ -e^{i(\omega_n+\omega_m-q)x}\left(|\omega_n+\omega_m-q|-|q|\right)\Big].$$

Consider the particular sub-cases:

- $g(x) = g\cos\omega x$ ($A_1 = A_2 = \frac{1}{2}g$, $\omega_1 = -\omega_2 = \omega$, all other zero). The correction can be conveniently rearranged to give

$$\delta\langle\mathcal{O}(x)\rangle = \epsilon^2 q\frac{g^2 s}{4}\Bigg[\frac{|q+2\omega|-|q|}{2\omega}\cos\left((2\omega+q)x\right) \\ -\frac{|q-2\omega|-|q|}{2\omega}\cos\left((q-2\omega)x\right) + \cos qx\Bigg],$$

which is, as expected, a real result. However note that the source modes are now coupled with the geometry. We can still write the relative correction $\Delta(x)$ by dividing by the source, and being careful to take into account that when the

source vanishes the result is zero and not divergent.

$$\Delta(x) = -\epsilon^2 \frac{g^2}{4}\left[\frac{|q+2\omega|-|q|}{2\omega}\frac{\cos\left((2\omega+q)x\right)}{\cos qx} - \frac{|q-2\omega|-|q|}{2\omega}\frac{\cos\left((q-2\omega)x\right)}{\cos qx} + 1\right].$$

This can be analysed as before, giving

$$\begin{aligned}\Delta(x)_{q\geq 2\omega} &= -\epsilon^2\frac{g^2}{4}\left[\frac{\cos\left((2\omega+q)x\right)}{\cos qx} + \frac{\cos\left((q-2\omega)x\right)}{\cos qx} + 2\right] \\ &= \epsilon^2\frac{g^2}{4}\left[\cos 2\omega x + 1\right] = \frac{1}{2}g_{tx}^2,\end{aligned} \tag{5.13}$$

$$\Delta(x)_{q<2\omega} = -\epsilon^2\frac{g^2}{4}\left[\frac{\cos\left((2\omega+q)x\right)}{\cos qx} + \left(\frac{q}{\omega}-1\right)\frac{\cos\left((2\omega-q)x\right)}{\cos qx} + 1\right]. \tag{5.14}$$

Interestingly, as with all the examples we considered above, the relative correction for the case $q > 2\omega$ factors into a contribution that only depends on the underlying geometry. This can be interpreted intuitively as follows. If the wavelength of the source ($\propto q^{-1}$) is much smaller than the wavelength of the geometry, the dual operator will not 'feel' the inhomogeneity, leading to a coupling similar to the constant geometry case discussed in Section 5.3.2.1. In Fig.5.2 we plot the correction for different configurations of (ω, q) and inhomogeneity strength ϵ.

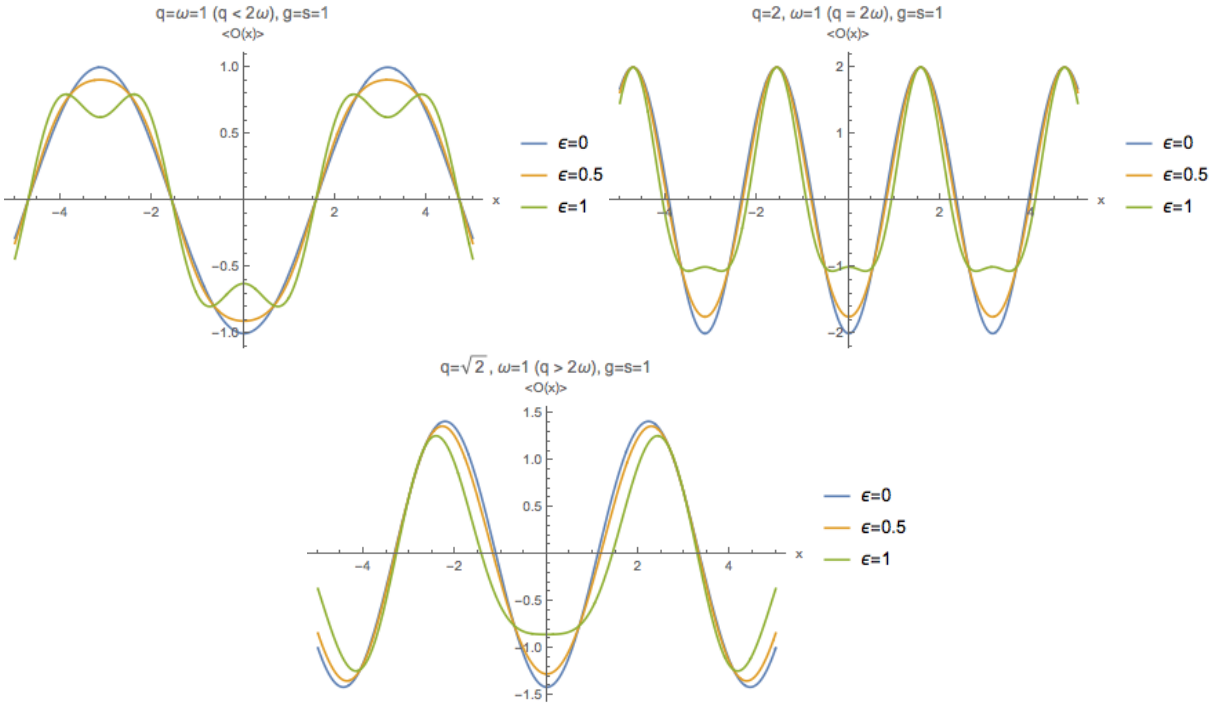

Figure 5.2: Expectation value of the boundary operator $\mathcal{O}$ Eq. (5.13) for source $s(x) = \cos qx$ and inhomogeneous geometry $g(x) = \cos \omega x$ with different configurations of (q, ω)

- $g(x) = \sum_{n=1}^{N} A_n \cos \omega_n x$. This polychromatic case is a direct extension of the above. It can be obtained by taking $N \to 2N$ and taking $A_n \to \frac{1}{2} A_n$ for $n = 1, \dots, 2N$, $\omega_n \to \omega_n$ for $n = 1, \dots, N$ and finally $\omega_n \to -\omega_n$ for $n = N+1, \dots, 2N$. By carefully splitting the sum and rearranging the terms, we get $\Delta(x) = \Delta_>(x) + \Delta_<(x)$ with

$$\Delta_>(x) = -\frac{\epsilon^2}{8} \sum_{n=1}^{N} \sum_{m=1}^{N} A_n A_m \left[\frac{|\omega_n + \omega_m + q| - |q|}{\omega_n + \omega_m} \frac{\cos\left((\omega_n + \omega_m + q)x\right)}{\cos qx} - \frac{|\omega_n + \omega_m - q| - |q|}{\omega_n + \omega_m} \frac{\cos\left((\omega_n + \omega_m - q)x\right)}{\cos qx} \right],$$

$$\Delta_<(x) = -\frac{\epsilon^2}{8} \sum_{n=1}^{N} \sum_{m=1}^{N} A_n A_m \left[\frac{|\omega_n - \omega_m + q| - |q|}{\omega_n - \omega_m} \frac{\cos\left((\omega_n - \omega_m + q)x\right)}{\cos qx} - \frac{|\omega_n - \omega_m - q| - |q|}{\omega_n - \omega_m} \frac{\cos\left((\omega_n - \omega_m - q)x\right)}{\cos qx} \right].$$

Note that since both terms are symmetric under the exchange $n \leftrightarrow m$, we can split the sum into a diagonal and an upper diagonal part, $\sum_{n,m} = \sum_{1 \le n \le N} + 2 \sum_{1 \le m < n \le N}$. The expressions can suggest that the diagonal part in $\Delta_<$ diverges. However this is not the case, since the denominators also vanish, and we have to take the limit carefully.

This polychromatic case is of particular interest since it can be used to simulate a discrete representation of disorder, as discussed in Appendix B. Defining $\Delta\omega = \frac{\pi}{Na}$ for some constant lattice spacing $a > 0$ and letting $A_n = \sqrt{\Delta\omega}$, $\omega_n = n\Delta\omega$ for $n = 1, \dots, N$ and adding random phases i.i.d. uniformly $\gamma \in [0, 2\pi)$ in the cosine arguments, $g(x)$ become a discrete representation of the Gaussian random process for large $N \gg 1$. As we will discuss in the next section, continuous disorder is more subtle, and we have to take the average at an early stage to make progress. Moreover, it is harder to implement it numerically since it can usually have discontinuous derivatives. For these reasons, this implementation is a useful representation and is specially suited for holography calculations, having been used in Chapter 4 and in many previous works in the literature [61, 88, 151]. In this case all modes ω_n are positive, and we can assume without loss of generality that $q > 0$. For convenience, we separate the sum in the correction in a diagonal

and a non-diagonal part, $\Delta = \Delta_{\mathrm{d}} + \Delta_{\mathrm{nd}}$ with

$$\Delta_{\mathrm{d}}(x) = -\frac{\epsilon^2}{4}\sum_{n=1}^{N} A_n^2 \,[2- \frac{|2\omega_n - q| - |q|}{2\omega_n}\frac{\cos\left((2\omega_n - q)x + 2\gamma_n\right)}{\cos qx} + \\ + \frac{\cos\left((2\omega_n + q)x + 2\gamma_n\right)}{\cos qx}\Big] \tag{5.15}$$

$$\Delta_{\mathrm{nd}} = -\frac{\epsilon^2}{4}\sum_{1\le m<n\le N}\frac{A_n A_m}{\cos qx}\Big[\cos\left((\omega^-_{nm} + q)x + \gamma_n - \gamma_m\right) + \\ + \cos\left((\omega^+_{nm} + q)x + \gamma_n + \gamma_m\right) + \\ - \frac{|\omega^+_{nm} - q| - |q|}{\omega^+_{nm}}\cos\left((\omega^+_{nm} - q)x + \gamma_n + \gamma_m\right) + \\ - \frac{|\omega^-_{nm} - q| - |q|}{\omega^-_{nm}}\cos\left((\omega^-_{nm} - q)x + \gamma_n - \gamma_m\right)\Big]. \tag{5.16}$$

where for convenience we abbreviated $\omega^{\pm}_{nm} = \omega_n \pm \omega_m$. Note that only the constant term in the diagonal part survives averaging over the i.i.d. phases γ_n. As expected, we reproduce the results for the constant geometry in Section 5.3.2.1 on average. In Fig.5.3 we plot the expectation value of the dual operator for $N = 10$ modes and fixed source $q = \sqrt{2}$ for a fixed realization of phases.

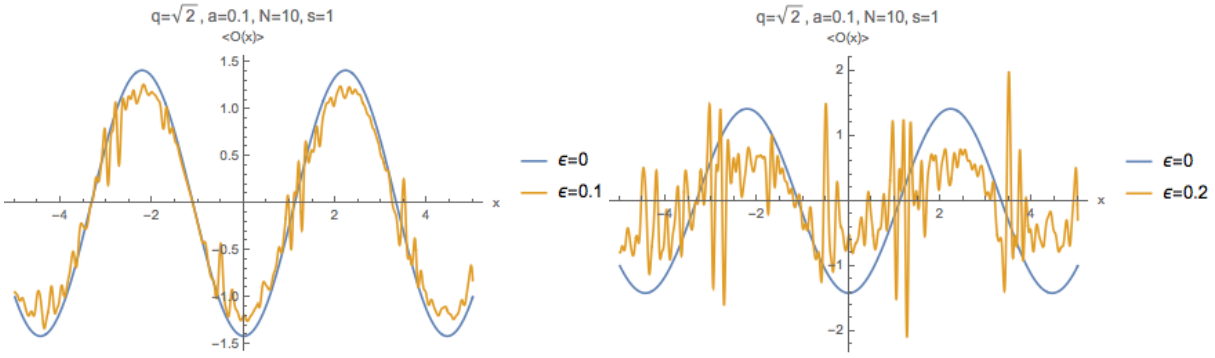

Figure 5.3: Expectation value of the boundary operator $\mathcal{O}$ Eq. (5.15) for source $s(x) = \cos\sqrt{2}x$ and discrete implementation of a disordered geometry $g(x) = \sum_{n=1}^{N} A_n \cos\left(\omega_n x + \gamma_n\right)$ for different amplitudes of disorder.

Delta source and two-point function We now consider the case $s_k = 1$ that leads to the corrections to the boundary-to-bulk propagator K. The integral Eq.(5.12) can be

done explicitly,

$$K_{(2)}(\rho;x) = \frac{\rho^{1/4}}{2}\sum_{n,m=1}^{N}\frac{A_nA_m}{\omega_n+\omega_m}\int_{\mathbb{R}}\frac{\mathrm{d}k}{2\pi}(k-\omega_n-\omega_m)\left(e^{-|k-\omega_n-\omega_m|\sqrt{\rho}}-e^{-|k|\sqrt{\rho}}\right)e^{ikx},$$
$$= \frac{1}{2\pi}\frac{\rho^{3/4}}{x^2+\rho}\sum_{n,m=1}^{N}A_nA_m\left[1-\frac{4e^{i\frac{(\omega_n+\omega_m)x}{2}}\sin\frac{(\omega_n+\omega_m)x}{2}}{\omega_n+\omega_m}\frac{x}{x^2+\rho}\right]. \tag{5.17}$$

Recall that the two-point function of the dual boundary operator is obtained by evaluating the boundary-to-bulk propagator at the boundary. Recalling that the zeroth order result is given by $\frac{1}{\pi x^2}$, this yields to a relative correction to two-point function given by

$$\frac{\delta\langle\mathcal{O}(x)\mathcal{O}(0)\rangle}{\langle\mathcal{O}(x)\mathcal{O}(0)\rangle_{(0)}} = \frac{\epsilon^2}{2}\sum_{n,m=1}^{N}A_nA_m\left[1-\frac{4e^{i\frac{(\omega_n+\omega_m)x}{2}}\sin\frac{(\omega_n+\omega_m)x}{2}}{(\omega_n+\omega_m)x}\right]. \tag{5.18}$$

Note that both terms are symmetric over $n\leftrightarrow m$. Thus we can split the sum into a diagonal term and a term where $n<m$,

$$\frac{\delta\langle\mathcal{O}(x)\mathcal{O}(0)\rangle}{\langle\mathcal{O}(x)\mathcal{O}(0)\rangle_{(0)}} = \frac{\epsilon^2}{2}\sum_{n=1}^{N}A_n^2\left(1-\frac{2e^{i\omega_nx}\sin\omega_nx}{\omega_nx}\right)+$$
$$+\epsilon^2\sum_{1\leq n<m\leq N}A_nA_m\left(1-\frac{4e^{i\frac{(\omega_n+\omega_m)x}{2}}\sin\frac{(\omega_n+\omega_m)x}{2}}{(\omega_n+\omega_m)x}\right)\Bigg].$$

Consider the following interesting examples,

- $g(x) = g\cos\omega x$.

  In this case we simply have

  $$\frac{\delta\langle\mathcal{O}(x)\mathcal{O}(0)\rangle}{\langle\mathcal{O}(x)\mathcal{O}(0)\rangle_{(0)}} = -\epsilon^2\frac{g^2}{2}\frac{\sin 2\omega x}{2\omega x}, \tag{5.19}$$

  which is proportional to a sinc function. Recall that we are looking at correlations of the point x with the origin. Thus the correction induced by the oscillating geometry suppress correlations of points closer to the origin. Note that for $\omega\gg 1$, the peak is sharper, while for $\omega\ll 1$ it is broader. Thus the bigger the wavelength of the inhomogeneous geometry, the less is the correction localised at $x=0$, see Fig.5.4. We can check that the limit $\omega\to 0$ reduces to the constant case discussed in Section 5.3.2.1.

- $g(x) = \sum_{n=1}^{N}A_n\cos(\omega_nx+\gamma_n)$.

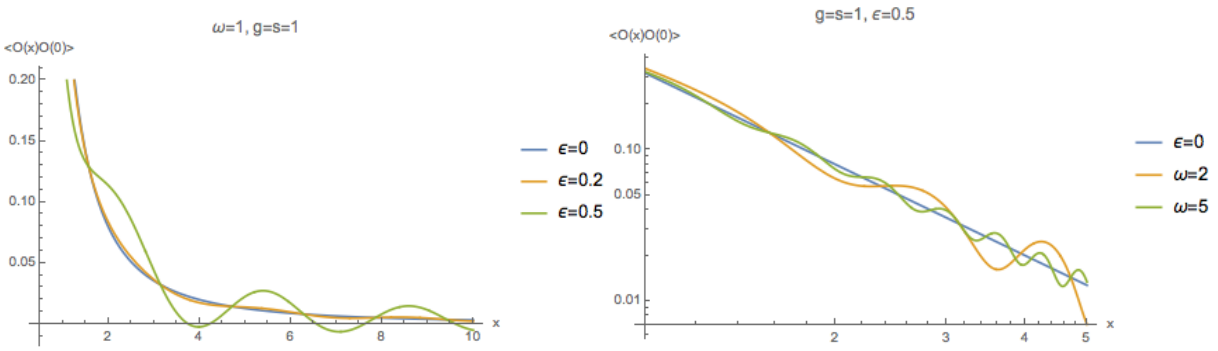

Figure 5.4: Two-point function $\langle \mathcal{O}(x)\mathcal{O}(0)\rangle = \langle \mathcal{O}(x)\mathcal{O}(0)\rangle_{(0)} + \epsilon^2\delta\langle \mathcal{O}(x)\mathcal{O}(0)\rangle$ for the oscillating geometry $g_{tx} = \epsilon\cos\omega x$, from Eq.(5.19). On the left, we fix the frequency and plot different amplitudes of ϵ, on the right we fix ϵ and plot different frequencies, in a log-log scale.

The result above can be easily generalised for many modes. Following the discussion in for the single cosine source, we have:

$$\begin{aligned}\frac{\delta\langle \mathcal{O}(x)\mathcal{O}(0)\rangle}{\langle \mathcal{O}(x)\mathcal{O}(0)\rangle_{(0)}} &= \frac{\epsilon^2}{4}\sum_{n=1}^{N}\sum_{m=1}^{N} A_n A_m\left[1 - \frac{\sin\left(\omega^+_{nm}x+\gamma_n-\gamma_m\right)}{\omega^+_{nm}x} - \frac{\sin\left(\omega^-_{nm}x+\gamma_n-\gamma_m\right)}{\omega^-_{nm}x}\right], \\ &= \frac{\epsilon^2}{4}\sum_{n=1}^{N} A_n^2\left[1-\frac{\sin(2\omega_n x+2\gamma_n)}{2\omega_n x}\right] \\ &+ \frac{\epsilon^2}{2}\sum_{1\le m<n\le N} A_n A_m\left[1 - \frac{\sin\left(\omega^+_{nm}x+\gamma_n-\gamma_m\right)}{\omega^+_{nm}x} - \frac{\sin\left(\omega^-_{nm}x+\gamma_n-\gamma_m\right)}{\omega^-_{nm}x}\right].\end{aligned} \tag{5.20}$$

Interestingly this discrete random process has mean zero.

Disordered Geometries

We now study the case where $g(x)$ is a centred random Gaussian field. As discussed in Appendix B, we can decompose g in its spectral modes $g(x) = \int_{\mathbb{R}} \frac{\mathrm{d}k}{2\pi} g_k e^{ikx}$, with g_k also given by a centered Gaussian process with $\mathbb{E}[g_k] = 0$ and $\mathbb{E}[g_k g_l] = g^2\delta(k-l)$. Equation (5.10) becomes a stochastic integro-differential equation, and is still intractable. However since it depends on the square of the geometry we can consider its non-trivial average. Defining $\bar{f}_k = \mathbb{E}[f_k]$ and averaging over g yield

$$\begin{aligned}4\rho^2\bar{f}_k'' - \left(\rho k^2 - \frac{3}{4}\right)\bar{f}_k &= -\rho^{5/4}g^2\int_{\mathbb{R}}\mathrm{d}q\ (k-2q)(k-q)e^{-|k-2q|\sqrt{\rho}}s_{k-2q}, \\ &= -\frac{\rho^{5/4}g^2}{4}\int_{\mathbb{R}}\mathrm{d}l\ l(k+l)e^{-|l|\sqrt{\rho}}s_l.\end{aligned} \tag{5.21}$$

As before, the constant source case give a trivial result. We now analyse non-trivial settings.

Plane wave source Let $s(x) = se^{iqx}$ with $q > 0$. Integrating Eq.(5.21) gives

$$4\rho^2 \bar{f}_k'' - \left(\rho k^2 - \frac{3}{4}\right) \bar{f}_k = -\frac{1}{4}\rho^{5/4} g^2 sq(k+q) e^{-|q|\sqrt{\rho}}. \tag{5.22}$$

The solution satisfying boundary conditions Eq.(5.9a) and (5.9b) is given by

$$\bar{f}_k(\rho) = \frac{1}{4}\rho^{1/4} g^2 s \frac{q}{k-q} \left[e^{-|q|\sqrt{\rho}} - e^{-|k|\sqrt{\rho}}\right]. \tag{5.23}$$

Note that the case $k = q$ can be treated by taking the limit of the above. Fourier transforming back,

$$\bar{\psi}_{(2)}(\rho, x) = \int_{\mathbb{R}} \frac{\mathrm{d}k}{2\pi} e^{ikx} \bar{f}_k(\rho) = \frac{1}{4}\rho^{1/4} g^2 s e^{iqx} \left[e^{-|q|\sqrt{\rho}} \mathrm{E}_1\left(iqx - q\sqrt{\rho}\right) - e^{|q|\sqrt{\rho}} \mathrm{E}_1\left(iqx + q\sqrt{\rho}\right)\right]. \tag{5.24}$$

The correction to the one-point function is given by

$$\overline{\Delta(x)} = \frac{\overline{\delta\langle\mathcal{O}\rangle}}{\langle\mathcal{O}\rangle_0} = \frac{\epsilon^2}{2} g^2 \left[\frac{ie^{-iqx}}{qx} + \mathrm{E}_1(iqx)\right]. \tag{5.25}$$

Oscillating source Let $s(x) = s\cos qx$. As before, by linearity of Eq.(5.21), we can build the oscillating case by summing two plane waves. Using that $\overline{\mathrm{E}_1(z)} = \mathrm{E}_1(\bar{z})$ we can simplify $\mathrm{E}_1(iqx) + \mathrm{E}_1(-iqx) = 2\mathrm{Re}\left[\mathrm{E}_1(iqx)\right] = -2\mathrm{Ci}(iqx)$, where $\mathrm{Ci}(x)$ is the cosine exponential function[29]. This leads to

$$\overline{\Delta(x)} = -\epsilon^2 g^2 \left[\frac{\sin qx}{qx} + \mathrm{Ci}(qx)\right]. \tag{5.26}$$

Delta source and two-point function Consider $s_k = 1$. Integrating the right-hand side of Eq.(5.21),

$$4\rho^2 \bar{f}_k'' - \rho k^2 \bar{f}_k + \frac{3}{4}\bar{f}_k = -\rho^{-1/4} g^2. \tag{5.27}$$

The regular solution at $\rho = \infty$ for the above is given by

$$f_k(\rho) = a_k \rho^{1/4} e^{-|k|\sqrt{\rho}} - \frac{g^2}{2\rho^{1/4}} + \frac{g^2}{4}\rho^{1/4} k e^{-k\sqrt{\rho}} \mathrm{Ei}(k\sqrt{\rho}) - \frac{g^2}{4}\rho^{1/4} k e^{k\sqrt{\rho}} \mathrm{Ei}(-k\sqrt{\rho}), \tag{5.28}$$

[29] Note that here the bars refer to the complex conjugate, and not to the average.

where $\mathrm{Ei}(x) = \int_{-x}^{\infty} t^{-1}e^{-t}\mathrm{d}t$ is the exponential integral functions. Close to the boundary $\rho = 0$ we have

$$f_k \underset{\rho=0}{\sim} -\frac{g^2}{2\rho^{1/4}} + a_k\rho^{1/4} + \frac{g^2}{2}\left(\gamma - 1 - \log k\sqrt{\rho}\right)\rho^{3/4} + \dots \,. \tag{5.29}$$

Therefore in order to preserve the zeroth order boundary condition we need to set $a_k = 0$. Note the appearance of two divergences: one proportional to $\rho^{-1/4}$ and the other proportional to $\log k\sqrt{\rho}$. As we will see next, they recombine when taking the Fourier transform and lead to a finite result.

Using the following Fourier transform that can be calculated from the definition of $\mathrm{Ei}(x)$,

$$\int_{-\infty}^{\infty} \frac{\mathrm{d}k}{2\pi} e^{-ak}\mathrm{Ei}(ak)e^{ikx} = -\frac{1}{2}\frac{|x| - ia\ \mathrm{sgn}(x)}{x^2 + a^2}, \qquad a > 0 \tag{5.30}$$

we can deduce that

$$\int_{-\infty}^{\infty} \frac{\mathrm{d}k}{2\pi} \left[e^{-ak}\mathrm{Ei}(ak) - e^{ak}\mathrm{Ei}(-ak)\right] e^{ikx} = \frac{ia\ \mathrm{sgn}(x)}{x^2 + a^2}. \tag{5.31}$$

Now using that $\mathcal{F}[ikf_k] = \partial_x f(x)$,

$$\int_{-\infty}^{\infty} \frac{\mathrm{d}k}{2\pi} \frac{k}{4} \left[e^{-ak}\mathrm{Ei}(ak) - e^{ak}\mathrm{Ei}(-ak)\right] e^{ikx} = -\frac{1}{2}\frac{a^2|x|}{(a^2 + x^2)^2} + \frac{1}{2}\delta(x). \tag{5.32}$$

Letting $a = \sqrt{\rho} > 0$ and taking into account the constant term leads to

$$K_{(2)}(\rho; x) = \int_{\mathbb{R}} \frac{\mathrm{d}k}{2\pi} f_k(\rho)e^{ikx} = -\frac{g^2}{2}\frac{\rho^{3/4}|x|}{(\rho + x^2)^2}. \tag{5.33}$$

Note that the first term in Eq.(5.28) leads to a delta function with opposite sign that exactly cancels the one coming from the derivative of the sign function. As discussed in Appendix A.3, this result is finite close to the boundary

$$K_{(2)}(\rho; x) \underset{\rho=0}{\sim} -\frac{g^2}{2}\frac{1}{|x|^3} + \dots \,. \tag{5.34}$$

Therefore the correction to the two-point function can be written as

$$\langle \mathcal{O}(x)\mathcal{O}(0)\rangle = \left(1 - \frac{\epsilon^2}{2}\frac{\pi}{|x|}\right)\frac{1}{\pi}\frac{1}{x^2}, \tag{5.35}$$

The effect of disorder is similar to the inhomogeneous case discussed in Section 5.3.2.2.

For points which are close together ($x = 0$) we have $|\frac{\delta\langle\mathcal{O}(x)\mathcal{O}(0)\rangle}{\langle\mathcal{O}(x)\mathcal{O}(0)\rangle_{(0)}}| \gg 1$ which indicates the breaking of the perturbative analysis. The minus sign of the correction indicates a suppression of the zeroth order result, see Fig. 5.5. We shall see that the exponent for which the correction blows up as $x \to 0$ depends on both the mass of the scalar field (here fixed to $m^2 = -3/4$) and on the type of disorder. In the following subsection, we will relax these conditions and explore the dependence of our results on these parameters.

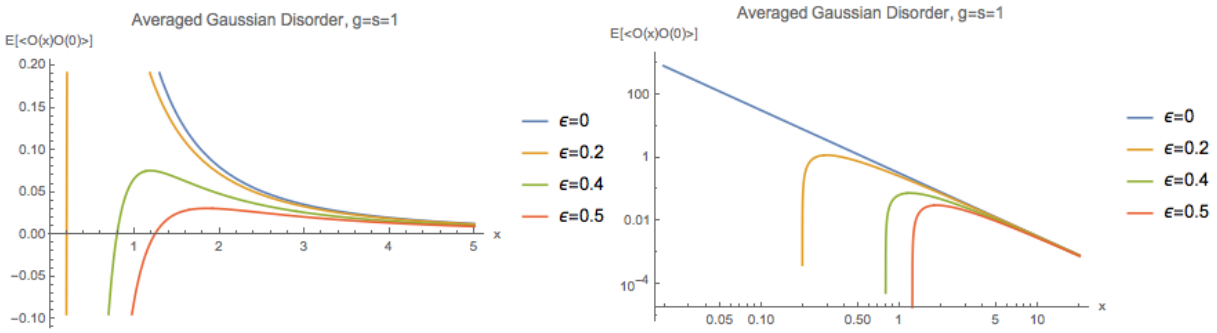

Figure 5.5: Averaged two-point function Eq. (5.35) for a disordered Gaussian geometry and different disorder strength ϵ. The plot on the right is the same as the one in the left, but in log-log scale.

Comments on other masses and correlated disorder

In this subsection we discuss how the results for the averaged two-point function generalise to different masses and correlated disorder.

We start by considering different masses. It is easy to check that for a generic mass parametrised by $\nu^2 = m^2 + 1$ the zeroth order solution of Eq.(5.4) that satisfies the boundary conditions Eqs.(5.3a),(5.3b) is given by,

$$f_k(\rho) = \frac{|k|^\nu}{2^{\nu-1}\Gamma(\nu)} K_\nu\left(|k|\sqrt{\rho}\right) s_k. \tag{5.36}$$

The boundary-to-bulk propagator is, as before, obtained by setting $s_k = 1$ and computing the Fourier transform, giving

$$K_{(0)}(\rho, x) = \frac{\rho^{1/2}}{2^{\nu-1}\Gamma(\nu)} \int_{\mathbb{R}} \frac{\mathrm{d}k}{2\pi} e^{ikx} |k|^\nu K_\nu\left(|k|\sqrt{\rho}\right) = \frac{\Gamma\left(\nu+\frac{1}{2}\right)}{\sqrt{\pi}\Gamma(\nu)} \frac{\rho^{\frac{\nu+1}{2}}}{\left(x^2+\rho\right)^{\nu+\frac{1}{2}}}. \tag{5.37}$$

Taking the near boundary limit, we obtain the expected dual two-point function,

$$\langle\mathcal{O}(x)\mathcal{O}(0)\rangle_{(0)} = \lim_{\rho\to 0} \rho^{-\frac{1+\nu}{2}} K_{(0)}(\rho, x) = \frac{\Gamma\left(\nu+\frac{1}{2}\right)}{\sqrt{\pi}\Gamma(\nu)} \frac{1}{|x|^{2\nu+1}} = \frac{\Gamma\left(\nu+\frac{1}{2}\right)}{\sqrt{\pi}\Gamma(\nu)} \frac{1}{|x|^{2\Delta_+-1}}, \tag{5.38}$$

which the the expected result for the two-point function of a conformal operator with mass dimension Δ_+. The minus one factor is, as before, due to the time dimensional reduction. The calculation of corrections induced by the disordered geometry are exactly as before, with the only difference that we use the general solution above as a source in Eq.(5.8). Averaging the right-hand side, we get the general equation

$$4\rho^2 \bar{f}_k'' - \left(\rho k^2 + \nu^2 - 1\right) \bar{f}_k = -\frac{\sqrt{\pi}\Gamma\left(\nu + \frac{3}{2}\right)}{\Gamma(\nu)} \rho^{-\nu/2}, \tag{5.39}$$

which reduces to Eq.(5.27) for $\nu = 1/2$. The general solution for the above is a combination of hypergeometric functions. So next we consider other values of ν for which the calculations are less cumbersome. Take for instance $\nu = 3/2$. In this case the solution satisfying the boundary conditions is given by

$$f_k(\rho) = -\frac{1}{\rho^{3/4}} + \frac{k}{4\rho^{1/4}} \left[e^{-k\sqrt{\rho}} \left(1 + k\sqrt{\rho}\right) \mathrm{Ei}\left(k\sqrt{\rho}\right) - e^{k\sqrt{\rho}} \left(1 - k\sqrt{\rho}\right) \mathrm{Ei}\left(-k\sqrt{\rho}\right)\right]. \tag{5.40}$$

The Fourier transform of the above can be computed exactly in the same way as in Section 5.3.2.3 and is given by

$$K_{(2)} = -\rho^{5/4} \frac{2|x|}{(\rho + x^2)^3}, \qquad \nu = 3/2.$$

Noting that for $\nu = 3/2$ we have $\Delta_+ = 1 + \nu = 5/2$, the dual two-point function is given by

$$\langle \mathcal{O}(x)\mathcal{O}(0)\rangle = \frac{2}{\pi}\left(1 - \frac{\epsilon^2}{2}\frac{\pi}{|x|}\right)\frac{1}{|x|^4}, \qquad \nu = 3/2.$$

This result follow exactly the one for $\nu = 1/2$, with the only difference that now the zeroth order result has a different mass dimension. It is not hard to check that the same is true for $\nu = 5/2$, where the averaged two-point function is given by

$$\langle \mathcal{O}(x)\mathcal{O}(0)\rangle = \frac{8}{3\pi}\left(1 - \frac{\epsilon^2}{2}\frac{3\pi}{|x|}\right)\frac{1}{|x|^6}, \qquad \nu = 5/2,$$

and now $2\Delta_+ - 1 = 6$. Although we have not manage to prove the general result, it seems that white noise always induce the same relative corrections in the two-point function. As we will discuss next, this is not completely surprising. For higher masses the dual operator is a more relevant deformation, but we are not changing the mass dimension of disorder.

To see this explicitly, note that the metric element g_{tx} should be dimensionless. Since we are imposing $g_{tx} = \epsilon \int \frac{\mathrm{d}k}{2\pi} e^{ikx} f_k$, we must have $[\epsilon] = -1 - [f_k]$. On the other hand, for Gaussian white noise $\mathbb{E}[f_k f_l] = \delta(k - l)$ and thus $2[f_k] = -1$. Therefore in this case we must have $[\epsilon] = -1 + 1/2 = -1/2$, i.e. Gaussian white noise is irrelevant. To change the effective

mass dimension of disorder, we can consider correlated disorder $\mathbb{E}[f_k f_l] = \sigma_k^2 \delta(k-l)$ with $\sigma_k^2 = |k|^\alpha$, $\alpha \in \mathbb{R}$. Note that since σ_k^2 is a variance, it needs to be a positive definite function. Generalising the previous discussion, this gives

$$[\epsilon] = -\frac{\alpha+1}{2}.$$

This is precisely what we found in the previous section: corrections to the two-point function decay faster in the IR limit $|x| \to \infty$ than the leading order result. Choosing $\alpha > 0$ will only make disorder more irrelevant. It is easy to check that for $\alpha > 0$, we get subleading powers of ρ which do not contribute to the two-point function.

We now explore the case $\alpha = -2$, when disorder becomes relevant. For simplicity, lets consider again $\nu = 1/2$. In this case, the integral in the right-hand side of Eq.(5.21) can be written as

$$\begin{aligned}\int \mathrm{d}q\, \frac{(k-2q)(k-q)}{q^2} e^{-|k-2q|\sqrt{\rho}} &= (2k\sqrt{\rho}+1)e^{k\sqrt{\rho}}E_2(k\rho) - (2k\sqrt{\rho}-1)e^{k\sqrt{\rho}}E_2(k\rho) - 4, \\ &= 2\rho^{-1/2} + k\Big[(2k\sqrt{\rho}+3)e^{k\sqrt{\rho}}\mathrm{Ei}(-k\sqrt{\rho}) + \\ &\qquad + (2k\sqrt{\rho}-3)e^{-k\sqrt{\rho}}\mathrm{Ei}(-k\sqrt{\rho})\Big],\end{aligned}$$

where $E_\alpha(z) = z^{\alpha-1}\int_z^\infty \mathrm{d}t\; t^{-\alpha}e^{-t}$ is the generalised exponential integral function, which in the last line we related to the exponential integral through the following recursive relation

$$p\; E_{p+1}(z) + z\; E_p(z) = e^{-z}.$$

together with $E_1(z) = -\mathrm{Ei}(-z)$. The regular solution at the Poincaré horizon which does not modify the source will be given by

$$\begin{aligned}f_k(\rho) &= -\rho^{3/4} - \frac{1}{2}\rho^{5/4}\left[(k\sqrt{\rho}+2)e^{k\sqrt{\rho}}\mathrm{Ei}(-k\sqrt{\rho}) - (k\sqrt{\rho}-2)e^{-k\sqrt{\rho}}\mathrm{Ei}(k\sqrt{\rho})\right], \\ &= -\rho^{3/4} - \rho^{3/4}F_+(k\sqrt{\rho}) + \frac{\rho^{5/4}k}{2}F_-(k\sqrt{\rho}), \\ &= -\rho^{3/4}\left[1 + F_+(\omega) - \frac{\omega}{2}F_-(\omega)\right],\end{aligned}$$

where in the last equality we defined $\omega = k\sqrt{\rho}$. We can compute the Fourier transform of the above in following the same recipes as discussed above. The boundary-to-bulk propagator is given by

$$K_{(2)}(\rho, x) = -\rho^{3/4}\frac{x^2|x|}{(\rho+x^2)^2},$$

and the correction to the boundary two-point function thus given by

$$\langle \mathcal{O}(x)\mathcal{O}(0)\rangle = \frac{1}{\pi}\frac{1}{|x|^2} - \frac{\epsilon^2}{|x|} = \frac{1}{\pi}\left(1-\epsilon^2\pi|x|\right)\frac{1}{|x|^2}.$$

Note that different from the results in the previous section, the correction induced by the correlated Gaussian disorder dominates the decay of the propagator at the IR, $|x| \to \infty$. For any fixed amplitude $\epsilon > 0$ and for $|x| > \frac{1}{\epsilon^2\pi}$ the correction becomes more important than the zero order result, which signals a breakdown of perturbation theory.

5.4 Numerical analysis

We have also performed a numerical analysis which allows us to confirm and extend our previous results beyond perturbation theory. Our first step is to compactify the interval of the radial coordinate. Following [151], we define y via

$$\rho = \frac{y^2}{(1-y)^2} \tag{5.41}$$

In this new coordinate, the boundary is located at $y = 0$ and the Poincaré horizon at $y = 1$. We redefine the scalar as

$$\psi = \frac{y^{1/2}}{(1-y)^{1/2}}\chi$$

We can check that the near boundary behaviour can be expressed in terms of χ as

$$\chi \approx \chi^{(0)} + y\langle O\rangle + \dots \tag{5.42}$$

Here $\chi^{(0)}$ and $\langle O\rangle$ correspond to the source and vacuum expectation value of the dual operator. Comparing with the pure AdS solution given in (5.5), we see that, at least for $g_{tx} = 0$ modes with non-zero momentum decay or grow exponentially at the horizon. After turning on g_{tx}, the near-horizon asymptotics become harder to analyse, but by continuity with the pure AdS case we demand that the field vanishes there.

We solve the equation of motion by discretising it on a homogeneous grid along both the radial coordinate y and the boundary coordinate x, and solving the resulting matrix equation in Mathematica. Since most of the variability occurs along x, we use $N_x = 450$ grid points along this direction, and $N_y = 50$ for the radial direction. After solving the wave equation, we extract the vacuum expectation value by taking a radial derivative of the solution at the boundary, as seen in (5.42).

We compute approximations to the one and two-point functions, concentrating on the case of disordered geometries. We do so by employing the spectral representation of disorder

discussed in Appendix B.3. More specifically, we take g_{tx} to be given Gaussian by using (B.4) with $\sigma(k_n) = 1$ with suitable modifications described in more detail below.

5.4.1 One-point correlation function

We consider one-point function of the scalar in the presence of the source

$$\chi^{(0)} = \cos(k_0 x).$$

As explained above, the vacuum expectation value corresponds to the derivative of the field at the boundary, as given by (5.42). Since the periodicities of the source and geometry need to fit in the same computational domain, the expansion of the disordered geometry will contain terms $\cos(2nk_0x + \gamma)$ with integer n, see Eq. (B.4). As seen in Section 5.3.2.2, these are potentially problematic since the commensurability of the source with the geometry induces extra near horizon divergences. To avoid this undesirable behaviour, we only consider cosines of odd momentum in the sum Eq.(B.4). We shall see that with this modification we can still obtain some generic features of disorder which match well with the perturbation theory results for small disorder amplitude, and extend them to higher values.

We extract the one-point function for $k_0 = 5$, and $N = 20$ for varying values of the disorder amplitude $\bar{V}$ as defined in Appendix B.3. For every $\bar{V}$, we generate a random geometry by providing random phases in Eq.(B.4). Once we have obtained a large number of them, we take the arithmetic average at each point x. We write the average vacuum expectation value as a suppression factor $\eta(\bar{V}, x)$ times the translational invariant result, given by $\langle O\rangle_0 := \langle O\rangle|_{\bar{V}=0} = -k_0 \cos(k_0 x)$. Hence, we define η by

$$\overline{\langle O\rangle}(x) = -\eta(\bar{V}, x) k_0 \cos(k_0 x) \tag{5.43}$$

For small disorder amplitudes the x-dependence of $\eta(\bar{V}, x)$ is very mild. However, at larger amplitudes the x-dependence of η becomes important. We show this in Fig. 5.6 where we plot the average of $\delta\langle O\rangle := \langle O\rangle_0 - \langle O\rangle$, normalised by $\langle O\rangle_0$, as a function of x.

In order to estimate the overall suppression, we track the value at the peak $\eta(\bar{V}, x = 0)$. We show our results in Fig 5.7. For small $\bar{V}$, we observe that the averaged one-point function displays the quadratic behaviour obtained in perturbation theory, although with different proportionality constant. At larger amplitudes, the power-law behaviour becomes milder. Moreover, we are able to fit the distribution of values of the vacuum expectation value at the peak with a Gaussian centred at the average value, see Fig 5.8.

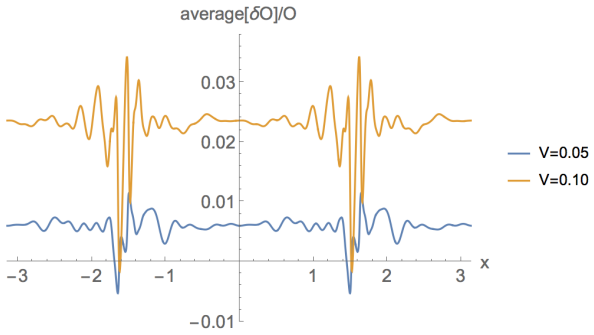

Figure 5.6: Change of the one-point function due to the presence of disorder as a function of x for different disorder amplitudes. We plot $\overline{\delta\langle O\rangle}/\langle O\rangle_0 = 1-\eta$, where η is defined in (5.43).

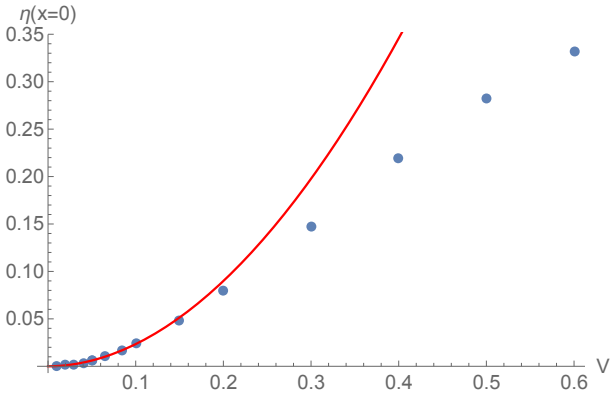

Figure 5.7: Dependence of the suppression of the peak of the vacuum expectation value, η, defined in (5.43), as a function of disorder. The solid red line is a fit we do for small $\bar{V}$, obtaining $\eta(x=0) \approx a\bar{V}^{\gamma}$ with $a = 2.05$, $\gamma = 1.94$. At higher $\bar{V}$ the exponent of the power law decreases.

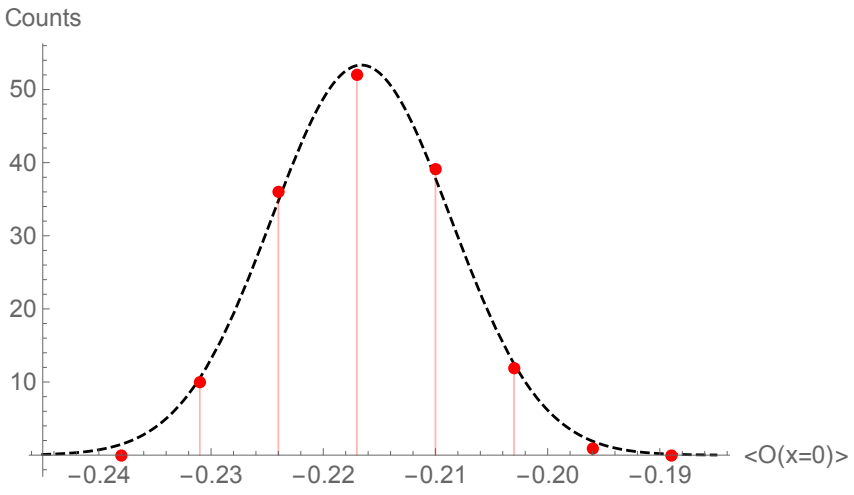

Figure 5.8: Distribution of the value of the vacuum expectation value at the peak, $\langle O\rangle(x=0)$, for $\bar{V} = 0.3$ for 150 runs. We fit this to a Gaussian, $f(x) = A\exp\left(-(x-\mu)^2/(2\sigma^2)\right)$, with parameters $A = 53.3$, $\mu = -0.21$, $\sigma = 8\times 10^{-3}$

5.4.2 Two-point correlation function

We now obtain an approximation to the two-point function in the presence of a disordered geometry. In principle, this entails a highly expensive calculation which requires inserting arbitrary sources at different points and taking the variation of the action with respect to them in the presence of a spatially dependent geometry. In order to gain some insight on the behaviour, we consider the more tractable calculation corresponding to the two-point function $G(x,0)$, which as explained above can be obtained by inserting a delta function source at $y=0$. In order to regularise the delta function, we follow the strategy of [228], i.e. we take as a source the boundary-to-bulk propagator evaluated at a small cutoff. We stress that we need to take into account the fact that in our numerics the x coordinate is periodic, which changes the form of the boundary-to-bulk propagator even in the absence of disorder $\bar{V}=0$. In fact, it is easy to show that for a box of length $2\pi/k_0$ the boundary-to-bulk propagator is given by

$$K(x,0;y)=\frac{\sinh\left(-\frac{y}{1-y}\right)}{\cos(k_0 x)-\cosh\left(-\frac{y}{1-y}\right)}$$

Note that here y refers to the radial variable introduced in Eq.(5.41).

Therefore, we approximate the two-point function $G(x,0)$ by the one-point function obtained in the presence of the source

$$\chi^{(0)}(x)=K(x,0;\delta) \tag{5.44}$$

at small δ. To test our approximation scheme, we first derive the results for pure AdS_3, $\bar{V}=0$. As expected, this approximation fails for $x\approx 0$. In particular, the so-obtained vacuum expectation values become very large and negative for small enough x. However, the results near the edge of the computational domain $x=\pi$ are well-behaved, and match well with the analytic result, see Fig 5.9. Therefore, we will be able to extract meaningful results away from the cores in this region[30].

The quantity of interest will be the ensemble average value of the one-point function in the presence of the source Eq.(5.44), $\overline{\langle O\rangle}(x)|_{\bar{V}}$. Normalizing this by the corresponding one-point function at $\bar{V}=0$, we define

$$\sigma(\bar{V},x)=\frac{\overline{\langle O\rangle}(x)|_{\bar{V}}}{\langle O\rangle|_{\bar{V}=0}}$$

In order to capture the behaviour away from the core, we take the spatial average in the

[30]Note that since we are using periodic boundary conditions, we cannot go infinitely far away from the cores of the delta functions.

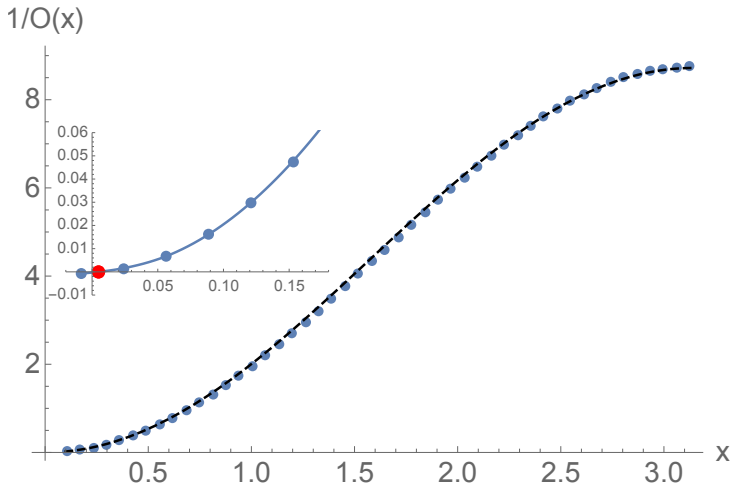

Figure 5.9: We show our numerical result for the inverse of the two-point function $G(x,0)$ evaluated as the one-point function in the presence of the source Eq.(5.44) for $\delta = 0.01$ and $\bar{V} = 0$. The blue dots represent the numerical data. The behaviour away from the core deviates only by a multiplicative factor ~ 1.09 from the analytic result obtained without cutoff $\langle O(x)\rangle^{-1} = k_0(1-\cos x)$. To illustrate this, we plot with the black dashed line the function $1.09k_0(1-\cos x)$ showing good agreement with the numerics. The inset shows the behaviour near $x = 0$. Here, the solid line shows interpolation of the numerical data, which indicates that two-point function acquires large, negative values near the core. The red dot marks the point where the numerics diverge.

interval $(2\pi/3, \pi)$, which we denote by

$$\tilde{\sigma}(\bar{V}) = \frac{3}{\pi}\int_{2\pi/3}^{\pi} \mathrm{d}x\ \sigma(\bar{V}, x) \tag{5.45}$$

This gives an estimate of the suppression of the two-point function in the presence of disorder.

We plot our results for this quantity with $k_0 = 5$, $N = 20$, $\delta = 0.01$ and varying $\bar{V}$ in Fig 5.10. Once again, we obtain a quadratic dependence of the suppression with the disorder amplitude.

5.5 Comparison with previous results in the literature

In the introduction, we reviewed different approaches to introduce disorder or spatial inhomogeneities in the holography literature. Now we discuss similarities and differences with the one introduced in this paper. A direct comparison is in general not possible in most cases. For instance the prediction for transport coefficients of [59, 70, 82–84, 86] requires the existence of a horizon and therefore are not applicable to our case. Even with no horizon, a comparison could be problematic because the assumption of a random chemical potential prevents, at least for a non-random background, any coherence effect. The addition of a random source, investigated in [63, 219], is, to the best of our knowledge,

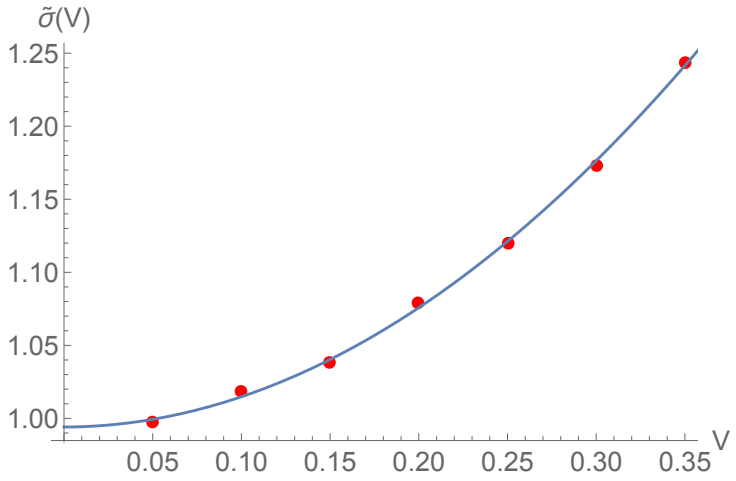

Figure 5.10: behaviour of $\tilde{\sigma}$ defined in Eq.(5.45) as a function of $\bar{V}$. The solid line corresponds to a fit with a model of the form $a + b\bar{V}^{\gamma}$ with $a = 0.99$, $b = 1.98$, $\gamma = 1.98$

not clearly connected to our approach. Instead of turning a source for the charge density, in our model we introduce a source for the stress energy tensor. From the gravitational perspective, we expect this to have a more significant effect because all fields couple to gravity. The equivalent field theory statement is that all operators propagate on the fixed boundary geometry. Moreover the geometry in this approach is not random, so no coherence effects are expected to be observed. It is an open question whether the observation of non-perturbative logarithmic corrections for marginal disorder in the two-point function, reported in [63,219], could occur in our setting. In order clarify these issues it would be necessary to carry out a full renormalization group analysis, beyond the scope of the paper, for the parameters for which the perturbative contribution from the disordered background becomes marginal. The result of such calculation would not only shed light on the existence of logarithmic corrections but also on the possible existence of a metal-insulator transition.

The approach closer to the one studied in the paper is maybe that of [61, 90, 94, 151] where a spatially random chemical potential, or scalar, in the boundary, backreacts in the gravity background that becomes inhomogeneous as well. However there are still important differences. At least perturbatively, interesting coherence effects are strongly suppressed, even if no horizon is present, because the only independent source of randomness comes from the scalar or chemical potential whose profile in the boundary is fixed by boundary conditions.

5.6 Conclusions

In this manuscript we have proposed a new approach to study disordered holographic field theories. We have computed numerically and analytically corrections due to a weakly disordered gravity background in the one and two-point function of the scalar dual boundary

operator for different choices of source and random component of the geometry g_{tx} (constant, a superposition of plane waves and finally a Gaussian random function). The main results can be summarised as follows:

- A constant geometry induces a negative constant correction that decreases the overall amplitude of the scalar one and two-point functions.
- The corrections induced by an oscillating geometry have a richer behaviour, and depend on the interaction with the source. In the simple case where the source is also an oscillating function, the perturbative correction to the one-point function can be positive or negative, depending on the relative sign of the geometry and source frequencies. For instance, if the source frequency is much bigger than the geometry's, the correction is similar in form to the constant case outlined above. However if the source frequency is smaller than the geometry's, the correction flips sign, adding constructively to the zeroth order one-point function.
- An oscillating sinusoidal geometry induces an oscillating but decaying correction to the two-point function, with an envelope $\sim |x|^{-\alpha}$ that depends on the scalar mass.
- The case in which the geometry is a superposition of oscillating modes is given, by linearity, by the sum of the single frequency results mentioned above.
- We have identified coherence effects between a sinusoidal source and the weakly random geometry introduced by a spectral decomposition. In certain region of parameters, the one-point function, which is sinusoidal, in the absence of disorder, becomes completely random even in the limit in which perturbation theory applies.
- The averaged corrections to the two-point function in the presence of a delta source and a weakly random, Gaussian distributed, gravity background, is negative and, for large distances, decays as a power-law with an exponent that depends on the type of disorder and the scalar mass. We have identified a range or parameters for which perturbation theory breaks down, as the power-law decay is slower than in the non-random case. This suggest an instability to a novel disorder driven fixed point which could eventually lead to a metal-insulator transition in the system.

6 | Chaotic-Integrable transition in the Sachdev-Ye-Kitaev model[†]

Quantum chaos is one of the distinctive features of the Sachdev-Ye-Kitaev (SYK) model, N Majorana fermions in $0+1$ dimensions with infinite-range two-body interactions, which is attracting a lot of interest as a toy model for holography. In this chapter, we show analytically and numerically that a generalised SYK model with an additional one-body infinite-range random interaction, which is a relevant perturbation in the infra-red, is still quantum chaotic, and retains most of its holographic features, for a fixed value of the perturbation and sufficiently high temperature. However a chaotic-integrable transition, characterised by the vanishing of the Lyapunov exponent and spectral correlations given by Poisson statistics [115], eventually occurs in the low-temperature limit.

6.1 Introduction

Fermionic models with random interactions of infinite range have been intensively investigated in a variety of contexts: from nuclear physics [229–234] to quantum chaos [235–240] and condensed matter physics [241]. Recently the study of these infinite range models has received a new impetus after Kitaev [100] found intriguing similarities with black hole physics that suggested its relevance in holography. More specifically, it was shown that the pattern of spontaneous and explicit conformal symmetry breaking in a simple model of N Majorana fermions with random two-body interactions of infinite range, from now on referred to as the Sachdev-Ye-Kitaev model (SYK), in the strong-coupling limit is identical to that of an anti-de Sitter background in two dimensions close to the horizon [101,242,243]. As it was discussed in Section 2.5.1, two-dimensional AdS is a ubiquitous geometry in applied holography, since it generically emerges as the near-horizon geometry of extremal black holes. As a consequence, it governs many of the important properties of quantum critical theories dual to these zero-temperature black holes. Besides sharing the same symmetry-

[2]This Chapter is based on Ref. [115], and was done in collaboration with Antonio M. García-García, Aurelio Romero-Bermúdez and Masaki Tezuka. The author would like to acknowledge A. M. García-García, M. Tezuka and A.R. Bermúdez for the numerical work in Section 6.3.3.

breaking patterns, both the SYK and AdS_2 have quantum chaotic features as the exponential growth for intermediate times of certain out-of-time correlation functions with the same universal exponent [101, 102]. The thermodynamic coefficients in the low-temperature free energy expansion, such as the zero temperature entropy density and the specific heat coefficient, are also shared by both models. The SYK model provides thus an ideal candidate for the field theory dual of the AdS_2 fixed point.

Research on the SYK model has also drawn considerable attention beyond the high-energy community. The astounding simplicity and intriguing non-Fermi liquid properties of the model have attracted the attention of condensed matter physicists, who saw the opportunity for using the solvable strongly-interacting model as a building block for engineering more complex phase diagrams. Interesting research lines currently being investigated include application to random matrix theory [104, 244–248], possible experimental realizations [112, 113, 249] and extensions involving non-random couplings [250, 251], higher spatial dimensions [106, 108, 110, 252, 253] and several flavours [254].

A natural question to ask [106, 108, 110, 250, 252–254] is to what extent the holographic properties are present in generalised SYK models. For instance, similar features are observed for non-random couplings [250] and in higher-dimensional realizations of the SYK [108,253] model. However, in some cases, the addition of more fermionic species can induce a transition to a Fermi liquid phase [106] or a metal-insulator transition [110, 252] which, at least superficially, spoils the holographic interpretation. In particular, if we take the perspective that the SYK model is an effective description for the infra-red fixed point of a higher theory, it is natural to study the stability of the model under deformations. In this chapter, we address this question by considering a simple relevant deformation of the SYK model, consisting in the addition of a random all-to-all one-body "hopping" term. We employ analytical and numerical techniques to study the thermodynamic and chaotic properties of this generalised model, which from now on is referred as *our model*.

The structure of the chapter is as follows. In Section 6.2, we review some of the key results concerning the vanilla SYK model. This section contains no original results, but illustrate some of the useful techniques we will need in the investigation of our model. Section 6.3 is the bulk of our original work. We introduce our generalised model and proceed with the analytical investigation of the thermodynamic and chaos properties of our model. Our results, which are also supported by an exact numerical analysis, suggest that although the thermodynamical properties of the model are dominated by the integrable deformation, there is a window of temperatures where the model is chaotic. Outside this window, our model undergoes a chaotic-integrable transition. Therefore, for a certain range of parameters, a holographic interpretation of the model is still plausible.

6.2 An overview of the SYK model

The SYK model is defined by N-Majorana fermions interacting via a $q/2$-body disordered all-to-all Hamiltonian,

$$H = i^{q/2} \sum_{1 \leq i_1 < i_2 < \cdots < i_q \leq N} J_{i_1 i_2 \ldots i_q} \chi_{i_1} \chi_{i_2} \cdots \chi_{i_q}. \tag{6.1}$$

The Majorana fermions satisfy the usual anti-commutation relations $\{\chi_i, \chi_j\} = \delta_{ij}$. Note that q is assumed to be even, and a factor of i is necessary to make the Hamiltonian hermitian when $q = 2 \bmod 4$. The disordered couplings $J_{i_1 i_2 \ldots i_q}$ are taken to be i.i.d. centred normal random variables with variance $\mathbb{E}[J^2_{i_1 i_2 \ldots i_q}] = J^2 (q-1)! N^{1-q}$, which is chosen such that the averaged energy is extensive. The constant J parametrises the amplitude of the quenched disorder fluctuations, and at $T = 0$ is the only length scale of the model, with $[J] = 1$ (in units of energy).

Note that since the disordered interaction term is all-to-all, there is no notion of spatial locality in the model, and therefore one is only interested in studying the time evolution of the model. At equilibrium, we can compute the partition function by performing a path integral in Euclidean time over a circle with radius $\beta = T^{-1}$,

$$\mathcal{Z} = \int_{\chi(\tau) = \chi(\tau + \beta)} \mathrm{D}\chi \; e^{-\int_0^\beta \mathrm{d}\tau (\chi \partial_\tau \chi - H(\tau))}, \tag{6.2}$$

where $L(\tau) = \chi \partial_\tau \chi - H(\tau)$ is the Lagrangian of the system. In particular, we are interested in the averaged free energy $-\beta F = \mathbb{E}[\log \mathcal{Z}]$, which give us information about the phase diagram of the model. However, as usual in quenched disorder models, it is hard to compute the average over a logarithm [255]. We, therefore, recur to the *replica trick*:

$$-\beta F = \mathbb{E}[\log \mathcal{Z}] = \lim_{n \to 0} \frac{1}{n} \left(\mathbb{E}\left[\mathcal{Z}^n\right] - 1 \right). \tag{6.3}$$

The replicated partition function $\mathcal{Z}^n$ is defined by taking the tensor product of n independent copies of the original Hilbert space. Its average is easier to compute,

$$\mathbb{E}[\mathcal{Z}^n] = \int \prod_{a=1}^{n} \mathrm{D}\chi_a \; \mathbb{E}\left[e^{-\sum_{a=1}^{n} \int_0^\beta \mathrm{d}\tau (\chi_a \partial_\tau \chi_a - H_a(\tau))} \right], \tag{6.4}$$

where the index $a = 1, \ldots, n$ labels the different replicas, and we have omitted the periodic boundary conditions to lighten notation. Note that the analytic continuation implied by the limit in Eq.(6.3) is not always well defined, a technical point which we avoid here. The average in Eq.(6.4) can be taken by noting that if X is a centred and normally distributed

random variable, then $\mathbb{E}[e^X] = e^{\frac{1}{2}\sigma^2}$, where σ^2 is the variance of X. This yields a term with $2q$ Majorana fermions that couple different replica indices. Performing two Hubbard-Stratonovich transformations and integrating out the Majoranas we obtain the following effective action,

$$\frac{S_{\text{eff}}}{N} = -\sum_{a,b=1}^{n} \text{Tr}\log\left(\delta_{ab}\delta(\tau-\tau')\partial_\tau - \Sigma_{ab}(\tau,\tau')\right) + \\ -\frac{1}{2}\int_0^\beta \mathrm{d}\tau \int_0^\beta \mathrm{d}\tau' \left[\Sigma_{ab}(\tau,\tau')G_{ba}(\tau',\tau) + \frac{J^2}{q}G_{ab}(\tau,\tau')^q\right] \tag{6.5}$$

where $G_{ab}(\tau,\tau') = N^{-1}\sum_{i=1}^{N}\chi_{i,a}(\tau)\chi_{i,b}(\tau')$ is a bilinear on the Majorana fields and Σ_{ab} is its Hubbard-Stratonovich conjugate. Note that, since the χ's anti-commute we have $G_{ab}(\tau,\tau') = -G_{ba}(\tau',\tau)$. In terms of the effective fields (G,Σ), the average replicated partition function is now given by $\mathbb{E}[\mathcal{Z}^n] = \int \mathrm{D}G\mathrm{D}\Sigma\, e^{-S_{\text{eff}}[G,\Sigma]}$. Note that, since the effective action is proportional to N, in the large-N limit the path integral is dominated by the saddle-points that extremise S_{eff}. In particular, we will be interested at *replica symmetric* saddle points for which $G_{ab} = \delta_{ab}G$ and $\Sigma_{ab} = \delta_{ab}\Sigma$, and the limit in Eq.(6.3) is trivial. The replica symmetric saddle solve the following *saddle-point equations*,

$$\partial_\tau G(\tau,\tau') - \int_0^\beta \mathrm{d}\tau'\, \Sigma(\tau,\tau')G(\tau',\tau'') = -\delta(\tau-\tau''), \tag{6.6}$$

$$\Sigma(\tau,\tau') = J^2 G_(\tau,\tau')^{q-1}. \tag{6.7}$$

Note these equations are the Wigner-Dyson equations for the two-point function of the theory. It is convenient to first study the saddle-point equations at $T = 0$, which simply means unwrapping the thermal circle and taking $\tau \in \mathbb{R}$. At a saddle, G gives the many-body Green's function and Σ the associated self-energy. For a time translational invariant ansatz, $G(\tau,\tau') = G(\tau-\tau')$ (same for Σ), it is convenient to write Eq.(6.6) in Fourier space

$$G(\omega_n) = -\left[i\omega_n + \Sigma(\omega_n)\right]^{-1}, \tag{6.8}$$

$$\Sigma(\omega_n) = J^2\int_0^\beta \mathrm{d}\tau\, e^{-i\omega_n\tau}G(\tau)^{q-1}, \tag{6.9}$$

where $\omega_n = \frac{\pi}{\beta}(2n+1)$ are the fermionic Matsubara frequencies. Once a solution to the saddle-point equations is found, we can compute the equilibrium thermodynamic properties of the model by inserting the pair of saddle solutions $(\bar{G},\bar{\Sigma})$ back into the effective action Eq.(6.5). For a replica symmetric, translational invariant saddle, the *free energy density* $f = F/N$ can

be written as,

$$-\beta f = -\frac{1}{2}\mathrm{Tr}\log\bar{G} - \frac{(\beta J)^2}{2}\left(1-\frac{1}{q}\right)\int_0^1 \mathrm{d}\theta\, \bar{G}(\theta)^q \tag{6.10}$$

where we have defined $\theta = \frac{\tau}{\beta} \in (0,1)$. For low temperatures $\beta \gg 1$, we expect to write the free energy as a power series in β^{-1},

$$-\beta F \underset{\beta\to\infty}{=} -\beta E_0 + S_0 + \frac{c}{2\beta} + O(\beta^{-2}), \tag{6.11}$$

where E_0 is the ground state energy, S_0 the zero temperature entropy and c the specific heat coefficient. We start by discussing the simplest case of $q = 2$, where an exact solution of the saddle-point equations can be found, and the thermodynamic coefficients in the above expansion computed exactly.

6.2.1 Integrable case, $q = 2$

In general Eqs.(6.6) and (6.7) do not have a closed form solution. The only exception is for $q = 2$, when $\Sigma(\omega) = J^2 G(\omega)$ and Eq.(6.8) is a quadratic polynomial in G. It can be solve exactly to give

$$G(\omega_n) = \frac{i}{2J}\left(-\frac{\omega_n}{J} + \sqrt{4+\left(\frac{\omega_n}{J}\right)^2}\right) = J^{-1}\int_{-2}^{2}\frac{\mathrm{d}\lambda}{2\pi}\frac{\sqrt{4-\lambda^2}}{\lambda - i\omega_n/J}, \tag{6.12}$$

where in the last equality we wrote the Green's function in terms of its *spectral representation*. The spectral representation allow us to analytically continue $G(\omega_n)$ to the whole complex plane by simply taking $z = i\bar{\omega}_n$.

$$G(z) = J^{-1}\int_{\mathbb{R}}\frac{\mathrm{d}\lambda}{2\pi}\frac{\rho(\lambda)}{\lambda - z/J}, \tag{6.13}$$

where $\rho(\lambda) = \sqrt{4-\lambda^2}\,\mathbb{I}_{[-2,2]}$ is the *spectral density*, given by the *Wigner semicircle law*. This result shouldn't come as a surprise, since for $q = 2$ the system is non-interacting, and the Hamiltonian is a simple Wigner matrix. From the spectral representation, it is possible to obtain the real-time retarded and advanced Green's functions by analytically continuing down to the real-frequency axis $G^{R/A}(\epsilon) = G(z = \epsilon \pm i0^+)$. The Matsubara Green's function can be computed from Eq.(6.12) by summing over the Matsubara frequencies,

$$G^\beta(\tau) = \frac{1}{\beta}\sum_{n\in\mathbb{Z}} e^{-i\omega_n\tau}G(\omega_n) = \frac{1}{\beta J}\int_{\mathbb{R}}\frac{\mathrm{d}\lambda}{2\pi}\frac{\rho(\lambda)e^{-\lambda J\tau}}{1+e^{\beta\lambda}}. \tag{6.14}$$

Note that, as expected, the Matsubara Green's function is anti-periodic in τ, $G^\beta(\tau+\beta) = -G(\tau)$. The free energy density $f = F/N$ can be computed by inserting the saddle-point solution $G^\beta(\tau)$ back into the action Eq.(6.5). While there is not a closed form expression for all $\beta > 0$, of particular interest are thermodynamic coefficients in the low-temperature expansion given in Eq.(6.11). By an explicit calculation it is easy to check that the integral terms in Eq.(6.5) do not contribute to these lowest order coefficients, and the leading contributions come from the Tr log term. It can be conveniently written in terms of the Matsubara frequencies as

$$\mathrm{Tr}\log G = \beta \sum_{n\in\mathbb{Z}} \log G(i\omega_n) e^{i\omega_n 0^+}. \tag{6.15}$$

We can rewrite the sum over frequencies as the residue of the complex integral $\int_\gamma \frac{\mathrm{d}z}{2\pi i}\log G(z)n(z)e^{z0^+}$ where $n(z) = (1+e^{\beta z})^{-1}$ and the contour γ englobes the poles at $z = i\omega_n$. The integrand also has a branch cut along the real axis. Since the integral decay at infinity, we can deform γ to wrap around the branch cut in the real axis. This leads to

$$\begin{aligned}\frac{1}{2}\mathrm{Tr}\log G &= \beta\int_\gamma \frac{\mathrm{d}z}{2\pi i}\log G(z)n(z)e^{z0^+}\\ &= \beta\int_{\mathbb{R}}\frac{\mathrm{d}\epsilon}{2\pi i}n(\epsilon)\left[\log G(\epsilon+i0^+) - \log G(\epsilon - i0^+)\right]\\ &= \beta\int_{\mathbb{R}}\frac{\mathrm{d}\epsilon}{\pi}n(\epsilon)\mathrm{Im}\log G^R(\epsilon) = \beta\int_{\mathbb{R}}\frac{\mathrm{d}\epsilon}{\pi}\frac{\mathrm{Arg}\, G^R(\epsilon)}{1+e^{\beta\epsilon}},\end{aligned} \tag{6.16}$$

In our case, G^R is simply obtained by analytically continuing Eq.(6.12). Thus,

$$\mathrm{Arg}\, G^R = \begin{cases}\frac{\pi}{2} - \tan^{-1}\left(\frac{-\epsilon/J}{\sqrt{4J^2-\epsilon^2}}\right) & \text{for } |\epsilon| < 2J,\\ \pi & \text{for } \epsilon \geq 2J,\\ 0 & \text{for } \epsilon \leq -2J,\end{cases} \tag{6.17}$$

giving

$$\begin{aligned}\frac{1}{2}\mathrm{Tr}\log G &= \beta J\int_{-2}^{2}\frac{\mathrm{d}\epsilon}{\pi}\frac{\frac{\pi}{2} - \tan^{-1}\left(\frac{-\epsilon}{\sqrt{4-\epsilon^2}}\right)}{1+e^{\beta J\epsilon}} + \beta\int_2^\infty \frac{\mathrm{d}\epsilon}{1+e^{\beta J\epsilon}}\\ &\underset{\beta\gg 1}{=} \beta J(\pi-1) + \log\left(1+e^{-2\beta J}\right) + \frac{\pi}{12\beta J} + O(\beta J^{-3}),\end{aligned} \tag{6.18}$$

where in the last equality we used the Sommerfeld expansion for the Fermi-Dirac distribution $n(\epsilon) \underset{\beta\gg 1}{=} \theta(-\epsilon) - \frac{\pi^2}{6(\beta J)^2}\delta'(\epsilon) + O(\beta J^{-4})$. The log term is exponentially decaying, and does not contribute in Eq.(6.11). Therefore we have $E_0 = (1-\pi)\,JN$, $s_0 = 0$ and $c = \frac{\pi}{6}\frac{N}{J}$.

6.2.2 Large-q analysis

The case $q = 2$ is somehow less interesting since the model is not interacting. On the other hand, for $q > 0$ an exact solution is not available, and one has to appeal to a perturbative approach in coupling at strong coupling $J\tau \gg 1$, discussed in Section 6.2.3. But before, we introduce another extreme limit where the model can be studied for all $J > 0$. The idea is to make a large-q expansion around the free fermion solution $G(\tau) = \frac{1}{2}\text{sgn}(\tau)$,

$$G(\tau) \underset{q\to\infty}{=} \frac{1}{2}\text{sgn}(\tau)\left(1 + \frac{1}{q}g(\tau) + O\left(q^{-2}\right)\right), \tag{6.19}$$

Note however that at large-q the self-energy Σ would scale as,

$$\Sigma(\tau) \underset{q\to\infty}{=} J^2 2^{1-q}\text{sgn}(\tau)e^{g(\tau)} + O(q^{-1}) \tag{6.20}$$

Therefore to have a self-consistent large-q expansion where the self-energy is suppressed at large-q, we have to rescale the coupling $J \to 2^{q-1}q^{-1}J^2$. [31] The $q \to \infty$ expansion around the free solution is therefore well-defined in the rescaled model. Inserting the expansion in the saddle-point Eq. (6.6) and simplifying, we get simple ordinary differential equation for g

$$\partial_\theta g(\theta) = 2(\beta J)^2 e^{g(\theta)}, \tag{6.21}$$

where again we work in the coordinate $\theta = \tau/\beta \in (0, 1)$. The equation above is a standard boundary value problem, with boundary conditions $g(0) = g(1) = 0$. The solution is simply given by

$$e^{g(\theta)} = \left[\frac{\cos\frac{\pi\nu}{2}}{\cos\left(\pi\nu\left(\frac{1}{2} - \theta\right)\right)}\right]^2, \qquad \beta J = \frac{\pi\nu}{\cos\frac{\pi\nu}{2}}. \tag{6.22}$$

Note that $\nu \in [0, 1]$ parametrises the flow of βJ. The weak-coupling regime $\beta J = 0$ is given by $\nu = 0$, while the strong-coupling regime $\beta J = \infty$ is given by $\nu = 1$. As in the previous section, we compute the free energy density by inserting the solution Eq.(6.22) in Eq.(6.10), keeping only the leading terms in q. A shortcut into the calculation is to first take a derivative $\partial_J(-\beta f)$, compute the integral term and then integrate the result to recover the full free energy density [102],

$$-\beta f = \frac{1}{2}\log 2 + \frac{\pi\nu}{q^2}\left[\tan\frac{\pi\nu}{2} - \frac{\pi\nu}{4}\right] + O\left(q^{-3}\right). \tag{6.23}$$

[31] Note that this rescaling represents a change in the variance of the original model.

To obtain the low-temperature (or strong-coupling) expansion of the free energy density in terms of βJ, we have to invert the power series of βJ in around $\nu = 1$,

$$1 - \nu \underset{\beta J \to \infty}{=} \frac{2}{\beta J} - \frac{4}{(\beta J)^2} + 8\left(1 + \frac{\pi^2}{24}\right) + O\left(\beta J^{-4}\right). \tag{6.24}$$

The low-temperature expansion of the free energy Eq.(6.23) is thus given by

$$-\beta f = \frac{1}{q^2}\beta J + \left(\frac{1}{2}\log 2 - \frac{\pi^2}{4q^2}\right) + \frac{2(6+\pi^2)}{3q^2}\frac{1}{\beta J} + O\left(\beta J^{-2}, q^{-3}\right), \tag{6.25}$$

and therefore we can identify, to leading order in large-q, the thermodynamic coefficients $E_0 = q^{-2}NJ$, $s_0 = S_0/N = \frac{1}{2}\log 2 - \frac{\pi^2}{4q^2}$ and $c = \frac{4(6+\pi^2)}{3q^2 J}N$. Differently from the $q = 2$ result, the interacting large-q model has a residual zero temperature entropy $s_0 > 0$ which is one of the distinctive holographic properties of the SYK model. Extrapolating this result down to $q = 2$, we can also observe a positive increase in the specific heat coefficient. These are generic features of $q > 2$.

6.2.3 Strong-coupling limit and conformal symmetry

For finite $q > 2$, there is no closed-form solution of the saddle-point equations. We, therefore, resort to a perturbative analysis in the coupling J. For high-temperature or weak-coupling $\beta J \ll 1$, the system is well-described by free fermions. The interesting region is the *strong-coupling* or low-temperature regime $\beta J \gg 1$. In this limit, the non-linear interaction term in the saddle-point Eq.(6.6) dominate over the derivative term. The saddle-point equation reads,

$$J^2 \int_0^\beta \mathrm{d}\tau'\, G(\tau - \tau')G(\tau' - \tau'')^{q-1} = \delta(\tau - \tau''). \tag{6.26}$$

It is easy to check that this equation is invariant under time reparametrization symmetry $\tau \to f(\tau)$, where the two-point functions transforms covariantly as

$$G(\tau - \tau') \to \left[f'(\tau)f'(\tau')\right]^{\Delta} G(f(\tau) - f(\tau')), \tag{6.27}$$

where we have defined $\Delta = 1/q \in \left(0, \frac{1}{2}\right)$, and $' = \partial_\tau$. This symmetry can be seen as an emerging *conformal symmetry* of the model in the strongly-coupled limit, under which the fermion-bilinear operator G transforms as an operator with conformal dimension Δ. The conformal symmetry suggests a procedure to solve the saddle-point equation. First, without loss of generality we can work at $T = 0$ by unwrapping the thermal circle and taking $\tau \in \mathbb{R}$, since finite temperature solutions can be obtained from the zero temperature ones through the reparametrization given by $\tau \to \tan \frac{\pi\tau}{\beta}$. Second, conformal symmetry suggests we can

find a particular solution with the scaling ansatz $G(\tau) = A\ \mathrm{sgn}(\tau)|\tau|^{-\alpha}$. Lastly, all other equivalent solutions can be found by applying the conformal mapping $\tau \to f(\tau)$.

Inserting the scaling ansatz in Eq.(6.26) yield

$$G_c(\tau) = b\frac{\mathrm{sgn}(\tau)}{|J\tau|^{2\Delta}}, \qquad\qquad b = \left[\frac{\tan \pi\Delta}{2\pi}\,(1-2\Delta)\right]^{\Delta}. \tag{6.28}$$

Note that this solution spontaneously break the reparametrization symmetry of the conformal action. It is not hard to check, however, that the scaling solution in Eq.(6.28) conserves a residual symmetry given by the Möbius transformations $\mathrm{SL}_2(\mathbb{R})$: $f : \tau \mapsto \frac{a\tau+b}{c\tau+d}$ with $ad-bc \neq 0$. According to Goldstone's theorem, this implies the existence of Goldstone modes living in the coset space $f \in \mathrm{Diff}(\mathbb{R})/\mathrm{SL}_2(\mathbb{R})$ which parametrise the set of different, but conformally equivalently set of solutions of Eq.(6.26). Among those, the finite temperature solution can be obtained from the scaling ansatz by compactifying back the line $f : \tau \to \tan \frac{\pi\tau}{\beta}$,

$$G_c^{\beta}(\theta) = b\left[\frac{1}{\beta J \sin \pi\theta}\right]^{2\Delta}, \qquad\qquad \theta = \frac{\tau}{\beta} \in (0,1). \tag{6.29}$$

We can focus on the finite temperature landscape of solutions by restricting to the Goldstone modes $f \in \mathrm{Diff}(S^1)/\mathrm{SL}_2(\mathbb{R})$ which characterise further reparametrizations of the thermal circle.

Note that, consistent with our assumptions, the scaling solution Eq.(6.28) is only well-defined in the strong-coupling region $|\tau J| \gg 1$. Similarly, at $T > 0$ the solution given by Eq.(6.29) is well-defined away from the boundary points $\{0, 1\}$. These ultra-violet (UV) divergence forbid us from simply inserting back the solutions in Eq.(6.10), as we did back in Sections 6.2.1 and 6.2.2. Also, the thermodynamic coefficients are not necessarily solely determined by the strict conformal solution. Indeed, it is possible to adapt the argument in Section 6.2.1 to include a UV regulator. As shown in Appendix E.2, by regularising the UV divergences in the on-shell action, we can compute the contribution of the conformal solution Eq.(6.29) to the low-temperature free energy density. The zero temperature entropy density $s_0 = S_0/N$ is completely determined by the conformal saddle, and is given by the following integral, also plotted in Fig.6.1

$$s_0 = \frac{1}{\pi}\int_0^1 \frac{\mathrm{d}u}{1-u^2}\left[\pi\left(\frac{1}{2}-\Delta\right) - u\tan^{-1}(u\cot\pi\Delta)\right], \tag{6.30}$$

Note that this result is consistent with the values we previously found for the cases $q = 2$ and $q = \infty$, and is indeed consistent with the exact numerical results for any q [245]. On the other hand, the specific heat cannot be computed from the conformal solution, and one needs to go to higher other terms that break conformal symmetry. Indeed, as we have seen

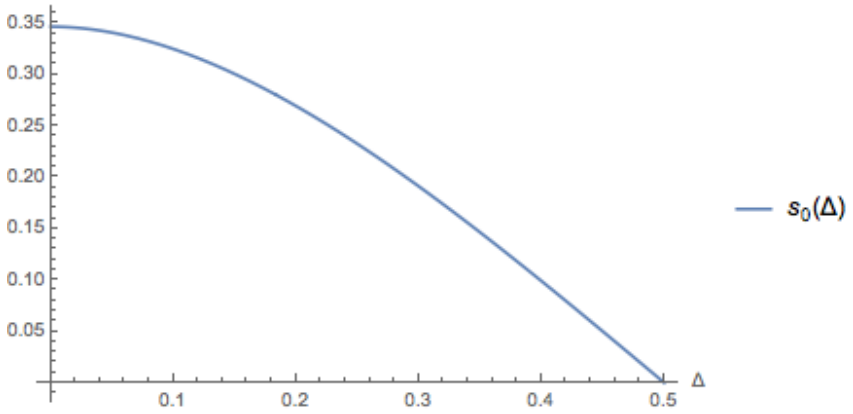

Figure 6.1: Zero temperature entropy density for the SYK model.

in both $q = 2$ or $q = \infty$, $c \propto J^{-1}$, suggesting that strictly at the conformal saddle $\beta J = \infty$ we have $c = 0$. The same is true for all higher order terms in the free energy expansion.

When we include the derivative term in Eq.(6.6), the degeneracy in the infinite dimensional manifold of conformally equivalent solutions is lifted. A diffeomorphism that previously connected equally good solutions of the saddle-point equations acquires a finite action cost proportional to the symmetry breaking term. This scenario is similar to the meson mass term that explicitly breaks chiral symmetry in QCD [256]. An effective field theory describing the action cost of these *pseudo-Goldstone* bosons is given by the celebrated *Schwarzian action* [102] (see [257] for a derivation),

$$S_{\text{eff}}[f] = N\frac{m}{J}\int \mathrm{d}\tau\, \{f(\tau), \tau\}, \tag{6.31}$$

where $m > 0$ is a positive real constant and $\{f, \tau\} = \left(\frac{f''}{f'}\right)' - \frac{1}{2}\left(\frac{f''}{f'}\right)$ is the *Schwarzian derivative*. One can check that $\{f, \tau\} = 0$ for $f \in \mathrm{SL}_2(\mathbb{R})$, and therefore the Schwarzian derivative does exactly what we expect: it assigns an action cost to diffeomorphisms in the coset space $\mathrm{Diff}(S^1)/\mathrm{SL}_2(\mathbb{R})$, and has kernel given by the residual symmetry group $\mathrm{SL}_2(\mathbb{R})$. Note also that, in the strict conformal limit $\tau J \gg 1$ the action cost vanish, signalling that all diffeomorphisms become massless. In particular, note that the cost associated with the thermal saddle $f(\tau) = \tan\frac{\pi\tau}{\beta}$ is given by $S_{\text{eff}} = \frac{2\pi^2 m}{\beta J}N$, which is precisely a contribution to the specific heat term in the low-temperature expansion of the free energy. This contribution was shown to be exact [246, 258–260], and is coherent with the aforementioned discussion that the specific heat coefficient term is given by the lowest order conformal symmetry breaking term. It was also recently shown that the density of states associated with the pseudo-Goldstone modes, obtained by exactly performing the path integral over $f \in \mathrm{Diff}(S^1)/\mathrm{SL}_2(\mathbb{R})$ weighted by S_{eff} follows Cardy's formula, which is consistent with previous results of Carlip for black holes [246, 261].

6.2.4 Out-of-time-order four point function and quantum chaos

The exponential growth of a certain out-of-time-order (OTO) four-point function has been recently proposed as a measure of quantum chaos in quantum field theories [262, 263]. This proposal was motivated by the remark that, in a semi-classical expansion of this correlator there is an exponential growth in a window around the Ehrenfest time $t_* \sim \lambda_{\rm L}^{-1} \log \hbar/S$, where S is the action and $\lambda_{\rm L}$ is the classic Lyapunov exponent of the system [263–265]. The growth rate of the OTO correlation function became a common quantitative measure of chaos for quantum mechanical systems. Research in this direction has gained further momentum in the high-energy physics community after it was shown that holographic field theories described by classic black holes are quantum chaotic in this sense [266, 267]. Since strong interactions are intimately related to chaos, this result has motivated Maldacena, Shenker and Stanford to conjecture a bound in the growth rate of the OTO correlator, which is only saturated by the 'infinitely' strongly-interacting holographic theories [268]. As we will shortly see, the fact that the SYK model saturates this bound is the strongest evidence of the holographic nature of the model [102].

The disorder averaged out-of-time order four-point function investigated in [268] is given by,

$$G_4(t_1, 0, t_2, 0) = \frac{1}{N^2} \sum_{i,j=1}^{N} \langle y\chi_i(t_1) y\chi_j(0) y\chi_i(t_2) y\chi_j(0) \rangle \tag{6.32}$$

where $y = e^{-\frac{1}{4}\beta H}$ and $t_1 > t_2$. Note that, instead of inserting the factor $e^{-\beta H}$ in front of the operator insertions, we have divided the thermal circle in four insertions sandwiched between the operators. It can be shown that this unusual definition act as a regularization for an otherwise divergent four-point function [268]. Strictly at $N = \infty$, the SYK four-point function is given by a trivial product of two disconnected two-point functions. At large-N, the OTO correlation function reads

$$G_4(t_1, 0, t_2, 0) = G^R(t_1) G^R(t_2) + \frac{1}{N} F(t_1, t_2) + O\left(N^{-2}\right) \tag{6.33}$$

where G^R is the retarded Green's function. The leading order non-trivial contribution $F(t_1, t_2)$ is given by a sum of ladder-diagrams $F = \sum_{n=0}^{\infty} F_n$. Each F_n is a ladder-diagram with n 'rungs', and satisfy the following recursive Bethe-Salpeter equation

$$F_{n+1}(t_1, t_2) = \int \mathrm{d}t_1 \mathrm{d}t_2 \; K(t_1, t_2, t_3, t_4) F_n(t_3, t_4), \tag{6.34}$$

with generating kernel K is given by

$$K(t_1,t_2,t_3,t_4) = J^2(q-1)G^R(t_{13})G^R(t_{24})G^<(t_{34})^{q-2}, \tag{6.35}$$

where $G^R(t) = \theta(t)\langle\{\chi(t),\chi(0)\}\rangle$ and $G^<(t) = \langle\chi(t),\chi(0)\rangle$ are the retarded and lesser Green's function, and we have defined $t_{12} = t_1 - t_2$. These real-time Green's function can be obtained from the Euclidean time one-point function $G(\tau)$ by analytic continuation to real time. Note however that for achieving the particular regularization in Eq.(6.32) the lesser function need to be continued with t_1 and t_2 separated by half of the thermal circle,

$$G^R(t) = \theta(t)\left[G(\tau = it - 0^+) + G(\tau = it + 0^+)\right] \tag{6.36}$$

$$G^<(t) = G\left(\tau = it + \frac{\beta}{2}\right) \tag{6.37}$$

Denoting the convolution in the space of anti-symmetric two-dimensional functions by $\star$, we can write Eq.(6.34) in a compact form $F_{n+1} = K \star F_n$. The sum of ladder diagrams can be rewritten as a power series in K, $F = \sum_{n=0}^{\infty} K^n \star F_0$, which could be formally summed to give $F = (1-K)^{-1}F_0$, which should be understood in the sense of operators. In principle, one can diagonalise K in the space of anti-symmetric two-dimensional functions and insert the operator $(1-K)$ in terms of the spectral decomposition of K. This cumbersome analysis was pursued in [102]. Here we will take a shortcut proposed by Kitaev [100]. The asymptotic behaviour of F is determined by ladder-diagrams with many rungs. One can therefore look for solutions $n \to \infty$ of Eq.(6.34). Note that these are precisely the eigenfunctions of K with eigenvalue 1,

$$F_\infty(t_1,t_2) = \int \mathrm{d}t_1 \mathrm{d}t_2 \; K(t_1,t_2,t_3,t_4)F_\infty(t_3,t_4) \tag{6.38}$$

Since we are after solutions that grow exponentially when $t_1, t_2 \to \infty$, we make the following separable ansatz: $F_\infty(t_1,t_2) = e^{\lambda_L \frac{t_1+t_2}{2}} f(t_{12})$. To proceed, we need an explicit expression for K. We start by looking at the large-q case where we have exact solutions for G.

Large-q

The leading order large-q solutions for the Euclidean propagator are given in Eq.(6.22). To leading order,

$$G^R(t) = \theta(t) + O(q^{-1}), \tag{6.39}$$

$$G^<(t)^{q-2} = 2^{2-q}e^{g(\tau=it+\beta/2)} + O(q^{-1}) = \frac{2^{2-q}(\pi\nu)^2}{(\beta J)^2}\frac{1}{\cosh^2\frac{\pi\nu}{\beta}t} + O(q^{-1}) \tag{6.40}$$

Inserting in Eq.(6.35) we get,

$$F(t_1,t_2)=2\left(\frac{\pi\nu}{\beta}\right)^2\int \mathrm{d}t_3\mathrm{d}t_4\,\frac{\theta(t_{13})\theta(t_{24})}{\cosh^2\frac{\pi\nu}{\beta}t_{34}}F(t_3,t_4). \tag{6.41}$$

We can make this integral equation into a differential equation by taking derivates with respect to t_1 and t_2 in both sides and noting that $\partial_x\theta(x)=\delta(x)$.

$$\partial_{t_1}\partial_{t_2}F(t_1,t_2)=2\left(\frac{\pi\nu}{\beta}\right)^2\frac{1}{\cosh^2\frac{\pi\nu}{\beta}t_{34}}F(t_1,t_2) \tag{6.42}$$

Inserting the aforementioned growth ansatz $F(t_1,t_2)=e^{\frac{\lambda(t_1+t_2)}{2}}f(t_{12})$ and changing coordinates to $y=\frac{\pi\nu}{\beta}t_{12}$ yield an ordinary differential equation for f,

$$\left[-\partial_y^2-\frac{2}{\cosh^2 y}\right]f_{\lambda_\mathrm{L}}(y)=-\left(\frac{\lambda_\mathrm{L}\beta}{2\pi\nu}\right)^2 f_{\lambda_\mathrm{L}}(y) \tag{6.43}$$

which is nothing but a one dimensional Schrödinger equation $\left(\partial_y^2+V(y)\right)\psi=E\psi$ with the well-known Poschl-Teller potential $V(y)=-2\mathrm{sech}^2 y$ and energy spectrum parametrised by $E_{\lambda_\mathrm{L}}=-\left(\frac{\lambda_\mathrm{L}\beta}{2\pi\nu}\right)^2$. It is easy to check it admits a bound state with energy $E_{\lambda_\mathrm{L}}=-1$ and normalised eigenstate $f(y)=\frac{1}{\sqrt{2}}\,\mathrm{sech}y$. This eigenvalue corresponds to a growth rate given $\lambda_\mathrm{L}=\frac{2\pi\nu}{\beta}$, which in turn imply the existence of an eigenfunction for the large-q generating kernel given by,

$$F_\infty(t_1,t_2)=\frac{1}{\sqrt{2}}e^{\frac{2\pi\nu}{\beta}\frac{t_1+t_2}{2}}\mathrm{sech}\frac{\pi\nu}{\beta}t_{12} \tag{6.44}$$

Note that since $\nu\in[0,1]$, this result is coherent with conjectured bound $\lambda_\mathrm{L}\leq\frac{2\pi}{\beta}$. Precisely at the strong-coupling limit $\beta J=\infty$ ($\nu=1$) the Lyapunov exponent λ_L saturates the bound. This result suggests that the conformal limit of the general $q>2$ SYK model should also saturate the bound.

Conformal limit

We now show that the generating kernel Eq.(6.35), when evaluated at the conformal limit $\beta J=\infty$, also admits an eigenvector which exponentially grows with a rate that saturates the chaos bound. Analytically continuing the Matsubara conformal one-point functions

Eq.(6.29) to real time,

$$G_c^R(t) = 2b\cos\pi\Delta\theta(t)\left[\frac{\pi}{\beta J\sinh\frac{\pi t}{\beta}}\right]^{2\Delta}, \tag{6.45}$$

$$G_c^<(t) = b\left[\frac{\pi}{\beta J\cosh\frac{\pi t}{\beta}},\right] \tag{6.46}$$

we can compute the conformal kernel $K(t_1,t_2,t_3,t_4) = J^2(q-1)G_c^R(t_{13})G_c^R(t_{24})G_c^<(t_{34})^{q-2}$. The large-$q$ eigenvalues Eq.(6.44) suggest a functional shape for an ansatz, $F_\infty(t_1,t_2) \propto e^{\frac{2\pi}{\beta}\frac{t_1+t_2}{2}}\mathrm{sech}^\alpha\frac{\pi t_{12}}{\beta}$ for some exponent α. By direct integration, it we can check that choosing $\alpha = 2\Delta+1$ indeed gives an eigenfunction of K with eigenvalue 1 [102]. This eigenfunction corresponds to the exponential growth expected, with growth rate saturating the chaos bound $\lambda_\mathrm{L} = \frac{2\pi}{\beta}$.

The saturation of the chaos bound, together with the emergent conformal symmetry at strong coupling and the finite entropy density at $T = 0$ are examples of the astounding similarity between the SYK model and extremal black holes. They suggest the SYK model, which is effectively described by a one-dimensional CFT in the infra-red as a strong candidate for the dual of the ubiquitous $\mathrm{AdS}_2 \times S^2$ IR fixed point of extremal black holes. However, from the point of view of condensed matter, the pure interaction Hamiltonian of the SYK model is simplistic and should be understood as an effective theory describing a fixed point from a more involved model. In the next section, we investigate whether these *holographic properties* discussed above are stable under the simplest relevant one-body deformation of the model.

6.3 A generalised SYK model

This section is the bulk of our original contribution to this field. We study the stability of the holographic properties discussed in Section 6.2 under the relevant one-body perturbation. For simplicity, unless otherwise stated, we restrict our analysis to the simplest non-trivial SYK model with $q = 4$. The Hamiltonian of our generalised model is given by

$$H = i\sum_{1\le i<j\le N}\kappa_{ij}\chi_i\chi_j + \sum_{1\le i<j<k<l\le N}J_{ijkl}\chi_i\chi_j\chi_k\chi_l, \tag{6.47}$$

where we take both couplings κ_{ij} and J_{ijkl} to be uncorrelated and normally distributed random variables, with mean zero and variances given by $\mathbb{E}[\kappa_{ij}^2] = \frac{\kappa^2}{N}$ and $\mathbb{E}[J_{ijkl}^2] = \frac{6J^2}{N^3}$. Since the random couplings are uncorrelated, terms which mix the two terms in Eq.(6.47) vanish. Following the same replica argument as in Section 6.2 and focusing on the replica

symmetric saddle yield the effective action

$$\frac{S_{\text{eff}}}{N} = -\frac{1}{2}\text{Tr}\log(\partial_\tau - \Sigma) + \frac{1}{2}\int_0^\beta \mathrm{d}\tau \int_0^\beta \mathrm{d}\tau' \left[G(\tau,\tau')\Sigma(\tau,\tau') - \frac{J^2}{4}G(\tau,\tau')^4 - \frac{\kappa^2}{2}G(\tau,\tau')^2\right]. \tag{6.48}$$

As before, the saddle-point equations can be conveniently written in Fourier space as

$$G(\omega_n) = -\left[i\omega_n + \Sigma(\omega_n)\right]^{-1}, \tag{6.49}$$

$$\Sigma(\omega_n) = \kappa^2 G(i\omega_n) + J^2 \int_0^\beta \mathrm{d}\tau\ e^{-i\omega_n\tau} G(\tau)^3, \tag{6.50}$$

where ω_n are the fermionic Matsubara frequencies. Our generalised model has two natural energy scales κ, J. Recall that for the original SYK model with $q = 2$, which here corresponds to $J = 0$, the saddle-point equations are exactly solvable. This case, which we will refer as *integrable*, did not enjoy from the holographic properties: the entropy density vanishes at $T = 0$, the specific heat coefficient is the same as the one of Fermi liquid theory and the semi-classical expansion of the OTO four-point function does not grow exponentially. On the other hand, for any $q > 2$ (and even $q = \infty$) the SYK model becomes *chaotic* in the sense we have previously defined in Section 6.2.4. But note that the one-body term is more relevant than the two-body, in the sense of the renormalization group. Heuristically, we expect that thermodynamic quantities that depend on the IR of the model, such as the entropy density and specific heat, will be dominated by the one-body behaviour. This is less clear for quantities such as the semi-classic growth rate of the OTO four-point function, which takes place in timescales of the order of the Ehrenfest time.

We start our investigation of these considerations by treating the two-body term as a deformation of the exact one-body theory and proceed by computing the corrections induced by the interactions in the thermodynamic properties.

6.3.1 Perturbative analysis of the thermodynamic properties

We carry out an analytical calculation of the low-temperature thermodynamic properties of the generalised one+two-body SYK model in the limit of large-N. Since the exact solution for the one-body Hamiltonian is known analytically, it is convenient to develop the perturbative approach around this exact ground state. For this purpose, we work in units of $\kappa = 1$ and for convenience set $J = \tilde{\kappa}$. For $\tilde{\kappa} = 0$, the model is integrable, and the exact solution for the Euclidean one-point function was found in Section 6.2.1,

$$G_0(\omega_n) = \frac{-i\omega_n + i\text{sgn}(\omega_n)\sqrt{4+\omega_n^2}}{2}, \tag{6.51}$$

where we will use the subscript "0" to denote quantities with respect $\tilde{\kappa} = 0$. For $\tilde{\kappa} > 0$, Eq.(6.49) is an integral equation, and cannot be solved exactly. We proceed with a perturbative solution in the limit $\tilde{\kappa} \ll 1$. Let

$$G(\omega_n) \underset{\tilde{\kappa}\ll 1}{=} G_0(\omega_n) + \tilde{\kappa}^2\, g(\omega_n) + O\left(\tilde{\kappa}^4\right). \tag{6.52}$$

Inserting in Eq.(6.49) and expanding in $\tilde{\kappa}$, we find

$$g(\omega_n) = -\frac{G_0(\omega_n)}{i\omega_n + 2G_0(\omega_n)}\sigma_0(\omega_n) \tag{6.53}$$

where we defined $\sigma_0(\omega) = \int \mathrm{d}\tau\; e^{i\omega\tau} G_0(\tau)^3$, which acts as a source for the first order correction. The prefactor can be written exactly,

$$\frac{G_0(\omega_n)}{i\omega_n + 2G_0(\omega_n)} = \frac{1}{2}\left[1 - \frac{\omega_n\, \mathrm{sgn}(\omega_n)}{\sqrt{4+\omega_n^2}}\right]. \tag{6.54}$$

Note that the only temperature dependence of $G_0(\omega_n)$ is through the Matsubara frequencies, and thus disappears upon analytic continuation $i\omega_n \to \epsilon + i0^+$. This is expected since $\tilde{\kappa} = 0$ is essentially a non-interacting system, and the spectral density should not be temperature dependent. However, for any $\tilde{\kappa} > 0$ the system is interacting, and we do expect non-trivial temperature dependence in $G(\omega_n)$. As we will see below, this comes exactly from the non-linearity induced by the σ_0 contribution. Since we do not have a closed form expression for σ_0, which involves the cube of the Matsubara propagator Eq.(6.14), we proceed with a low-temperature expansion. The first step is to find a low-temperature expansion of Eq.(6.14). Since the spectral density is compactly supported and the integrand is bounded, by the Lebesgue dominated convergence theorem we can do a series expansion under the integral. For a detailed discussion, see Appendix E.3. Integrating term by term results in

$$\begin{aligned} G_0^\beta(\tau) \underset{\beta\gg 1}{=} &\left(-\frac{5\pi^8}{32768\beta^9} + \frac{\pi^6}{1024\beta^7} - \frac{\pi^4}{128\beta^5} + \frac{\pi^2}{8\beta^3} + \frac{1}{\beta}\right)\csc \pi\theta + \\ &+ \left(\frac{1025\pi^8}{4096\beta^9} - \frac{91\pi^6}{512\beta^7} + \frac{5\pi^4}{32\beta^5} - \frac{\pi^2}{4\beta^3}\right)\csc^3\pi\theta + \left(-\frac{7245\pi^8}{2048\beta^9} + \frac{105\pi^6}{128\beta^7} - \frac{3\pi^4}{16\beta^5}\right)\csc^5\pi\theta + \\ &+ \left(\frac{4725\pi^8}{512\beta^9} - \frac{45\pi^6}{64\beta^7}\right)\csc^7\pi\theta - \frac{1575\pi^8}{256\beta^9}\csc^9\pi\theta + O(\beta^{-11}), \end{aligned} \tag{6.55}$$

where as usual we defined $\theta = \tau/\beta \in (0,1)$. We now expand $G_0^\beta(\tau)^3$ in $1/\beta$ and perform the Fourier transform to get $\sigma_0(\omega_n) = \int_0^\beta \mathrm{d}\tau\; e^{i\omega_n\tau} G_0^\beta(\tau)^3$. Inserting this into Eq.(6.53), together with Eq.(6.54), we get an expression for $g(\omega_n)$ that should be added to the zeroth order solution Eq.(6.51). Analytically continuing this expression $i\omega_n \to \epsilon + i0^+$ and expanding in low frequencies gives an approximation for the analytic continuation of Eq.(6.52) $G^R(\epsilon) =$

$G(i\omega_n \to \epsilon)$:

$$
\begin{aligned}
G^R(\epsilon) \underset{\epsilon \ll 1}{=} \epsilon & \left[\left(-\frac{3\pi^7}{8192\beta^8} - \frac{3\pi^3}{128\beta^4} + \frac{\pi}{8\beta^2} \right) \tilde{\kappa}^2 - \frac{1}{2} \right] + \\
& + \tilde{\kappa}^2 \epsilon^3 \left(-\frac{3\pi^7}{65536\beta^8} - \frac{913\pi^5}{645120\beta^6} - \frac{17\pi^3}{3840\beta^4} - \frac{\pi}{64\beta^2} + \frac{1}{8\pi} \right) \\
& + \tilde{\kappa}^2 \epsilon^7 \left(-\frac{9\pi^7}{1048576\beta^8} - \frac{913\pi^5}{5160960\beta^6} - \frac{41\pi^3}{20480\beta^4} - \frac{\pi}{384\beta^2} + \frac{1}{128\pi} \right) \\
& + \tilde{\kappa}^2 \epsilon^7 \left(-\frac{15\pi^7}{8388608\beta^8} - \frac{913\pi^5}{27525120\beta^6} - \frac{121\pi^3}{393216\beta^4} - \frac{17\pi}{30720\beta^2} + \frac{7}{3840\pi} \right) + \\
& + i\epsilon^2 \left[\left(\frac{913\pi^5}{322560\beta^6} + \frac{23\pi^3}{7680\beta^4} + \frac{\pi}{16\beta^2} - \frac{1}{4\pi} \right) \tilde{\kappa}^2 - \frac{1}{8} \right] \\
& + i\epsilon^4 \left[\left(\frac{311\pi^3}{122880\beta^4} + \frac{5\pi}{1536\beta^2} + \frac{1}{64\pi} \right) \tilde{\kappa}^2 - \frac{1}{128} \right] + \\
& + i\epsilon^6 \left[\left(\frac{7\pi}{15360\beta^2} + \frac{1}{3840\pi} \right) \tilde{\kappa}^2 - \frac{1}{1024} \right] + i\epsilon^8 \left[\frac{59\tilde{\kappa}^2}{2580480\pi} - \frac{5}{32768} \right] + O(\epsilon^9, \tilde{\kappa}^4).
\end{aligned}
\tag{6.56}
$$

where we have conveniently separated the real and imaginary parts. The real part of the retarded Green's function is odd, while the imaginary part which gives the spectral density is even. Note that the effect of interactions is mainly to renormalise the coefficients of the free $\tilde{\kappa} = 0$ model, with both zero and finite temperature contributions. This reflects the fact that the interactions are irrelevant compared to the one-body term. At zero temperature $\beta = \infty$, corrections only appear at order ϵ^2. This means that the low-frequency behaviour of the ground state of the system is unchanged.

The calculation of the low-temperature free energy density follows exactly the same procedure as for $\tilde{\kappa} = 0$, which we highlighted in Section 6.2.1. As before, the thermodynamic coefficients are determined by the Tr log term, which can be written as an integral over the phase of the retarded Green's function Eq.(6.16). For $\tilde{\kappa} > 0$, we only have access to the IR low frequency result in Eq.(6.56). Naively inserting this in Eq.(6.16) leads to UV divergences due to unboundedness of the integrals. Note this was not needed for $\tilde{\kappa} = 0$ since the compact support of the spectral function comes naturally from the exact solution. This UV divergence is expected since the perturbative IR solution does not hold for large frequencies. We, therefore, introduce an UV cutoff λ to regularise the integrals. We will show that this leads to cutoff dependent ground state energy, but cutoff independent entropy and specific heat. This is expected given that these coefficients depend only on the IR behaviour of G^R. Indeed it is also possible to compute the exact specific heat coefficient in Eq.(6.18) by using only the low-temperature expansion of the exact G_0^R, as discussed in Appendix E.1. Although there is some freedom in the choice of λ, it is largely constrained by non-perturbative properties of the spectral function $\rho(\epsilon) = 2\text{Im}\, G_R$, which must satisfy

the sum rule $\int \frac{d\epsilon}{2\pi}\rho(\epsilon) = 1$ and positivity $\rho(\epsilon) \geq 0$. These constraints give us a consistent way to fix the cutoff: we choose λ such that $\int_{-\lambda}^{\lambda} \frac{d\epsilon}{2\pi}\rho(\epsilon) = 1$ [32]. This ensures that $|\epsilon| < \lambda$ saturates the spectral weight, and therefore for $|\epsilon| \geq \lambda$ the perturbative solution breaks down. It is easy to check that this choice automatically satisfies positivity of ρ. With this discussion in mind, we take

$$\text{Arg } G^R = \begin{cases} \frac{\pi}{2} - a(\epsilon, \tilde{\kappa}, \beta) & \text{for } |\epsilon| < \lambda, \\ \pi & \text{for } \epsilon \geq \lambda, \\ 0 & \text{for } \epsilon \leq -\lambda, \end{cases} \tag{6.57}$$

where we define $a(\epsilon, \tilde{\kappa}, \beta) = \tan^{-1}\left(\frac{\text{Re } G^R}{\text{Im } G^R}\right)$ with G^R given in Eq.(6.56). As in Eq.(6.18), the integral over (λ, ∞) gives an exponentially decaying term that does not contribute to the thermodynamic coefficients. The remaining integral over $(-\lambda, \lambda)$ can be integrated numerically using the cutoff estimated from the sum-rule for ρ.[33]. To extract the specific heat coefficient, we subtract the zero temperature result and multiply by a factor β^2. According to Eq.(6.11), the result should asymptote to $c/2$ as $\beta \to \infty$. These are shown in Fig. 6.2 and Fig. 6.3 respectively.

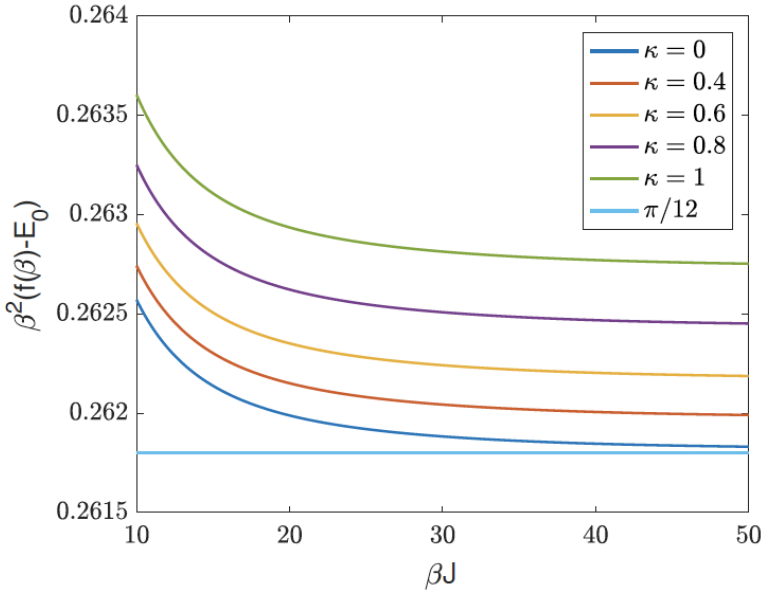

Figure 6.2: Numerical integration of $\beta^2(f - E_0)$, which asymptotes to $c/2N$ at low temperatures.

One can observe in Fig. 6.2 an order 10^{-3} correction in $c/2N$ for small $\tilde{\kappa}$. While this correction is consistent with the exact diagonalisation results in Section 6.3.3, it can also be an artefact of perturbation theory. We thus study the dependence of $c/2N$ in $\tilde{\kappa}$ as we go

[32] Note that since ρ is even, without loss of generality we can take a symmetric interval $(-\lambda, \lambda)$.

[33] We have also checked numerically that, as long and positivity of ρ is respected, changes in the cutoff do not affect the results for the thermodynamic coefficients c and s_0.

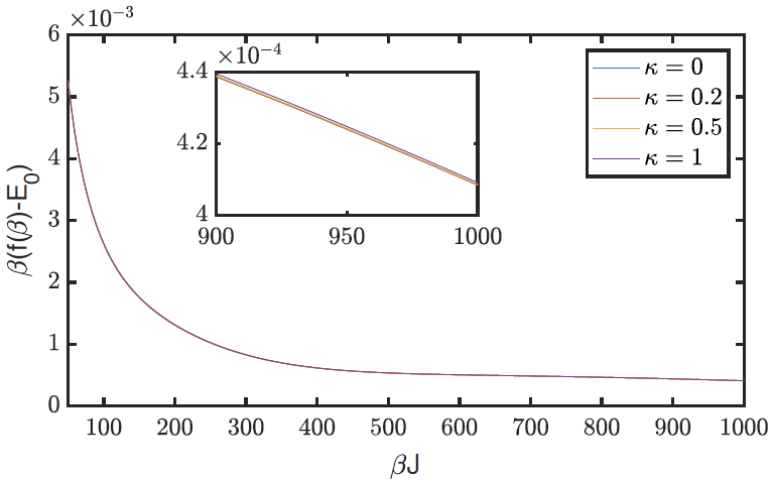

Figure 6.3: Numerical integration of $\beta(f - E_0)$, which asymptotes to s_0 at low temperatures.

higher orders in perturbation theory for $G^R(\epsilon)$. This is shown in Fig. 6.4. The specific heat

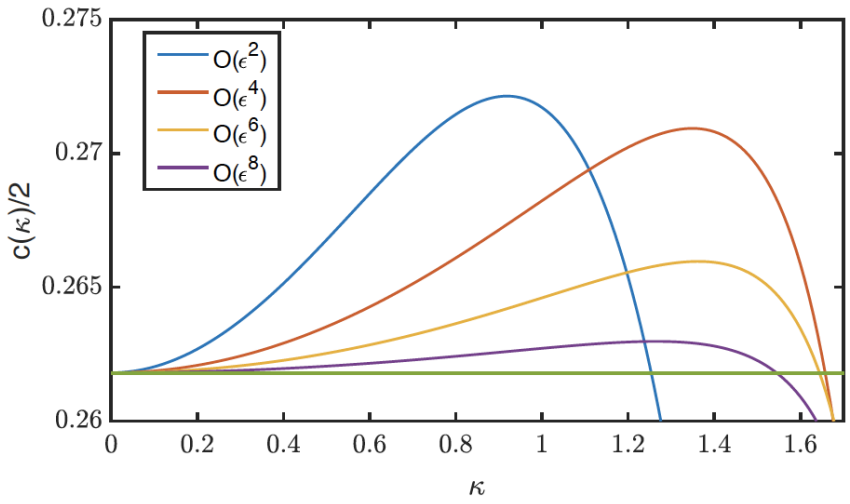

Figure 6.4: Specific heat coefficient $c/2N$, from Eqs.(6.16), (6.56), (6.11), as a function of $\tilde{\kappa}$ for different orders in perturbation theory.

coefficient $c/2$ increases with $\tilde{\kappa}$. However, the higher order we go in perturbation theory for small frequencies ϵ, the smaller is the increase for a given $\tilde{\kappa}$. This suggests that a fully non-perturbative calculation of $c(\tilde{\kappa})$ could lead to a $\tilde{\kappa}$ independent specific heat coefficient at least in the limit $\tilde{\kappa} \ll 1$.

Indeed this can also be understood analytically. First we need to identify which term gives this contribution. The integral over the $\pi/2$ factor in Eq.(6.57) gives only a cutoff

dependent contribution to the ground state energy $\frac{\beta\lambda}{2}$, and is unimportant in what concerns c. The remaining piece can again be studied using the Sommerfeld expansion,

$$-\beta\int_{-\lambda}^{\lambda}\frac{\mathrm{d}\epsilon}{\pi}\frac{a(\epsilon,\tilde{\kappa},\beta)}{1+e^{\beta\epsilon}}\underset{\beta\gg 1}{=}-\beta\int_{-\lambda}^{0}\frac{\mathrm{d}\epsilon}{\pi}a(\epsilon,\tilde{\kappa},\beta)+\frac{\pi}{6\beta}\frac{\mathrm{d}}{\mathrm{d}\epsilon}\,a(\epsilon,\tilde{\kappa},\beta)|_{\epsilon=0}+O(\beta^{-3}). \tag{6.58}$$

From Eq.(6.56), we can check that $\frac{\mathrm{d}}{\mathrm{d}\epsilon}\,a|_{\epsilon=0}=-\frac{1}{2}$ for any $\tilde{\kappa}$ and β. Thus this term is identical to the integrable $\tilde{\kappa}=0$ result. Since a is now temperature dependent, possible corrections to the specific heat coefficient can come from the integral of a over $(-\lambda,0)$ or from the higher order odd derivatives. However a simple series expansion of a reveals that the leading order temperature dependence in a comes at order $O(\epsilon^9)$, which is beyond the scope of the perturbative result in Eq.(6.56). One can check that, had we gone only to order $O(\epsilon^4)$ in G^R, the first order temperature dependence would have been at order $O(\epsilon^5)$. Going to order $O(\epsilon^6)$ pushes the leading order temperature dependence of a to order $O(\epsilon^7)$, and finally going to order $O(\epsilon^8)$ pushes it to $O(\epsilon^9)$. This analytical argument is fully consistent with the evaluation of c from Eq.(6.16) depicted in Fig.6.4.

In Section 6.3.3 we give numerical exact diagonalisation results for the low-temperature thermodynamic coefficients. Corrections to the $\tilde{\kappa}=0$ specific heat coefficient $c=\pi/6$ and entropy density $s_0=0$ for $\tilde{\kappa}\ll 1$ are found to be of order $O(10^{-3})$ or lower. Our large-N perturbative results are in good agreement with the numerics. They also corroborate the claim that the ground state of our model is dominated by the one-body term in the Hamiltonian.

6.3.2 Perturbative large-q analysis of the Lyapunov exponent

In the previous section, we have shown that the thermodynamic properties of the modified SYK are dominated by the relevant one-body term in the infra-red, a result which is consistent with the naive expectations of power-counting. However, as we mentioned in Section 6.3, it is not clear whether the same is true for the Lyapunov exponent, which is a property of the model at shorter timescales.

In Section 6.2.2 we have shown that the Lyapunov exponent of the general $q/2$-body SYK model could be computed exactly, at all coupling scales, in the limit where $q\gg 1$ and the rescaled coupling $J^2\to 2^{q-1}q^{-1}J^2$ is held fixed. Motivated by this result, in this section, we develop a similar analysis for our mixed model, in the case where we generalise the two-body term to a $q/2$-body term. Since the Lyapunov exponent of the $q=2$ SYK model vanishes, it is more natural to switch perspectives from the previous section and study the perturbative effect of the integrable term in the chaotic $q/2$-body term. Note, however, that this perturbative approach should be taken with a pinch of salt. The reason is that, as we saw in the previous section, the one-body term is more relevant than the $q/2$-body term,

and therefore a perturbative analysis can be ill-defined in the IR. With this disclaimer in mind, by closely following the method presented in Section 6.2.2, we show that despite the naive perturbative expansion in $\kappa \ll 1$ being singular, it captures the relevant physics we are interested. For any fixed $\kappa \ll 1$, we identify a range of temperatures for which the Lyapunov exponent is non-zero, though never saturates the bound on chaos. We also show that it vanishes for sufficiently low temperatures. This striking result is in full qualitative agreement with the numerics presented in Section 6.3.3 for the model Eq.(6.47), which corroborates the existence of a chaotic-to-integrable transition in this type of generalised SYK model.

We will work with the following Hamiltonian,

$$H = i \sum_{1\leq i<j\leq N} \kappa_{ij}\chi_i\chi_j + i^{q/2} \sum_{1\leq i_1<i_2<\cdots<i_q\leq N} J_{i_1 i_2 \ldots i_q}\chi_{i_1}\chi_{i_2}\cdots\chi_{i_q}, \tag{6.59}$$

which is the $q/2$-body generalization of the original model Eq.(6.47). As before $J_{i_1 i_2 \ldots i_q}$ and κ_{ij} are uncorrelated normally distributed random variables with zero average and variance $\frac{2^{q-1}}{q}\frac{(q-1)!J^2}{N^{q-1}}$ and $\frac{\kappa^2}{qN}$ respectively. Note that, following the discussion in 6.2.2, we have rescaled the coupling constants: $\kappa^2 \to \kappa^2/q$ and $J^2 \to J^2 2^{q-1}/q$. The large-q limit is then defined by taking $q \gg 1$ and keeping the rescaled couplings fixed [102]. We follow the same replica procedure described in Section 6.2 to get the following effective action

$$\frac{S_{\text{eff}}}{N} = -\frac{1}{2}\text{Tr}\log(\partial_\tau - \Sigma) + \frac{1}{2}\int_0^\beta \mathrm{d}\tau \int_0^\beta \mathrm{d}\tau' \left[G(\tau,\tau')\Sigma(\tau,\tau') - \frac{J^2}{2^{1-q}q^2}G(\tau,\tau')^q - \frac{\kappa^2}{2q}G(\tau,\tau')^2\right]. \tag{6.60}$$

As opposed in Section 6.2.2, for $q \gg 1$ we can consistently expand

$$G(\tau) \underset{\beta\kappa\ll 1}{=} \frac{1}{2}\text{sgn}(\tau)\left(1 + \frac{1}{q}g(\tau) + O(q^{-2})\right). \tag{6.61}$$

Closely following the steps in Section 6.2.2, we insert the above expansion in the saddle-point equations and simplify to get

$$\partial_\theta^2 g = 2(\beta J)^2 e^{g(\theta)} + (\beta\kappa)^2, \tag{6.62}$$

where as usual $\theta = \tau/\beta \in [0,1)$. This equation should be compared with Eq.(6.21). Together with the finite temperature boundary conditions $g(0) = g(1) = 0$, this equation defines a non-linear boundary value problem for g. For $\kappa = 0$, the solution was given in Eq.(6.22), and we reproduce here for convenience,

$$e^{g_{(0)}(\theta)} = \left[\frac{\cos\frac{\pi\nu}{2}}{\cos\left[\pi\nu\left(\frac{1}{2}-\theta\right)\right]}\right]^2, \qquad \beta J = \frac{\pi\nu}{\cos\frac{\pi\nu}{2}}. \tag{6.63}$$

Note that, as before, $\nu \in [0,1]$ parametrises the flow of βJ. In the limit $\kappa/J \ll 1$, we can linearise Eq.(6.62) around $g_{(0)}$. More explicitly, we substitute $g(\theta) = g_{(0)}(\theta) + (\kappa/J)^2\, g_{(1)}(\theta) + O(\kappa^4 J^{-4})$ into Eq.(6.62) to get the equation satisfied by $g_{(1)}$:

$$\left(\partial_x^2 - \frac{2}{\cos^2(x)}\right) g_{(1)}(x) = \left(\frac{\beta J}{\pi\nu}\right)^2 , \tag{6.64}$$

where we changed the θ-coordinate to $x = \pi\nu\left(\frac{1}{2} - \theta\right) \in \left[-\frac{\pi\nu}{2}, \frac{\pi\nu}{2}\right]$ and the corresponding boundary conditions in this coordinate are given by $g_{(1)}\left(\frac{\pi\nu}{2}\right) = g_{(1)}\left(-\frac{\pi\nu}{2}\right) = 0$. The solution of this boundary-value problem is given by

$$g_{(1)}(x) = \left(\frac{\beta J}{(\pi\nu}\right)^2 [\alpha(x)\tan x + \log\cos x + x\tan x + B(\nu)(x\tan x + 1)] \tag{6.65}$$

where we have defined,

$$\alpha(x) = \int^x \mathrm{d}t\ \log\cos t \tag{6.66}$$

$$B(\nu) = -\frac{-\alpha\left(-\frac{\pi\nu}{2}\right)\tan\left(\frac{\pi\nu}{2}\right) + \alpha\left(\frac{\pi\nu}{2}\right)\tan\left(\frac{\pi\nu}{2}\right) + \pi\nu\tan\left(\frac{\pi\nu}{2}\right) + 2\log\cos\left(\frac{\pi\nu}{2}\right)}{\pi\nu\tan\left(\frac{\pi\nu}{2}\right) + 2} \tag{6.67}$$

Note that $B(\nu)$ is a negative monotonically decreasing function of ν bounded by $B(0) = 0$ and $B(1) = \log 2 - 1$, and α is a transcendental function that can be explicitly written in terms of dilogarithms. Similar to Section 6.2.4 the out-of-time order four point correlator is generated by repeated convolution with a real-time retarded kernel, which in the generalised large-q model is given by simplifies considerably,

$$K_R(t_1,t_2,t_3,t_4) = \theta(t_{13})\theta(t_{24})\left[2J^2 e^{g(\tau = it_{34} + \beta/2)} + q^{-1}\kappa^2\right]. \tag{6.68}$$

Thus, at large-q the second term is sub-leading. As in Section 6.2.4, the asymptotic growth rate of the OTO four-point function can be obtained from solving the eigenvalue problem $F_\infty = K_R \star F_\infty$ on the space of antisymmetric two-dimensional functions for the eigenvalue 1. The integral eigenvalue equation can be converted to a partial differential equation by taking partial derivatives with respect to ∂_{t_1} and ∂_{t_2} on both sides,

$$\partial_{t_1}\partial_{t_2} F(t_1,t_2) = 2J^2 e^{g(\tau = it_{12} + \beta/2)} F(t_1,t_2). \tag{6.69}$$

Searching for solutions with exponential growth, $F(t_1,t_2) = e^{\frac{\lambda_L(t_1+t_2)}{2}} f(t_{12})$ and changing

coordinates to $y = \frac{\pi\nu}{\beta} t_{12}$, the above simplifies to

$$\left[\partial_y^2 + 2\left(\frac{\beta J}{\pi\nu}\right)^2 e^{g(x\to iy)}\right] f(y) = \left(\frac{\beta\lambda_{\rm L}}{2\pi\nu}\right)^2 f(y) \tag{6.70}$$

As in Section 6.2.2, the equation above has the form of a one-dimensional Schrödinger equation for the eigenfunction f with eigenvalues $E_\lambda = -\left(\frac{\beta\lambda_{\rm L}}{2\pi\nu}\right)^2$ in the potential $V(y) = -2\left(\frac{\beta J}{\pi\nu}\right)^2 e^{g(iy)}$. We have shown in Section 6.2.2 that for $\kappa = 0$ this equation admits an eigenvalue $E^{(0)}_{\lambda_{\rm L}} = -1$ with eigenstate $f^{(0)}_{\lambda_{\rm L}}(y) = \frac{1}{\sqrt{2}}{\rm sech} y$, which corresponds to an exponential growth with Lyapunov exponent given by $\lambda_{\rm L} = \frac{2\pi}{\beta}\nu$. We are interested in studying what happens to this bound state when we add the $\kappa/J \ll 1$ correction to the potential. Or in a more suggestive notation, when we consider $V(y) = V_{(0)}(y) + (\kappa/J)^2 V_{(1)}(y)$ where $V_{(1)}(y) = e^{g_{(0)}(x\to iy)} g_{(1)}(x \to iy)$ with $g_{(1)}(x)$ given by Eq.(6.65). By standard quantum mechanical perturbation theory, the correction in the energy $E_\lambda = E^{(0)}_\lambda + (\kappa/J)^2 E^{(1)}_\lambda$ is given by

$$\begin{aligned} E^{(1)}_\lambda &= \left\langle f^{(0)} \left| \frac{2}{\cosh^2(y)} g_{(1)}(iy) \right| f^{(0)} \right\rangle \\ &= \frac{1}{2}\int_{\mathbb{R}} {\rm d}y \frac{g_{(1)}(iy)}{\cosh^4(y)} = \frac{1}{2}\left(\frac{\beta J}{\pi\nu}\right)^2 \left[B(\nu) + \frac{19}{18} - \log 2\right] = \left(\frac{\beta J}{\pi\nu}\right)^2 \delta E(\nu), \end{aligned} \tag{6.71}$$

where $2\delta E(\nu) \equiv B(\nu) + \frac{19}{18} - \log 2$. Therefore the correction to the bound-state energy is given by

$$E_{\lambda_{\rm L}} = -1 + \left(\frac{\beta\kappa}{\pi\nu}\right)^2 \delta E(\nu) = -1 + \left(\frac{\kappa}{J}\right)^2 \frac{\delta E(\nu)}{\cos^2\frac{\pi\nu}{2}}. \tag{6.72}$$

Letting $E_{\lambda_{\rm L}} = -\left(\frac{\beta\lambda_{\rm L}}{2\pi\nu}\right)^2$ we obtain the correction to the Lyapunov exponent,

$$\frac{\beta\lambda_{\rm L}}{2\pi} = \sqrt{1 - \left(\frac{\kappa}{J}\right)^2 \frac{\delta E(\nu)}{\cos^2\frac{\pi\nu}{2}}} \underset{\beta\kappa\ll 1}{=} \nu - \left(\frac{\kappa}{J}\right)^2 \frac{\nu\delta E(\nu)}{2\cos^2\frac{\pi\nu}{2}} + O\left(\kappa^4 J^{-4}\right). \tag{6.73}$$

In Fig.6.5 we plot the Lyapunov exponent for different values of κ with $J = 1$. This is to be compared with the exact numerical data from Fig.(6.9). Although we do not get exact agreement between the critical values of β_* for which $\lambda_{\rm L} = 0$, the qualitative behaviour is similar. For $\kappa = 0$ we get the saturation of the bound at low temperatures. For any finite $\kappa > 0$, there is a range of temperatures where a non-zero Lyapunov exponent persists, although this range decrease rapidly as we increase κ.

We estimate the critical temperature β_* for which $\lambda_{\rm L}$ crosses the real axis by doing a

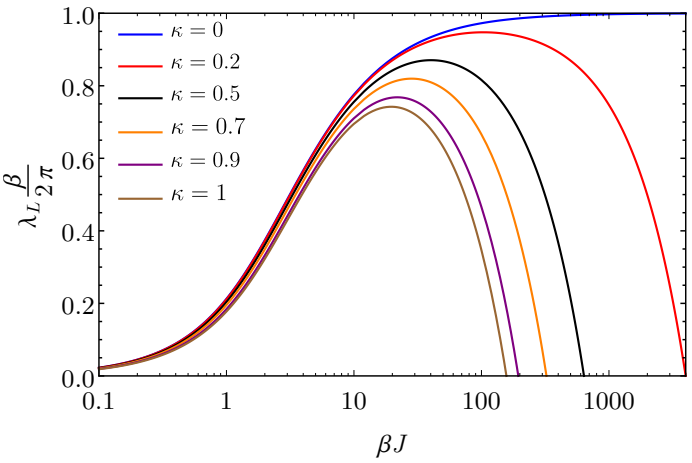

Figure 6.5: Lyapunov exponent $\lambda_{\rm L}$, Eq.(6.73), as a function of the inverse temperature βJ, in units of $1/k_B$, for different values of κ and $J = 1$. Note that $\frac{\beta\lambda_{\rm L}}{2\pi} \sim |\beta - \beta_*|$ vanishes linearly near the transition, with a slope of approximately $\frac{-2\kappa}{\pi\sqrt{72}}$. These results are in good quantitative agreement with those shown in Fig. 6.9.

low-temperature expansion of Eq.(6.73). For $\beta J \gg 1$, we have

$$1 - \nu \underset{\beta J \gg 1}{=} \frac{2}{\beta J} - \frac{4}{(\beta J)^2} + \frac{24 + \pi^2}{3(\beta J)^3} + O\left((\beta J)^{-4}\right). \tag{6.74}$$

Inserting in Eq.(6.73) and expanding,

$$\frac{\beta\lambda}{2\pi} = 1 - \frac{(\beta\kappa)^2}{\pi^2}\left[\frac{1}{72} + \frac{19 - 18\log\pi}{36\beta J} + O\left((\beta J)^{-2}\right)\right]. \tag{6.75}$$

Thus, assuming the transition occurs for large $\beta\kappa$ we obtain that, to lowest order in $\beta\kappa$, the transition should occur when

$$(\beta\kappa)_* = \sqrt{72}\pi. \tag{6.76}$$

This estimate gives $\beta_* \approx 133$ for $\kappa = 0.2$ and $\beta_* \approx 53$ for $\kappa = 0.5$, which is in very good agreement with Fig.6.5 and with the large-N result obtained numerically for $q = 4$ in Fig. 6.9.

Similarly, one can also expand Eq.(6.73) in $\beta J \ll 1$. This gives the following high-temperature behaviour

$$\frac{\beta\lambda}{2\pi} \underset{\beta J \ll 1}{=} \frac{\beta J}{\pi} - \frac{(\beta J)^3}{8\pi} + \frac{(\beta\kappa)^2}{\pi}\left[\frac{-19 + 18\log 2}{\beta J} + O(\beta J)\right], \tag{6.77}$$

where the $O\left((\beta\kappa)^2\right)$ correction is negative, indicating that chaos is weakened also in this regime of high temperatures.

6.3.3 Numerical analysis

In Section 6.3.1 and 6.3.2 we argued that despite the fact that the thermodynamic properties of our modified model are dominated by the one-body term, there is a stable range of parameters where the model should still be chaotic. These analytical results relied on two distinct perturbative settings. In this section, we give numerical support to this claim. The numerical analysis is, alike the previous sections, divided into two parts: thermodynamics and Lyapunov exponent. The thermodynamics of the model was computed using two complementary numerical techniques: exact diagonalisation of the Hamiltonian Eq.(6.47) for $N \leq 34$ and exact solution of the replica symmetric saddle-point Eq.(6.49), valid at large-N. The later was also used for in the numerical solution of the eigenvalue problem for the exponential growth of the OTO four-point function. All the numerical results corroborate with our analytical predictions.

I would like to acknowledge that all the numerical results presented here have been done by my collaborators A.M. García-García, M. Tezuka and A.R. Bermúdez, and have been published as part of a collaborative work in [115]. I present these results here for consistency.

Thermodynamics

We initiate our analysis of Eq. (6.47) with the study of thermodynamic properties by exact diagonalisation. The results in this section are given in units where $J = 1$. For a given set of parameters we have obtained at least 10^6 eigenvalues. We have computed, following [104, 245], the low temperature limit of the entropy by using standard thermodynamic relations and a finite size scaling. The latter is necessary as the zero temperature limit of the entropy density s_0 vanishes for any finite fixed N. For the standard SYK model s_0 is finite, however our results are consistent with a vanishing s_0 for any κ. This is in agreement with the theoretical expectation that, in the large-N limit and deep in the infrared, where the conformal prediction applies, the first term in Eq. (6.47) is irrelevant. The entropy associated to the second term in Eq. (6.47) vanishes at zero temperature [100].

We note that a vanishing s_0 does not compromise the existence of a gravity-dual interpretation [269]. The specific heat, linear in the low temperature limit with a slope c which is proportional to the number of Majoranas fermions N, is qualitatively similar to the one in the unperturbed SYK model [100]. This is the expected behaviour in a field theory with the gravity dual. For small κ, the two-body random perturbation is not important and $c \approx 0.5N/\kappa$. However, for $\kappa > 1$ we have observed a steady increase of c with κ.

The zero temperature limit of the entropy, s_0, was obtained by exact diagonalisation of the Hamiltonian Eq. (6.48) for different N and κ. We note that for any finite N the entropy will vanish in the $T \to 0$ limit [34]. Therefore, to justify a zero entropy in this limit

[34] The reason is simply that for finite N there is a gap of the order 2^{-N} so that degeneracy is not exact.

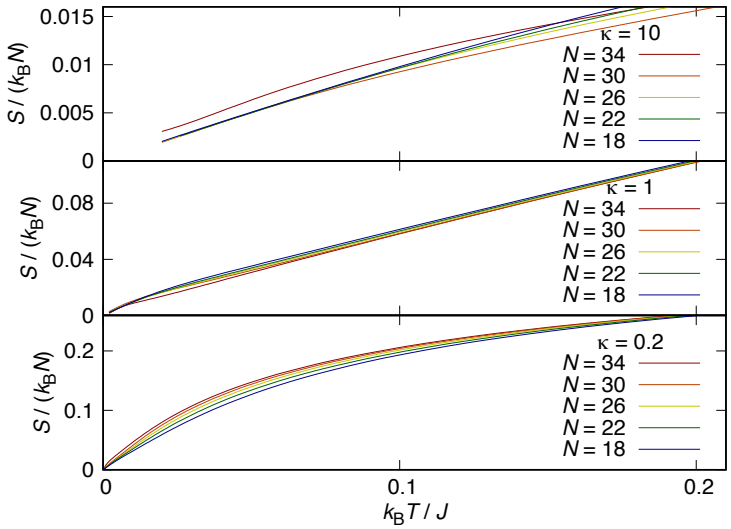

Figure 6.6: Entropy S as a function of temperature T from the exact diagonalisation of Eq.(6.48) for different N's and κ where k_B stands for the Boltzmann constant. The number of eigenvalues employed is mentioned in the main text. The weak dependence on N is consistent with a vanishing zero temperature entropy.

it is necessary to extrapolate the finite N numerical results to the $N \to \infty$ limit. However, this does not seem strictly necessary as the N dependence, depicted in Fig. 6.6, is very weak, especially for $\kappa \geq 1$. A simple extrapolation of the curves for larger N to the $T = 0$ limit leads to a zero-temperature entropy which is smaller than 10^{-3} for all κ's. These results are fully consistent with the $N \to \infty$ results, which have been obtained by fitting $\frac{\log Z}{N} = -E_0\beta + s_0 + \frac{c}{2\beta} + \frac{c_1}{\beta^2} + \frac{c_2}{\beta^3}$ for $J = 1$. In order to obtain $\frac{\log Z}{N}$ we solve Eq. (6.49) as described previously in Refs. [102, 253]. We use a Fast Fourier transform to switch between frequency and time domains and solve iteratively until convergence. For $\omega_n = 2\pi T(n + 1/2)$ we take $-N_\omega/2 < n < N_\omega/2 - 1$, with $N_\omega = 2^{24}$ and $N_t = 4N_\omega$ points in the frequency and time domains.

We now move to the study of the low temperature limit of the specific heat $C(T)$ per Majorana obtained by exact diagonalisation. For that purpose we employ the following thermodynamic expression:

$$C(T) = \left\langle \frac{1}{NZ} \sum_k \frac{(E_k - \bar{E})^2}{T^2} e^{-\beta E_k} \right\rangle , \tag{6.78}$$

where Z is the partition function, $\langle \ldots \rangle$ stands for ensemble average and k labels the eigenvalues for a given disorder realisation with average $\bar{E}$.

We carry out quenched averages, namely, the specific heat is computed separately for each disorder realisation. The final specific heat is the arithmetic average over all disorder realisations. We then fit the low temperature limit by a low order polynomial in temperature. The coefficient of the linear term is the specific heat coefficient, c, which in units of N and

with the coupling constant set to one, is $\pi/(6\kappa)$ for $\kappa \to \infty$ and ≈ 0.4 for the unperturbed two-body SYK model ($\kappa = 0$) [102, 245]. As shown in Fig. 6.7, for large κ, c is indeed very close to $\pi/(6\kappa)$. Only for $\kappa \ll 1$ we observe a moderate increase of c. This is a

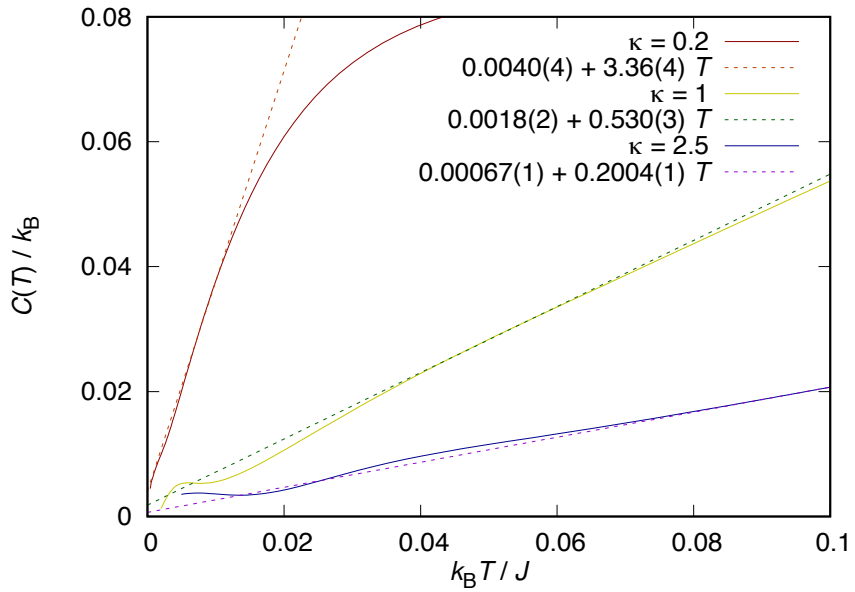

Figure 6.7: Specific heat $C(T)$ as a function of temperature, in units of J/κ_B, obtained from Eq.(6.78) and the exact diagonalisation of Eq.(6.48) for $N = 34$ and different κ's. The specific heat is clearly linear in the low temperature limit with a slope that it is close to the $\kappa = 0$ prediction $c = \pi/6$ for any $\kappa \leq 1$.

further confirmation that the ground state and lowest energy excitations of the Hamiltonian Eq.(6.48) are mostly controlled by the random-mass term. We cannot study arbitrarily small κ because it would require to reach very low temperatures that compromise the numerical accuracy of the results. We have checked that the obtained specific heat coefficient c is robust to changes in the fitting interval. We have observed that for $N \leq 30$ the value of c does not have a monotonic dependence on N which makes it difficult to carry out a finite size scaling analysis. For that reason, unless otherwise stated, the fitting is restricted to the largest $N = 34$ that can be reached numerically. Finally, in Fig. 6.8, we compare the specific heat coefficient c obtained from the large-N fitting of $\frac{\log Z}{N}$, as explained above with the exact diagonalisation result given in Fig. 6.7. Deviations are consistent with $1/N$ corrections only taken into account in the latter.

Lyapunov exponent

As discussed in Section 6.2.4 the exponential growth rate of OTO four-point functions provide a measure of quantum chaos. In the SYK model, the OTO correlation function is a sum of ladder diagrams recursively generated by convolution with a kernel composed of the

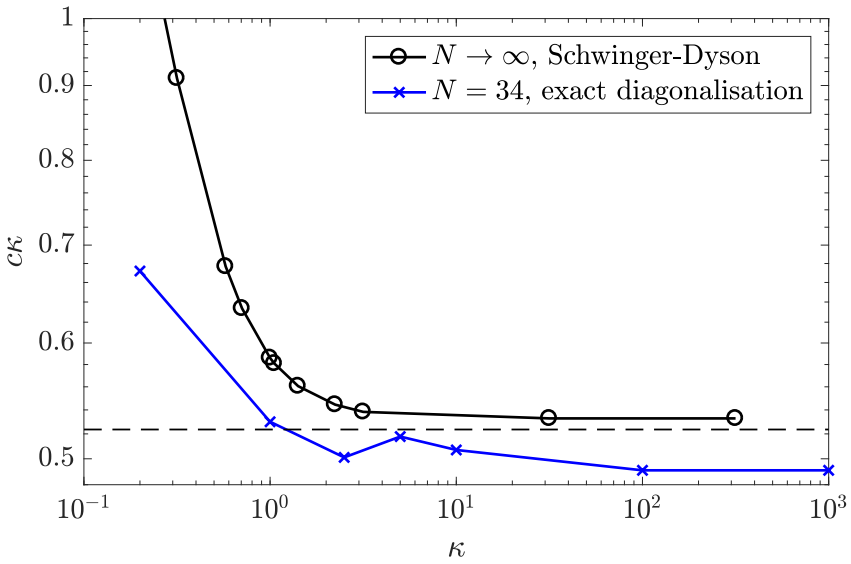

Figure 6.8: Specific heat coefficient c as a function of κ. The exact diagonalisation result, shown in blue crosses, is the slope of the fitting curve in Fig. 6.7. The black dots are obtained from fitting $-\beta\frac{F}{N} = \frac{\log Z}{N}$ obtained from the numerical solution of the large-N saddle point equations Eq.(6.49). The dashed line corresponds to $c = \pi/(6\kappa)N$, the analytical value when the Hamiltonian only contains the random-mass term [102]. Differences between the two results are consistent with $1/N \sim 0.03$ corrections only retained in the exact diagonalisation result.

retarded and lesser one-point functions. In our generalised model it can be written as

$$K(t_1, t_2, t_3, t_4) = G^R(t_1)G^R(t_2)\left[3J^2 G^<(t_3 - t_4)^2 + \kappa^2\right]. \tag{6.79}$$

Following our previous discussion in Sections 6.2.4 and 6.3.2, the growth rate of the OTO is determined by the eigenfunction satisfying the following eigenvalue problem,

$$F(t_1, t_2) = \int_{\mathbb{R}} \mathrm{d}t_3 \int_{\mathbb{R}} \mathrm{d}t_4 \; K(t_1, t_2, t_3, t_4)F(t_3, t_4). \tag{6.80}$$

Therefore, to know whether our model is chaotic or not, it suffice to solve the eigenvalue problem and evaluate the asymptotic of F. In this section we pursue this strategy numerically.

In order to numerically compute the exact retarded and lesser one-point functions, we follow the strategy employed in Refs. [102, 106]. We analytically continue $i\omega_n \to \epsilon + i0^+$ the saddle point Eq.(6.49) and solve it using the spectral representation of the retarded Green's function. Substituting the ansatz: $\mathcal{F}(t_1, t_2) = e^{\lambda_L(t_1+t_2)/2} f(t_{12})$, where $t_{12} = t_1 - t_2$, into Eq. (6.38) and expressing it in the frequency domain, we obtain the following eigenvalue equation for $f(\omega)$:

$$f(\epsilon') = \left|G^R\left(\epsilon' + i\frac{\lambda_L}{2}\right)\right|^2 \left[\kappa^2 f(\epsilon') + 3J^2 \int \frac{\mathrm{d}\epsilon}{2\pi} g_{lr}(\epsilon' - \epsilon) f(\epsilon)\right] \tag{6.81}$$

where $\epsilon' = \epsilon_1 - i\lambda_L/2$ and $g_<(\epsilon) = \int \mathrm{d}t\, e^{i\epsilon t} G_<(t)^2$. Finally, we compute λ_L by imposing the existence of a non-degenerate eigenvalue equal to one so that Eq. (6.81) is satisfied.

Results, depicted in Fig. 6.9, show the system displays chaotic behaviour, namely, the Lyapunov exponent λ_L is finite, for all studied values of κ and sufficiently high temperature. However, even in the strong coupling limit, λ_L never approaches the bound $\lambda_L = 2\pi k_B T/\hbar$. Indeed, for a given temperature, λ_L decreases as κ increases and eventually vanishes for sufficiently strong κ or, for a fixed κ, for sufficiently low temperature. This is fully consistent with the previous results that suggested a chaotic-integrable transition for a fixed κ and sufficiently low temperature. Therefore, chaos is robust to the introduction of a relevant one-body perturbation but the Lyapunov exponent never reaches the saturation value and eventually vanishes.

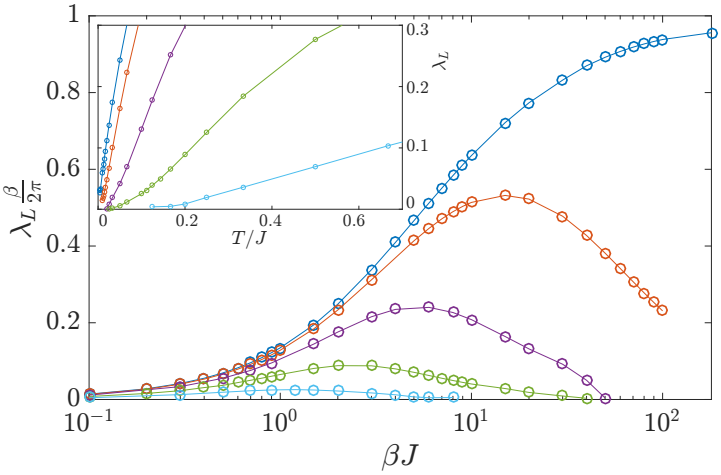

Figure 6.9: Lyapunov exponent λ_L in the model of Eq. (6.47) with $J = 1$ as a function of β and κ. From top to bottom $\kappa = 0,\ 0.2,\ 0.5,\ 1,\ 2$. A finite λ_L, which is a signature of quantum chaos, is observed for a fixed κ and not too low temperature. For sufficiently low temperatures, and $\kappa > 0$, we identify a $T^*(\kappa)$ such that $\lambda_L = 0$ for any $T < T^*(\kappa)$ which signals a chaotic-integrable transition. Inset: Zoomed in region in low temperature limit. Except for $\kappa = 0$ (dark blue), λ_L vanishes for any $T \leq T^*(\kappa)$.

6.4 Conclusion

In this chapter, we have discussed the stability of the holographic properties of the SYK model under a relevant, one-body all-to-all deformation of the Hamiltonian. The model was introduced in Section 6.3, where we have also derived the large-N saddle-point equations. In Section 6.3.1, we introduced a perturbative scheme around the ground state of the model, which is dominated by the one-body term. We proceeded by analytically computing the low-temperature expansion of the free energy, and determined the zero temperature entropy density and specific heat coefficient. Since these thermodynamic coefficients are determined

by the long-time, infra-red properties of the model, they are consistent with the ones for the pure integrable model and are largely unaffected by the leading order two-body perturbation. While the long-time equilibrium properties of the model are expected to be dominated by the relevant term, this is less clear for properties that depend on intermediate time scales, such as the exponential growth of the OTO four-point function around the Ehrenfest time. In Section 6.3.2 we pursued this question by studying the large-q expansion of the model around the chaotic $q/2$-model. Although this expansion is singular, we showed that it surprisingly captures the relevant physics. Our results suggest that chaos is stable for a range of temperatures. Finally, in Section 6.3.3 we concluded by presenting exact numerical results supporting to our analytical results. Both the exact diagonalisation and large-N numerical estimate of the thermodynamic coefficients agree with our analytical results in the region they overlap. Furthermore, the numerical solution of the eigenvalue problem is in qualitative agreement with our large-q analysis, and suggests that chaos is stable for a non-trivial range of temperatures. We note that spectral statistics for this model has been studied in [115], and further corroborates our conclusions.

7 | Conclusion

In this dissertation we have investigated several aspects in the study of translational symmetry breaking in holographic field theories. Our journey started with a pragmatic introduction to the tools and techniques of applied holography, followed by a review of the previous literature that prompted our research questions. Translational symmetry breaking was first motivated by the unphysical infinite dc-conductivity of the simplest charged holographic theory. Although the early Stueckelberg-based models have been successful in addressing this issue, and correctly reproduce the behaviour of standard metals, they fail to capture the physics of metal-insulator transitions in the strong relaxation regime. We have shown that introducing a non-minimal coupling between the axion field and the Ricci tensor can lead to a crossover towards an insulator-like behaviour at strong relaxation. However, since the effects of disorder are only incorporated in Stueckelberg-based models through momentum dissipation, it became clear that this phenomenological approach is limited. A move towards genuinely disordered models inevitably involves breaking translational invariance explicitly at the level of the dual geometry. We investigated two complementary approaches in this direction. The first consisted in introducing a disordered chemical potential in an initially translational invariant theory. We have shown that this deformation drives the theory to a non-trivial disordered fixed point which can be studied analytically by judiciously choosing the distribution of disorder. Our second approach, instead, took as a starting point a non-perturbative disordered solution of Einstein's equations. We have studied how disorder affects a probe scalar field living in this random geometry, and have found compelling signs of coherence in the one and two-point functions of dual boundary operator. This is the first time coherence effects are observed in a holographic field theory. Finally, we changed sides in the duality and investigated the SYK model, an interacting many-body model which was recently shown to possess black hole-like properties suggesting the existence of a gravity dual. Our work has shown that these holographic properties of the model are robust against the most natural one-body perturbation of the model.

We now summarise our key original results in more detail.

Summary of results

In Chapter 3 we have introduced an asymptotically AdS Brans-Dicke (BD) model where we coupled a scalar field to the Ricci tensor in the Einstein-Hilbert action. First, we studied the model in the presence of translational symmetry, taking the scalar field to be a function of the holographic radius. In this case, the background was found analytically and can be heuristically pictured as the dual of a metal with a varying coupling constant. Although the dc-conductivity is divergent - as expected for translational invariant geometries - we obtained analytical results for the regular part of the dc-conductivity σ_Q, which was shown to deviate from the result in Einstein-Maxwell-dilaton (EMd) theories. In contrast, the shear viscosity to entropy ratio η/s was shown to saturate the KSS bound. As a consistency check, we also reproduce these results using a shortcut consisting of mapping our Brans-Dicke theory to EMd via a conformal transformation. Interestingly, we note that exactly the same procedure can be applied to general $f(R)$ theories, and find the analogous results for σ_Q and η/s to this general family of translational invariant theories. In the second part of the chapter, we break translational symmetry by taking the scalar to be a function of the Stueckelberg field. The finite dc-conductivity of the model has been calculated analytically and is given as a function of the background at the horizon. Unfortunately in this case an analytical solution for the geometry is not available, and we proceed by solving the field equations numerically. Although the dc-conductivity is always positive, we observe a crossover between $\frac{\mathrm{d}\sigma_{\mathrm{dc}}}{\mathrm{d}T} < 0$ and $\frac{\mathrm{d}\sigma_{\mathrm{dc}}}{\mathrm{d}T} > 00$ as we increase the relaxation strength, a behaviour commonly referred in the holography community as *insulating-like*. However, we argue that this insulator-like behaviour is mostly due to the screening of charge in dual field theory. We have also computed the ac-conductivity and showed that it scales linearly with frequency for low-frequencies, strong relaxation and low-temperatures. Common to other effective theories of momentum relaxation, the shear viscosity to entropy ratio is always above the KSS bound.

In Section 4 we studied the break of translational invariance in a holographic field theory by introducing a zero mean normally distributed chemical potential. Although this deformation is a priori relevant, we showed that the power spectrum of disorder can be tuned to make it marginal or irrelevant. We proceeded with a perturbative calculation around the weak disorder limit. At zero temperature, the first order random correction to the geometry can be found analytically and was shown to be suppressed in the IR for irrelevant disorder. For marginal disorder, the perturbative corrections to the geometry diverge logarithmically in the IR, indicating the breakdown of the perturbative expansion around the translational invariant ground state. We showed that this divergence can be resumed, and yield an emergent Lifshitz scaling in the IR geometry. The perturbative correction to the dc-conductivity is positive, reflecting the fact that the weakly-disordered chemical potential introduces charge into the system. The story is similar for the finite

temperature analysis, although in this case the analytical calculations are more intricate. At finite temperature, the black hole acquires an effective charge and the thermal conductivity has the expected Drude peak that signals the breaking of translational invariance. However, the electric conductivity is not affected by the random chemical potential to leading order in the disorder strength.

Section 5 continued with the investigation of inhomogeneous holographic theories. We have introduced a family of three-dimensional exact solutions of Einstein's equations indexed by a free function which was taken to depend on the spacelike boundary coordinate. We introduced a massive scalar field to probe the effects of the inhomogeneous background. The corrections to the translational invariant one and two-point functions of the dual boundary scalar operator were calculated analytically, for different choices of inhomogeneity in the geometry. In particular, in the case where the source is also an oscillating function, the perturbative correction to the one-point function can be positive or negative, depending on the relative sign of the geometry and source frequencies. We have also identified coherence effects between a sinusoidal source and the weakly random geometry introduced by a spectral decomposition. In a certain region of parameters, the one-point function, which is sinusoidal, in the absence of disorder, becomes completely random even in the limit in which perturbation theory applies. The averaged corrections to the two-point function in the presence of a delta source and a weakly random, normally distributed, gravity background, is negative and, for large distances, decays as a power-law with an exponent that depends on the type of disorder and the scalar mass. We have identified a range of parameters for which perturbation theory breaks down, as the power-law decay is slower than in the translational invariant case. This suggests an instability to a novel disorder driven fixed point which could eventually lead to a metal-insulator transition in the system.

Finally, in Section 6 we have investigated the thermodynamic and chaotic properties of a generalized SYK model consisting of a one plus two-body uncorrelated all-to-all random terms. We have shown that the ground state of this generalised model is dominated by the one-body term, which is relevant in the sense of the renormalisation group. Therefore, we proceeded with a perturbative analysis of the model around the one-body solution and calculated the low-temperature expansion of the free energy. The zero temperature entropy density and specific heat coefficients were found to be unchanged to leading order. Next, we have generalized the two-body term to a $q/2$-body term and have studied the OTO four-point function in the large-q limit. A singular perturbative expansion around the interacting term revealed that the Lyapunov exponent characterising the exponential growth of the OTO correlation function is finite for a range of temperatures. This result suggests that chaos is stable in the generalised model. Outside the stability window, we speculate that this model undergoes a chaotic-integrable transition. Numerical results supporting our perturbative analytical calculations are also provided.

A look into the future

In the course of writing this dissertation, at least five works motivated by disordered holographic theories have appeared [270–274], illustrating the dynamism of this fairly young field. In these last lines, we draw the attention to a couple of open problems which we speculate will drive the field in the years to come.

In Chapter 4 we have discussed how Lifshitz geometries arise in the infra-red from the resummation of the perturbative expansion of weak marginal disorder. Our work suggests that Lifshitz scaling is generic for marginal disorder in holographic theories. Very recent work by Aharony and Narovlansky [270,273] takes a step forward in analysing the renormalization group flow of general disordered quantum field theories[35] and has shown that the emergence of a dynamical scaling exponent is generic. This is yet an example of general quantum field theory result which was first motivated by holography. Surprisingly, in this work, the authors propose to take the dynamical critical exponent z as a beta function for the renormalisation group flow and develop an analytical treatment of the Callan-Symanzik equations. The analogy between Einstein's equations and the renormalisation group flow discussed in Section 2.3.3 could give valuable insight in transposing this non-perturbative treatment to holography. It would be interesting to investigate the possibility of finding the full disordered geometry, or at least its average, from the Einstein's equations.

A similar direction which remains largely unexplored is the study of thermalisation in disordered holographic theories. From the gravity perspective, thermalisation is related to the problem of black hole formation. Work by Pretorius and Choptuik has identified an emerging scale invariance near the black hole formation point, very similar to a phase transition in critical systems [275]. Disorder has been recently shown to slow down or even prevent thermalisation in some condensed matter systems, a phenomenon known as many-body localisation [51,276,277]. It would be interesting to investigate whether disorder can drive the gravitational collapse away from the black hole fixed point to the equivalent of a many-body localised phase.

Our work in Chapter 5 have only studied one instance of a random geometry. Asymptotic AdS_3 solutions of Einstein's Equations have been classified in [225], and there are other families in which disorder could be introduced in a similar fashion. It would be interesting to investigate whether introducing disorder in other metric components could lead to a similar universal behaviour and, if not so, identify the physics behind these differences. Second, since temperature tends to suppress coherence effects in disordered systems, in this work we have chosen to study holographic field theories at strictly zero temperature. However, finite temperature solutions in three dimensions have also been classified [278], and our work could be therefore also generalized in this direction. In particular, it would be interesting to study the low-temperature regime and compare it with our results. Third, we

[35] Not necessarily holographic or marginal.

have only considered Gaussian distributed disorder with delta-like correlations. However, our formalism is easily generalisable to more general forms of disorder where correlations between points become important. Fourth, a renormalization group treatment, feasible for marginal random perturbations, would shed light on the existence, or not, of a novel non-trivial disordered driven fixed point which signals an instability toward a metal-insulator transition in the system.

A | Auxiliary calculations

A.1 Scalar field dynamics in AdS$_{d+1}$

Consider a massive scalar field ψ minimally coupled to a fixed AdS$_{d+1}$ geometry. The action is given by,

$$\begin{aligned} S[\psi] &= \frac{1}{2}\int \mathrm{d}^{d+1}x \left(\mathrm{d}\psi \wedge \star \mathrm{d}\psi - m^2\psi^2\right) \\ &= -\frac{1}{2}\int \mathrm{d}^{d+1}x \left(\mathrm{d}\star \mathrm{d}\psi - m^2\psi\right)\psi + \frac{1}{2}\int \mathrm{d}^{d}x\, \psi \star \mathrm{d}\psi. \end{aligned} \tag{A.1}$$

The equations equation of motion are given by

$$\left(\Delta_g - m^2\right)\psi = 0. \tag{A.2}$$

We now fix a local Poincaré II chart $x^a = (r, t, \mathbf{x})$ (see Section 2.2.1) in which the metric is given by $\mathrm{d}s^2 = r^{-2}\left(\mathrm{d}r^2 - \mathrm{d}t^2 + \mathrm{d}\mathbf{x}^2\right)$. We can exploit the fact that the geometry is static and homogeneous to write the scalar field in Fourier space,

$$\psi(r,t,\mathbf{x}) = \int_{-\infty}^{\infty}\frac{\mathrm{d}\omega}{2\pi}\int_{\mathbb{R}^{d-1}}\frac{\mathrm{d}^{d-1}k}{(2\pi)^{d-1}}e^{-i\omega t + i\mathbf{k}\cdot\mathbf{x}}\,\psi_{\omega,\mathbf{k}}(r)$$

where Eq.(A.2) simplifies to a second order ordinary differential equation,

$$\partial_r^2\psi_k - \frac{d-1}{r}\partial_z\psi_k + \left(k^2 + \frac{m^2}{r^2}\right)\psi_k = 0 \tag{A.3}$$

with $k^2 = -\omega^2 + \mathbf{k}^2$. Letting $\psi = r^{(d+1)/2}\phi$ and defining $\nu^2 = \frac{d^2}{4} + m^2$, Eq.(A.3) simplifies to a modified Bessel Equation

$$(kr)^2\phi_k'' + (kr)\phi_k' - \left(\nu^2 + (kr)^2\right)\phi_k = 0. \tag{A.4}$$

with general solution given by a linear combination of the modified Bessel Functions

$$\phi_k(z) = a_k K_\nu(kr) + b_k I_\nu(kr). \tag{A.5}$$

Requiring that $\nu > 0$ imply that $m^2 > -d^2/4$ (note that $d > 0$), which is the celebrated *Breitenlohner-Freedman (BF) bound*. According to the holographic dictionary in Section (2.3), we should impose that the solution remain bounded at the Poincaré horizon $r = \infty$. The behaviour of the Bessel functions in the asymptotic region $r \to \infty$ is given by

$$K_\nu(kr) \sim e^{-kr}, \qquad I_\nu(kr) \sim e^{kr}. \tag{A.6}$$

Note that since $k^2 = -\omega^2 + \mathbf{k}^2$, it can be positive or negative, these cases need to be considered separately.

Case $k^2 > 0$: In this case, the general solution solution blows up as $r \to \infty$. Therefore regularity at the Poincaré Horizon requires imposing $b_k = 0$. Near the boundary $r = 0$, $K_\nu(kr) \sim \frac{\Gamma(\nu)}{2}(\frac{kr}{2})^{-\nu} + \frac{\Gamma(-\nu)}{2}(\frac{kr}{2})^{\nu}$. Therefore,

$$\psi_k(r) \underset{r\to 0}{=} r^{d-\Delta}\psi_{(0)}(k) + r^{\Delta}\psi_{(1)}(k) + \dots, \tag{A.7}$$

where we have defined $\psi_{(0)}(k) = a_k 2^{\nu-1}\Gamma(\nu)\ k^{d-\Delta}$, $\psi_{(1)}(k) = a_k 2^{\nu-1}\Gamma(-\nu)\ k^{\Delta}$ and $\Delta = d/2 + \nu$. Note that since $\Delta > 0$ the first term in Eq.A.7 always decay as we approach the boundary. This is not always the case for the second term, since $d - \Delta = d/2 - \nu$ can either positive or negative. We say the mode $\psi_{(0)}(k)$ is *normalisable*, while the mode $\psi_{(1)}(k)$ is only normalisable in the range $-d^2/4 < m^2 < 1 - d^2/4$. Within this range, both modes can be used to construct a Hilbert space in the boundary space, and each choice lead to a quantisation scheme. The Hilbert Spaces are related through a canonical transformation, since $(\psi_{(0)}, \psi_{(1)})$ are conjugated pairs [279]. Outside this range, only one mode is normalisable and there is a natural choice of quantisation for building the boundary Hilbert Space.

For later reference, we write the full solution for $k^2 > 0$

$$\psi(r, x) = r^{\frac{d+1}{2}} \int \frac{\mathrm{d}^d k}{(2\pi)^d} e^{ik\cdot x}\ a_k\ K_\nu(kz)$$

Case $k^2 < 0$: In this case k is purely imaginary, and we can parametrise $k = i\beta$ for $\beta \in \mathbb{R}$. The results above are still valid, up to the change $kr \to i\beta r$. The independent solutions are now given by $\psi_\pm = K_{\pm\nu}(i\beta r)$, and have regular asymptotics $\sim e^{\pm i\beta r}$ as $r \to \infty$. We therefore have two independent solutions for ψ, one corresponding to an incoming plane wave at the Poincaré horizon and one being emitted by the horizon. In terms

of the duality, these two independent regular solutions ultimately correspond to the advanced and retarded real-time propagators. As before, m^2 must satisfy the BF bound and we have normalisable and non-normalisable modes. We refer the reader to [280] for a detailed discussion.

A.2 Holographic renormalisation

In this Appendix we discuss the details of holographic renormalisation in our inhomogeneous geometry. Let $\mathcal{M}$ be the underlying manifold defined by the geometry in Eq.(5.1). The action for the probe scalar is given by

$$\begin{aligned} S[\psi] &= \frac{1}{2}\int_{\mathcal{M}} \mathrm{d}^3x \left(\mathrm{d}\psi \wedge \star \mathrm{d}\psi + m^2\psi^2\right) \\ &= -\frac{1}{2}\int_{\mathcal{M}} \mathrm{d}^3x\, \psi \left(\mathrm{d}\star \mathrm{d}\psi - m^2\psi\right) + \frac{1}{2}\int_{\partial\mathcal{M}} \mathrm{d}^2x\, \psi \star \mathrm{d}\psi. \end{aligned}$$

Thus on-shell we have

$$S_{\text{on-shell}}[\psi] = \frac{1}{2}\int_{\partial\mathcal{M}} \mathrm{d}^2x\, \sqrt{-\gamma}\, \psi n^a \partial_a \psi, \tag{A.8}$$

where n is the normal unit vector pointing outwards of the boundary $\partial\mathcal{M}$ and γ is the respective induced metric. Note that strictly at the conformal boundary $\rho = 0$ Eq.(A.8) is divergent. To regularise this divergence, we evaluate the on-shell action at a slice $\rho = \lambda \ll 1$ which we later take to zero. The normal unit vector pointing outward the fixed $\rho = \lambda$ surface is then given by $n = -2\rho\, \partial_\rho|_{\rho=\lambda}$, while the induced metric is

$$\mathrm{d}s^2 = \lambda^{-1} g_{(0)}(x)\mathrm{d}x^\mu \mathrm{d}x^\nu = \lambda^{-1}\left(-\mathrm{d}t^2 + \mathrm{d}x^2 + 2g_{tx}(x)\mathrm{d}t\mathrm{d}x\right)$$

and thus $\sqrt{-\gamma} = \lambda^{-1}\sqrt{-g_{(0)}}$ with $\sqrt{-g^{(0)}} = \sqrt{1+g_{tx}^2}$. Note that $g^{(0)}$ is interpreted holographically as the metric where the dual boundary field theory lives. Inserting in the on-shell action,

$$S_{\text{on-shell}}[\psi] = -\int \mathrm{d}t\mathrm{d}x\, \sqrt{-g_{(0)}}\, \psi\partial_\rho\psi|_{\rho=\lambda}.$$

As with the pure AdS case, the above on-shell action needs to be renormalised. Solutions to Eq. (5.2) satisfy the following near-boundary expansion

$$\psi(\rho, x) = \rho^{\frac{1-\nu}{2}} s(x) + \rho^{\frac{1+\nu}{2}} A(x) + \ldots,$$

where all higher order terms have positive exponents. Thus we have

$$\begin{aligned} S_{\text{on-shell}}[\psi] &= -\int \mathrm{d}t\mathrm{d}x\ \sqrt{-g_{(0)}}\Big(\lambda^{\frac{1-\nu}{2}} s(x) + \lambda^{\frac{1+\nu}{2}} A(x) + \dots\Big)\times \\ &\qquad\qquad \times\Big(\frac{1-\nu}{2}\lambda^{-\frac{1+\nu}{2}} s(x) + \frac{1+\nu}{2}\lambda^{\frac{\nu-1}{2}} A(x) + \dots\Big), \\ &= -\int \mathrm{d}t\mathrm{d}x\ \sqrt{-g_{(0)}}\left(\frac{1-\nu}{2}\lambda^{-\nu} s(x)^2 + s(x)A(x) + \dots\right). \end{aligned}$$

Note that the highest diverging is in the term $\propto s^2$. To remediate this particular divergence, we add the following boundary counter-term to the action

$$S_{\text{ct}}^{(0)} = \frac{1-\nu}{2}\int_{\partial\mathcal{M}} \mathrm{d}^2x\sqrt{-\gamma}\ \psi^2|_{\rho=\lambda} = \frac{1-\nu}{2}\int \mathrm{d}t\mathrm{d}x\sqrt{-g_{(0)}}\ \left(\lambda^{-\nu} s(x)^2 + 2s(x)A(x) + \dots\right).$$

In most of the manuscript we work with $\nu = 1/2$, for which other divergences are not present, and therefore the only counter term required is the above. However, for larger values of ν there is a finite tower of higher divergences between the leading term $\propto \int s(x)^2$ and the term $\propto \int s(x)A(x)$ which we have omitted in the ellipsis, and which should also be taken into account in order to obtain a finite one-point function. For instance, the next order divergence would be of order $O\left(\lambda^{-(\nu-1)}\right)$, which can be remediated by adding a derivative term $S_{\text{ct}}^{(1)} = \frac{1}{2\nu-2}\int_{\partial\mathcal{M}} \mathrm{d}^2\sqrt{-\gamma}\psi\ \Delta_\gamma\psi|_{\rho=\lambda}$. Higher order terms can be treated in the same way, adding higher derivative terms $S_{\text{ct}}^{(k)}$ accordingly (for a complete discussion, see [131]). However note these derivative terms do not contribute to the coefficient of the one-point function $\propto \int s(x)A(x)$. Accounting for all the divergences, the renormalised action reads

$$S_{\text{ren}} = \lim_{\lambda\to 0}\left(S_{\text{on-shell}} + S_{\text{ct}}\right) = -\frac{1}{2}\int \mathrm{d}t\mathrm{d}x\ \sqrt{-g_{(0)}}\ 2\nu\ s(x)A(x). \tag{A.9}$$

The expression above makes clear that the leading coefficient $s(x)$ in the expansion of ψ acts as a source for a dual operator $\langle\mathcal{O}(x)\rangle = 2\nu\ A(x)$. The expectation value of the dual is then simply given by

$$\langle\mathcal{O}(x)\rangle = \frac{1}{\sqrt{-g_{(0)}}}\frac{\delta\left(-S_{\text{ren}}\right)}{\delta s(x)} = 2\nu\ A(x)$$

A.3 Boundary-to-bulk propagator and boundary two-point function

Consider a probe scalar field ψ living in an asymptotically AdS_{d+1} geometry with metric tensor g. As previously discussed, the equation of motion for the scalar is given by $(\Delta_g - m^2)\,\psi = 0$. We define the *bulk-to-bulk propagator* $G(x,y)$ as the Green's function for

this equation. In other words, it is the solution of

$$(\Delta_g - m^2)G(x,y) = \frac{i}{\sqrt{-g}}\delta^{d+1}(x-y). \tag{A.10}$$

Note that if we couple the scalar field with a source by adding a term $(\Delta_g - m^2)\psi = J$, then knowing bulk-to-bulk propagator we can build a solution

$$\psi(x) = \int \mathrm{d}^{d+1}y\sqrt{-g}\; G(x,y)J(y).$$

In a neighbourhood of the boundary, by the Fefferman-Graham theorem we can write the asymptotically AdS metric in a coordinate chart $x^a = (\rho, x^\mu)$ as

$$\mathrm{d}s^2 = \frac{\mathrm{d}\rho^2}{4\rho^2} + \frac{1}{\rho}g_{\mu\nu}(\rho, x^\mu)\mathrm{d}x^\mu \mathrm{d}x^\nu,$$
$$g(\rho, x^\mu) \underset{\rho=0}{\sim} g_{(0)}(x^\mu) + \rho g_{(1)}(x^\mu) + O(\rho^2),$$

where $g_{(0)}(x^\mu)$ defines the metric at the conformal boundary located at $\rho = 0$. At a slice close to the boundary $\rho = \lambda \ll 1$, we have

$$\sqrt{-g} = \frac{\sqrt{-g_{(0)}}}{2\lambda^{1+d/2}}.$$

And therefore evaluating Eq.(A.10) at $\rho = 0$ for one of the arguments make the right-hand side zero. This defines the so called *Boundary-to-bulk propagator*

$$(\Delta_g - m^2)K(\rho; x^\mu, y^\mu) = 0$$

which depends only on one radial variable. As we will see next, it propagates solutions from the boundary to the bulk. Recall that according to the holographic dictionary solutions of the bulk equations of motion define a dual source at the boundary according to

$$\lim_{\rho\to 0}\rho^{-\Delta_-/2}\psi(\rho, x^\mu) = s(x^\mu),$$

where $\Delta_\pm = \frac{d}{2} \pm \nu$ with $\nu = \sqrt{\frac{d^2}{4} + m^2}$. Thus by imposing boundary conditions

$$\lim_{\rho\to 0}\rho^{-\Delta_-/2}K(\rho; x^\mu, y^\mu) = \delta^d(x^\mu - y^\mu),$$

we find that the K satisfies

$$\psi(\rho, x^\mu) = \int \mathrm{d}^d y\; K(\rho; x^\mu, y^\mu)s(y^\mu).$$

This justifies the terminology boundary-to-bulk propagator, since it propagates the source $s(x^\mu)$ living in the boundary into a scalar field satisfying the Bulk equations of motion.

From this relation it is also possible to see that the bulk-to-bulk and boundary-to-bulk propagators are related to the boundary tree-level boundary two-point function. Since we have

$$\langle \mathcal{O}(x^\mu) \rangle = (2\nu) \lim_{\rho \to 0} \rho^{-\Delta_+/2} \psi(\rho, x^\mu)$$

we see that if we define the boundary tree-level two-point function

$$G_{(0)}(x^\mu, y^\mu) = \langle \mathcal{O}(x^\mu)\mathcal{O}(y^\mu) \rangle = (2\nu) \lim_{\rho \to 0} \rho^{-\Delta_+/2} K(\rho; x^\mu, y^\mu)$$

it satisfies the usual linear-response relation

$$\langle \mathcal{O}(x^\mu) \rangle = \int \mathrm{d}^d y \; G_{(0)}(x^\mu, y^\mu) s(y^\mu)$$

between the source and the expected value.

B | Notes on random fields

B.1 Implementation

Consider a random function $f : \mathbb{R}^d \to \mathbb{R}$. A useful trick to parametrise the randomness in f is to work in the spectral representation (a.k.a. Fourier space)

$$f(\mathbf{x}) = \int_{\mathbb{R}^d} \frac{\mathrm{d}^d k}{(2\pi)^d}\, f(\mathbf{k}) e^{i\mathbf{k}\cdot\mathbf{x}}, \tag{B.1}$$

where $f(\mathbf{k})$ are random Fourier coefficients. In other words: we exchanged randomness in real space for randomness in Fourier space. Without loss of generality we can parametrise the Fourier coefficients $f(\mathbf{k}) = a_\mathbf{k} + ib_\mathbf{k}$ where $a_{-\mathbf{k}} = a_\mathbf{k}$ and $b_{-\mathbf{k}} = -b_\mathbf{k}$ for reality of $f(\mathbf{x})$. We say f is a *Gaussian random field* when the Fourier coefficients $(a_\mathbf{k}, b_\mathbf{k})$ are drawn from a Gaussian distribution

$$P[f(\mathbf{k})] = P[a_\mathbf{k}, b_\mathbf{k}] = \frac{1}{\pi\sigma_\mathbf{k}} e^{-\frac{a_\mathbf{k}^2 + b_\mathbf{k}^2}{\sigma_\mathbf{k}^2}} = \frac{1}{\pi\sigma_\mathbf{k}} e^{-\frac{|f(\mathbf{k})|^2}{\sigma_\mathbf{k}^2}}, \tag{B.2}$$

where $\sigma_\mathbf{k}$ is the standard deviation, and for simplicity we centred the distribution at zero. In other words, we have $\mathbb{E}[f(\mathbf{k})] = 0$ and $\mathbb{E}[f(\mathbf{k})f(\mathbf{q})] = \sigma_\mathbf{k}^2 \delta(\mathbf{k} + \mathbf{q})$. It is important for the distribution to be normalised:

$$\int \mathrm{D}f(\mathbf{k})\; P[f(\mathbf{k})] = \int_{-\infty}^{\infty} \mathrm{d}a_\mathbf{k} \int_{-\infty}^{\infty} \mathrm{d}b_\mathbf{k}\; P[a_\mathbf{k}, b_\mathbf{k}] = 1, \qquad \forall \mathbf{k}. \tag{B.3}$$

Moments of any functional $Q[f(\mathbf{k})]$ of the random field can be easily computed using the characterisation above:

$$\mathbb{E}[Q[f(\mathbf{k})]] = \int \mathrm{D}f(\mathbf{k})\; P[f(\mathbf{k})]\; Q[f(\mathbf{k})] = \int_{-\infty}^{\infty} \mathrm{d}a_\mathbf{k} \int_{-\infty}^{\infty} \mathrm{d}b_\mathbf{k}\; \frac{Q[a_\mathbf{k}, b_\mathbf{k}]}{\pi\sigma_\mathbf{k}^2} e^{-\frac{a_\mathbf{k}^2 + b_\mathbf{k}^2}{\sigma_\mathbf{k}^2}}.$$

This can then be Fourier transformed to real space. As a simple example, lets compute a two-point function of the random field,

$$\begin{aligned}\mathbb{E}[f(\mathbf{x})f(\mathbf{y})] &= \int \frac{\mathrm{d}^d k}{(2\pi)^d} \int \frac{\mathrm{d}^d q}{(2\pi)^d} e^{i\mathbf{k}\cdot\mathbf{x}} e^{i\mathbf{q}\cdot\mathbf{y}} \mathbb{E}[f(\mathbf{k})f(\mathbf{q})] \\ &= \int \frac{\mathrm{d}^d k}{(2\pi)^d} \int \frac{\mathrm{d}^d q}{(2\pi)^d} e^{i\mathbf{k}\cdot\mathbf{x}} e^{i\mathbf{q}\cdot\mathbf{y}} \sigma^2_{\mathbf{k}} \delta(\mathbf{k}+\mathbf{q}) \\ &= \int \frac{\mathrm{d}^d k}{(2\pi)^d} e^{i\mathbf{k}\cdot(\mathbf{x}-\mathbf{y})} \frac{\sigma^2_{\mathbf{k}}}{(2\pi)^d},\end{aligned}$$

where $(2\pi)^{-d}\sigma^2_{\mathbf{k}}$ is commonly known as the *power spectrum* of the random field. For the simple case where the power spectrum is a constant $\sigma^2_{\mathbf{k}} = (2\pi)^d \bar{V}^2$, we have $\mathbb{E}[f(\mathbf{x})f(\mathbf{y})] = \bar{V}^2\delta(x-y)$ which means the distribution of $f(\mathbf{x})$ in real space is also Gaussian. Conversely, considering a non-trivial power spectrum lead to non-trivial correlations for the random field. Therefore the spectral representation of a random field is a convenient way of generating non-gaussian distributions while still working with Gaussian objects in Fourier space.

B.2 Cutoffs

However this construction is not very useful for actual applications. For instance, note that as $\mathbf{x}$ approaches $\mathbf{y}$ we get an ultra-violet divergence. This for instance can be very inconvenient in the case we are treating, since in our equations we have a lot of terms that go as 'disorder squared' at the same point. To remediate this problem, we will resolve this long wavelength divergence by introducing an ultra-violet (UV) cutoff λ and integrate only over modes $|\mathbf{k}| < \lambda$. A pictorial way to interpret this cutoff is to say that λ introduce a length scale $a = \pi/\lambda$ that corresponds to an underlying lattice. Modes with frequencies below this scale are then ignored. This would imply for instance that $\mathbb{E}[f(\mathbf{x})^2] = \bar{V}^2/a$. As we take the lattice spacing $a \to 0$ we recover the expected UV divergence.

While UV divergences are a consequence of the way we introduce disorder, there can be IR divergences that are emergent in the problem, and indicate a change of behaviour in the system. Or in terms of the renormalisation group: the system flows towards a disordered fixed point. To resolve these divergences one usually introduce a box of size L, and in the end of calculation one aims to study how the system behaves as L is increased. IR singularities in the thermodynamic limit $L \to \infty$ indicate a flow towards a new phase.

B.3 Discrete

Although the continuum implementation simplifies analytical calculations, numerically one needs a discretisation that takes into account the aforementioned observations. From now on

we restrict ourselves to the case of interest, namely $d = 1$. Note that according to Eq. (B.2) the norm of $|f(\mathbf{k})|$ is drawn from a Gaussian distribution, while the phase is drawn from the uniform distribution on $[0, 2\pi]$. This remark leads to a useful discrete representation of the continuous spectral decomposition. We start by discretising uniformly our box of size L in N intervals of size a, i.e. $L = Na$. This implies the quantisation of the modes $k_n = n\Delta k$ with $\Delta k = \frac{\pi}{Na} = \frac{\lambda}{N}$. The thermodynamic limit then becomes $N \to \infty$. The spectral decomposition Eq. (B.1) becomes,

$$f(x) = \sum_{n=-N}^{N} f_n e^{ik_n x} = \sum_{n=1}^{N} A_n \cos(k_n x + \gamma_n), \tag{B.4}$$

where $A_n \in \mathbb{R}_{>0}$ corresponds to the amplitude of the Fourier modes and $\gamma_n \in [0, 2\pi]$ the phase. As we remarked above, in this representation each A_n is a random variable taking values in a Gaussian distribution, while each γ_n is a random variable taking values uniformly in $[0, 2\pi)$. However a useful simplification is to make A_n deterministic and only keep the phases random. One can then check that taking $A_n = \bar{V}\sqrt{\sigma(k_n)\Delta k}$ and averaging uniformly in $[0, 2\pi)$,

$$\mathbb{E}[\cdots] = \lim_{N\to\infty} \int_0^{2\pi} \prod_{n=1}^{N} \frac{\mathrm{d}\gamma_n}{2\pi} (\cdots), \tag{B.5}$$

imply that for $\sigma(k_n) = 1$ in the thermodynamic limit $\mathbb{E}[f(x)f(y)] = \bar{V}^2\delta(x - y)$. In other words, we reproduce the Gaussian behaviour with a simpler setup in which only the phases fluctuate. Similarly, we can obtain non-Gaussianity by choosing a non-trivial function $\sigma(k_n)$.

C | Brans-Dicke Holography

C.1 An asymptotically AdS Brans-Dicke Black Hole

As we have previously discussed in section 3.2.2.3, the action (3.10) can be brought to the Einstein frame via a conformal transformation. In this frame, the BD action maps to an EMD model. Solutions for this action have been widely studied for different choices of potential [157–159, 171]. For completeness, we give here a particular explicit black brane solution with AdS assymptotics. In the language of ref. [159] this corresponds to a $\delta = \gamma$ solution.

$$\mathrm{d}\bar{s}^2 = -f(u)\mathrm{d}t^2 + \frac{\mathrm{d}r^2}{f(u)} + r^2 R(u)\delta_{ij}\mathrm{d}x^i\mathrm{d}x^j \tag{C.1}$$

$$f(u) = \frac{2\Lambda(\alpha^2+1)^2 b^{2\gamma}}{(d-1)(\alpha^2-d)}u^{2(1-\gamma)} - \frac{m}{u^{(d-1)(1-\gamma)-1}} + \frac{2q^2(\alpha^2+1)^2 b^{-2(d-2)\gamma}}{(d-1)(\alpha^2+d-2)}u^{2(d-2)(\gamma-1)} \tag{C.2}$$

$$R(u) = \left(\frac{b}{u}\right)^{2\gamma} \tag{C.3}$$

$$\bar{\phi}(r) = \frac{(d-1)\alpha}{2(1+\alpha^2)}\log\frac{b}{u} \tag{C.4}$$

$$\bar{V}(\bar{\phi}) = 2\Lambda e^{\frac{4\alpha\bar{\phi}}{d-1}} = \left(\frac{b}{u}\right)^{2\gamma} \tag{C.5}$$

$$\bar{a}'_t = -\frac{qY}{u^{d-1}}\left(\frac{b}{u}\right)^{-(d-3)\gamma}, \tag{C.6}$$

where we defined $\gamma = \alpha^2/(1+\alpha^2)$, with α as in Eq. (3.8). This solution has four free parameters (γ, b, q, m). γ is a function of the Brans-Dicke parameter ξ

$$\gamma = \frac{\alpha^2}{1+\alpha^2} = \frac{1}{1+\alpha^{-2}} = \frac{(d-3)^2}{(d-1)^2+8+4(d-1)\xi}$$

The black brane horizon radius is found by imposing $f(u_0) = 0$. This allow us to solve for one of the parameters as functions of u_0 and the others, e.g. $m = m(u_0, q, b, \gamma)$. The parameter b sets the scale of the dilaton $\bar{\phi}$ and can be set to unit by a coordinate rescaling.

An interesting case is given by $d = 3$, where $\gamma = \alpha = 0$ and the scalar field is constant.

In this case the solution above reduces to the well known AdS Reissner-Nordstrom solution. Note that $\gamma = \alpha = 0$ also for $\xi \to \infty$, which is the well known Einstein limit of Brans-Dicke theory. In this limit, the solution also reduces to $d+1$ dimensional Reissner-Nordstrom. q is the charge density of the background and m is related to the energy density (ADM mass) as we will discuss below.

To construct an asymptotically AdS black hole solution for our Brans-Dicke theory Eq. (3.1) we take the inverse conformal mapping on the solution above. The Brans-Dicke black hole is then given by

$$\begin{aligned}
\mathrm{d}s^2 &= -A(r)\mathrm{d}t^2 + B(r)\mathrm{d}r^2 + r^2 c(r)\delta_{ij}\mathrm{d}x^i\mathrm{d}x^j \\
A(r) = \phi^{-\frac{2}{d-1}} f(u) \quad B(r) &= \frac{\phi^{-\frac{2}{d-1}}}{f(u)}\,, \quad c(r) = \phi^{-\frac{2}{d-1}} R(u) = \left(\frac{b}{u}\right)^{\frac{2(d-5)}{d-3}\gamma} \\
V(\phi) &= 2\Lambda\phi^2 \\
a_t' &= -\frac{qY}{u^{d-1}}\left(\frac{b}{u}\right)^{-(d-3)\gamma} \\
\phi(r) &= \left(\frac{b}{u}\right)^{\frac{2(d-1)\gamma}{d-3}}\,.
\end{aligned}$$

Note that in particular this transformation preserves the position of the horizon u_0. The temperature can then be computed

$$4\pi T = |A(u_0)| = \frac{(d-\alpha^2)m}{\alpha^2+1} u_0^{(d-1)(\gamma-1)} - \frac{4q^2(\alpha^2+1)b^{-2(d-2)\gamma}}{\alpha^2+d-2} u_0^{(2d-3)(\gamma-1)-\gamma}$$

which again reduces to the RN temperature for $\gamma = \alpha = 0$. The free energy density can be computed by the properly renormalised euclidean action. We refer the curious reader to [281] for the details of the calculation and just quote the answer here,

$$\begin{aligned}
f &= \beta\left(\frac{(d-1)b^{(d-1)\gamma}m}{\alpha^2+1}\right) - \frac{b^{(d-1)\gamma}u_0^{(d-1)(1-\gamma)}}{4\pi} - \beta\frac{q^2}{2((d-3)(1-\gamma)+1)}\frac{1}{u_0^{1+(d-3)(1-\gamma)}} \\
&= \beta\epsilon - s - \beta\mu q,
\end{aligned}$$

for $\beta = T^{-1}$ and we defined

$$\epsilon = \frac{(d-1)b^{(d-1)\gamma}m}{\alpha^2+1}\,, \quad s = \frac{b^{(d-1)\gamma}u_0^{(d-1)(1-\gamma)}}{4\pi}\,, \quad \mu = \frac{q^2}{2((d-3)(1-\gamma)+1)}\frac{1}{u_0^{1+(d-3)(1-\gamma)}}.$$

The energy density (ADM mass), entropy density and chemical potential. In particular note that the above satisfy the first law $\mathrm{d}\epsilon = T\mathrm{d}s + \mu\mathrm{d}\rho$ for $4\pi\rho = \int_{\mathcal{M}} \star F = q$ the charge density.

C.2 Gravitational background with $Z \neq 1$, $Y = 1$ and $V \neq 1$ in four bulk dimensions

In Fig. C.1 we show the metric functions, defied in Eq. (3.11), at nonzero temperature for the model defined in Eq. (3.10) and couplings given in Eq. (3.30).

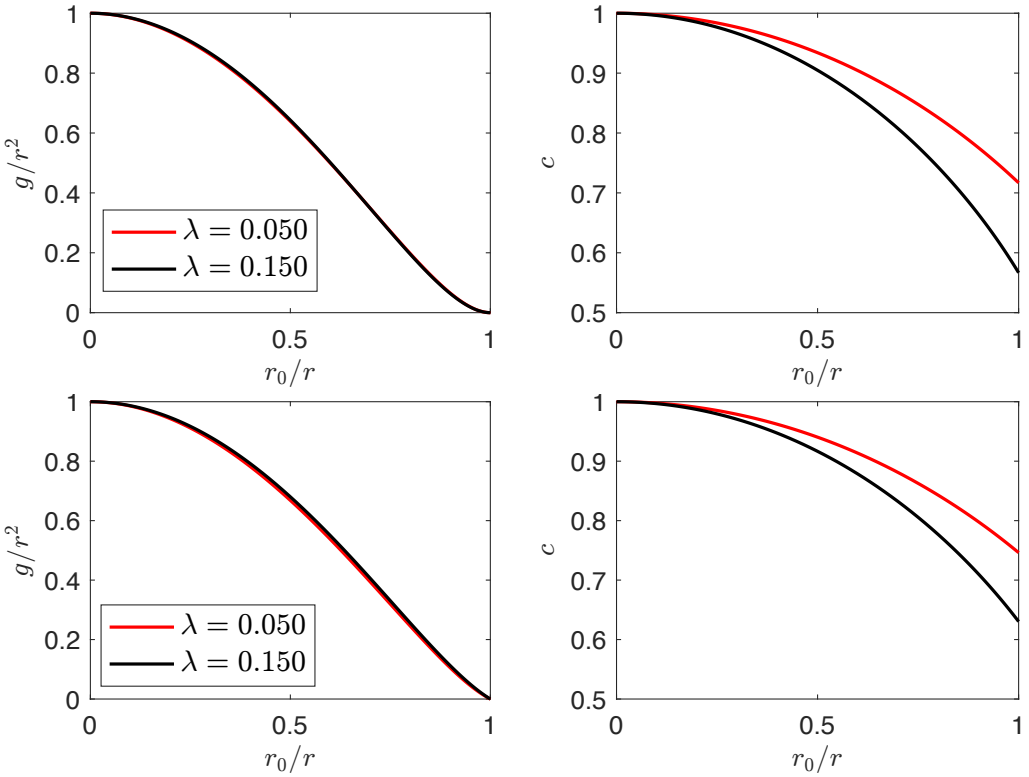

Figure C.1: Metric functions g (blackening factor) and c, Eq. (3.11) for two different temperatures; top row: $T = 10^{-4}$ and bottom row: $T = 0.08$. We fix the charge density $\rho = 1$, $\kappa = 1$ and $\lambda_{\text{eff}} = \lambda\alpha^2 = 0.15$. Each line corresponds to $\alpha^2 = \lambda_{\text{eff}}/\lambda$ for the corresponding λ, which is given in the legends. The legends also refer to the right-hand side figures. Moreover, for a fixed temperature and λ_{eff}, the dc conductivity is different for the two choices of λ and α. We conclude that, in the presence of V in the action, λ and α are two independent parameters associated with the translational symmetry breaking.

The lines correspond to a fixed $\lambda_{\text{eff}} \equiv \lambda\alpha^2$ but different λ and α, defined in Eq. (3.33). Most notably, the function c at the horizon shows a difference of about 20%, while the blackening factor is very similar throughout the bulk. Fig.C.1 shows that the model defined in Eqs.(3.10) and (3.30) contains three independent parameters, κ, α and λ.

D | Disorder in Eintein-Maxwell backgrounds

D.1 Conductivity at finite temperature

Consider the Einstein-Maxwell system at finite temperature with an inhomogeneous chemical potential in both boundary directions. We work in coordinates such that the horizon is at $\bar{r}=1$ and the boundary at $\bar{r}=0$. To zeroth order in perturbation theory, Einstein's Equations fix the usual Schwarzschild blackening factor. Looking for solutions of the type

$$\begin{aligned} ds^2 &= \frac{r_0^2}{\bar{r}^2}\left[-f(\bar{r})(1+\bar{V}^2\alpha(\bar{r},\mathbf{x}))\mathrm{d}t^2+\frac{r_0^2\mathrm{d}\bar{r}^2}{f(\bar{r})}+(1+\bar{V}^2\beta(\bar{r},\mathbf{x}))(\mathrm{d}x^2+\mathrm{d}y^2)\right], \\ A &= \bar{V}\varphi(\bar{r},\mathbf{x})\mathrm{d}t. \end{aligned}$$

The second order equations read:

$$2\bar{r}f\partial_{\bar{r}}^2\alpha+2\bar{r}r_0^2\nabla^2\alpha+(3\bar{r}f'-6f)\partial_{\bar{r}}\alpha+2(\bar{r}f'-4f)\partial_{\bar{r}}\beta=-\bar{r}^3r_0^2f^{-1}\left[f(\partial_{\bar{r}}\varphi)^2+r_0^2(\nabla\varphi)^2\right], \tag{tt}$$

$$2\bar{r}f\partial_{\bar{r}}^2\alpha+4\bar{r}f\partial_{\bar{r}}^2\beta+(3\bar{r}f'-2f)\partial_{\bar{r}}\alpha+2(\bar{r}f'-2f)\partial_{\bar{r}}\beta=\bar{r}^3r_0^2f^{-1}\left[(f\partial_{\bar{r}}\varphi)^2-r_0^2(\nabla\varphi)^2\right], \tag{$\bar{r}\bar{r}$}$$

$$f'\partial_x\alpha+2f\partial_x\partial_{\bar{r}}(\alpha+\beta)=-\frac{1}{2}\bar{r}^2r_0^2f^{-1}\partial_x\varphi\partial_{\bar{r}}\varphi, \tag{$\bar{r}x$}$$

$$2\bar{r}f\partial_{\bar{r}}^2\beta+2\bar{r}r_0^2\nabla^2\beta+2r_0^2\partial_x^2\alpha-2f\partial_{\bar{r}}\alpha+2(\bar{r}f'-4f)\partial_{\bar{r}}\beta=\bar{r}^3r_0^2f^{-1}\left[f(\partial_{\bar{r}}\varphi)^2-r_0^2\left((\partial_x\varphi)^2-(\partial_y\varphi)^2\right)\right] \tag{xx}$$

$$f'\partial_y\alpha+2f\partial_y\partial_{\bar{r}}(\alpha+\beta)=-\frac{1}{2}\bar{r}^2r_0^2f^{-1}\partial_y\varphi\partial_{\bar{r}}\varphi, \tag{$\bar{r}y$}$$

$$f\partial_y\partial_x\alpha=\bar{r}^2r_0^2\partial_x\varphi\partial_y\varphi, \tag{xy}$$

$$2\bar{r}f\partial_{\bar{r}}^2\beta+2\bar{r}r_0^2\nabla^2\beta+2\bar{r}r_0^2\partial_y^2\alpha-2f\partial_{\bar{r}}\alpha+2(\bar{r}f'-4f)\partial_{\bar{r}}\beta=\bar{r}^3r_0^2f^{-1}\left[f(\partial_{\bar{r}}\varphi)^2+r_0^2\left((\partial_x\varphi)^2-(\partial_y\varphi)^2\right)\right] \tag{yy}$$

where we introduced $\nabla = (\partial_x, \partial_y)$. It is convenient to look at the following linear combinations,

$$4f^{1/2}\partial_{\bar{r}}\left(\bar{r}^{-2}f^{1/2}\partial_{\bar{r}}\beta\right) + 2\bar{r}^{-2}\nabla^2\beta = -r_0^2 f^{-1}\left[f(\partial_{\bar{r}}^2\varphi)^2 + r_0^2(\nabla\varphi)^2\right], \tag{D.1}$$

$$(3+f)^2 f^{-1/2}\partial_{\bar{r}}\left(\frac{f^{3/2}}{\bar{r}^2(3+f)}\partial_{\bar{r}}\alpha\right) + 2\bar{r}^{-2}r_0^2 f\nabla^2\alpha + \bar{r}^{-2}r_0^2(f-3)\nabla^2\beta = r_0^2 f^{-1}\,\mathbb{E}[3f(\partial_{\bar{r}}\varphi)^2 + r_0^2(\nabla\varphi)^2], \tag{D.2}$$

where we took $-tt + \bar{r}\bar{r} + xx + yy$ and $3/2(f+1) + 1/2(f-3)(\bar{r}\bar{r} - xx - yy)$ respectively. Note in particular that these equations reduce to (4.20a) and (4.20b) over averaging. The source can be expanded in the spectral basis as

$$\varphi(\bar{r}, \mathbf{x}) = \sum_{\mathbf{k}} \varphi_{\mathbf{k}}(\bar{r}) \prod_{i\in\{x,y\}} \cos\left(\theta_{\mathbf{i},\mathbf{k}}\right),$$

where $\mathbf{k} = (k_x, k_y) = (n_x, n_y)k_0/N$ with $n_x, n_y \in \{1, 2, \ldots, N-1\}$ and $\theta_{i,k_i} = k_i x^i + \gamma_i$ for $\gamma_i \in [0, 2\pi)$ i.i.d. uniformly distributed random variables. We have opted for a discrete representation here for clarity, but this should not change the result. Recall that $\varphi_{\mathbf{k}}(\bar{r})$ can be obtained from Maxwell's Equations (4.19), but an explicit solution is not needed for our purposes.

Further, we can write

$$\begin{aligned}
(\partial_{\bar{r}}\varphi)^2 &= \left(\sum_{\mathbf{k}} \varphi'_{\mathbf{k}} \prod_i \cos\theta_{i,\mathbf{k}}\right)\left(\sum_{\mathbf{l}} \varphi'_{\mathbf{l}} \prod_i \cos\theta_{i,\mathbf{l}}\right) = \sum_{\mathbf{k},\mathbf{l}} \varphi'_{\mathbf{k}}\varphi'_{\mathbf{l}} \prod_i \cos\theta_{i,\mathbf{k}}\cos\theta_{i,\mathbf{l}} \\
&= \frac{1}{2}\sum_{\mathbf{k},\mathbf{l}} \varphi'_{\mathbf{k}}\varphi'_{\mathbf{l}} \prod_i \left(\cos\theta^-_{i,\mathbf{k},\mathbf{l}} + \cos\theta^+_{i,\mathbf{k},\mathbf{l}}\right) \\
&= \frac{1}{2}\sum_{\mathbf{k}} (\varphi'_{\mathbf{k}})^2 \prod_i (1 + \cos 2\theta_{i,\mathbf{k}}) + \frac{1}{2}\sum_{\mathbf{k}\neq\mathbf{l}} \varphi'_{\mathbf{k}}\varphi'_{\mathbf{l}} \prod_i \left(\cos\theta^-_{i,\mathbf{k},\mathbf{l}} + \cos\theta^+_{i,\mathbf{k},\mathbf{l}}\right), \\
(\nabla\varphi)^2 &= \frac{1}{2}\sum_{\mathbf{k},\mathbf{l}} (\mathbf{k}\cdot\mathbf{l})\varphi_{\mathbf{k}}\varphi_{\mathbf{l}} \prod_i \left(\cos\theta^-_{i,\mathbf{k},\mathbf{l}} - \cos\theta^+_{i,\mathbf{k},\mathbf{l}}\right) \\
&= \frac{1}{2}\sum_{\mathbf{k}} k^2(\varphi_{\mathbf{k}})^2 \prod_i (1 - \cos 2\theta_{i,\mathbf{k}}) + \frac{1}{2}\sum_{\mathbf{k}\neq\mathbf{l}} (\mathbf{k}\cdot\mathbf{l})\varphi_{\mathbf{k}}\varphi_{\mathbf{l}} \prod_i \left(\cos\theta^-_{i,\mathbf{k},\mathbf{l}} - \cos\theta^+_{i,\mathbf{k},\mathbf{l}}\right),
\end{aligned}$$

where we have defined $\theta^{\pm}_{i,k_i,l_i} = \theta_{i,k_i} \pm \theta_{i,l_i}$. This determines the spectral decomposition of the metric coefficients in terms of the sources. For example, we can write $\alpha(\bar{r}, \mathbf{x}) =$

$\alpha_{\text{hom}}(\bar{r}) + \alpha_{\text{inh}}(\bar{r}, \mathbf{x})$ with

$$\alpha_{\text{inh}}(\bar{r}, \mathbf{x}) = \sum_{\mathbf{k}} \alpha^0_{\mathbf{k}}(\bar{r}) \prod_i \cos 2\theta_{i,\mathbf{k}} + \sum_{\mathbf{k}\neq\mathbf{l}} \alpha^+_{\mathbf{k},\mathbf{l}}(\bar{r}) \prod_i \cos \theta^+_{i,\mathbf{k},\mathbf{l}} + \sum_{\mathbf{k}\neq\mathbf{l}} \alpha^-_{\mathbf{k},\mathbf{l}}(\bar{r}) \prod_i \cos \theta^-_{i,\mathbf{k},\mathbf{l}}, \tag{D.3}$$

with a similar expression for β. By linearity, the task of solving equations (D.1) now reduces to solving coupled ODEs for $\alpha_{\text{hom}}, \beta_{\text{hom}}$, α^0, β^0 and $\alpha^\pm, \beta^\pm$. This is in principle doable but cumbersome, and does not bring any insight. Examples of explicit solutions for zero and finite temperature backgrounds in a similar context were given in references [33, 92, 94]. However for the purposes of applying the formula (4.21) we do not need the full solution.

By linearity of the mean, we just need to compute terms like $\mathbb{E}[\cos\theta_k]$,$\mathbb{E}[\cos 2\theta_n \cos\theta_k]$ and $\mathbb{E}[\cos\theta^\pm_{nm}\cos\theta_k]$ for $n \neq m$. The first is trivially zero since it is the integral of one cosine over a full period. To compute the other terms, we use the angle sum rule $\cos\theta^\pm_{nm} = \cos\theta_n\cos\theta_m \mp \sin\theta_n \sin\theta_m$. In order to have a nonzero integral we need all cosines and sines to group into a single power, since any single cosine vanishes when integrated over. For the second term, this will only happen when $k = n$, but in this case the integrals are over $\cos^3\theta$ and $\sin^2\theta\cos\theta$ which vanish on a period. In the third term, there will be always a cosine or sine left over since $n \neq m$. Thus $\mathbb{E}[\cos\alpha_k] = \mathbb{E}[\cos 2\theta_n\cos\theta_k] = \mathbb{E}[\cos\theta^\pm_{nm}\cos\theta_k] = 0$ generically. The result quoted in section 4.4.4 follows.

E | Auxiliary material for the SYK model

E.1 Specific heat from low-frequencies

In this appendix we illustrate how the zero temperature entropy density and specific heat coefficients from the $q = 2$ model, calculated exactly in Section 6.2.1 can alternatively computed only from the infra-red information. At low

The retarded Green's function is obtained by analytically continuing $\omega_n \to \epsilon + i0^+$ in Eq.(6.12),

$$G^R(\epsilon) = \frac{-\epsilon + i\sqrt{4J^2 - \epsilon^2}}{2J^2}, \qquad \epsilon \in \mathbb{R}, \tag{E.1}$$

and the exact spectral density $\rho(\epsilon) = 2\text{Im}G^R = \sqrt{4 - (\epsilon/J)^2}\mathbb{I}_{[-2J,2J]}$ is given by the celebrated Wigner semi-circle law. At low-frequencies $\epsilon/J \ll 1$, the retarded Green's function is given by

$$G^R(\epsilon) = -\frac{\epsilon}{2J^2} + \frac{i}{2J}\left[1 - \frac{1}{8}\left(\frac{\epsilon}{J}\right)^2 - \frac{1}{128}\left(\frac{\epsilon}{J}\right)^4 + O(\epsilon^{-6})\right] \tag{E.2}$$

Note that computing the spectral density from only this infra-red expansion we completely miss the fact ρ is compactly supported, which is related to the fact that for $|\epsilon| > 2J$ the retarded propagator G^R becomes real. Of course this should be expected, since the tails of the spectral density are related to the high-frequency behaviour. Note that a naive extrapolation of this result to the region $\epsilon/J \gg 1$ gives an ultra-violet divergence, illustrated in Fig. E.1. As a consequence, this UV divergence prevent us from computing the integral in Eq.(6.16) which runs over frequencies in the whole real line. However, if we are only interested in infra-red quantities, we can remediate this divergence by introducing a sharp UV cutoff λ, which we consistently fix using the non-perturbative constraints that the spectral should density satisfy:

- $\int \frac{\mathrm{d}\epsilon}{2\pi}\rho(\epsilon) = 1$ (Conservation of spectral weight),
- $\rho(\epsilon) \geq 0$ (Positivity).

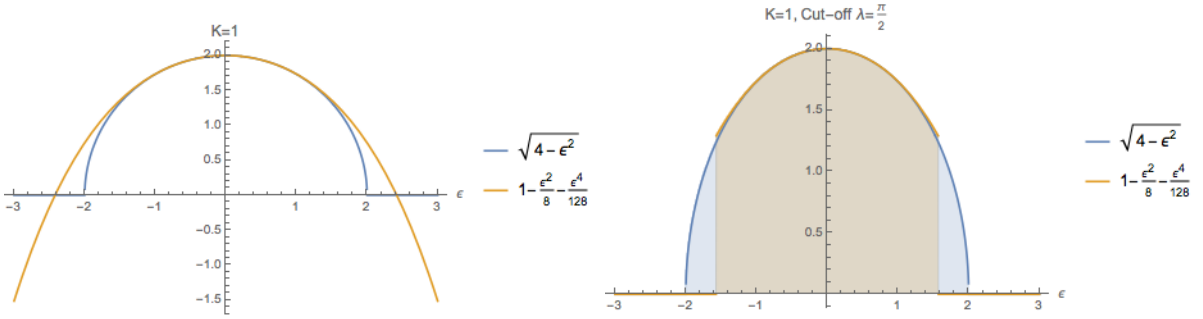

Figure E.1: Exact semi-circle law against low-frequency expansion for $J = 1$, with and without cut-off.

Since the decay of the true ρ need to be such that this sum rule is satisfied, saturation of spectral weight at a given interval indicates that the low frequency approximation starts to break down at outside the interval. Let $\lambda > 0$ and consider the integral,

$$\int_{-\lambda}^{\lambda} \frac{\mathrm{d}\epsilon}{2\pi}\rho(\epsilon) = \lambda\left(\frac{2}{\pi} - \frac{\lambda^2}{12\pi} + O(\lambda^4)\right) \leq \frac{2\lambda}{\pi} \tag{E.3}$$

Note that we without loss of generality we can consider the symmetric interval $(-\lambda, \lambda)$ since ρ is an even function. Since higher order terms only improve our estimate, a conservative choice is to take $\lambda = \frac{\pi K}{2}$. This ensures that the sum rule is satisfied to leading order. Moreover, note that for $|\epsilon| < \lambda$ we have $\rho(\epsilon) > 0$, so positivity is also satisfied.

We can now take

$$\arg G^R(\epsilon) = \begin{cases} \frac{\pi}{2} - \tan^{-1}\left(\frac{-\epsilon/2K}{1-\frac{1}{8}(\epsilon/K)^2-\frac{1}{128}(\epsilon/K)^4+\ldots}\right) & \text{for } |\epsilon| < \lambda, \\ \pi & \text{if } \epsilon \geq \lambda, \\ 0 & \text{if } \epsilon \leq \lambda. \end{cases} \tag{E.4}$$

Following the same steps of Section 6.2.1, for $\epsilon \geq \lambda$ the integral over the constant π factor contributes with the exponentially decaying term $\log\left(1 + e^{-\beta K}\right)$ which does not contribute to the low temperature expansion. This last is completely determined by the integral over $|\epsilon| < \lambda$. This last is composed from two pieces. The first is

$$\frac{\beta}{2}\int_{-\lambda}^{\lambda} \frac{\mathrm{d}\epsilon}{1+e^{\beta\epsilon}} = \frac{\beta\lambda}{2} = \frac{\pi}{4}\beta J \tag{E.5}$$

which is a cutoff dependent contribution to the ground state energy. Note that, as we discussed before, naively taking $\lambda \to \infty$ would lead to divergences here. The second integral

is given by

$$-\beta J\int_{-\lambda}^{\lambda}\frac{\mathrm{d}\epsilon}{\pi}\frac{\tan^{-1}\left(\frac{-\epsilon/2}{1-\frac{\epsilon^2}{8}-\frac{\epsilon^4}{128}+\ldots}\right)}{1+e^{\beta J\epsilon}}\approx \tag{E.6}$$

$$\begin{aligned}
&-\beta J\int_{-\lambda}^{\lambda}\frac{\mathrm{d}\epsilon}{\pi}\tan^{-1}\left(\frac{-\epsilon/2}{1-\frac{\epsilon^2}{8}-\frac{\epsilon^4}{128}+\ldots}\right)\left[\theta(-\epsilon)-\frac{\pi^2}{6}\frac{\delta'(\epsilon)}{(\beta J)^2}+O(\beta J^{-4})\right]\\
&=\beta J\int_{-\lambda}^{0}\frac{\mathrm{d}\epsilon}{\pi}\tan^{-1}\left(\frac{-\epsilon/2}{1-\frac{\epsilon^2}{8}-\frac{\epsilon^4}{128}+\ldots}\right)+\frac{\pi^2}{12\beta J}+O(\beta K^{-3})\\
&=0.208\beta J+\frac{\pi^2}{12\beta J}+O(\beta J^{-3})
\end{aligned} \tag{E.7}$$

To this we have to add the factor $\frac{\pi}{4}\beta J$ coming from the first integral. Putting together, we have $E_0 = -0.993\ KN$, $s_0 = 0$ and $c = \frac{\pi}{6}\frac{N}{J}$. As expected, we miss contributions to the ground state energy, but it is easy to check that considering higher order terms in the ϵ/J expansion improve this result. In the other hand the specific heat comes entirely from the derivative of the phase factor (and therefore from the first order term in the $\epsilon \ll J$ expansion), and the result from the expansion is exact.

Below we plot a comparison the the free energy density $F(\beta)/N$ as computed via the exact integral Eq.(6.18) against the one obtained via the approximation Eq.(E.4), up to order $(\epsilon/J)^2$ and order $(\epsilon/J)^4$ for $J = 1$. On the left, we plot $-\beta^2(f(\beta) - E_0)$ which, for $\beta \gg 1$ should go to $c/2 = \pi/12$. We have good agreement in both cases.

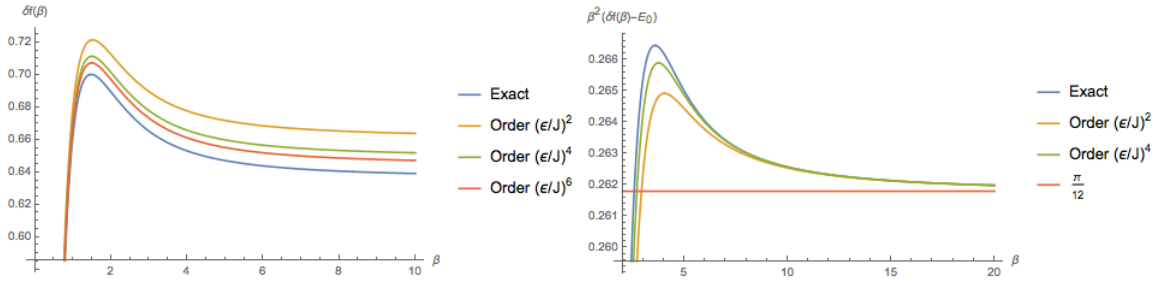

Figure E.2: Comparison between exact contribution to the free energy density from Eq.(6.18) and the approximated one, from Eq.(E.4), for $J = 1$.

E.2 Regularisation of the conformal free energy

In this appendix we discuss the regularisation of the Tr log term for the conformal propagator. The trace is written as a sum over Matsubara frequencies,

$$\mathrm{Tr}\log G = \beta\sum_{n\in\mathbb{Z}}\log G(i\omega_n)e^{i\omega_n 0^+}. \tag{E.8}$$

In the conformal limit, the Matsubara propagator is divergent in the UV. Therefore, the first step in computing this sum consists of adding and subtracting an also UV divergent free fermion propagator $G_0(i\omega_n) = (i\omega_n)^{-1}$. One of the terms can be regularised by using zeta function regularisation,

$$\mathrm{Tr}\log G_0 = -\beta \sum_{n\in\mathbb{Z}} \log i\omega_n = -\log 2$$

therefore the regularised Tr log term reads,

$$\mathrm{Tr}\log G = -\frac{1}{\beta}\log 2 + \beta \sum_{n\in\mathbb{Z}} \left(\log G(i\omega_n) - \log G_0\right) e^{i\omega_n 0^+}.$$

Next, we follow almost exactly the same steps as in the discussion of the $q = 2$ case in Eq.(6.16) to rewrite the remaining sum in the real axis,

$$\mathrm{Tr}\log G = -\log 2 + \beta \int_{\mathbb{R}} \frac{\mathrm{d}\epsilon}{\pi} \left(\mathrm{Arg}G^R(\epsilon) - \mathrm{Arg}G_0^R(\epsilon)\right) n(\beta\epsilon) \tag{E.9}$$

where we have defined $n(\beta\epsilon) = (1 + e^{\beta\epsilon})^{-1}$. Note that since $G_0^R = (\epsilon - i0^+)^{-1}$, we have $\mathrm{Arg}G_0^R = \pi\left(\theta(\epsilon) - \frac{1}{2}\right)$, and the integral for the free propagator is simply given by

$$\beta \int_{\mathbb{R}} \mathrm{d}\epsilon \left(\theta(\epsilon) - \frac{1}{2}\right) n(\beta\epsilon) = \log 2 - \frac{\beta}{2}\int_{\mathbb{R}} \mathrm{d}\epsilon\, n(\beta\epsilon). \tag{E.10}$$

Therefore, we rewrite Eq.(E.9) as

$$\mathrm{Tr}\log G = \beta \int_{\mathbb{R}} \frac{\mathrm{d}\epsilon}{\pi} \left(\mathrm{Arg}G^R(\epsilon) - \frac{\pi}{2}\right) n(\beta\epsilon). \tag{E.11}$$

Noting that $n(-\beta\epsilon) = 1 - n(\beta\epsilon)$, we can further rewrite the above as

$$\mathrm{Tr}\log G = \frac{\beta}{2\pi}\int_{-\infty}^{0} \mathrm{d}\epsilon \left[\mathrm{Arg}G^R(\epsilon) - \frac{\pi}{2}\right] + \frac{\beta}{2\pi}\int_{-\infty}^{\infty} \mathrm{d}\epsilon\, \frac{\mathrm{Arg}G^R(\epsilon)\mathrm{sgn}(\epsilon)}{e^{\beta|\epsilon|}+1} - \frac{\log 2}{2} \tag{E.12}$$

We now proceed with the evaluation of $\mathrm{Arg}G^R(\epsilon)$. In the conformal limit, the Matsubara propagator is given by

$$G_c^\beta(\theta) = b\left[\frac{1}{\beta J \sin\pi\theta}\right]^{2\Delta}, \qquad \theta = \frac{\tau}{\beta} \in (0,1). \tag{E.13}$$

and therefore in Fourier space,

$$G(i\omega_n) = 2i\frac{(2\pi)^{2\Delta-1} b^\Delta (\beta J)^{1-2\Delta}\cos(\pi\Delta)}{\Gamma(2\Delta)\sin(2\pi\Delta)}\Gamma\left(\Delta + \frac{\beta\omega_n}{2\pi}\right)\Gamma\left(\Delta - \frac{\beta\omega_n}{2\pi}\right)\sin\left(\pi\Delta - \frac{\beta\omega_n}{2}\right).$$

where $\beta\bar{\omega}_n = \pi(2n+1)$ are the usual fermionic Matsubara frequencies. We can now take an analytic continuation $i\omega_n \to \epsilon - i0^+$ to the complex plane to get

$$G^R(\epsilon) = 2i\frac{(2\pi)^{2\Delta-1}b^{\Delta}(\beta J)^{1-2\Delta}\cos(\pi\Delta)}{\Gamma(2\Delta)\sin(2\pi\Delta)}\Gamma\left(\Delta + i\frac{\beta\epsilon}{2\pi}\right)\Gamma\left(\Delta - i\frac{\beta\epsilon}{2\pi}\right)\sin\left(\pi\Delta + i\frac{\beta\epsilon}{2}\right) \tag{E.14}$$

and therefore,

$$\mathrm{Arg}G^R(\epsilon) = \frac{\pi}{2} - a(\epsilon) = \frac{\pi}{2} - \tan^{-1}\left(\cot\pi\Delta\tanh\frac{\beta\epsilon}{2}\right). \tag{E.15}$$

where $a(\epsilon)$ is defined for notational convenience. Note that all terms in Eq.(E.12) are functions of $\beta\epsilon$ only. Therefore we can write all the integrals in terms of the dimensionless frequency $\bar{\epsilon} = \beta\epsilon$. This integral should give the first terms in the expansion of the free energy density $-\beta f(\beta) = \beta E_0 + s_0 + O(\beta^{-1})$. However, it is not hard to show that the first integral in Eq.(E.12) is divergent at $\epsilon = -\infty$, which is a statement that the conformal ground state energy density E_0 is divergent. To further remove this divergence, we subtract the $f(\beta = \infty)$, which is equivalent to subtracting $a(-\infty)$ inside the integral. The remaining integral is not a function of β, and therefore contribute only to the zero temperature entropy density,

$$s_0 = \frac{1}{2\pi}\int_{-\infty}^{0} \mathrm{d}\bar{\epsilon}\ [a(\bar{\epsilon}) - a(-\infty)] + \frac{1}{2\pi}\int_{-\infty}^{\infty}\mathrm{d}\bar{\epsilon}\ \frac{a(\bar{\epsilon})\mathrm{sgn}(\bar{\epsilon})}{e^{|\bar{\epsilon}|}+1} \tag{E.16}$$

Note that since $a(-\infty) = \cot\pi\Delta$, the integral of $a(\omega) - a(-\infty)$ over $(-\infty, 0]$ is now finite, as claimed. Letting $t = \cot\pi\Delta$ and $u = \tanh\frac{\omega}{2}$ gives the result in Eq.(6.30)

E.3 Expansion of integral in Eq.(6.14)

Consider the integral,

$$I(\theta, a) = \int_{-a}^{a}\frac{\mathrm{d}\lambda}{\pi}\frac{e^{-x\theta}}{1+e^{-x}}\sqrt{1-\left(\frac{x}{a}\right)^2} = \int_{-\infty}^{\infty}\frac{\mathrm{d}\lambda}{\pi}\frac{e^{-x\theta}}{1+e^{-x}}\sqrt{1-\left(\frac{x}{a}\right)^2}\mathbb{I}_{(-2,2)}(x), \quad \theta\in[0,1). \tag{E.17}$$

which is related to Eq.(E.3) by $\mathcal{G}(\theta) = (\beta J)^{-1}I(\theta, \beta K)$ and $\mathbb{I}(-2,2)(x) = 1$ for $x \in (-a, a)$ and 0 otherwise. The question we want to answer is

$$\lim_{a\to\infty}\int_{-\infty}^{\infty}\frac{\mathrm{d}\lambda}{\pi}\frac{e^{-x\theta}}{1+e^{-x}}\sqrt{1-\left(\frac{x}{a}\right)^2}\mathbb{I}_{(-a,a)}(x) \stackrel{?}{=} \int_{-\infty}^{\infty}\frac{\mathrm{d}\lambda}{\pi}\frac{e^{-x\theta}}{1+e^{-x}}\lim_{a\to\infty}\sqrt{1-\left(\frac{x}{a}\right)^2}\mathbb{I}_{(-a,a)}(x) \tag{E.18}$$

First, note that

$$0 < \sqrt{1 - \left(\frac{x}{a}\right)^2}\,\mathbb{I}_{(-a,a)}(x) \leq 1, \qquad \forall x \in (-a, a) \tag{E.19}$$

Thus,

$$\left|\int_{-\infty}^{\infty} \frac{\mathrm{d}x}{\pi} \frac{e^{-x\theta}}{1+e^{-x}} \sqrt{1 - \left(\frac{x}{a}\right)^2}\,\mathbb{I}_{(-a,a)}(x)\right| \leq \int_{-\infty}^{\infty} \frac{\mathrm{d}x}{\pi} \left|\frac{e^{-x\theta}}{1+e^{-x}} \sqrt{1 - \left(\frac{x}{a}\right)^2}\,\mathbb{I}_{(-a,a)}(x)\right| \leq \int_{-\infty}^{\infty} \frac{\mathrm{d}x}{\pi} \frac{e^{-x\theta}}{1+e^{-x}} \tag{E.20}$$

Since

$$\int_{-\infty}^{\infty} \frac{\mathrm{d}x}{\pi} \frac{e^{-x\theta}}{1+e^{-x}} = \frac{1}{\sin \pi\theta}, \qquad \theta \in (0,1) \tag{E.21}$$

By Lebesgue dominated convergence theorem we can exchange the limits for $\theta \in (0,1)$. Commutation of limits justifies the series expansion under the integral. Note however that at the boundaries $\theta = 0, 1$, the integral Eq.(E.21) diverges, and therefore dominated convergence only applies at the open interval $(0,1)$.

Bibliography

[1] J. H. Schwarz, "The second superstring revolution," arXiv:9607067 [hep-th].

[2] J. Maldacena, "The large-N limit of superconformal field theories and supergravity," *International journal of theoretical physics* **38** no. 4, (1999) 1113–1133.

[3] E. Witten, "Anti De Sitter Space And Holography," arXiv:9802150 [hep-th].

[4] S. Gubser, I. Klebanov, and A. Polyakov, "Gauge theory correlators from non-critical string theory," *Physics Letters B* **428** no. 1-2, (May, 1998) 105–114.

[5] O. Aharony, S. S. Gubser, J. Maldacena, H. Ooguri, and Y. Oz, "Large N field theories, string theory and gravity," *Physics Reports* **323** no. 3-4, (Jan., 2000) 183–386.

[6] G. Policastro, D. T. Son, and A. O. Starinets, "Shear Viscosity of Strongly Coupled N=4 Supersymmetric Yang-Mills Plasma," *Physical Review Letters* **87** no. 8, (Aug., 2001) 081601.

[7] **STAR** Collaboration, J. Adams *et al.*, "Experimental and theoretical challenges in the search for the quark-gluon plasma: The star collaboration's critical assessment of the evidence from rhic collisions," *Nuclear Physics A* **757** no. 1, (2005) 102 – 183.

[8] G. Policastro, D. T. Son, and A. O. Starinets, "From AdS/CFT correspondence to hydrodynamics," *Journal of High Energy Physics* **2002** no. 09, (Sept., 2002) 043–043.

[9] S. Cremonini, "The Shear Viscosity to Entropy Ratio: a status report," *Modern Physics Letters B* **25** no. 23, (Sep, 2011) 1867–1888.

[10] P. Kovtun, D. T. Son, and A. O. Starinets, "Holography and hydrodynamics: diffusion on stretched horizons," *Journal of High Energy Physics* no. 10, (Oct, 2003) 064–064.

[11] P. Kovtun, D. Son, and A. Starinets, "Viscosity in Strongly Interacting Quantum Field Theories from Black Hole Physics," *Physical Review Letters* **94** no. 11, (Mar., 2005) 111601.

[12] J. D. Edelstein, J. P. Shock, and D. Zoakos, "The ads/cft correspondence and nonâĂŘperturbative qcd," *AIP Conference Proceedings* **1116** no. 1, (2009) 265–284.

[13] L. P. Kadanoff, "Scaling laws for ising models near T_c," *Physics Physique Fizika* **2** (Jun, 1966) 263–272. https://link.aps.org/doi/10.1103/PhysicsPhysiqueFizika.2.263.

[14] K. G. Wilson, "Renormalization group and critical phenomena. i. renormalization group and the kadanoff scaling picture," *Phys. Rev. B* **4** (Nov, 1971) 3174–3183. https://link.aps.org/doi/10.1103/PhysRevB.4.3174.

[15] L. P. Kadanoff, "Scaling and universality in statistical physics," *Physica A: Statistical Mechanics and its Applications* **163** no. 1, (1990) 1 – 14.

[16] J. Cardy, *Scaling and Renormalization in Statistical Physics*. Cambridge Lecture Notes in Physics. Cambridge University Press, 1996.

[17] J. Cardy, "Conformal field theory and statistical mechanics," 0807.3472 [cond-mat.stat-mech].

[18] S. A. Hartnoll, P. K. Kovtun, M. Müller, and S. Sachdev, "Theory of the Nernst effect near quantum phase transitions in condensed matter and in dyonic black holes," *Physical Review B* **76** no. 14, (Oct, 2007) 144502.

[19] A. Karch and A. O'Bannon, "Metallic AdS/CFT," *Journal of High Energy Physics* **2007** no. 09, (Sept., 2007) 024–024.

[20] D. T. Son, "Toward an ads/cold atoms correspondence: A geometric realization of the schrödinger symmetry," *Phys. Rev. D* **78** (Aug, 2008) 046003.

[21] A. Adams, K. Balasubramanian, and J. McGreevy, "Hot spacetimes for cold atoms," *Journal of High Energy Physics* **2008** no. 11, (2008) 059.

[22] S. A. Hartnoll and C. P. Herzog, "Impure AdS/CFT correspondence," *Physical Review D* **77** no. 10, (May, 2008) 106009.

[23] S. A. Hartnoll, C. P. Herzog, and G. T. Horowitz, "Holographic superconductors," *Journal of High Energy Physics* **2008** no. 12, (Dec., 2008) 015–015.

[24] J. Maldacena, D. Martelli, and Y. Tachikawa, "Comments on string theory backgrounds with non-relativistic conformal symmetry," *Journal of High Energy Physics* **2008** no. 10, (2008) 072.

[25] S. A. Hartnoll and K. Yoshida, "Families of IIB duals for nonrelativistic CFTs," *Journal of High Energy Physics* **2008** no. 12, (2008) 071.

[26] C. P. Herzog, M. Rangamani, and S. F. Ross, "Heating up galilean holography," *Journal of High Energy Physics* **2008** no. 11, (2008) 080.

[27] S. S. Gubser, "Breaking an Abelian gauge symmetry near a black hole horizon," *Physical Review D* **78** no. 6, (Sept., 2008) 065034.

[28] S. A. Hartnoll, C. P. Herzog, and G. T. Horowitz, "Building a Holographic Superconductor," *Physical Review Letters* **101** no. 3, (July, 2008) 031601.

[29] S. S. Gubser, C. P. Herzog, S. S. Pufu, and T. Tesileanu, "Superconductors from superstrings," *Phys. Rev. Lett.* **103** (Sep, 2009) 141601.

[30] S. Gubser and F. Rocha, "Gravity Dual to a Quantum Critical Point with Spontaneous Symmetry Breaking," *Physical Review Letters* **102** no. 6, (Feb., 2009) 061601.

[31] G. Parisi, *Field Theory, Disorder and Simulations*. World Scientific Publishing Co., Inc., River Edge, NJ, USA, 1993.

[32] P. A. Lee, "Disordered electronic systems," *Reviews of Modern Physics* **57** no. 2, (Apr., 1985) 287–337.

[33] S. A. Hartnoll and J. E. Santos, "Disordered Horizons: Holography of Randomly Disordered Fixed Points," *Physical Review Letters* **112** no. 23, (June, 2014) 231601.

[34] A. Altland and B. Simons, *Condensed Matter Field Theory*. Cambridge University Press, 2nd edition ed., March, 2010.

[35] P. W. Anderson, "Absence of diffusion in certain random lattices," *Physical Review* **109** (1958) 1492–1505.

[36] J. T. Edwards and D. J. Thouless, "Numerical studies of localization in disordered systems," *Journal of Physics C: Solid State Physics* **5** no. 8, (1972) 807.

[37] R. Abou-Chacra, D. J. Thouless, and P. W. Anderson, "A selfconsistent theory of localization," *Journal of Physics C: Solid State Physics* **6** no. 10, (May, 1973) 1734.

[38] E. Abrahams, P. W. Anderson, D. C. Licciardello, and T. V. Ramakrishnan, "Scaling Theory of Localization: Absence of Quantum Diffusion in Two Dimensions," *Physical Review Letters* **42** no. 10, (Mar., 1979) 673–676.

[39] D. Vollhardt and P. Wolfle, "Anderson localization in $d \leq 2$ dimensions: A self-consistent diagrammatic theory," *Phys. Rev. Lett.* **45** (Sep, 1980) 842–846.

[40] F. Scheffold, R. Lenke, R. Tweer, and G. Maret, "Localization or classical diffusion of light?," *Nature* **398** (03, 1999) 206.

[41] M. Störzer, P. Gross, C. M. Aegerter, and G. Maret, "Observation of the critical regime near anderson localization of light," *Phys. Rev. Lett.* **96** (Feb, 2006) 063904.

[42] T. Schwartz, G. Bartal, S. Fishman, and M. Segev, "Transport and anderson localization in disordered two-dimensional photonic lattices," *Nature* **446** no. 7131, (03, 2007) 52–55.

[43] M. Segev, Y. Silberberg, and D. N. Christodoulides, "Anderson localization of light," *Nature Photonics* **7** no. 3, (Mar, 2013) 197–204.

[44] R. Weaver, "Anderson localization of ultrasound," *Wave Motion* **12** no. 2, (1990) 129 – 142.

[45] J. Billy, V. Josse, Z. Zuo, A. Bernard, B. Hambrecht, P. Lugan, D. Clément, L. Sanchez-Palencia, P. Bouyer, and A. Aspect, "Direct observation of anderson localization of matter waves in a controlled disorder," *Nature* **453** (06, 2008) 891 EP –.

[46] L. Fleishman and P. W. Anderson, "Interactions and the Anderson transition," *Physical Review B* **21** no. 6, (Mar., 1980) 2366–2377.

[47] J. Rammer and A. Schmid, "Destruction of phase coherence by electron-phonon interactions in disordered conductors," *Phys. Rev. B* **34** (Jul, 1986) 1352–1355.

[48] T. V. Shahbazyan and M. E. Raikh, "Surface plasmon in a two-dimensional anderson insulator with interactions," *Phys. Rev. B* **53** (Mar, 1996) 7299–7307.

[49] D. M. Basko, I. L. Aleiner, and B. L. Altshuler, "On the problem of many-body localization," `arXiv:0602510 [cond-mat]`.

[50] D. Basko, I. Aleiner, and B. Altshuler, "Metal–insulator transition in a weakly interacting many-electron system with localized single-particle states," *Annals of Physics* **321** no. 5, (May, 2006) 1126–1205.

[51] D. A. Huse, R. Nandkishore, and V. Oganesyan, "Phenomenology of fully many-body-localized systems," *Phys. Rev. B* **90** (Nov, 2014) 174202.

[52] D. A. Abanin and Z. Papić, "Recent progress in many-body localization," *Annalen der Physik* **529** no. 7, (2017) 1700169.

[53] D. Vegh, "Holography without translational symmetry," `arXiv:1301.0537`.

[54] T. Andrade and B. Withers, "A simple holographic model of momentum relaxation," *Journal of High Energy Physics* **2014** no. 5, (May, 2014) 101.

[55] B. Goutéraux, "Charge transport in holography with momentum dissipation," *Journal of High Energy Physics* **2014** no. 4, (Apr., 2014) 181.

[56] R. A. Davison and B. Goutéraux, "Momentum dissipation and effective theories of coherent and incoherent transport," *Journal of High Energy Physics* **2015** no. 1, (Jan, 2015) 39.

[57] R. A. Davison and B. Goutéraux, "Dissecting holographic conductivities," *Journal of High Energy Physics* **2015** no. 9, (Sep, 2015) 90.

[58] A. Donos, B. Goutéraux, and E. Kiritsis, "Holographic metals and insulators with helical symmetry," *Journal of High Energy Physics* **2014** no. 9, (Sept., 2014) 38.

[59] A. Donos and J. P. Gauntlett, "The thermoelectric properties of inhomogeneous holographic lattices," *Journal of High Energy Physics* **2015** no. 1, (Jan, 2015) 35.

[60] A. Donos and J. P. Gauntlett, "Holographic Q-lattices," *Journal of High Energy Physics* **2014** no. 4, (Apr, 2014) 40.

[61] A. M. García-García and B. Loureiro, "Marginal and irrelevant disorder in einstein-maxwell backgrounds," *Phys. Rev. D* **93** (Mar, 2016) 065025.

[62] S. Ryu, T. Takayanagi, and T. Ugajin, "Holographic conductivity in disordered systems," *Journal of High Energy Physics* **2011** no. 4, (Apr, 2011) 115.

[63] M. Fujita, Y. Hikida, S. Ryu, and T. Takayanagi, "Disordered systems and the replica method in AdS/CFT," *Journal of High Energy Physics* **2008** no. 12, (Dec., 2008) 065–065.

[64] M. Blake, D. Tong, and D. Vegh, "Holographic Lattices Give the Graviton an Effective Mass," *Physical Review Letters* **112** no. 7, (Feb., 2014) 071602.

[65] M. Blake and D. Tong, "Universal resistivity from holographic massive gravity," *Phys. Rev. D* **88** (Nov, 2013) 106004.

[66] A. Donos and J. P. Gauntlett, "Holographic helical superconductors," *Journal of High Energy Physics* **2011** no. 12, (Dec., 2011) 91.

[67] A. Donos and S. A. Hartnoll, "Metal-insulator transition in holography," arXiv:1212.2998.

[68] A. Donos and J. P. Gauntlett, "Helical Superconducting Black Holes," *Physical Review Letters* **108** no. 21, (May, 2012) 211601.

[69] A. Donos and J. P. Gauntlett, "Black holes dual to helical current phases," *Physical Review D* **86** no. 6, (Sept., 2012) 064010.

[70] A. Donos and J. P. Gauntlett, "On the thermodynamics of periodic ads black branes," *Journal of High Energy Physics* **2013** no. 10, (Oct, 2013) 38.

[71] Y. Ling, P. Liu, C. Niu, J.-P. Wu, and Z.-Y. Xian, "Holographic superconductor on q-lattice," *Journal of High Energy Physics* **2015** no. 2, (Feb, 2015) 59.

[72] Y. Ling, P. Liu, and J.-P. Wu, "A novel insulator by holographic q-lattices," *Journal of High Energy Physics* **2016** no. 2, (Feb, 2016) 75.

[73] S. Kachru, A. Karch, and S. Yaida, "Holographic lattices, dimers, and glasses," *Physical Review D* **81** no. 2, (Jan., 2010) 026007.

[74] S. A. Hartnoll and D. M. Hofman, "Locally Critical Resistivities from Umklapp Scattering," *Physical Review Letters* **108** no. 24, (June, 2012) 241601.

[75] G. T. Horowitz, J. E. Santos, and D. Tong, "Optical conductivity with holographic lattices," *Journal of High Energy Physics* **2012** no. 7, (Jul, 2012) 168.

[76] G. T. Horowitz, J. E. Santos, and D. Tong, "Further evidence for lattice-induced scaling," *Journal of High Energy Physics* **2012** no. 11, (Nov, 2012) 102.

[77] P. Chesler, A. Lucas, and S. Sachdev, "Conformal field theories in a periodic potential: Results from holography and field theory," *Physical Review D* **89** no. 2, (Jan., 2014) 026005.

[78] A. El Azrak, R. Nahoum, N. Bontemps, M. Guilloux-Viry, C. Thivet, A. Perrin, S. Labdi, Z. Z. Li, and H. Raffy, "Infrared properties of $YBa_2Cu_3O_7$ and $Bi_2Sr_2Ca_{n-1}Cu_nO_{2n+4}$ thin films," *Phys. Rev. B* **49** (Apr, 1994) 9846–9856.

[79] D. van der Marel, F. Carbone, A. Kuzmenko, and E. Giannini, "Scaling properties of the optical conductivity of bi-based cuprates," *Annals of Physics* **321** no. 7, (2006) 1716 – 1729. July 2006 Special Issue.

[80] M. R. Norman and A. V. Chubukov, "High-frequency behavior of the infrared conductivity of cuprates," *Phys. Rev. B* **73** (Apr, 2006) 140501.

[81] P. Anderson, "Infrared conductivity of cuprate metals: Detailed fit using luttinger liquid theory," `cond-mat/9506140`.

[82] A. Donos and J. P. Gauntlett, "Thermoelectric DC conductivities from black hole horizons," *Journal of High Energy Physics* **2014** no. 11, (Nov., 2014) 81.

[83] A. Donos and J. P. Gauntlett, "Navier-stokes equations on black hole horizons and dc thermoelectric conductivity," *Phys. Rev. D* **92** (Dec, 2015) 121901.

[84] A. Donos, J. P. Gauntlett, T. Griffin, and L. Melgar, "Dc conductivity of magnetised holographic matter," *Journal of High Energy Physics* **2016** no. 1, (Jan, 2016) 113.

[85] E. Banks, A. Donos, and J. P. Gauntlett, "Thermoelectric dc conductivities and stokes flows on black hole horizons," *Journal of High Energy Physics* **2015** no. 10, (Oct, 2015) 103.

[86] A. Donos, J. P. Gauntlett, and V. Ziogas, "Diffusion in inhomogeneous media," *Phys. Rev. D* **96** (Dec, 2017) 125003.

[87] H. B. Zeng, "Possible anderson localization in a holographic superconductor," *Phys. Rev. D* **88** (Dec, 2013) 126004.

[88] D. Areán, A. Farahi, L. A. Pando Zayas, I. S. Landea, and A. Scardicchio, "Holographic superconductor with disorder," *Physical Review D* **89** no. 10, (May, 2014) 106003.

[89] D. Areán, A. Farahi, L. A. Pando Zayas, I. Salazar Landea, and A. Scardicchio, "Holographic p-wave superconductor with disorder," *Journal of High Energy Physics* **2015** no. 7, (Jul, 2015) 46.

[90] A. Adams and S. Yaida, "Disordered holographic systems: Functional renormalization," *Phys. Rev. D* **92** (Dec, 2015) 126008.

[91] A. Adams and S. Yaida, "Disordered holographic systems: Marginal relevance of imperfection," *Physical Review D* **90** no. 4, (Aug., 2014) 046007.

[92] S. A. Hartnoll, D. M. Ramirez, and J. E. Santos, "Emergent scale invariance of disordered horizons," *Journal of High Energy Physics* **2015** no. 9, (Sep, 2015) 160.

[93] S. Kachru, X. Liu, and M. Mulligan, "Gravity duals of Lifshitz-like fixed points," *Physical Review D* **78** no. 10, (Nov., 2008) 106005.

[94] D. K. O'Keeffe and A. W. Peet, "Perturbatively charged holographic disorder," *Phys. Rev. D* **92** (Aug, 2015) 046004.

[95] M. Araújo, D. Areán, and J. M. Lizana, "Noisy branes," *Journal of High Energy Physics* **2016** no. 7, (Jul, 2016) 91.

[96] A. Lucas, "Hydrodynamic transport in strongly coupled disordered quantum field theories," *New Journal of Physics* **17** no. 11, (2015) 113007.

[97] S. c. v. Grozdanov, A. Lucas, S. Sachdev, and K. Schalm, "Absence of disorder-driven metal-insulator transitions in simple holographic models," *Phys. Rev. Lett.* **115** (Nov, 2015) 221601.

[98] S. Grozdanov, A. Lucas, and K. Schalm, "Incoherent thermal transport from dirty black holes," *Phys. Rev. D* **93** (Mar, 2016) 061901.

[99] T. N. Ikeda, A. Lucas, and Y. Nakai, "Conductivity bounds in probe brane models," *Journal of High Energy Physics* **2016** no. 4, (Apr, 2016) 7.

[100] A. Kitaev, "A simple model of quantum holography." KITP strings seminar and Entanglement 2015 program, 12 February, 7 April and 27 May 2015, http://online.kitp.ucsb.edu/online/entangled15/.

[101] J. Maldacena, D. Stanford, and Z. Yang, "Conformal symmetry and its breaking in two-dimensional nearly anti-de sitter space," *Progress of Theoretical and Experimental Physics* **2016** no. 12, (2016) 12C104.

[102] J. Maldacena and D. Stanford, "Remarks on the Sachdev-Ye-Kitaev model," *Phys. Rev. D* **94** (Nov, 2016) 106002.

[103] J. Engelsöy, T. G. Mertens, and H. Verlinde, "An investigation of ads2 backreaction and holography," *Journal of High Energy Physics* **07** no. 7, (2016) 1–30.

[104] J. S. Cotler, G. Gur-Ari, M. Hanada, J. Polchinski, P. Saad, S. H. Shenker, D. Stanford, A. Streicher, and M. Tezuka, "Black holes and random matrices," *Journal of High Energy Physics* **05** no. 5, (2017) 118.

[105] X.-Y. Song, C.-M. Jian, and L. Balents, "A strongly correlated metal built from sachdev-ye-kitaev models," `arXiv:1705.00117`.

[106] S. Banerjee and E. Altman, "Solvable model for a dynamical quantum phase transition from fast to slow scrambling," *Phys. Rev. B* **95** (Apr, 2017) 134302.

[107] X. Chen, R. Fan, Y. Chen, H. Zhai, and P. Zhang, "Competition between chaotic and nonchaotic phases in a quadratically coupled sachdev-ye-kitaev model," *Phys. Rev. Lett.* **119** (Nov, 2017) 207603.

[108] Y. Gu, X.-L. Qi, and D. Stanford, "Local criticality, diffusion and chaos in generalized sachdev-ye-kitaev models," *Journal of High Energy Physics* **05** no. 5, (2017) 125.

[109] A. Haldar and V. B. Shenoy, "Strange half metals and mott insulators in syk models," 1703.05111.

[110] S.-K. Jian and H. Yao, "Solvable sachdev-ye-kitaev models in higher dimensions: From diffusion to many-body localization," *Phys. Rev. Lett.* **119** (Nov, 2017) 206602.

[111] A. M. García-García and M. Tezuka, "Many-body localization in a finite-range sachdev-ye-kitaev model," 1801.03204.

[112] I. Danshita, M. Hanada, and M. Tezuka, "Creating and probing the Sachdev–Ye–Kitaev model with ultracold gases: Towards experimental studies of quantum gravity," *Progress of Theoretical and Experimental Physics* **2017** no. 8, (2017) 083I01.

[113] D. I. Pikulin and M. Franz, "Black hole on a chip: Proposal for a physical realization of the sachdev-ye-kitaev model in a solid-state system," *Phys. Rev. X* **7** (Jul, 2017) 031006.

[114] A. Chew, A. Essin, and J. Alicea, "Approximating the sachdev-ye-kitaev model with majorana wires," *Phys. Rev. B* **96** (Sep, 2017) 121119.

[115] A. M. García-García, B. Loureiro, A. Romero-Bermúdez, and M. Tezuka, "Stability of chaos in a generalised sachdev-ye-kitaev model," 1707.02197.

[116] J. Maldacena, "The large-N limit of superconformal field theories and supergravity," *International Journal of Theoretical Physics* **38** no. 4, (Apr, 1999) 1113–1133.

[117] C. V. Johnson, "D-Brane Primer," arXiv:0007170 [hep-th].

[118] J. Polchinski, "TASI Lectures on D-Branes," arXiv:9611050 [hep-th].

[119] I. R. Klebanov, "TASI Lectures: Introduction to the AdS/CFT Correspondence," arXiv:0009139 [hep-th].

[120] J. L. Petersen, "Introduction to the Maldacena Conjecture on AdS/CFT," *International Journal of Modern Physics A* **14** no. 23, (Sept., 1999) 3597–3672.

[121] A. V. Ramallo, "Introduction to the AdS/CFT correspondence," arXiv:1310.4319 [hep-th].

[122] G. Hooft, "A planar diagram theory for strong interactions," *Nuclear Physics B* **72** no. 3, (1974) 461 – 473.

[123] A. Strominger and C. Vafa, "Microscopic origin of the bekenstein-hawking entropy," *Physics Letters B* **379** no. 1, (1996) 99 – 104.

[124] G. T. Horowitz and A. Strominger, "Counting states of near-extremal black holes," *Phys. Rev. Lett.* **77** (Sep, 1996) 2368–2371.

[125] L. Susskind, "The world as a hologram," *Journal of Mathematical Physics* **36** no. 11, (Sept., 1995) 6377.

[126] E. Witten, "Anti-de sitter space, thermal phase transition, and confinement in gauge theories," `arXiv:9803131 [hep-th]`.

[127] J. P. Gauntlett, J. Sonner, and T. Wiseman, "Holographic superconductivity in m theory," *Phys. Rev. Lett.* **103** (Oct, 2009) 151601.

[128] C. Fefferman and C. R. Graham, "Conformal Invariants," *Élie Cartan et les Mathématiques d'aujourd'hui* (1985) 95.

[129] S. Ferrara and C. Fronsdal, "Conformal Maxwell theory as a singleton field theory on AdS , IIB 3-branes and duality," *Classical and Quantum Gravity* **15** no. 8, (Aug., 1998) 2153–2164.

[130] M. E. Peskin and D. V. Schroeder, *An Introduction to quantum field theory*. Addison-Wesley, Reading, USA, 1995.

[131] K. Skenderis, "Lecture notes on holographic renormalization," *Classical and Quantum Gravity* **19** no. 22, (2002) 5849.

[132] M. Bianchi, D. Z. Freedman, and K. Skenderis, "Holographic renormalization," *Nuclear Physics B* **631** no. 1, (2002) 159 – 194.

[133] G. W. Gibbons and S. W. Hawking, "Cosmological event horizons, thermodynamics, and particle creation," *Physical Review D* **15** no. 10, (May, 1977) 2738–2751.

[134] D. T. Son and A. O. Starinets, "Minkowski-space correlators in AdS/CFT correspondence: recipe and applications," *Journal of High Energy Physics* **2002** no. 09, (Sept., 2002) 042–042.

[135] C. P. Herzog and D. T. Son, "Schwinger-Keldysh propagators from AdS/CFT correspondence," *Journal of High Energy Physics* **2003** no. 03, (Mar., 2003) 046–046.

[136] N. Iqbal and H. Liu, "Universality of the hydrodynamic limit in AdS/CFT and the membrane paradigm," *Physical Review D* **79** no. 2, (Jan., 2009) 025023.

[137] T. Faulkner, H. Liu, J. McGreevy, and D. Vegh, "Emergent quantum criticality, Fermi surfaces, and AdS_2," *Physical Review D* **83** no. 12, (June, 2011) 125002.

[138] H. Liu, J. McGreevy, and D. Vegh, "Non-Fermi liquids from holography," *Physical Review D* **83** no. 6, (Mar., 2011) 065029.

[139] A. Strominger, "AdS_2 quantum gravity and string theory," *Journal of High Energy Physics* **1999** no. 01, (1999) 007.

[140] J. Maldacena, J. Michelson, and A. Strominger, "Anti-de sitter fragmentation," *Journal of High Energy Physics* **1999** no. 02, (1999) 011.

[141] J. Michelson and A. Strominger, "The Geometry of (Super) Conformal Quantum Mechanics," *Communications in Mathematical Physics* **213** no. 1, (Sep, 2000) 1–17.

[142] J. A. de Azcárraga, J. M. Izquierdo, J. C. Pérez Bueno, and P. K. Townsend, "Superconformal mechanics, black holes, and nonlinear realizations," *Phys. Rev. D* **59** (Mar, 1999) 084015.

[143] G. Gibbons and P. Townsend, "Black holes and calogero models," *Physics Letters B* **454** no. 3, (1999) 187 – 192.

[144] P. Claus, M. Derix, R. Kallosh, J. Kumar, P. K. Townsend, and A. Van Proeyen, "Black holes and superconformal mechanics," *Phys. Rev. Lett.* **81** (Nov, 1998) 4553–4556.

[145] J. Michelson and A. Strominger, "Superconformal multi-black hole quantum mechanics," *Journal of High Energy Physics* **1999** no. 09, (1999) 005.

[146] S. Bellucci, A. Galajinsky, E. Ivanov, and S. Krivonos, "Ads2/cft1, canonical transformations and superconformal mechanics," *Physics Letters B* **555** no. 1, (2003) 99 – 106.

[147] S. A. Hartnoll, "Lectures on holographic methods for condensed matter physics," *Classical and Quantum Gravity* **26** no. 22, (Nov., 2009) 224002.

[148] R. A. Davison, B. Goutéraux, and S. A. Hartnoll, "Incoherent transport in clean quantum critical metals," *Journal of High Energy Physics* **2015** no. 10, (Oct, 2015) 112.

[149] K.-Y. Kim, K. K. Kim, Y. Seo, and S.-J. Sin, "Coherent/incoherent metal transition in a holographic model," *Journal of High Energy Physics* **2014** no. 12, (Dec, 2014) 170.

[150] M. Blake, "Momentum relaxation from the fluid/gravity correspondence," *Journal of High Energy Physics* **2015** no. 9, (Sep, 2015) 10.

[151] S. A. Hartnoll, "Theory of universal incoherent metallic transport," *Nature Physics* **11** (Dec, 2014) 54–61.

[152] A. M. García-García, B. Loureiro, and A. Romero-Bermúdez, "Transport in a gravity dual with a varying gravitational coupling constant," *Phys. Rev. D* **94** (Oct, 2016) 086007.

[153] H. Goenner, "Some remarks on the genesis of scalar-tensor theories," *General Relativity and Gravitation* **44** no. 8, (Jun, 2012) 2077–2097.

[154] C. Brans and R. H. Dicke, "Mach's principle and a relativistic theory of gravitation," *Phys. Rev.* **124** (Nov, 1961) 925–935.

[155] G. Kang, "Black hole area in Brans-Dicke theory," *Physical Review D* **54** no. 12, (Dec, 1996) 7483–7489.

[156] A. Sheykhi and M. Yazdanpanah, "Thermodynamics of charged brans–dicke ads black holes," *Physics Letters B* **679** no. 4, (2009) 311 – 316.

[157] A. Sheykhi, M. H. Dehghani, and S. H. Hendi, "Thermodynamic instability of charged dilaton black holes in ads spaces," *Phys. Rev. D* **81** (Apr, 2010) 084040.

[158] C. Charmousis, B. Goutéraux, B. Soo Kim, E. Kiritsis, and R. Meyer, "Effective holographic theories for low-temperature condensed matter systems," *Journal of High Energy Physics* **2010** no. 11, (Nov, 2010) 151.

[159] E. Kiritsis and J. Ren, "On holographic insulators and supersolids," *Journal of High Energy Physics* **2015** no. 9, (Sep, 2015) 168.

[160] S. Chakrabarti, S. Chakrabortty, and S. Jain, "Proof of universality of electrical conductivity at finite chemical potential," *Journal of High Energy Physics* **2011** no. 2, (2011) .

[161] S. Jain, "Universal thermal and electrical conductivity from holography," *Journal of High Energy Physics* **2010** no. 11, (Nov, 2010) 92.

[162] A. M. García-García and A. Romero-Bermúdez, "Drude weight and mazur-suzuki bounds in holography," *Phys. Rev. D* **93** (Mar, 2016) 066015.

[163] M. Baggioli and O. Pujolàs, "On holographic disorder-driven metal-insulator transitions," *Journal of High Energy Physics* **2017** no. 1, (Jan, 2017) 40.

[164] B. Goutéraux, E. Kiritsis, and W.-J. Li, "Effective holographic theories of momentum relaxation and violation of conductivity bound," *Journal of High Energy Physics* **2016** no. 4, (Apr, 2016) 122.

[165] S. Gopalakrishnan, M. Müller, V. Khemani, M. Knap, E. Demler, and D. A. Huse, "Low-frequency conductivity in many-body localized systems," *Phys. Rev. B* **92** (Sep, 2015) 104202.

[166] G. T. Horowitz and J. E. Santos, "General relativity and the cuprates," *Journal of High Energy Physics* **2013** no. 6, (Jun, 2013) 87.

[167] G. Gibbons and K.-i. Maeda, "Black holes and membranes in higher-dimensional theories with dilaton fields," *Nuclear Physics B* **298** no. 4, (Mar, 1988) 741–775.

[168] D. Garfinkle, G. T. Horowitz, and A. Strominger, "Charged black holes in string theory," *Physical Review D* **43** no. 10, (May, 1991) 3140–3143.

[169] B. Goutéraux and E. Kiritsis, "Generalized holographic quantum criticality at finite density," *Journal of High Energy Physics* **2011** no. 12, (Dec, 2011) 36.

[170] C. H. Brans, "The roots of scalar-tensor theory: an approximate history," arXiv:0506063 [gr-qc].

[171] C. J. Gao and S. N. Zhang, "Higher-dimensional dilaton black holes with cosmological constant," *Physics Letters B* **605** no. 1–2, (2005) 185 – 189.

[172] I. L. Shapiro and H. Takata, "Conformal transformation in gravity," *Physics Letters B* **361** no. 1-4, (Nov, 1995) 31–37.

[173] I. L. Shapiro, "On the conformal transformation and duality in gravity," *Classical and Quantum Gravity* **14** no. 2, (Feb, 1997) 391–405.

[174] T. P. Sotiriou and V. Faraoni, "$f(R)$ theories of gravity," *Reviews of Modern Physics* **82** no. 1, (Mar, 2010) 451–497.

[175] T. P. Sotiriou, S. Liberati, and V. Faraoni, "Theory of Gravitation Theories: A No-Progress Report," *International Journal of Modern Physics D* **17** no. 03n04, (Mar, 2008) 399–423.

[176] I. L. Shapiro and H. Takata, "One-loop renormalization of the four-dimensional theory for quantum dilaton gravity," *Physical Review D* **52** no. 4, (Aug, 1995) 2162–2175.

[177] R. Brustein and A. J. M. Medved, "Ratio of shear viscosity to entropy density in generalized theories of gravity," *Physical Review D* **79** no. 2, (Jan, 2009) 021901.

[178] R. Brustein, D. Gorbonos, and M. Hadad, "Wald's entropy is equal to a quarter of the horizon area in units of the effective gravitational coupling," *Physical Review D* **79** no. 4, (Feb, 2009) 044025.

[179] S. Nojiri and S. D. Odintsov, "Unified cosmic history in modified gravity: From f(r) theory to lorentz non-invariant models," *Physics Reports* **505** no. 2, (2011) 59 – 144.

[180] S. Chatterjee, M. Parikh, and S. Sarkar, "The black hole membrane paradigm in $f(R)$ gravity," *Classical and Quantum Gravity* **29** no. 3, (Feb, 2012) 035014, 1012.6040.

[181] R. Pourhasan, "Spacetime entanglement with f(R) gravity," *Journal of High Energy Physics* **2014** no. 6, (Jun, 2014) 4.

[182] A. Donos and J. P. Gauntlett, "Novel metals and insulators from holography," *Journal of High Energy Physics* **2014** no. 6, (Jun, 2014) 7.

[183] J. Santos, J. S. Alcaniz, M. J. Reboucas, and F. C. Carvalho, "Energy conditions in f(R)-gravity," *Phys. Rev. D* **76** (2007) 083513.

[184] R. Emparan, D. Grumiller, and K. Tanabe, "Large-d gravity and low-d strings," *Phys. Rev. Lett.* **110** (Jun, 2013) 251102.

[185] A. M. García-García and A. Romero-Bermúdez, "Conductivity and entanglement entropy of high dimensional holographic superconductors," *Journal of High Energy Physics* **2015** no. 9, (2015) 1–32.

[186] R. A. Davison, "Momentum relaxation in holographic massive gravity," *Physical Review D* **88** no. 8, (Oct., 2013) 086003.

[187] S. A. Hartnoll, D. M. Ramirez, and J. E. Santos, "Entropy production, viscosity bounds and bumpy black holes," *Journal of High Energy Physics* **2016** no. 3, (Mar, 2016) 170.

[188] X. H. Ge, Y. Ling, C. Niu, and S. J. Sin, "Thermoelectric conductivities, shear viscosity, and stability in an anisotropic linear axion model," *Phys. Rev. D* **92** no. 10, (2015) 1–31.

[189] M. Sadeghi and S. Parvizi, "Hydrodynamics of a black brane in gauss–bonnet massive gravity," *Classical and Quantum Gravity* **33** no. 3, (2016) 035005.

[190] P. Burikham and N. Poovuttikul, "Shear viscosity in holography and effective theory of transport without translational symmetry," *Phys. Rev. D* **94** (Nov, 2016) 106001.

[191] A. Rebhan and D. Steineder, "Violation of the holographic viscosity bound in a strongly coupled anisotropic plasma," *Phys. Rev. Lett.* **108** no. 2, (2012) 2–5.

[192] K. A. Mamo, "Holographic rg flow of the shear viscosity to entropy density ratio in strongly coupled anisotropic plasma," *Journal of High Energy Physics* **2012** no. 10, (Oct, 2012) 70.

[193] S. I. Finazzo, R. Critelli, R. Rougemont, and J. Noronha, "Momentum transport in strongly coupled anisotropic plasmas in the presence of strong magnetic fields," *Phys. Rev. D* **94** (Sep, 2016) 054020.

[194] L. Alberte, M. Baggioli, and O. Pujolàs, "Viscosity bound violation in holographic solids and the viscoelastic response," *Journal of High Energy Physics* **2016** no. 7, (Jul, 2016) 74.

[195] I. Giannakis, D. Hou, J.-r. Li, and H.-c. Ren, "Low shear viscosity due to anderson localization," *Phys. Rev. D* **77** (Jan, 2008) 027701.

[196] T. Faulkner, N. Iqbal, H. Liu, J. McGreevy, and D. Vegh, "Charge transport by holographic Fermi surfaces," *Physical Review D* **88** no. 4, (Aug., 2013) 045016.

[197] J. Fröhlich and T. Spencer, "Absence of diffusion in the Anderson tight binding model for large disorder or low energy," *Communications in Mathematical Physics* **88** no. 2, (1983) 151–184.

[198] W.-M. Wang and Z. Zhang, "Long Time Anderson Localization for the Nonlinear Random Schrödinger Equation," *Journal of Statistical Physics* **134** no. 5-6, (Nov., 2008) 953–968.

[199] A. Lucas, S. Sachdev, and K. Schalm, "Scale-invariant hyperscaling-violating holographic theories and the resistivity of strange metals with random-field disorder," *Physical Review D* **89** no. 6, (Mar., 2014) 066018, arXiv:1401.7993.

[200] A. Lucas and S. Sachdev, "Conductivity of weakly disordered strange metals: From conformal to hyperscaling-violating regimes," *Nuclear Physics B* **892** (Mar, 2015) 239–268, arXiv:1411.3331.

[201] A. Lucas and S. Sachdev, "Memory matrix theory of magnetotransport in strange metals," *Phys. Rev. B* **91** (May, 2015) 195122.

[202] S. A. Hartnoll, D. M. Ramirez, and J. E. Santos, "Thermal conductivity at a disordered quantum critical point," *Journal of High Energy Physics* **2016** no. 4, (Apr, 2016) 22.

[203] D. Arean, L. A. P. Zayas, I. S. Landea, and A. Scardicchio, "The Holographic Disorder-Driven Supeconductor-Metal Transition," arXiv:1507.02280.

[204] B. Kramer and A. MacKinnon, "Localization: theory and experiment," *Reports on Progress in Physics* **56** no. 12, (Dec., 1993) 1469–1564.

[205] P. W. Anderson, D. J. Thouless, E. Abrahams, and D. S. Fisher, "New method for a scaling theory of localization," *Physical Review B* **22** no. 8, (Oct., 1980) 3519–3526.

[206] T. Andrade, A. M. García-García, and B. Loureiro, "Coherence effects in disordered geometries with a field-theory dual," *Journal of High Energy Physics* **2018** no. 3, (Mar, 2018) 187.

[207] S. John, "Electromagnetic absorption in a disordered medium near a photon mobility edge," *Phys. Rev. Lett.* **53** (Nov, 1984) 2169–2172.

[208] P. W. Anderson, "The question of classical localization a theory of white paint?," *Philosophical Magazine B* **52** no. 3, (1985) 505–509.

[209] Y. Bardoux, M. M. Caldarelli, and C. Charmousis, "Shaping black holes with free fields," *Journal of High Energy Physics* **2012** no. 5, (May, 2012) 54.

[210] T. Andrade, S. A. Gentle, and B. Withers, "Drude in d major," *Journal of High Energy Physics* **2016** no. 6, (Jun, 2016) 134.

[211] T. Andrade, "A simple model of momentum relaxation in Lifshitz holography," arXiv:1602.00556.

[212] R. A. Davison, K. Schalm, and J. Zaanen, "Holographic duality and the resistivity of strange metals," *Phys. Rev. B* **89** (Jun, 2014) 245116.

[213] A. Amoretti, A. Braggio, N. Maggiore, N. Magnoli, and D. Musso, "Thermo-electric transport in gauge/gravity models with momentum dissipation," *Journal of High Energy Physics* **2014** no. 9, (Sep, 2014) 160.

[214] R. A. Davison, K. Schalm, and J. Zaanen, "Holographic duality and the resistivity of strange metals," *Phys. Rev. B* **89** (Jun, 2014) 245116.

[215] M. Baggioli and O. Pujolàs, "Electron-phonon interactions, metal-insulator transitions, and holographic massive gravity," *Phys. Rev. Lett.* **114** (Jun, 2015) 251602.

[216] F. Aprile and T. Ishii, "A simple holographic model of a charged lattice," *Journal of High Energy Physics* **2014** no. 10, (Oct., 2014) 151.

[217] Y. Ling, C. Niu, J.-P. Wu, and Z.-Y. Xian, "Holographic lattice in Einstein-Maxwell-dilaton gravity," *Journal of High Energy Physics* **2013** no. 11, (Nov., 2013) 6, arXiv:1309.4580.

[218] P. Chesler, A. Lucas, and S. Sachdev, "Conformal field theories in a periodic potential: Results from holography and field theory," *Phys. Rev. D* **89** (Jan, 2014) 026005.

[219] O. Aharony, Z. Komargodski, and S. Yankielowicz, "Disorder in large-n theories," *Journal of High Energy Physics* **2016** no. 4, (Apr, 2016) 13.

[220] J. Cardy, "Logarithmic conformal field theories as limits of ordinary cfts and some physical applications," *Journal of Physics A: Mathematical and Theoretical* **46** no. 49, (2013) 494001.

[221] O. Saremi, "Disorder in Gauge/Gravity Duality, Pole Spectrum Statistics and Random Matrix Theory," arXiv:1206.1856.

[222] M. Taylor and W. Woodhead, "Inhomogeneity simplified," *The European Physical Journal C* **74** no. 12, (Dec, 2014) 3176.

[223] B. L. Altshuler, D. Khmel'nitzkii, A. I. Larkin, and P. A. Lee, "Magnetoresistance and hall effect in a disordered two-dimensional electron gas," *Phys. Rev. B* **30** (Dec, 1980) 228–232.

[224] C. Fefferman and C. R. Graham, "The ambient metric," arXiv:0710.0919 [math].

[225] K. Skenderis and S. N. Solodukhin, "Quantum effective action from the AdS/CFT correspondence," *Physics Letters, Section B: Nuclear, Elementary Particle and High-Energy Physics* **472** no. 3-4, (Oct, 2000) 316–322.

[226] P. Breitenlohner and D. Z. Freedman, "Positive Energy in anti-De Sitter Backgrounds and Gauged Extended Supergravity," *Phys. Lett.* **115B** (1982) 197–201.

[227] P. Breitenlohner and D. Z. Freedman, "Stability in Gauged Extended Supergravity," *Annals Phys.* **144** (1982) 249.

[228] R. A. Janik, J. Jankowski, and P. Witkowski, "Conformal defects in supergravity - backreacted Dirac delta sources," *JHEP* **07** (2015) 050, arXiv:1503.08459 [hep-th].

[229] O. Bohigas and J. Flores, "Two-body random hamiltonian and level density," *Physics Letters B* **34** no. 4, (1971) 261 – 263.

[230] J. French and S. Wong, "Validity of random matrix theories for many-particle systems," *Physics Letters B* **33** no. 7, (1970) 449 – 452.

[231] J. French and S. Wong, "Some random-matrix level and spacing distributions for fixed-particle-rank interactions," *Physics Letters B* **35** no. 1, (1971) 5 – 7.

[232] O. Bohigas and J. Flores, "Spacing and individual eigenvalue distributions of two-body random hamiltonians," *Physics Letters B* **35** no. 5, (1971) 383 – 386.

[233] K. Mon and J. French, "Statistical properties of many-particle spectra," *Annals of Physics* **95** no. 1, (1975) 90 – 111.

[234] T. A. Brody, J. Flores, J. B. French, P. A. Mello, A. Pandey, and S. S. M. Wong, "Random-matrix physics: spectrum and strength fluctuations," *Rev. Mod. Phys.* **53** (Jul, 1981) 385–479.

[235] J. Verbaarschot and M. Zirnbauer, "Replica variables, loop expansion, and spectral rigidity of random-matrix ensembles," *Annals of Physics* **158** no. 1, (1984) 78 – 119.

[236] L. Benet, T. Rupp, and H. A. Weidenmüller, "Nonuniversal behavior of the k-body embedded gaussian unitary ensemble of random matrices," *Phys. Rev. Lett.* **87** (Jun, 2001) 010601.

[237] L. Benet and H. A. Weidenmüller, "Review of the k -body embedded ensembles of gaussian random matrices," *Journal of Physics A: Mathematical and General* **36** no. 12, (2003) 3569.

[238] M. Srednicki, "Spectral statistics of the k-body random-interaction model," *Phys. Rev. E* **66** (Oct, 2002) 046138.

[239] V. Kota, "Embedded random matrix ensembles for complexity and chaos in finite interacting particle systems," *Physics Reports* **347** no. 3, (2001) 223 – 288.

[240] J. Gomez, K. Kar, V. Kota, R. Molina, A. Relano, and J. Retamosa, "Many-body quantum chaos: Recent developments and applications to nuclei," *Physics Reports* **499** no. 4–5, (2011) 103 – 226.

[241] S. Sachdev and J. Ye, "Gapless spin-fluid ground state in a random quantum heisenberg magnet," *Phys. Rev. Lett.* **70** (May, 1993) 3339–3342.

[242] A. Almheiri and J. Polchinski, "Models of ads_2 backreaction and holography," *Journal of High Energy Physics* **11** no. 11, (2015) 1–19.

[243] K. Jensen, "Chaos in ads_2 holography," *Phys. Rev. Lett.* **117** (Sep, 2016) 111601.

[244] Y.-Z. You, A. W. W. Ludwig, and C. Xu, "Sachdev-ye-kitaev model and thermalization on the boundary of many-body localized fermionic symmetry-protected topological states," *Phys. Rev. B* **95** (Mar, 2017) 115150.

[245] A. M. García-García and J. J. M. Verbaarschot, "Spectral and thermodynamic properties of the sachdev-ye-kitaev model," *Phys. Rev. D* **94** (Dec, 2016) 126010.

[246] A. M. García-García and J. J. M. Verbaarschot, "Analytical spectral density of the sachdev-ye-kitaev model at finite n," *Phys. Rev. D* **96** (Sep, 2017) 066012.

[247] T. Kanazawa and T. Wettig, "Complete random matrix classification of SYK models with N=0, 1 and 2 supersymmetry," arXiv:1706.03044 [hep-th].

[248] C. Krishnan, K. V. P. Kumar, and S. Sanyal, "Random matrices and holographic tensor models," *Journal of High Energy Physics* **2017** no. 6, (Jun, 2017) 1–26.

[249] L. García-Álvarez, I. L. Egusquiza, L. Lamata, A. del Campo, J. Sonner, and E. Solano, "Digital quantum simulation of minimal AdS/CFT," *Phys. Rev. Lett.* **119** (Jul, 2017) 040501.

[250] E. Witten, "An SYK-Like Model Without Disorder," arXiv:1610.09758 [hep-th].

[251] I. R. Klebanov and G. Tarnopolsky, "Uncolored random tensors, melon diagrams, and the sachdev-ye-kitaev models," *Phys. Rev. D* **95** (Feb, 2017) 046004.

[252] C.-M. Jian, Z. Bi, and C. Xu, "Model for continuous thermal metal to insulator transition," *Phys. Rev. B* **96** (Sep, 2017) 115122.

[253] R. A. Davison, W. Fu, A. Georges, Y. Gu, K. Jensen, and S. Sachdev, "Thermoelectric transport in disordered metals without quasiparticles: The sachdev-ye-kitaev models and holography," *Phys. Rev. B* **95** (Apr, 2017) 155131.

[254] D. J. Gross and V. Rosenhaus, "A generalization of sachdev-ye-kitaev," *Journal of High Energy Physics* **02** no. 2, (2017) 93.

[255] M. Mézard, G. Parisi, and M. A. Virasoro, *Spin Glass Theory and Beyond*. Singapore: World Scientific, 1987.

[256] S. Scherer, "Chiral perturbation theory: Introduction and recent results in the one-nucleon sector," *Progress in Particle and Nuclear Physics* **64** no. 1, (2010) 1 – 60.

[257] D. Bagrets, A. Altland, and A. Kamenev, "Sachdev–ye–kitaev model as liouville quantum mechanics," *Nuclear Physics B* **911** (2016) 191–205.

[258] D. Bagrets, A. Altland, and A. Kamenev, "Power-law out of time order correlation functions in the syk model," *Nuclear Physics B* **921** (2017) 727 – 752.

[259] V. V. Belokurov and E. T. Shavgulidze, "Exact solution of the schwarzian theory," *Phys. Rev. D* **96** (Nov, 2017) 101701.

[260] D. Stanford and E. Witten, "Fermionic localization of the schwarzian theory," *Journal of High Energy Physics* **2017** no. 10, (Oct, 2017) 8.

[261] S. Carlip, "Entropy from conformal field theory at killing horizons," *Classical and Quantum Gravity* **16** no. 10, (1999) 3327.

[262] S. H. Shenker and D. Stanford, "Black holes and the butterfly effect," *JHEP* **03** (2014) 067, arXiv:1306.0622 [hep-th].

[263] B. Swingle, G. Bentsen, M. Schleier-Smith, and P. Hayden, "Measuring the scrambling of quantum information," *Phys. Rev. A* **94** (Oct, 2016) 040302.

[264] A. Larkin and Y. N. Ovchinnikov, "Quasiclassical method in the theory of superconductivity," *Sov Phys JETP* **28** no. 6, (1969) 1200–1205.

[265] G. Berman and G. Zaslavsky, "Condition of stochasticity in quantum nonlinear systems," *Physica A: Statistical Mechanics and its Applications* **91** no. 3, (1978) 450 – 460.

[266] S. H. Shenker and D. Stanford, "Multiple shocks," *Journal of High Energy Physics* **2014** no. 12, (Dec, 2014) 46.

[267] D. A. Roberts, D. Stanford, and L. Susskind, "Localized shocks," *Journal of High Energy Physics* **2015** no. 3, (Mar, 2015) 51.

[268] D. S. Juan Maldacena, Stephen H. Shenker, "A bound on chaos," *Journal of High Energy Physics* **08** no. 8, (2016) 106.

[269] B. Goutéraux, B. Kim, and R. Meyer, "Charged dilatonic black holes and their transport properties," *Fortschritte der Physik* **59** no. 7-8, (2011) 723–729.

[270] V. Narovlansky and O. Aharony, "The renormalization group in quantum quenched disorder," 1803.08529 [cond-mat.str-el].

[271] R. Narayanan, C. Park, and Y.-L. Zhang, "Entanglement Entropy of Randomly Disordered System," 1803.01064 [hep-th].

[272] M. Ammon, M. Baggioli, A. Jiménez-Alba, and S. Moeckel, "A smeared quantum phase transition in disordered holography," 1802.08650 [hep-th].

[273] O. Aharony and V. Narovlansky, "The renormalization group flow in field theories with quenched disorder," 1803.08534 [cond-mat.str-el].

[274] A. Donos, J. P. Gauntlett, T. Griffin, and V. Ziogas, "Incoherent transport for phases that spontaneously break translations," 1801.09084 [hep-th].

[275] F. Pretorius and M. W. Choptuik, "Gravitational collapse in 2+1 dimensional AdS spacetime," *Physical Review D* **62** no. 12, (Nov., 2000) 124012.

[276] E. Canovi, D. Rossini, R. Fazio, G. E. Santoro, and A. Silva, "Quantum quenches, thermalization, and many-body localization," *Physical Review B* **83** no. 9, (Mar., 2011) 094431, arXiv:1006.1634.

[277] K. Agarwal, S. Gopalakrishnan, M. Knap, M. Müller, and E. Demler, "Anomalous diffusion and griffiths effects near the many-body localization transition," *Phys. Rev. Lett.* **114** (Apr, 2015) 160401.

[278] C. Li and J. Lucietti, "Three-dimensional black holes and descendants," *Physics Letters B* **738** no. Supplement C, (2014) 48 – 54.

[279] P. Minces and V. O. Rivelles, "Scalar field theory in the AdS/CFT correspondence revisited," *Nuclear Physics B* **572** no. 3, (Apr., 2000) 651–669, arXiv:9907079 [hep-th].

[280] V. Balasubramanian, P. Kraus, and A. Lawrence, "Bulk versus boundary dynamics in anti–de Sitter spacetime," *Physical Review D* **59** no. 4, (Jan., 1999) 046003.

[281] A. Sheykhi and H. Alavirad, "Topological Black Holes in Brans–Dicke–Maxwell Theory," *International Journal of Modern Physics D* **18** no. 11, (Nov, 2009) 1773–1783.